AN INVESTIGATION OF THE EFFECTS OF PHOSPHATES AND OTHER ADDITIVES ON THE CALCIUM OXIDE-ALUMINA SYSTEM

A Thesis submitted in fulfilment of the
requirements for the degree of
Doctor of Philosophy
in the University of Leeds

by

Fathy Helmy MOSALAMY, B.Sc., M.Sc. (Research).

This work was carried out under the supervision of
D.E.C. Corbridge, B.Sc., Ph.D., M.Inst.P., F.C.S.

Department of Ceramics,
Houldsworth School of Applied Science,
The University,
Leeds LS2 9JT.

NOVEMBER, 1978.

"In the name of the GOD,
Most Gracious, Most Merciful"

Dedicated to:

My parents

My Wife, and

My Son AMRO

ABSTRACT

The work described in this thesis is concerned with the investigation of the influence of different additives (H_3PO_4, $AlPO_4$, H_3BO_3, BPO_4, CrO_3 and $CrPO_4$) on the strength and properties of materials in the $CaO-Al_2O_3$ system.

Sample fabrication involved initial mixing with water and selected additive followed by one of three treatments: (1) casting at room temperature, followed by firing in the range 300-1300°C; (2) hot-pressing under constant pressure (207 MNm^{-2}) for constant time (30 minutes) over a wide range of temperature (50-700°C); (3) hot-pressing under constant pressure (207 MNm^{-2}) for constant time (30 minutes) at constant temperature (300°C), followed by firing in air in the range 300-1300°C.

With H_3PO_4 additive, cast at room temperature, strengths were found to be directly related to the quantity of aluminum phosphate formed *in situ*. Under hot-pressing conditions, aluminum phosphate was formed within a short time (30 minutes), and at a relatively low temperature (200-700°C), the quantity depending on the $\frac{C}{C+A}$ ratio. A relationship was derived between the $\frac{C}{C+A}$ ratio and the minimum hot-pressing temperature at which anhydrous aluminum phosphate is formed.

Small quantities (~ 5%) of (H_3PO_4 + H_3BO_3) or preformed BPO_4 were found to increase considerably the strength (~ 300 MNm^{-2}) of CA and CA_2 after firing above 1200°C. One of the components formed, $9Al_2O_3.2B_2O_3$, does not appear to be a cementitious material, however.

The work confirms that the compound $4CaO.3Al_2O_3.CrO_3$ is produced in the system $CaO.Al_2O_3.CrO_3$ on firing above 900°C. This compound may contribute to the high strength (~ 160 MNm^{-2}) obtained with some mixes containing CrO_3 additive.

The study carried out on pure materials showed that pure calcium dialuminate (CA_2), if hot-pressed at low temperatures (100-150°C), hydrates to give C_3AH_6 and a product which has a very high strength

($\sim$260 MNm^{-2}). Hot-pressing of CA, CA_2 and Secar "250" cement samples at 150°C led to the highest strength values (253, 260 and 310 MNm^{-2}), whereas hot-pressing at 300°C showed a marked decrease in strength (113, 47 and 150 MNm^{-2}). A correlation between generated microstructure and strength was established.

Strength-porosity relationships were studied using three different empirical equations. These relationships showed a strong dependence on the starting material and the type of additive used.

Generally, hot-pressing at low temperature (300°C), followed by firing, led to higher strength than those achieved by casting at room temperature followed by firing. With some mixes, strengths were found to be four to five times higher in the former than the latter case.

ACKNOWLEDGMENTS

Praise be to GOD, Lord of the Worlds, by whose grace this work has been completed.

The author would like to thank Dr. D.E.C. Corbridge for his supervision and help during the course of the work. He is especially indebted to Professor R.J. Brook for his helpful discussions relating to the strength aspects, and for his encouragement. The ready advice from Dr. W.E. Worrall on matters relating to chemical analysis is also sincerely acknowledged; and also is his and Dr. A.J. Moulson's interest in reading and commenting on the thesis.

The author is very grateful to the Egyptian Government for its financial support and to the Building Research Institute, Cairo, Egypt, for leave of absence.

It is a special pleasure to thank Miss S.H. Toon for her patience and her skillful typing of the thesis.

To my wife, very special thanks for her support and encouragement throughout the entire course of the research.

LIST OF NOTATIONS AND ABBREVIATIONS

Cement chemists' shorthand notation is used throughout this work:

$C = CaO$

$A = Al_2O_3$

$H = H_2O$

$S = SiO_2$

$F = Fe_2O_3$

Other abbreviations used routinely are:

$\frac{C}{C+A}$ ratio = $\frac{CaO}{CaO + Al_2O_3}$ molar ratio

w/c ratio = water:cement ratio

w/s ratio = water:solids ratio

H.A.C. = High-alumina cement

H.p. = hot-pressed

XRD = X-ray diffraction

XRF = X-ray fluorescence

DTA = Differential thermal analysis

IR = Infra-red spectroscopy

SEM = Scanning electron microscopy.

All percentages are by weight unless otherwise stated.

CONTENTS

LIST OF FIGURES

LIST OF TABLES

CHAPTER 1

INTRODUCTION

The aim of this investigation was to advance our understanding of the nature of the reaction between different calcium aluminate phases and various bonding agents (phosphoric acid, aluminum phosphate, phosphoric acid + boric acid, boron phosphate, phosphoric acid + chromium trioxide and chromium phosphate). It was intended to establish the conditions under which known refractory or cementitious materials such as various polymorphic forms of aluminum phosphate might be formed. This investigation has included work on the influence of these bonding agents on the cold strength of calcium aluminate phases after firing over a wide range of temperatures.

In addition, commercial material, "Secar 250" cement, mixed with the above bonding agents, and pure starting materials without any additives were also studied under hot-pressing conditions.

The systems chosen for this study were:

(1) $CaO-Al_2O_3-P_2O_5-H_2O$

(2) $CaO-Al_2O_3-P_2O_5-B_2O_3-H_2O$

(3) $CaO-Al_2O_3-P_2O_5-CrO_3-H_2O$

(4) $CaO-Al_2O_3-H_2O$.

The technique of hot-pressing was also selected as a fabrication process in this investigation in order to:

(1) study the reaction between calcium aluminate phases and different bonding agents under hot-pressing conditions;

(2) evaluate the materials with respect to strength;

(3) study the relationship between porosity and strength;

(4) obtain a better assessment of factors involved in strength generation.

To reduce the number of interacting parameters the fabrication conditions (viz. temperature, pressure and time) were chosen so that pressure and time were constant (207 MNm^{-2} and 30 minutes respectively) where the hot-pressing temperature was the only variable (in the range 50 - 700°C). The effect of grain size on strength was reduced to a minimum by keeping the specific surface area of all the starting materials nearly the same except α-Al_2O_3.

There are two main groups of parameters that affect the mechanical properties of ceramics[1]: material properties (such as microstructure, internal strains, specimen shape and size), and environmental conditions (such as temperature, atmosphere, strain rate, rate of stress). The key mechanical property is strength, and the present work has been devoted to the influence of the material properties and environmental conditions upon the strength of the product.

Various methods of strength measurement were used for the different types of specimens. Although, ideally, the same geometry of loading should have been used for all the types of specimen, this was found to be impractical because of the variety of shape of the specimens. Compression tests were carried out on small cubes of side 12.7 mm prepared under ambient conditions, fired in air at different temperatures. The compacted specimens using the hot-pressing technique were in the form of small cylinders or discs. The strengths of the cylindrical samples were determined as compressive strength; strengths of samples in disc form were determined by a diametral compression test. In this latter test the disc was loaded in compression across a diameter and failure occurred from the uniform tensile stress acting perpendicular to the loaded diameter thus giving an indirect measure of tensile strength.

X-ray, D.T.A., I.R. and microscopic techniques were used to identify and study the phases produced in the reactions. The microstructures of some of these specimens were also examined.

CHAPTER 2

LITERATURE SURVEY

2.1 The $CaO-Al_2O_3$ System

The importance of this system led to the pioneering and classic studies of Rankin and co-workers[2,3]. Some of their original conclusions have since been modified, particularly the stoichiometry of the compounds C_5A_3 and C_3A_5 whose correct compositions are $C_{12}A_7$[4] and CA_2[5] respectively. An alumina-rich compound CA_6 was reported by Toropov et al.[6] in 1940 and its existence was confirmed by Gentile et al.[7] in 1963. The remaining calcium-aluminates, C_3A and CA, have received the greatest attention because of their importance in cements of various kinds. Nurse et al.[8] investigated the $CaO-Al_2O_3$ system in a moisture-free atmosphere and this is represented by the phase diagram shown in Fig. 2.1. This work, which refers to strictly anhydrous conditions, probably represents the most nearly correct diagram. Four stable compounds occur in this system: $3CaO.Al_2O_3$, $CaO.Al_2O_3$, $CaO.2Al_2O_3$ and $CaO.6Al_2O_3$. All these compounds melt incongruently and have primary crystallisation fields in the binary system. If the system is studied in air of normal humidity, and not in a strictly moisture-free atmosphere, a further metastable compound $12CaO.7Al_2O_3$ can also occur in addition to the four stable compounds. It is not binary and contains some hydroxyl groups[9].

2.1.1 Tricalcium aluminate C_3A

This component is present in Portland Cement, and hydrates more rapidly than any other calcium aluminate phase, but by itself produces little or no hydraulic strength in mortars[10]. It belongs to the cubic system having a = 7.6 Å , it melts incongruently at 1539 ± 5°C, dissociating into CaO and a liquid of composition (wt %) CaO 57.2, Al_2O_3 42.8[8].

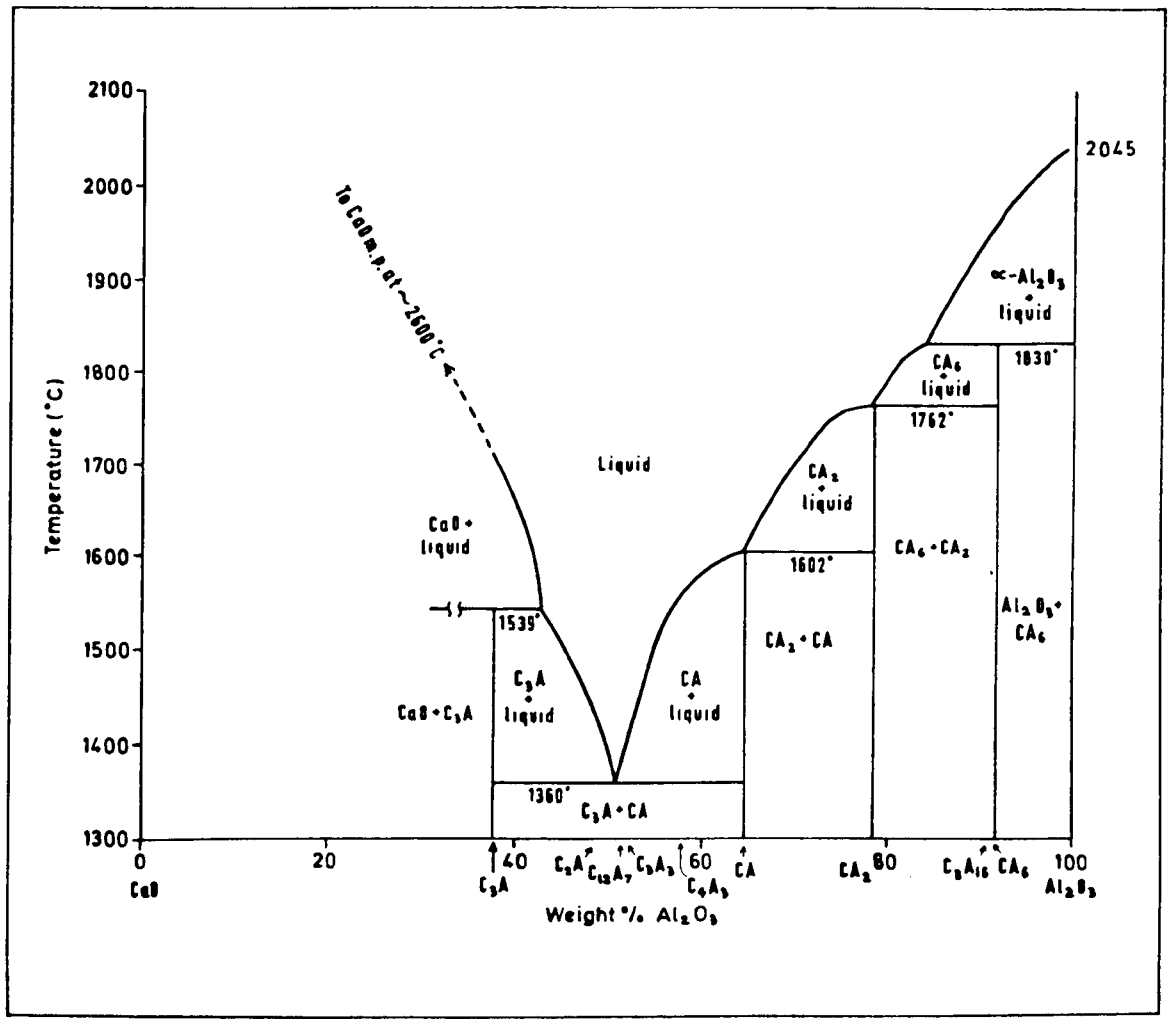

FIG. 2.1: The system $CaO-Al_2O_3$ in moisture-free atmospheres (Reference 8).

2.1.2 Monocalcium aluminate CA

The structure of this phase was partially investigated by Heller[11] and the general character of the structure was reported by Dougill[12]. The cell dimensions were a = 8.69, b = 8.09, c = 15.21 ± 0.02 Å, β = 90°.8'[10]. Pure CA forms prismatic or irregular grains which although monoclinic are frequently pseudohexagonal. Its structure is based on that of β-tridymite with all the Si^{4+} replaced by Al^{3+} and Ca^{2+} in cavities of the framework of AlO_4 tetrahedra. It melts incongruently at 1602 ± 5°C to $2CaO.Al_2O_3$ and liquid of approximately composition (wt %) CaO 36, Al_2O_3 64[8]. It has very desirable hydraulic properties[13] and is the most important constituent of anhydrous high-alumina cement which is responsible for the rapid hydration and high early strength.

2.1.3 Monocalcium dialuminate CA_2

This compound was first reported by Rankin and Wright[3] and was given the formula CA_2 by Tavasci[14] in 1935. A number of workers[15,16] agree that this compound is monoclinic and isomorphous with $SrO.2Al_2O_3$ and its cell dimensions are a = 12.862 Å, b = 8.86 Å, c = 5.43 Å, β = 106°50'. It melts incongruently at 1762 ± 5°C to give CA_6 and liquid of approximate composition (wt %) CaO 22, Al_2O_3 78[8]. The high alumina cements, depending on their CaO/Al_2O_3 ratio, contain mainly CA plus CA_2[13]. The CA_2 phase hydrates very slowly and it was considered that it might be hydraulically inert at ordinary temperature if completely pure[8,9]. It was reported that in alkaline solution, the rate of reaction with water can be significantly increased[10]. Bobrov et al.[17] in 1975 studied the effect of temperature on the hydration of CA_2. They concluded that when pure CA_2 was hydrated below 20°C, CAH_{10} was not formed unless a small amount of CA was present. Below 40°C, the hydration led to the formation of hexagonal hydroaluminate, C_2AH_8, where at or above 40°C cubic hydroaluminate, C_3AH_6, was formed.

2.1.4 Monocalcium hexa-aluminate, CA_6

This phase was first reported as a new compound at the higher alumina end of the $CaO-Al_2O_3$ system and assigned the formula C_3A_{16} by Lagerqvist et al.[5] The confirmation and the existence of this compound was studied and modified to CA_6 by other investigators[7,18]. The compound has hexagonal symmetry and it was suggested that its structure is isomorphous with magneto-plumbite ($PbO.6Fe_2O_3$).[19] The cell dimensions are a = 5.536, c = 21.825 Å [19]. This compound melts incongruently at 1830 ± 15°C to corundum and a liquid of approximate composition (wt %) CaO 16, Al_2O_3 84[8]. High alumina cements having a high Al_2O_3 content often contain CA_6[13]. This phase does not appear to hydrate in water and is relatively inert to hydration under neutral conditions.

2.1.5 The compound $C_{12}A_7$

This was formally known as pentacalcium trialuminate C_5A_3[3]. There is still some controversy regarding the stability of this compound and details can be found elsewhere.[9,10,20] The compound $C_{12}A_7$ is cubic and its cell dimension is a = 11.95Å[20]. The $C_{12}A_7$ phase which might be expected in normal aluminous cements depending on CaO/Al_2O_3 ratios, is an undesirable constituent because it hydrates very rapidly and causes "flash setting"[13]. This results in partial hardening of the wet concrete before it can be placed.

2.2 The $CaO-Al_2O_3-H_2O$ System

The stability relations and equilibria in the $CaO-Al_2O_3-H_2O$ system have received much attention in recent years. Jones[21] and other investigators[13,22,23,24] have studied this system at various temperatures. The effect of temperature on this system is shown in Fig. 2.2, in which the stable solubility curves for γ-AH_3 and C_3AH_6 are omitted.

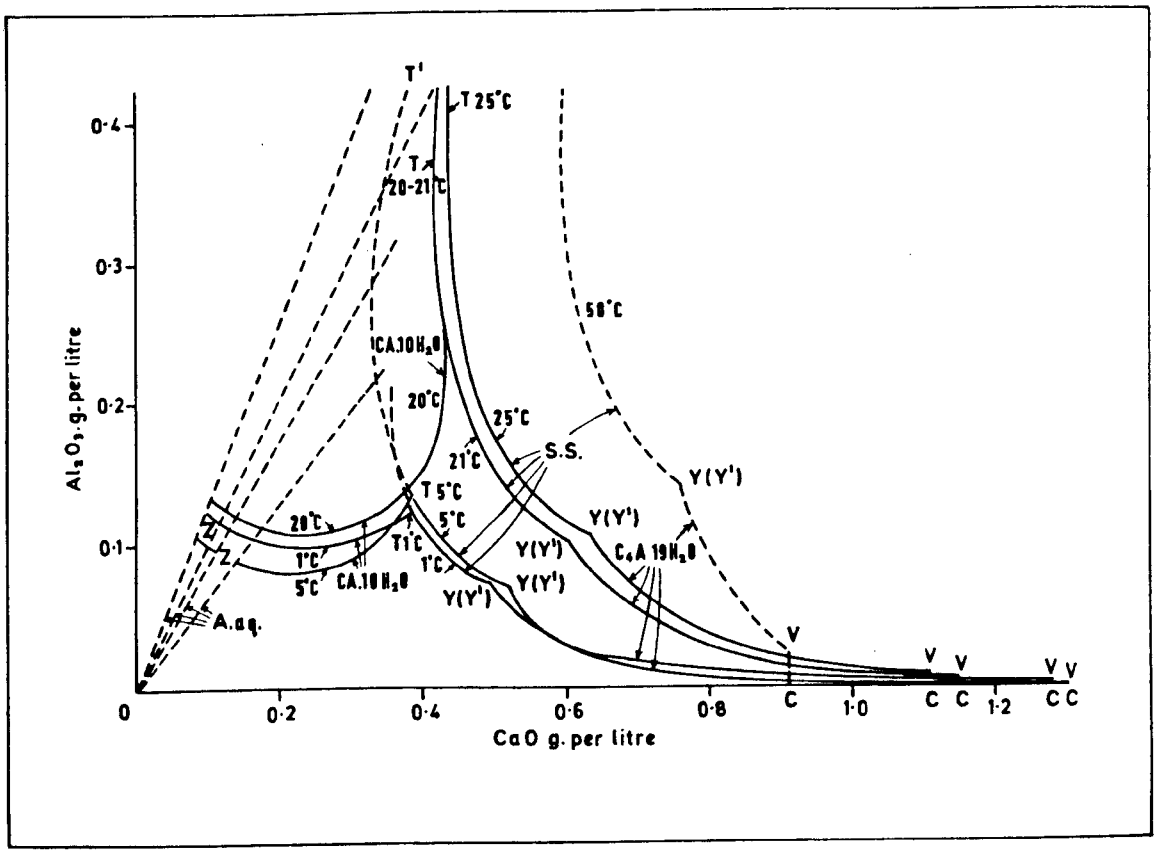

FIG. 2.2: The system $CaO-Al_2O_3-H_2O$ at various temperatures (Reference **21**).

All the investigators[13 21,22] agree that the appearance of the CAH_{10} phase at 21°C, but not at 25°C. It appears from Fig. 2.2 that C_2AH_8 and C_4AH_{19} have the highest solubilities at both 21 and 25°C. A possible lower hydrate of dicalcium aluminate, C_2AH_3, may be formed above about 100°C[21]. All the investigators[13,21,22] agree that C_3AH_6 is fundamentally stable up to about 215°C, whereas above this temperature $C_4A_3H_3$ is formed. Majumdar and Roy[25] investigated this system in the range 100 to 1000°C involving high pressure. It was concluded that only three stable hydrated phases, $Ca(OH)_2$, C_3AH_6 and $C_4A_3H_3$, are formed in this system. More details on the $CaO-Al_2O_3-H_2O$ system can be found elsewhere.[13,21,22,23,24,25]

2.3 Aluminous Cements

The development of aluminous cements dates back to as early as 1865. France was the pioneer in manufacturing these cements and recognised their interesting properties such as high early strength and resistance to chemical action of sulphate. Aluminous cement is obtained by fusing or sintering a mixture of aluminous and calcaceous materials and grinding the resultant product to a fine powder[9]. Two types of calcium aluminate cements are produced commercially. The first type has a typical bulk chemical composition (in wt %) CaO 36-40, Al_2O_3 40-50, SiO_2 4-9, iron oxide 1-15, TiO_2 1-3, alkali 0-1, and MgO 0-2[13]. This type of cement is usually referred to as normal aluminous cement or "Ciment fondu". The second type of cement has a much higher Al_2O_3 content; typically (in wt %) Al_2O_3 72-82, and CaO 15-27. Iron oxide, silica and other impurities are usually kept below a level of 1-4%. This type of cement is usually called high-alumina cement[13].

2.3.1 Composition and constitution of aluminous cements

The most important constituent of this cement is calcium mono-aluminate CA, since the strength of this type of cement is primarily determined by its content of CA. It is slow setting, particularly if rapidly cooled from the molten condition, but it subsequently hardens with great rapidity. In cements with higher Al_2O_3/CaO ratio, calcium dialuminate CA_2 is also formed. It was reported that the compound $C_{12}A_7$ might be present in commercial cements[13]. Calcium hexa-aluminate CA_6 does not exist in aluminous cements, but may be formed when concrete made with this cement and corundum aggregates is heated to high temperature. The phase β-C_2S is often detected in those cements containing less than 10% SiO_2. But in those having higher SiO_2 content gehlinite C_2AS predominates[9]. It is necessary to keep the silica content of aluminous cements low since C_2AS has little or no hydraulic activity under normal conditions. Another interesting phase which sometimes occurs in aluminous cements is the "Pleochroite" "unstable C_5A_3" phase. Many investigators[3,26,27,28,29] have examined this phase and more than one formula has been suggested. The exact composition of pleochroite is still uncertain[30]. Rankin and Wright[3], Aruja[26] have proposed the formula $5CaO.3Al_2O_3$. Parker[27] has suggested the formula $6CaO.4(Al,Fe^{3+})_2O_3.(Mg.Fe^{2+})O.SiO_2$ as a ferrous-ferric iron-substituted solid solution based on the quaternary phase $6CaO.4Al_2O_3.MgO.SiO_2$. More recently Midgely[28] has proposed the formula $22CaO.17Al_2O_3.3FeO.2SiO_2$. More details about this phase can be found elsewhere.[3,9,13,26,27,28,29,30] At the same time, this cement contains a relatively higher proportion of iron oxide, in ferrous and ferric states. It was reported[13,31] that little iron substitution can occur in CA and $C_{12}A_7$. The solid solutions are now known to extend from $2CaO.Fe_2O_3$ towards a hypothetical $2CaO.Al_2O_3$ and the mechanism of the solid solution is replacement of Fe^{3+} by Al^{3+}. The mineralogical composition of high-alumina cement is variable and

influenced by the ratio of ferrous to ferric iron[8]. Ferrous iron may be present as wüstite or in a glass phase. The formation of a compound with the formula $CaO.TiO_2$ (perovskite) in cements containing TiO_2 was also reported[9,13]. More details about the composition and constitution can be found elsewhere.[9,13,31,32]

2.3.2 Hydration of aluminous cements

Aluminous cement is a hydraulic material, i.e. it sets and hardens by chemical reaction with water and remains stable in the presence of water. This subject has been investigated by numerous authors.[32,33,34,35] It is generally agreed that the hydration of either CA or aluminous cement in pastes at 21°C gives CAH_{10} as a major product[33]. It was reported[34] that some gel appears to be formed in the first few hours and this seems to be alumina gel rather than CAH_{10}. This alumina gel on ageing gradually crystallises as gibbsite ($Al_2O_3.3H_2O$). The extent to which CAH_{10} or C_2AH_8 predominates in the hydration products depends on the temperature and also on the cement[9]. When pure CA is hydrated the critical temperature above which C_2AH_8 is formed is about 23°C[9]. The hexagonal hydrate CAH_{10} is of interest in connection with conversion because this hydrate compound is unstable both at normal and at higher temperatures and transformed into the cubic stable hydrate compound C_3AH_6. Recently Roy and Gouda[36] found that on hot-pressing aluminous cements, C_3AH_6 is formed initially; a subsequent potentially destructive conversion is thereby avoided. Also, the alumina hydrate boehmite (AlO.OH) is formed rather than gibbsite ($Al_2O_3.3H_2O$). They had suggested that the reaction apparently proceeds as follows:

$$3[CaO.Al_2O_3] + 8H_2O \longrightarrow 3CaO.Al_2O_3.6H_2O + 4AlO.OH.$$

Therefore, the hydration reaction in aluminous cements pastes can be formulated as follows:

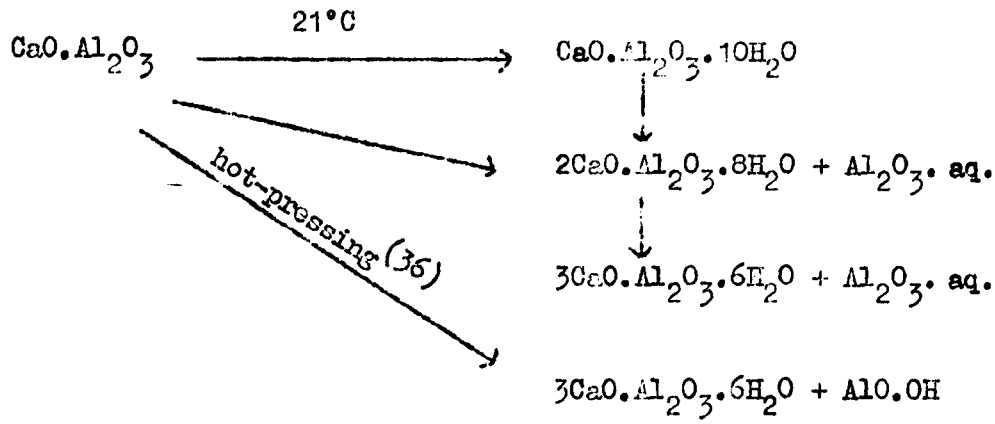

Much attention has been directed towards a more detailed study of the conversion phenomenon since the failure of some H.A.C. concrete beams have been reported in 1974. Long-term research into the characteristics of H.A.C. concrete was started to assess all the factors which affect the degree and the rate of conversion[37,38]. The compound $C_{12}A_7$ if present is believed to hydrate to C_2AH_8. The dicalcium aluminate hydrate, with ferric oxide replacing part of the alumina $C_2(AF)H_8$, is also reported from the ferrite compound in the cement[39]. The product of hydration of C_2S is a calcium silicate hydrate, in which the number of molecules of water is not known with certainty[40]. The hydrations of other compounds, particularly those containing iron, are still not clear[8] and details can be found elsewhere[9,13].

2.3.3 Refractory properties and effect of heat treatment on H.A.C. and H.A.C. Castable

The use of hydraulic aluminous cement for refractory application is now well known. However there is a region of low strength at temperatures between that at which the hydraulic bond is destroyed and that at which the cement becomes truly ceramic by sintering. Heindl and Post[41] presented data on the change in strength of H.A.C. with firebrick grog on firing. Schneider[42] studied the effect of elevated temperatures on the strength using neat white H.A.C. and concluded that many changes in the mechanical properties of the cement were directly related to

corresponding changes in composition. Tseung and Carruthers[43] investigated the degree of hydration achieved and its effect on the strength of refractory concrete before and after firing. They demonstrated that high curing-temperature for a restricted time (75°C for 6 hours) could provide a substantial increase in strength not only at room temperature, but also after the castable had been fired at any temperature up to the point at which ceramic bonding occurred. Wood and Driebach[44] studied the effect of curing-temperature on the strength of castable material using H.A.C. and white H.A.C. Generally their strength results after firing up to 1000°C were in agreement with the previous observation. Midgely[34] studied the mineralogy of set H.A.C. and the strength at elevated temperatures, as in Table 2.1.

Temp. of heating °C	Compressive Strength psi	Mineralogy
18	24.000	CAH_{10}, alumina gel
110	11.000	C_3AH_6, γ-AH_3
200	9.950	$C_{12}A_7$, amorphous Al_2O_3, $Ca(OH)_2$
300	11.300	" "
400	10.650	" "
500	9.800	" "
700	9.500	$C_{12}A_7$, amorphous Al_2O_3, CaO
800	9.000	" "
900	5.400	CA, trace $C_{12}A_7$
1000	5.000	CA

Table 2.1: Strength and Mineralogy of set H.A.C. after heating to various temperatures (Ref. 34).

Dutta et al.[45] in their investigation, found also that the cold strength of castable refractories using high purity calcium aluminate cement decreases after firing at different temperatures up to 1200°C.

2.4 Phosphate bonding

The bonding properties of a number of phosphate materials have been recognised for many years. Phosphate bonds are of particular interest in the field of refractories because of the high fusion temperatures of many phosphates. Heating is usually involved in establishing the bond. Kingery[46] stated that phosphate bonding is accomplished by three methods: (i) the reaction between siliceous materials and phosphoric acid, (ii) the reaction between oxides and phosphoric acid, and (iii) the direct addition or formation in situ of acid phosphates. Phosphoric acid itself acts as the bonding material, the addition of aluminum, magnesium, iron and beryllium oxide will increase the bonding power. These substances are all amphoteric or weakly basic and have moderate sized ionic radii. In contrast the addition of calcium, barium and thorium oxide, which are highly basic, or have a large ionic radii, will decrease the effectiveness of phosphoric acid as a bonding material.

Bechtel and Floss[47,48] reported on the bonding of ceramics with monoaluminum phosphate, $Al(H_2PO_4)_3$. They bonded fireclay, bauxite and silica and obtained a high strength value in the intermediate temperature range of 600-1000°C. Preuser[49] discussed the chemical setting of refractories by dilute phosphoric acid. Considerable strength was produced at 200 to 300°C. Reinhart[50] published a comprehensive review of binders for ceramics. Sheets and co-workers[51] used phosphoric acid to make castable refractories. They introduced the concept of adding an inhibitor: Rodin 78, a complex amine, was used to reduce the phenomenon known as bloating which results from the reaction between phosphate and metallic iron. Direct calorimetric analysis (DCA) studies[52] on tabular alumina-phosphoric acid mixture, suggests that no acid/alumina reaction occurs up to ~127°C. Most of the reaction occurs over the temperature range 127-427°C, and involves the formation of aluminum phosphates and possibly formation and melting of pyrophosphoric acid.

At about 510°C a change in the slope occurs that remains up to 732°C. Continuous changes in slope occur over the temperature range 732-1327°C arising from the formation of aluminum phosphate bonding phases and phase transitions. These authors also confirmed that the addition of Cr_2O_3 increases the thermal stability of phosphate bond. Ersin and William[53] studied the effects of chemical agents, added to phosphoric acid in controlling the formation of aluminum phosphate and preventing premature hardening. Palfreyman[54] published data on hot strength of high alumina refractories. Values of more than 13.8 MNm^{-2} were found for fused mullite specimens bonded with ground calcined alumina and 5 of 85% H_3PO_4. It is impossible to make any general statement about the properties of phosphate bonds without specifying the type of bond used and the composition and grading of the aggregate; particularly if one is to compare the relative properties of different binder systems.[54,55] Sicka[56] patented a foamed ceramic made from fly ash and phosphoric acid. McCarthy and Lovette[57] described a hot pressing method for firing a solid radioactive waste in a phosphate glass. Chvatal[58] introduced aluminum-chromium phosphate binder. These phosphates have good thermal stability. Chvatal's results have been confirmed by others[52]. Aluminum chlorophosphate hydrate was recently introduced also as a bonding material[59,60]. It is a dry powder, readily soluble in water. It decomposes on heating directly to $AlPO_4$ without forming intermediate metaphosphate. An extensive review on phosphate ceramics was given recently by Westman[61] and Cassidy[62].

There is very little literature about the hot pressing of phosphate bonded alumina[63], and no record of phosphate bonded calcium aluminate phases under hot-pressing conditions. At the same time no investigations have been reported on the use of either a mixture of boric acid + phosphoric acid or boron phosphate as a bonding agent for different materials in the $CaO-Al_2O_3$ system.

The effect of phosphates in a cement clinker on its setting properties were also reported. Koyanogi[64] reported that small quantities of monocalcium phosphate retarded the setting of cement by preventing the hydration of calcium aluminate. Nurse[65] reported that P_2O_5 in raw materials may cause difficulties in firing, erratic setting, and slow strength development.

2.4.1 The $CaO-Al_2O_3-P_2O_5$ system

Phase relationships in this system were studied by Stone et al.[66] as shown in Fig. 2.3. A partial equilibrium diagram for the system $Al_2O_3-P_2O_5$ covering the composition range between the two binary compounds aluminum metaphosphate ($Al(PO_3)_3$) and aluminum orthophosphate $AlPO_4$ is shown also in Fig. 2.4[67]. By far the most interesting compound in the system is $AlPO_4$. Kolb[68] found that when pure $AlPO_4$ (cristobalite form) was heated to about 1500°C it began to decompose liberating P_2O_5 and forming Al_2O_3 as given in Table 2.2.

Temp./°C	Duration/ hour	Composition %	
		$AlPO_4$	Al_2O_3
1500	1	93.7	6.3
1650	1	86.8	13.2
1800	1	86.5	13.5
2200	Not stated	-	100

Table 2.2: Thermal stability of $AlPO_4$ in air (Ref. 68)

Bagman and Ershov[68] reported on the bonding characteristics of calcium phosphate in the system $CaO-P_2O_5$. They concluded that monocalcium phosphate formed at 600°C, had no bonding properties. Di-, tri- and tetracalcium phosphates formed at 800°, 1000° and 1200°C respectively had bonding properties, the tricalcium phosphate being the most active.

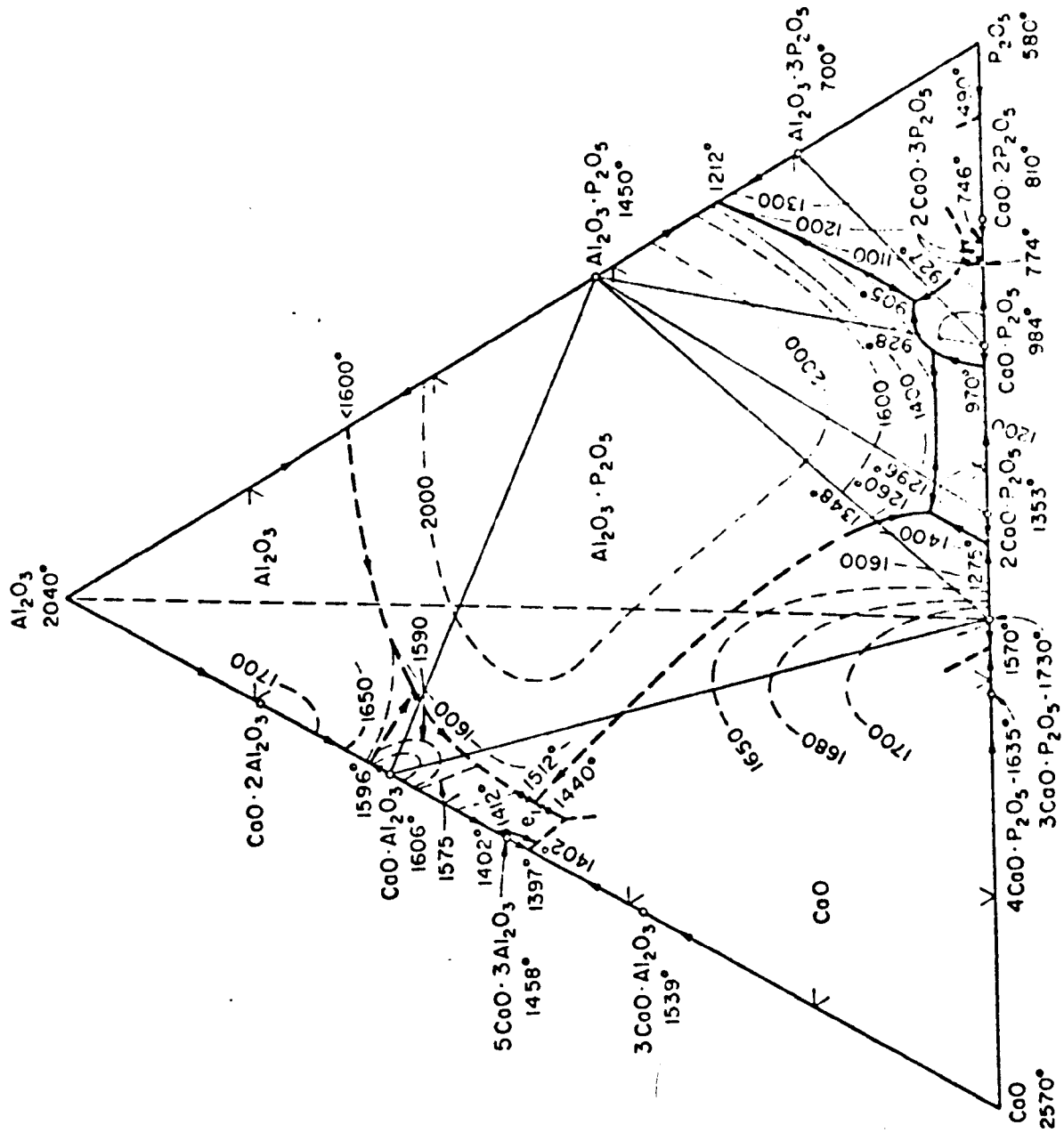

FIG. 2.3: The System Al_2O_3-CaO-P_2O_5 (Reference 66).

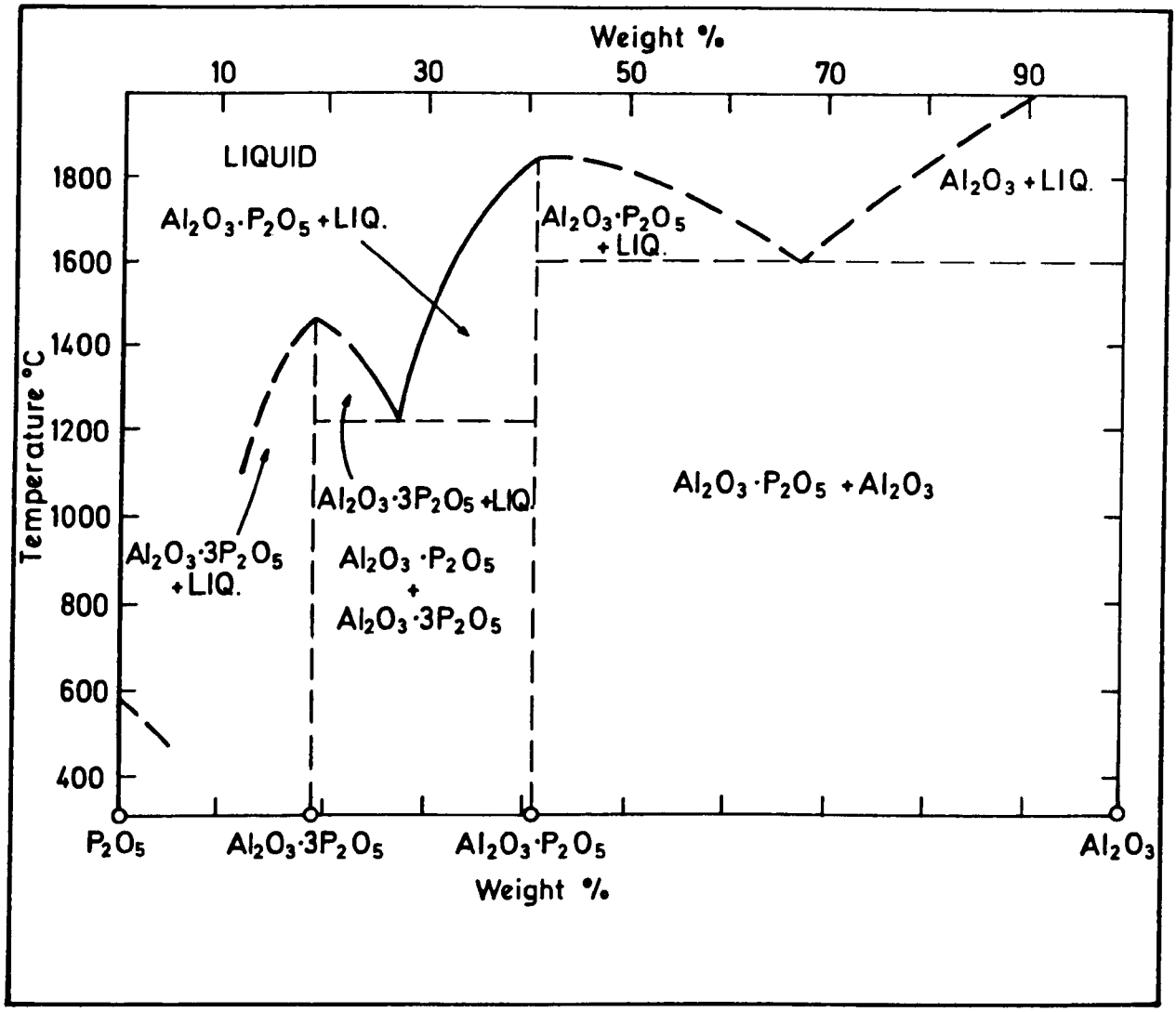

FIG. 2.4 : The system Al_2O_3-P_2O_5 (Reference 67).

2.5 Compounds isostructural with silica

The existence of phases with structures analogous to those of silica has long been known. Buerger[70] has discussed the physico-chemical basis of the structures of such compounds in detail. It was suggested[71] that silica type structures are only formed by ABO_4-type compounds when $(r_A + r_B)/2 < 0.55$ and recently Corbridge[72] summarised all compounds isostructural with silica in Table 2.3.

$(r_A+r_B)/2$	Quartz		Tridymite		Cristobalite	
	Low	High	Low	High	Low	High
0.42	SiO_2	SiO_2	SiO_2	SiO_2	SiO_2	SiO_2
0.43	$AlPO_4$	$AlPO_4$	$AlPO_4$	$AlPO_4$	$AlPO_4$	$AlPO_4$
0.29	BPO_4				BPO_4	
0.48	$GaPO_4$				$GaPO_4$	$GaPO_4$
0.49	$FePO_4$	$FePO_4$				
0.50	$MnPO_4$				$MnPO_4$	$MnPO_4$
0.34					$BAsO_4$	
0.48	$AlAsO_4$					
0.54	$GaAsO_4$					

Table 2.3: ABO_4-type compounds with silica structures (Ref. 72)

2.5.1 Aluminium phosphate

The structures of the $AlPO_4$ polymorphs parallel those of silica very closely. It has been classified as a half-breed derivative of silica[70], in which $2Si^{4+}$ ions are replaced by an Al^{3+} ion and a P^{5+} ion. Tröndel and Winkhaus[73] and earlier investigators observed that the crystalline forms of $AlPO_4$ have a remarkable structural resemblance to quartz, tridymite and cristobalite including the high forms. They also noted that the reconstructive inversions in $AlPO_4$ proceeded much faster than do

the corresponding silica inversions. Huttenlocher[74] and Strunz[75] reported the structural relationship between berlinite and low-quartz, but the first accurate lattice parameters were published by Brill and De Bretteville[76]. Using commercially prepared aluminum phosphate as a starting material, Beck[77] investigated the inversion characteristics of various $AlPO_4$ polymorphs. Shafer and Roy[78] presented revised values for some of the reconstructive inversion temperatures. Corbridge[72] summarised the six different forms of $AlPO_4$ analogous to those of silica in Fig. 2.5.

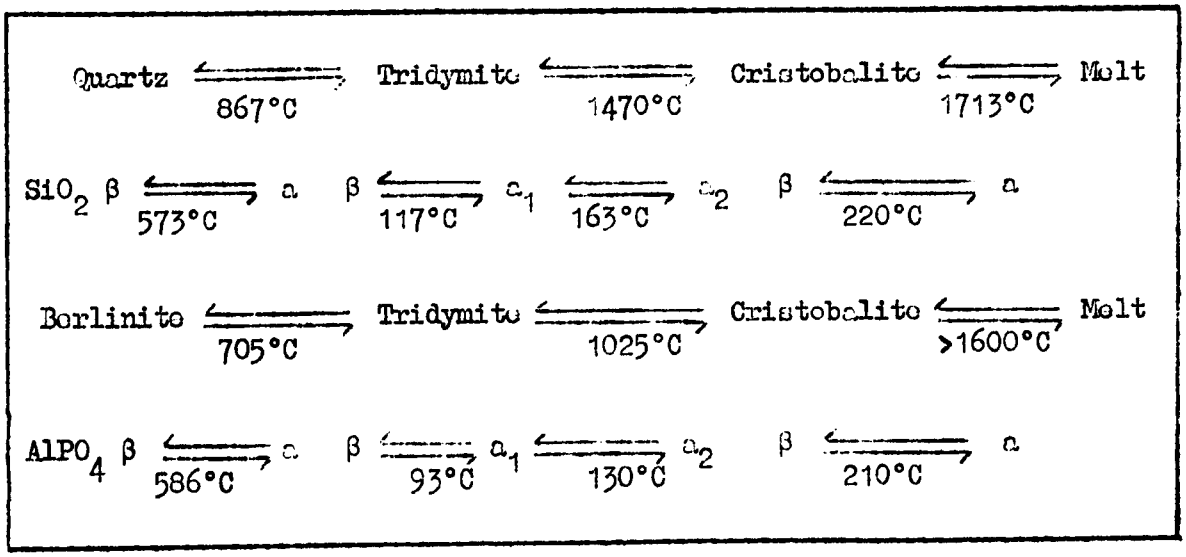

Fig. 2.5: Phase transformation of SiO_2 and $AlPO_4$ (Reference 72)

In both series of compounds the $\alpha \leftrightarrow \beta$ transitions take place comparatively readily but the transitions involving major changes of structure are much more sluggish[72]. All these compounds are characterised by their hardness and high melting point, their insolubility and resistance to hydration. The $AlPO_4$ analogues of the high-pressure forms of silica, namely Coesite, Keatite, Stishovite, have not yet been established[72]. Infrared adsorption spectra of SiO_2-$AlPO_4$ mixtures suggest that isomorphous substitution can occur at high temperatures, only up to about 5% in each series[79].

2.5.2 Boron phosphate

Boron phosphate is the only binary compound in the system B_2O_3-P_2O_5 which has long been known[60]. It was reported that boron phosphate exists in quartz[81,82] and high and low cristobalite forms[83,84]. Shafer et al.[78] showed that the structure was of a low cristobalite form and thus disproved the structure suggested by Schulze[84]. They indicated also that a possible boron phosphate analogue to quartz was formed under mild hydrothermal conditions. Corbridge[72] reported only two forms of boron phosphate as shown in Table 2.3. Buerger[70] described BPO_4 as a half-breed derivative of silica, where $2Si^{4+}$ ions were replaced by B^{3+} and P^{5+} ions. Both P^{5+} and B^{3+} ions were shown to be tetrahedrally coordinated with oxygen[85]. Unlike some half-breed derivatives of silica, BPO_4 does not have a high-low cristobalite type inversion above room temperature. Hummel et al.[86] reported that boron phosphate does not exhibit an appreciable rate of vaporisation until a temperature above 1450°C is reached, where Rickles[87] reported that BPO_4 sublimes at 1235°C.

Anhydrous chromium orthophosphate exists in two crystalline forms as well as in the amorphous state[88]. Brown-black amorphous material may be made by heating the hydrated forms. Alternatively, purple-grey amorphous material can be made by flame spraying a chromic/phosphoric acid mixture in gas flame at about 700°C[88].

$$2CrO_3 + 2H_3PO_4 \longrightarrow 2CrPO_4 + 3H_2O + 3O$$

Further heat treatment of amorphous varieties leads (irreversibly) to the formation of khaki-coloured β-$CrPO_4$ and above about 1150°C to dark blue-green α-$CrPO_4$.

$$CrPO_4.nH_2O \longrightarrow \text{Amorphous} \longrightarrow \beta\text{-}CrPO_4 \longrightarrow \alpha\text{-}CrPO_4 \longrightarrow \text{m.p. } 1850°C$$

The irreversibility of the phase transitions in $CrPO_4$ could be associated with a reduction of Cr coordination number from 6 to 4 and be compared

with the reversibility of the silica transformation which do not involve any change in coordination number from 4. Chromium phosphate, $CrPO_4$, has many of the silica-type structures. It is very insoluble, hard, chemically inert and has a high melting point ($>1850°C$). Although $(r_A + r_B)/2 = 0.49$, silica-type structures do not seem to exist for $CrPO_4$.[72]

2.6 Hot Pressing

The term hot-pressing, or pressure sintering, refers to the densification of a powder or paste by simultaneous application of heat and pressure. The development of high-performance ceramic materials with closely controlled microstructures and greatly improved properties (e.g. mechanical, thermal, electrical, optical and magnetic) by hot pressing represents one of the most important contemporary areas of ceramic processing. Hot pressing has numerous advantages over conventional cold-pressing and sintering processes[89]. By hot pressing improved microstructure and mechanical properties of a material are generally obtained relative to its porous form. Such materials are denser, stronger, and exhibit higher thermal conductivity. They are hard, durable and have a good surface finish. Owing to their low porosity and permeability they can resist various environmental effects. Sufficient pressure must be applied to compress the material in the die and to eliminate as much as possible the gases entrapped within the powders or pastes as well as the gases that are generated during sintering cycles. Many non-oxide ceramics, e.g. carbides, borides, nitrides, can only be sintered in the pure state by hot pressing to achieve densities sufficient for high-performance applications. Such materials generally have high vapour or decomposition pressures at sintering temperatures, as well as low atomic mobilities, making it difficult to achieve densification without pressure. A number of

modifications of uniaxial pressure sintering have been developed which can be considered thermochemical in nature[90]. These are: decomposition hot pressing[91], reactive hot pressing[92], including phase transformation[93], reaction hot pressing[94] and liquid phase hot pressing[95].

Hot pressing has been recently applied to cement paste[36,96,97]. Very high values of compressive strength have been reported using pressures (172.5 - 345 MNm^{-2}) in the range of temperatures 150-250°C for 30 minutes.

2.7 Mechanical Properties

It has long been recognised that the theoretical strength of a material is much greater than that found in practice. Theoretical estimates, based on atomic cohesion models, indicate that the theoretical fracture strength is approximately $E/10$ (E is Young's modulus), yet most materials fail at stresses between $E/10^2$ and $E/10^3$ [98]. The presence of cracks, either those that exist prior to stressing or those that are induced during stressing, are believed to be the cause of these discrepancies between theoretical and observed strength. The maximum attainable strength of a solid depends in the first place on the strength of its individual atomic bonds. In an ideal solid subjected to tensile stresses, the solid will elongate elastically until the atoms are sufficiently separated that their attractive forces no longer counterbalance the applied force, and fracture occurs along an entire plane of atoms. The theoretical strength is then expressed by this equation[98]:

$$\sigma_{th} = \left(\frac{E\gamma_o}{r_o}\right)^{\frac{1}{2}} \qquad \ldots\ldots\ldots (2.1)$$

where E = Young's modulus

γ_o = thermodynamic surface energy

r_o = atomic separation (i.e. interatomic distance).

Theoretical strength, of course, could only be attained in materials which are theoretically dense, and by eliminating either the pre-existing cracks or the phenomenon leading to crack nucleation during stressing. Even then, it has been reported that in polycrystalline materials grain boundaries frequently serve as locales of dislocations, weakening the material[1]. Inglis[99] was the first to show analytically that the stresses at the periphery of a crack are much greater than elsewhere in a stressed body. Albeit his calculations showed that cracks are likely sources of failure at applied stress much less than the theoretical fracture stress, they did not lead to an expression for crack instability, i.e. crack extension and failure.

Griffith[100] was the first to explain the discrepancy between the theoretical and practical strength. He defined a brittle material as a continuous medium which contains defects (microcracks) and assumed that the defect generates a stress concentration under an applied stress. His reasoning was based on the premise that the free energy of a cracked body and the applied forces should not increase during crack extension.

For a sharp elliptical crack of length 2C (which is equivalent to a surface crack of length C) in a thin infinite sheet of material under a tensile stress, Griffith postulated that for plane stress conditions

$$\sigma_f = \left(\frac{2E\gamma_o}{\pi C}\right)^{\frac{1}{2}} \qquad \ldots\ldots (2.2)$$

where σ_f = critical applied stress

E = Young's modulus

γ_o = thermodynamic surface energy

C = crack length.

Application of equation (2.2) to a range of ceramic materials predicts strengths which are up to an order of magnitude too small. This is because apart from thermodynamic surface energy consideration, other mechanisms concurrent with crack extension that dissipate energy,

e.g. dislocation motion, cleavage step formation and subsidiary cracking are not accounted for.

In contemporary fracture mechanics of ceramics, Υ is not referred to as surface energy but as the material's fracture energy, which takes into account all energy contributions.

The modified Griffith equation which forms the basis of fracture mechanics can be written as[101]:

$$\sigma_f = \frac{1}{Y}\left(\frac{2E\Upsilon_i}{C}\right)^{\frac{1}{2}} \qquad \ldots\ldots (2.3)$$

where σ_f = fracture stress

Y = a constant related to the crack and specimen geometry

Υ_i = effective surface energy for fracture initiation

C = the size of the largest inherent surface flaw.

2.7.1 Grain size-strength relationship

Several empirical formulae have been derived to define the relationship between the strength of polycrystalline bodies and their average grain size. Orowan[102] was the first to suggest that the strength of a polycrystalline material is inversely proportional to one-half power of its mean grain diameter by this equation:

$$\sigma = Kd^{-\frac{1}{2}} \qquad \ldots\ldots (2.4)$$

where σ = strength of brittle polycrystalline material

d = mean grain diameter

K = empirical constant.

Petch[103] modified Orowan's concept somewhat and proposed that the relation between strength and grain size could be represented by the formula:

$$\sigma = \sigma_o + Kd^{-\frac{1}{2}} \qquad \ldots\ldots\ldots (2.5)$$

where σ_o and K are constants characteristic of the material. Knudsen[104] was one of the first to show very explicitly the dependence of strength on grain size by equation 2.6:

$$\sigma = Kd^{-a} \qquad \ldots\ldots\ldots (2.6)$$

This expression differs from that proposed by Orowan in that the value of the exponent of d is not a fixed value of $-\frac{1}{2}$ but apparently differs for different materials and perhaps also for different test methods. Recently, the dependence of strength upon (grain size)$^{-\frac{1}{2}}$ has been extensively reviewed by Rice[105]. More details about this relationship can be found elsewhere[1,106,107].

2.7.2 Porosity-strength relationship

Porosity is a phase almost always present in polycrystalline ceramics and it significantly affects the strength. Experimentally, it has been found that the strength of porous ceramics decreases in a way that is nearly exponential with porosity. Various specific analytical relationships have been suggested for the effect of porosity. An empirical relationship suggested by Ryskewitsch[108] is:

$$\sigma = \sigma_o \exp(-nP) \qquad \ldots\ldots\ldots (2.7)$$

where n ranges from 4 to 7 and where P is the volume fraction of porosity.

In a more extensive study, Coble and Kingery[109] studied porous polycrystalline aluminas measuring the strength as a function of porosity at several temperatures. Their results were fitted to an

empirical equation of the form:

$$0.6P = \exp. - [\sigma/8000(1-P)] \quad \ldots\ldots\ldots (2.8)$$

By incorporating both grain size (d) and porosity (P) effect on strength (σ), the relationship 2.9 was suggested[110]:

$$\sigma = Kd^{-a} \exp.(-bP) \quad \ldots\ldots\ldots (2.9)$$

where K, a and b are empirical constants.

Recently, Roy and Gouda[36,96,97] proposed that the relationship between strength and porosity in hot-pressed cement pastes can be expressed in the following form:

$$P = P_o \exp.(-KS) \quad \ldots\ldots\ldots (2.10)$$

where P = the porosity

P_o = porosity at zero strength

S = the compressive strength

K = an empirical constant.

Many other proposed relationships between strength and porosity can be found elsewhere.[1,105,108-111]

CHAPTER 3

EXPERIMENTAL TECHNIQUES

3.1 Preparation of Raw Materials

3.1.1 Calcium monoaluminate (CA) and calcium dialuminate (CA_2)

Pure calcium monoaluminate and calcium dialuminate were synthesised by grinding together stoichiometric proportions of analar calcium carbonate and aluminium oxide, in a rubber-lined mill charged with sintered alumina balls[43]. The ground mixtures were heated in re-crystallised alumina crucibles at 1500°C for 5 hours, in an automatically controlled gas furnace. The resulting sintered masses were then pulverised in a percussion mortar and finally ground in an alumina planetary ball-mill to -325 mesh. The mixture was heated again at the same temperature, for the same period, and checked by X-ray analysis. Heating was repeated until the X-ray powder pattern of the mixture was in full agreement with the lattice spacings of published data (A.S.T.M. card No. 1-0888 for CA and No. 7-82 for CA_2).

3.1.2 Calcium hexa-aluminate CA_6

Calcium hexa-aluminate was prepared from stoichiometric proportions of analar calcined alumina (-300 B.S. mesh) and calcium carbonate. These materials were thoroughly mixed in a mechanical agate mortar, pressed into pellets at ~ 80 MNm^{-2} with 5% starch solution and fired for 5 hours at 1500°C in an automatically controlled gas furnace in air[112]. The pellets were repeatedly fired, crushed, ground and examined by X-ray diffraction until no free corundum remained, and the pattern agreed with the published data for CA_6 (A.S.T.M. card No. 7-85).

Analar α-Al_2O_3 used in this study was supplied from B.D.H. Chemical Company, England.

Secar "250" cement used in this study was supplied from Lafarge Aluminous Cement Co. Ltd., England. All the prepared raw materials were kept in plastic bags and placed in tight metal tins.

The chemical analysis, surface area, and other physical properties of the starting materials are shown in Table 3.1.

Type of Analysis		CA	CA_2	CA_6	Secar 250 cement	Al_2O_3
Chemical analysis (XRF) (% w/w)	Al_2O_3	64.55	78.20	90.95	71.74	
	SiO_2	-	-	-	-	
	CaO	34.92	21.32	8.60	27.88	
	Fe_2O_3	-	-	-	0.10	
	FeO	-	-	-	-	
	MgO	0.30	0.22	0.12	0.22	
	TiO_2	-	-	-	-	
	Na_2O	0.22	0.20	0.18	0.42	
	K_2O	-	-	-	-	
	Total	99.99	99.94	99.85	100.36	
X-ray diffractometry		CA only	CA_2 only	CA_6 ~ 2% Al_2O_3	58% CA 42% CA_2	α-Al_2O_3 only
Specific surface area B.E.T. N_2 adsorption m^2gm^{-1}		0.57	0.619	0.734	0.676	1.47
Density g/cc		2.95	2.865	3.69	2.85	3.94

Table 3.1: Analysis of the Starting Materials

3.2 Bonding Agents

The phosphoric acid (H_3PO_4) used in this study was provided by B.D.H. Chemical Company, England. It was 85% concentrated with a specific gravity of 1.75 $gm.ml^2$.

Good quality cristobalite-type aluminum phosphate ($AlPO_4$) was prepared by heating precipitated anhydrous $AlPO_4$ (purchased from B.D.H.) at 1300°C for 90 hours[113].

Boric acid (H_3BO_3) was supplied by B.D.H. Chemical Company, England.

Boron phosphate (BPO_4) was prepared by drying a mixture of boric acid and phosphoric acid ($B_2O_3:P_2O_5 = 1$) at 80°C and then heating to 1000°C for 12 hours[67].

Chromium trioxide (CrO_3) was provided by B.D.H. Chemical Company, England.

Chromium phosphate, the α, β and amorphous forms, were provided by my supervisor, Dr. Corbridge[88].

3.3 Fabrication of Specimens

3.3.1 Room temperature fabrication

Cubes of side 12.7 mm made at room temperature were used in this study. When casting, sufficient material to fill eight cubes was mixed with the requisite quantity of water and bonding agent on a glass plate using a palette knife. The process was completed in about 5 minutes. The moulds were then loaded after lubrication (by Rocol, invisible film lubricant; Rocol House, Swillington, Leeds, England). Gentle tapping and a vibrating spatula (Spatula Vibrant Mettler LV2) were used to ensure that no air had been trapped inside the paste. Finally the surface of the mould was finished off with a palette knife. This process could be completed within 10 minutes. The samples were then set aside at room temperature for 24 hours, and then extracted from the moulds for heat treatment.

3.3.2 Hot pressing fabrication

3.3.2.1 The hot pressing equipment

The hot pressing equipment consisted of a hot pressing cell, hydraulic press with pump, pressure gauge and furnace.

(i) Hot pressing cell: Hot pressing was carried out in a die assembly consisting of two plungers (one 45 mm and the other 22 mm in length) made from Nimonic 115 alloy and a cylindrical die (internal diameter ~ 12.7 mm) made from Nimonic 105 alloy (Henry Wiggin Co., Hereford). The control thermocouple (Pt-Pt/13% Rh) was held horizontally by the furnace and rested in a hole drilled into the die, such that the thermocouple bead was only 10.2 mm from the edge of the specimen. To minimise die seizure on the plungers, there was 76 μm clearance between the plungers and the die.

(ii) Pressure equipment: A hand hydraulic pump was used to supply the pressure required to the press. Pressure was read from the gauge and was maintained constant during the course of a run by normal adjustment of the pump.

(iii) Furnace: Specimens were heated in an internally wound 'Kanthal' wire resistance tube furnace. The furnace was controlled by a Eurotherm Thyristor Controller (Model PID/SCR/25A/240V/0-1600°C/Pt-Pt 13% Rh) and a heating rate of ~ 30°C min^{-1} was used up to the required temperature and hold for the required time. The temperature could be obtained from the dial of the furnace controller and was found by potentiometer to be accurate to ± 5°C. The hot pressing apparatus is shown diagrammatically in Figure 3.1.

3.3.2.2 Sample preparation

A constant weight of the powder material, a constant w/s ratio with the chosen percent from the selected bonding agent was mixed with the aid

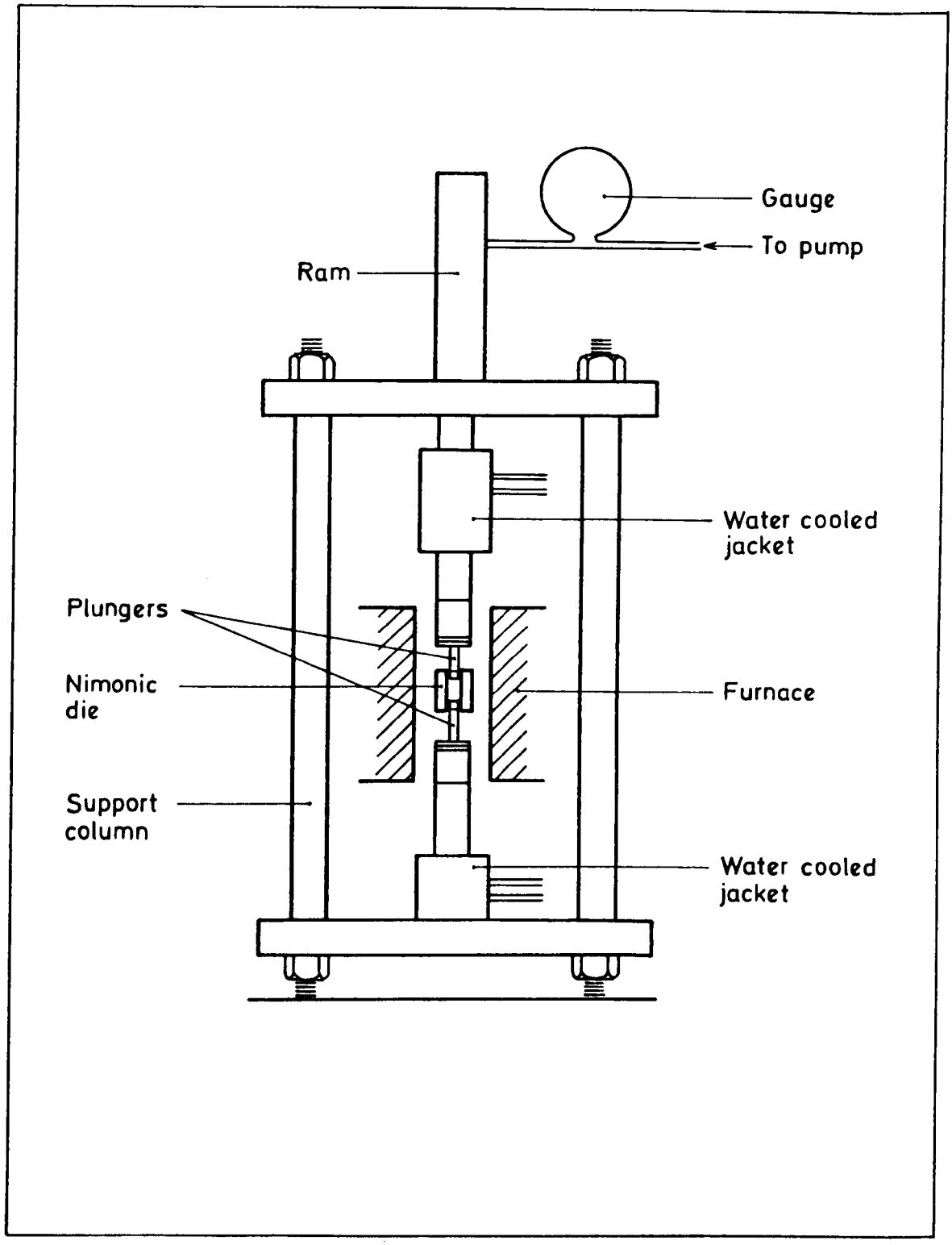

FIG. 3.1: The Hot-Pressing Equipment, Schematic

of a trowel on a glass plate for three minutes. Then the paste was transferred to the hot pressing cell. Before each run, the plungers and inner surface of the die were coated with graphite to act as a lubricant (Dag colloidal graphite in alcohol, Acheson Colloids Ltd., Plymouth). Then the cell was transferred inside the furnace where the longer plunger stood on the lower pedestal, the die being supported only by frictional forces from the specimen. The specimen was compressed by the action of the upper ram upon the smaller plunger. The thermal expansion of Nimonic alloy is larger compared to most ceramic materials. Therefore to avoid jamming of specimens during cooling, specimens which heated up to 600 and 700°C were extracted at high temperatures (500 and 600°C). To extract the sample, the pressure was released and the ram was raised. The extractor ring was then placed on top of the die and the pressure reapplied; the extractor ring pushing the die down leaving the specimen free. The final specimen was either a cylinder ($\sim$12.5 mm diameter x 15-18 mm high) or a disc having diameter $\sim$12.5 mm and thickness 6-8 mm.

3.3.3 Heat treatment of the samples

All the samples which were fabricated at room temperature and some from those fabricated under hot pressing conditions(under 207 MNm^{-2} pressure at 300°C for 30 minutes) were subjected to heat treatment. Heating was carried out for different times at different temperatures up to 1300°C in thermostatically controlled electric muffle furnace under ambient conditions. After heating samples were allowed to cool down naturally in the furnace to room temperature.

3.3.4 Curing of the samples

Some of the hot-pressed samples were cured immediately after removal from the cell in 100% relative humidity and at the same room temperature for 24 hours. The specimens were immersed in water after this time until

the time of testing. Samples of 24 hours were tested directly after removal from the moist closet and without immersing in water.

3.4 Methods of Strength Measurements

3.4.1 Compressive strength

Specimens used for measuring compressive strength were cubes of side 12.7 mm, fabricated at room temperature, and cylinders of diameter 12.7 mm and height 15-18 mm fabricated by hot pressing. The surfaces of the specimens were carefully polished on fine sand paper in order to remove irregularities. The dimensions of the specimen were determined using a micrometer screw gauge. To help transmit the load to the specimen faces uniform pieces of cardboard about 0.1 mm thick were used at both faces. The compressive load was determined on an Avery-Denison testing machine (Civil Engineering Department, Leeds University) using a loading rate of 3 KN/min. The compressive strength was estimated from:

$$\sigma_c = P/A \qquad \ldots\ldots\ldots (3.1)$$

where σ_c = compressive strength MN/m^2, P = the load at which failure occurs, N, and A = the nominal area of the specimen, mm^2.

3.4.2 Indirect tensile strength

For those specimens which were in the form of small discs (12.5 mm diameter and 6-8 mm thickness) obtained by hot pressing, measurement of flexural strength would have necessitated cutting out and testing very small bars. To avoid these problems the "diametral compression test" was adopted. In this test the solid disc is compressed along a diameter between two platens. The compression induces a uniform tensile stress field perpendicular to the loaded diameter[114]. At the lines of application of the load, highly localised stress concentrations can occur unless pieces of low elastic modulus material are interposed between platen and specimen. Failure of specimen is in tension and the

indirect tensile strength of the specimen was computed from the following relation:

$$\sigma = \frac{2P}{\pi Dt} \qquad \ldots\ldots (3.2)$$

where σ = indirect tensile strength, MN/m^2

P = load at which failure occurred, N

D = diameter of the specimen, mm

t = thickness of the specimen, mm.

The tensile strength values reported are the averages of three test specimens. Where individual values deviated more than 10% from the average of the three measurements, the average of the remaining two values was reported.

To apply the compression, the disc specimen was placed in a compression cage, previously used by Briggs[115], using bench model 1026 Instron tensile machine. The slowest possible strain rate (corresponding to a crosshead speed of .5 mm min^{-1}) was used. Cardboard of thickness 0.1mm was interposed between specimen and platen to reduce the high localised stresses which occur there. This method was shown by Spriggs et al.[116] and by Griob et al.[117] to give strength values about half those obtained in four-point bending. Spriggs et al.[116] also found that the results obtained from the diametral compression test were similar to those obtained from direct tension.

3.5 X-ray Diffraction Procedure

3.5.1 Identification of crystal phases

The crystalline phases present in the specimens were identified using an X-ray diffraction technique. Nickel-filtered CuKα radiation (λ = 1.5405 Å) at 40 KV 20 mA was used throughout in a Philips PW1310 diffractometer. The specimen was crushed with a percussion mortar and hand ground for 10 minutes after sieving through 320 mesh. Rectangular

type specimen holder made of aluminum 2 mm thick was used to pack ~ 0.2g of sample. Scanning speeds 1° 2θ/min. were used in routine work, using time constant 2 seconds and chart speed 2 cm/min. The full scale deflection was set to 400 cps, scatter and receiving slit widths of 1° and a focus slit width 0.1° was constant in all the work.

Alignment of the goniometer was checked by comparing the pattern of a standard silicon specimen with the known tabulated line positions. There was no detectable difference between the two.

3.5.2 Quantitative analysis

Quantitative analysis of some crystalline phases in the mixture was adopted using direct comparison method[118]. In this method it is necessary to have a standard crystalline sample, and in some cases a series of pure reference crystalline samples are needed[119]. In choosing diffraction lines to measure, the overlapping or closely adjacent lines from different phases should be avoided. Therefore, this method depends on comparing the intensity of a diffracted ray of the required phase in a mixture by the intensity of the same diffracted ray in the standard sample. In order to get the "correct count" the background scattering was subtracted from the peak scattering, either in the mixture or in the standard sample[120]. .2 g of the powder sample was charged into the sample holder which has a cover glass plate at the bottom, and compacted as strongly as possible by using fingers. The bottom cover plate was then taken off and the original bottom surface of the compacted sample was then exposed to the X-ray beam instead of the upper surface. By using this technique the experimental error due to variations in surface smoothness, sample compactness and the level of the sample to be exposed could be effectively reduced. The more detailed conditions for the measurements were given above in the relevant section, except that scanning speed used was ¼° 2θ/min.

The accuracy of this method was checked with a set of samples mechanical mixtures, containing known weights of different phases. There was a good agreement between the results and the known compositions.

3.6 Scanning Electron Microscopy

Scanning electron microscopy was used in the course of this work. The electron microscope used in the present work was a Cambridge S600 Stereoscan operated at 30 KVA and 45° for tilted angle. The fracture surfaces after the mechanical strength test were examined by this technique. These samples were prepared by gluing the specimen onto an aluminium holder with bostik adhesive and sputtering on a 10 nm thick gold/palladium coating, to form a conducting film so as to prevent charging.

3.7 Density measurements

Bulk density was calculated by weighing the samples and measuring their dimensions with a micrometer. Density measuredments were checked with a mercury densitometer (Doulton Research Ltd.). The agreement between the two methods was to within $\pm$ .01 gm/cc.

True density was determined by pyknometer method (details in B.S. 1902 Part 1A, 1966), using paraffin oil instead of distilled water.

The porosities were calculated from the densities using the following expression:

$$p = \frac{\rho_T - \rho_B}{\rho_T} \times 100\% \qquad \ldots\ldots\ldots (3.3)$$

where p = porosity

ρ_T = true density and ρ_B is the bulk density.

3.8 Differential Thermal Analysis

The DTA technique is designed so as to detect any thermal changes accompanying chemical or structural transformations during the heating of a particular material. The DTA apparatus consists of a specially designed sample holder which has two compartments; in one is placed the sample and in the other a thermally inert material. The sample holder is heated up at a constant rate, and the temperature difference between the two samples is monitored by means of opposing thermocouples. The actual temperature of the inert material is also monitored by a thermocouple. When a transformation in the sample occurs, which causes liberation or absorption of heat, then the temperature difference between the sample and the inert material will change. Therefore a plot of temperature difference against inert temperature will show a peak.

Differential thermal analysis apparatus 673-4 (Stanton Redcroft Ltd.) using a potentiometric recorder RE 571.20 was used in this study. A Pt-Pt/13% Rh thermocouple assembly was used with a high gain, low noise, low drift DC amplifier. Calcined alumina was used as inert material. A sample of 100 mg (-53μ m) was housed in a dimped platinum-rhodium crucible using standard procedure for packing. The heating and cooling rates in all the experiments were 10^{o}C/min.

The calculation of the heat of reaction (ΔH) was carried out also on some experiments; calibration of the apparatus is given in Appendix 1.

3.9 Chemical Analysis

The major elements, CaO, Al_2O_3, SiO_2, MgO, Na_2O and K_2O, of some samples were quantitatively analysed with a Philips 12/2 automatic X-ray fluorescence spectrometer using a fused disc method. The flux for fusion of samples was used in the following proportions:

Powder sample = 0.56 g
Spectroflux 110 (lithium tetraborate) = 2.24 g

The sample and flux were weighed in a platinum crucible, then fused initially in an electric muffle furnace at 1000°C for 20 mins., then again for 10 mins. on a gas burner. The hot melt was agitated with a platinum wire, then cast and pressed into a circular disc of 30 mm in diameter and 1 mm in thickness by using a copper wire ring on a steel plate. The disc was analysed for the above major elements using an Ag X-ray tube under conditions of 36 KV 44 mA. The analytical crystal was "ThAP". Using standard discs all the calibrations and corrections were automatically processed by a computer programme which was available.

3.10 Infrared Absorption Spectroscopy

The characteristic IRS of any material can serve as a basis for qualitative and quantitative analysis. An infrared spectrophotometer, model SP1100 (made by Unicam, England) was used in this study in the range from 4000-400 cm^{-1} (25 - 2.5 micron). The potassium bromide pellet method was used[121]. Before measurement, potassium bromide and the samples were freed from the adsorbed water by drying at 110°C overnight. Two mg of the sample ($\sim < 2\mu$) was mixed with 1 g of potassium bromide in an automatic agate mortar for 10 minutes. A constant weight, 200 mg, of the mixture was pressed in pellet die under vacuum using 8 ton pressure for about 5 minutes, to give a transparent disc (13 mm diameter x 0.5 mm thickness). The pellets after fabrication were kept in plastic bags inside a desiccator to preserve them from any moisture.

CHAPTER 4

PHOSPHORIC ACID AND PREFABRICATED ALUMINUM PHOSPHATE ADDITIVES

4.1 Phosphoric Acid

Phosphoric acid (85%) was used as a bonding agent, and mixed with different weight ratios of α-Al_2O_3, CA_6, CA_2, CA and the commercial material Secar "250" Cement. Room temperature casting followed by firing at different temperatures up to 1300°C for 24 hours and hot pressing technique (under 207 MNm^{-2} pressure, for 30 minutes in the range 50 - 700°C) were applied. In addition, samples prepared under hot-pressing conditions (207 MNm^{-2} pressure, at 300°C for 30 minutes) were also fired in air for 24 hours in the range 300-1300°C.

4.1.1 Results

4.1.1.1 α-Al_2O_3 + H_3PO_4

(a) Samples cast at room temperature, followed by firing

The same procedures previously described (Sections 3.3.1 and 3.3.3) were followed to mix and fire α-Al_2O_3 with 5 and 10 wt% H_3PO_4 using 0.25 w/s ratio.

D.T.A., Fig. 4.1, and Table 4.1 show that this reaction produced an endothermic peak at ~230°C and three exothermic peaks at approximately 660, 747 and 1045°C.

X-ray analyses show that the process involved first the formation of the type $Al(H_2PO_4)_3$. However, on subsequent heating the final bonding phase was almost entirely aluminum phosphate, $AlPO_4$. X-ray diffraction patterns, Fig. 4.2, show that $AlPO_4$ (tridymite form) was detected in those samples fired at 900°C for 24 hours. On the other hand, $AlPO_4$ (cristobalite form) was found in samples fired at higher temperatures (i.e. 1200 and 1300°C).

Cold crushing strengths of these mixes were measured, and dependence

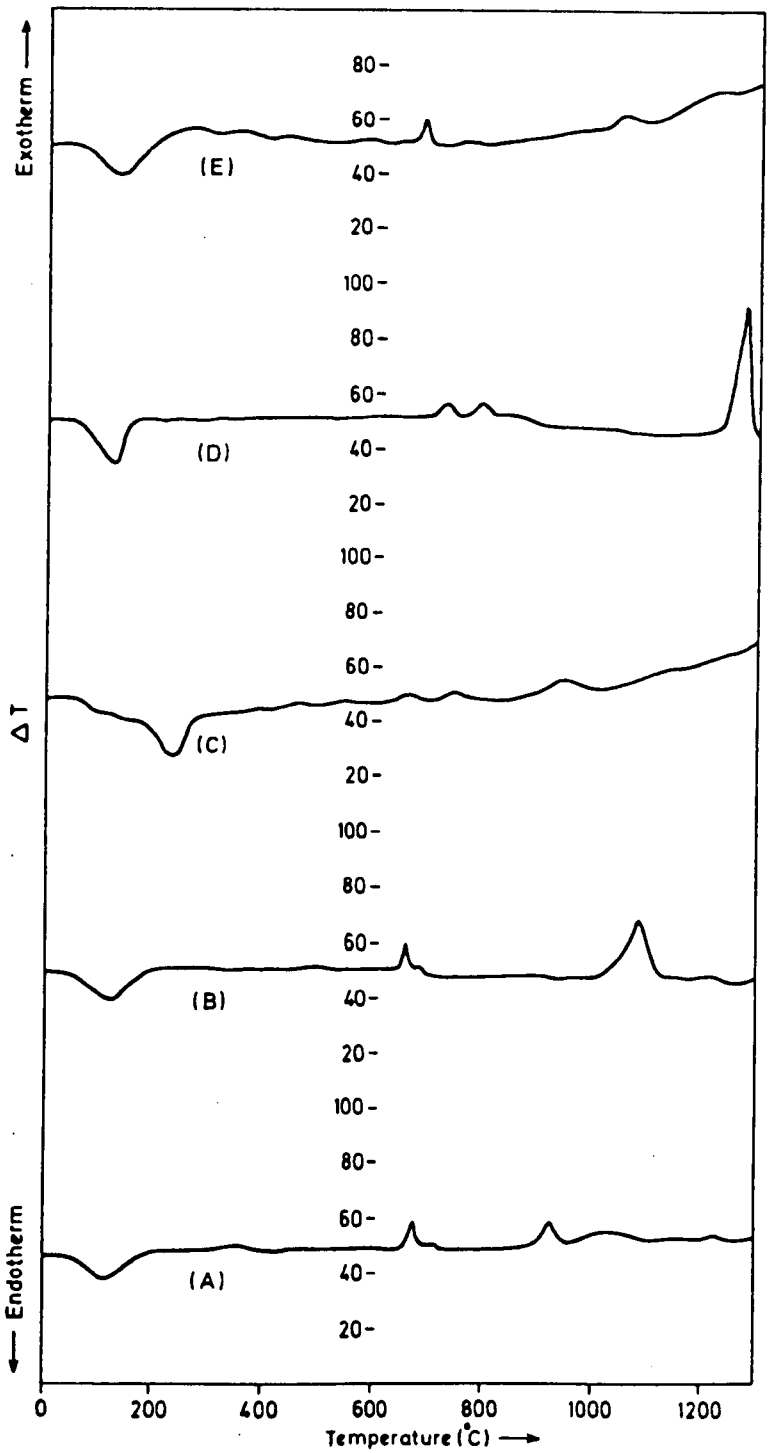

Fig. 4.1: D.T.A. traces of (A) CA + 10% H_3PO_4, (B) CA_2 + 10% H_3PO_4, (C) Secar "250" + 10% H_3PO_4, (D) CA_6 + 10% H_3PO_4, (E) α-Al_2O_3 + 10% H_3PO_4.

Mixture	Exothermic Reaction			ΔT °C	Peak Area (A) deg.S.mg^{-1}	Coefficient const. (K) x10^{-3} cal/deg.S	ΔH cal/mg (x10^{-3})
	Start °C	Peak °C	End °C				
α-Al_2O_3 + 10% H_3PO_4	628	660	692	.04	.096	9.826	-.9439
	713	750	788	.08	.192	-	-
	1015	1045	1082	.06	.147	-	-
CA_6 + 10% H_3PO_4	701	726	751	.10	.160	9.826	-1.572
	767	792	812	.09	.185	7.73	-0.6957
	1234	1271	1305	1.26	2.64	-	-
CA_2 + 10% H_3PO_4	645	656	671	.258	.252	9.826	-2.476
	671	682	701	-	-	-	-
	1016	1080	1123	.336	1.31	-	-
CA + 10% H_3PO_4	658	675	713	.337	.39	9.826	-3.84
	910	925	970	.2025	.486	9.84	-4.78
Secar "250" + 10% H_3PO_4	673	692	712	.225	.3375	9.826	-.3316
	1015	1048	1089	.072	.189	-	-

Table 4.1: Summary of D.T.A. results of α-Al_2O_3, CA_6, CA_2, CA and Secar "250" + 10% H_3PO_4.

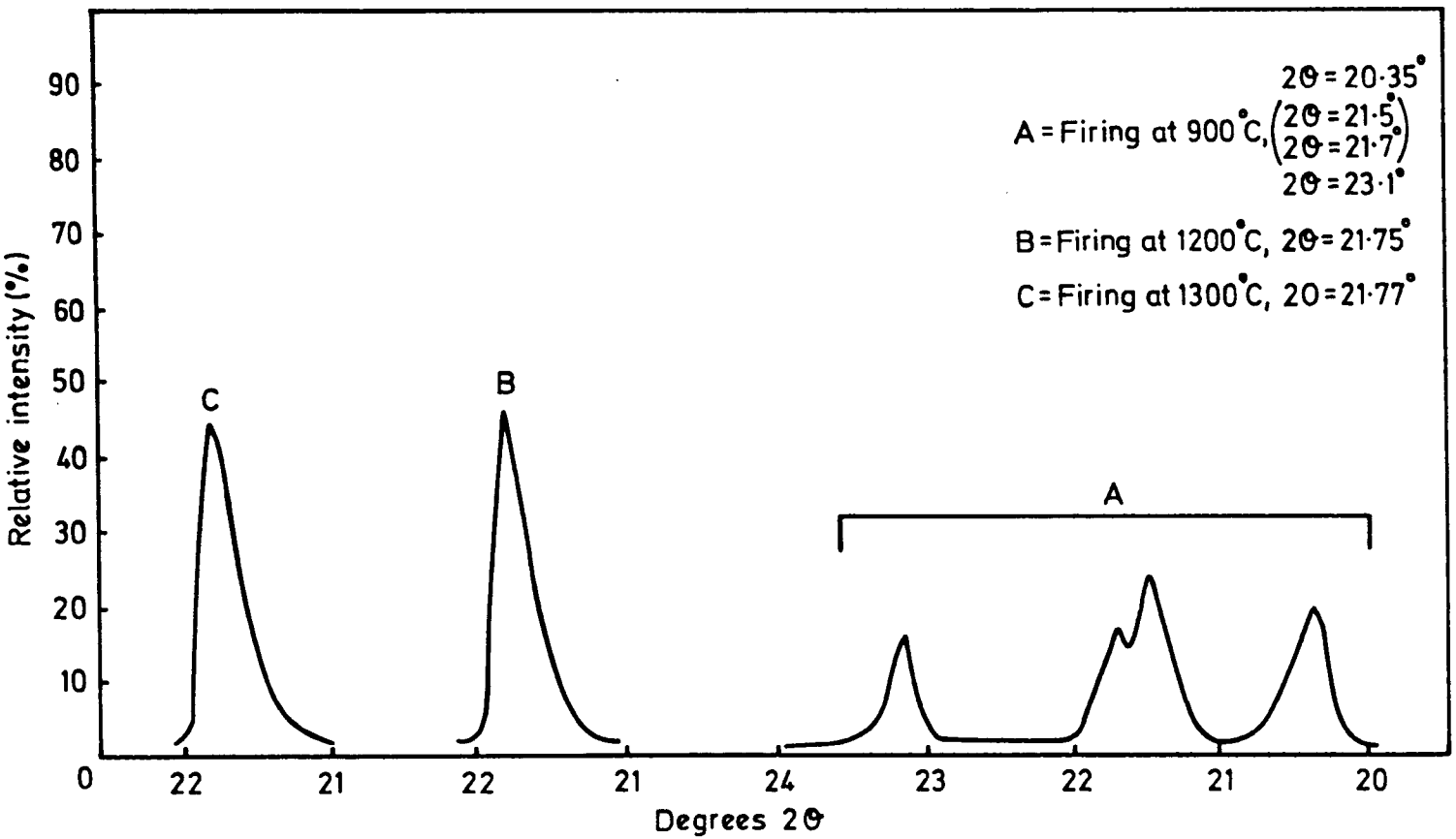

Fig. 4.2: X-ray diffractometer traces for the composition α-Al_2O_3 + 10% H_3PO_4, room temperature casting, fired at different temperatures, near the 2θ values corresponding to the main tridymite and cristobalite peaks of $AlPO_4$.

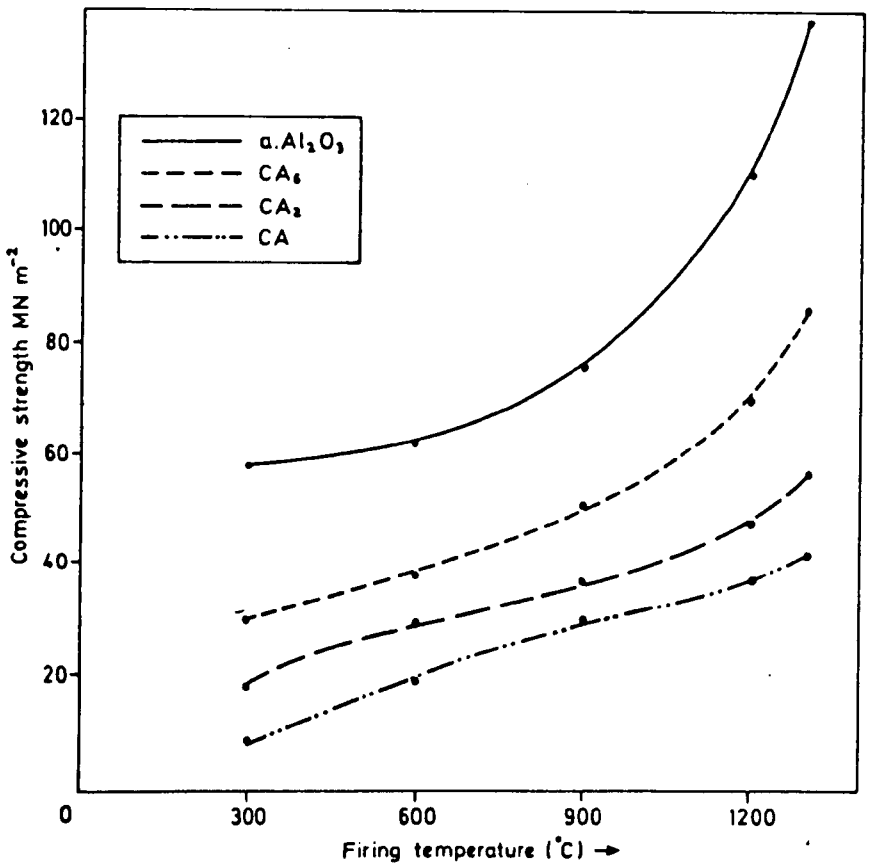

Fig. 4.3: Dependence of strength upon firing temperatures. Samples mixed with 10% H_3PO_4, cast at room temperature, fired for 24 hours.

Firing Temp. °C	α-Al_2O_3 + 5% H_3PO_4				α-Al_2O_3 + 10% H_3PO_4			
	B.D. g.cc	Porosity (%)	$AlPO_4$ (%)	Comp.St. MNm^{-2}	B.D. g.cc	Porosity (%)	$AlPO_4$ (%)	Comp.St. MNm^{-2}
300	2.22	41.5	-	27.73	2.32	38.9	-	58.9
600	2.21	41.84	2.78	34.15	2.305	39.34	3.16	62.17
900	2.23	41.3	3.81	55.3	2.327	38.8	5.55	76.00
1200	2.38	37.4	5.9	91.2	2.509	33.9	10.64	110.34
1300	2.62	31	4.87	95.87	2.70	30.95	12.78	138.56

B.D. = Bulk density; Comp.St. = Compressive strength.

Table 4.2: Compressive strength, density, porosity (%) and the percentage of aluminium phosphate in the mixtures α-Al_2O_3 + 5 and 10% H_3PO_4, fired at different temperatures for 24 hours.

of strength upon firing temperatures is shown in Fig. 4.3. Quantitative analysis of the percentage of anhydrous $AlPO_4$ formed *in situ* after firing at different temperatures, density, porosity, and cold crushing strength are given in Table 4.2.

(b) Hot-Pressing

A combination of 10 wt% phosphoric acid and 90 wt% of α-Al_2O_3 was mixed using .08 w/s ratio. Preparation of the samples was carried out as previously described (Section 3.3.2.2). Hot-pressing of this mixture was carried out under constant pressure (207 MNm^{-2}) for constant time (30 minutes) over a wide range of temperatures (50 - 700°C). In addition, some samples were prepared under hot-pressing conditions (207 MNm^{-2} pressure, at 300°C for 30 minutes), followed by firing in air between 300-1300°C for 24 hours.

X-ray analysis showed that variscite, $AlPO_4.2H_2O$, was formed as a direct reaction between alumina and phosphoric acid under hot-pressing conditions at about 50°C. By increasing hot-pressing temperature to 100°C a noticeable increase in the variscite peaks occurred. After hot-pressing at 200°C, a strong peak representing anhydrous $AlPO_4$ (cristobalite form) at $2\theta = 21.75^\circ$ appeared, as shown in Fig. 4.4. After hot-pressing at 300°C, two peaks appeared at $2\theta = 21.62^\circ$ and 21.5°. On further increasing the hot-pressing temperature to 400, 500, 600 and 700°C under the same conditions, the peak $2\theta = 21.5^\circ$ was predominating. These results can be shown in Fig. 4.5. The I.R. spectra are given in Fig. 4.6.

The other group of samples which were fired in air (in the range 300-1300°C, for 24 hours) after hot-pressing (207 MNm^{-2} pressure, at 300°C for 30 minutes) were also examined by XRD and I.R. After firing at 300°C, two strong peaks representing $AlPO_4$ were detected at $2\theta = 21.43^\circ$ and 21.68°. After firing at 600°C, the peak which was at $2\theta = 21.43^\circ$ increased, whereas the intensity of the other peak at $2\theta = 21.68^\circ$

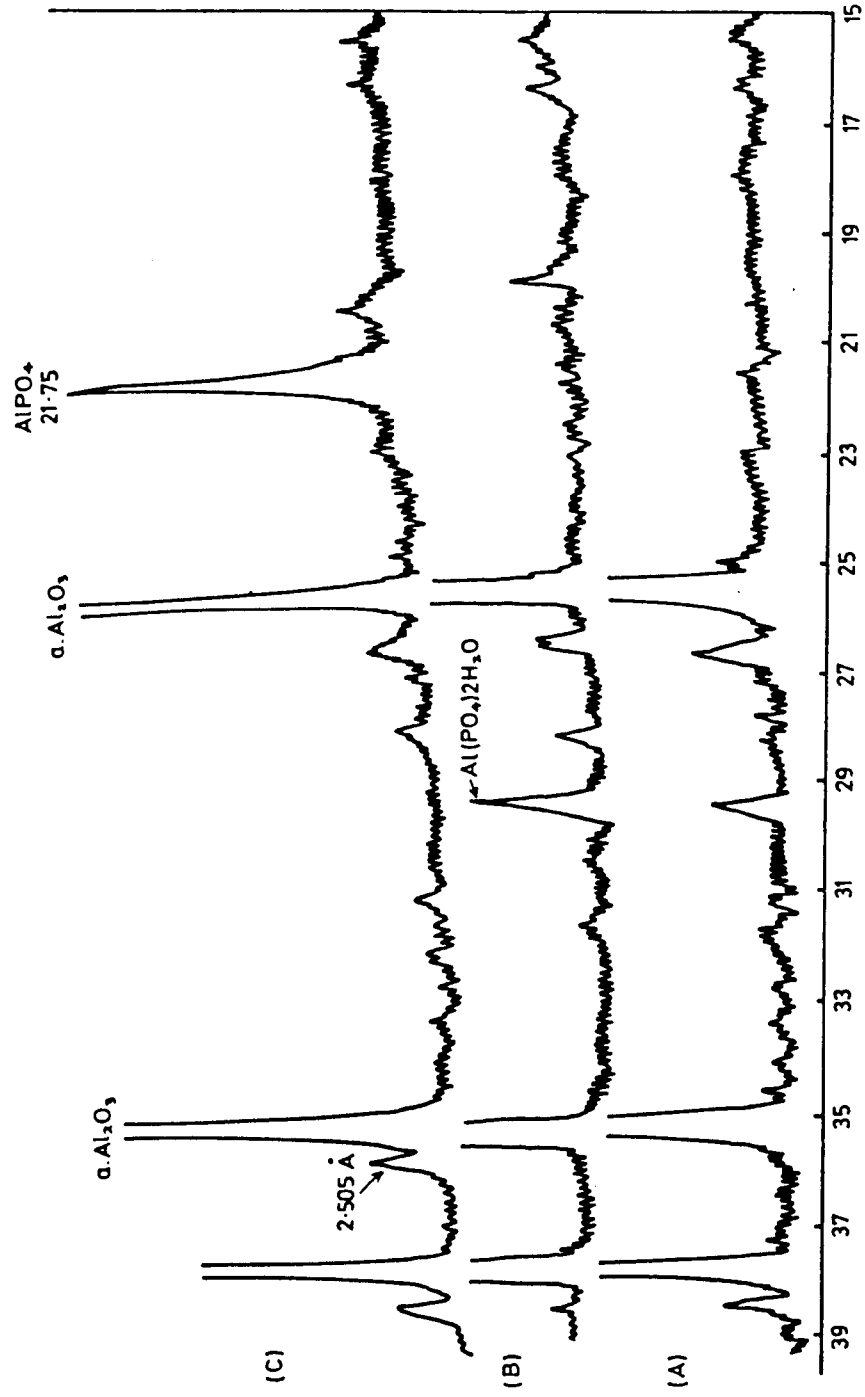

Fig. 4.4: X-ray diffractometer traces of the mixture α-Al_2O_3 + 10% H_3PO_4, hot-pressed at (A) 50°C, (B) 100°C, (C) 200°C, under 207 MNm^{-2} pressure for 30 minutes.

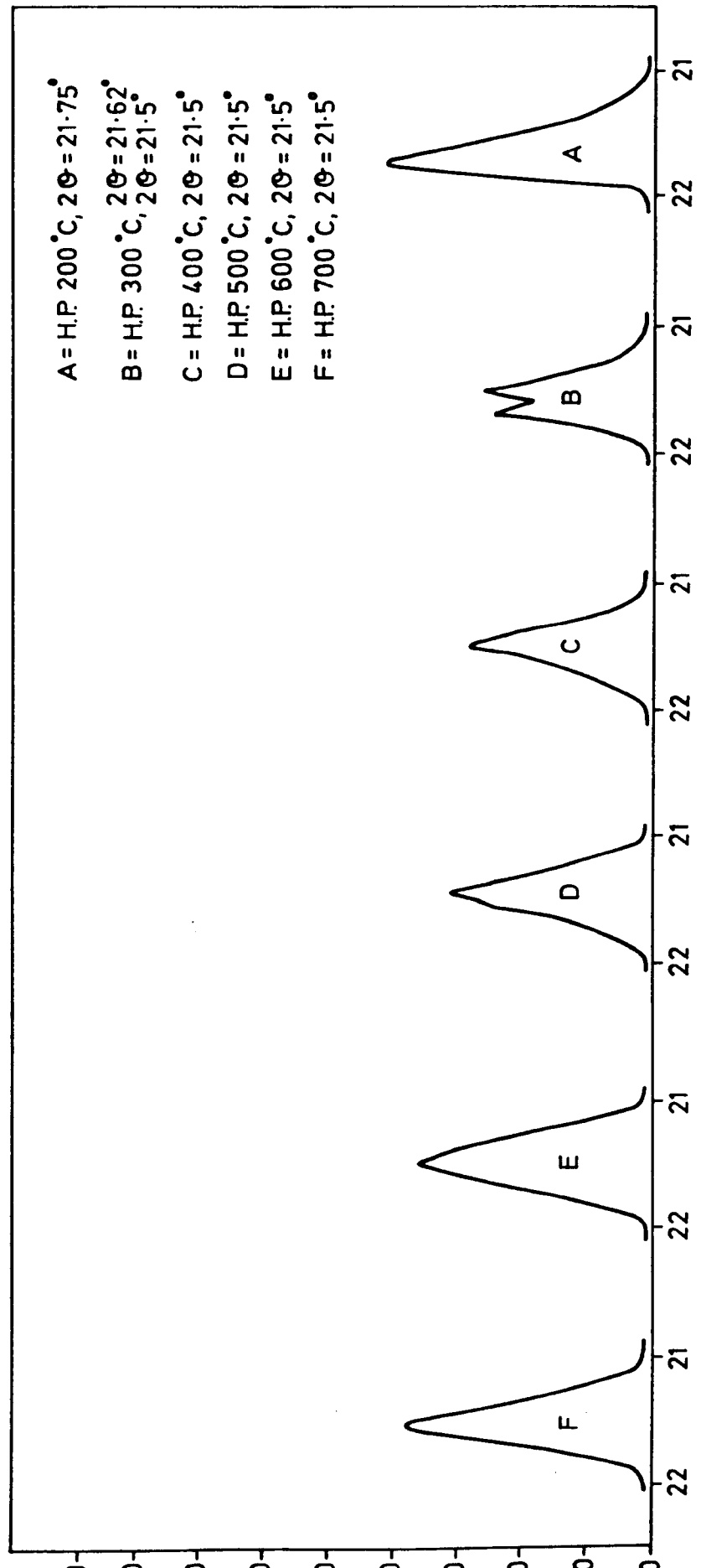

Fig. 4.5: X-ray diffractometer traces of the mixture α-Al_2O_3 + 10% H_3PO_4 hot-pressed at different temperatures, under 207 MNm^{-2} pressure, for 30 minutes. Traces near the 2θ value corresponding to the main peak of tridymite and cristobalite forms of $AlPO_4$.

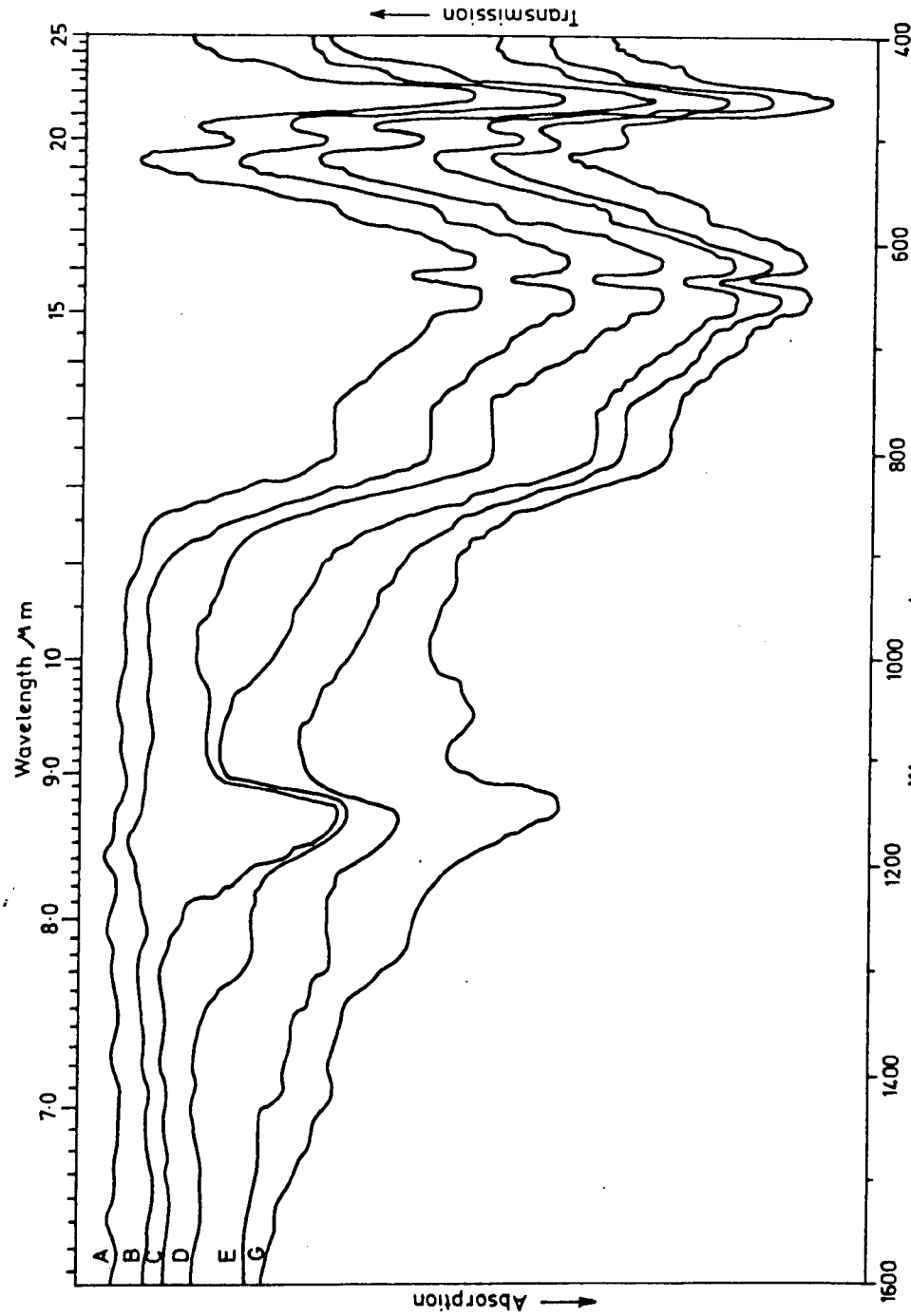

Fig. 4.6: Infra-red spectra of α-Al_2O_3 mixed with 10 wt% H_3PO_4 and hot pressed at (A) 50°C, (B) 100°C, (C) 200°C, (D) 300°C, (E) 500°C, (G) 700°C, under 207 MNm^{-2} pressure, for 30 minutes.

decreased and shifted to $2\theta = 21.65^{\circ}$. After firing at 900°C, the only peak which appeared was at $2\theta = 21.44^{\circ}$, and firing at 1200°C showed a small increase in intensity and a shift to $2\theta = 21.495^{\circ}$. At the same time, a small peak appeared at $2\theta = 21.65^{\circ}$. Finally, firing at 1300°C showed no change in the positions of the previous peaks, and only a small increase in the intensity of the peak $2\theta = 21.65^{\circ}$. These changes are given in Fig. 4.7. The I.R. spectra are shown in Fig. 4.8.

Dependence of strength upon hot-pressing temperature is shown in Fig. 4.9 and Table 4.3. Changes in the microstructure with hot-pressing temperatures and firing temperatures are shown in Figs. 4.10 and 4.11. The relationships between strengths and firing temperatures are given in Figs. 4.12 and 4.13. The mechanical properties and related physical properties are given in Table 4.4.

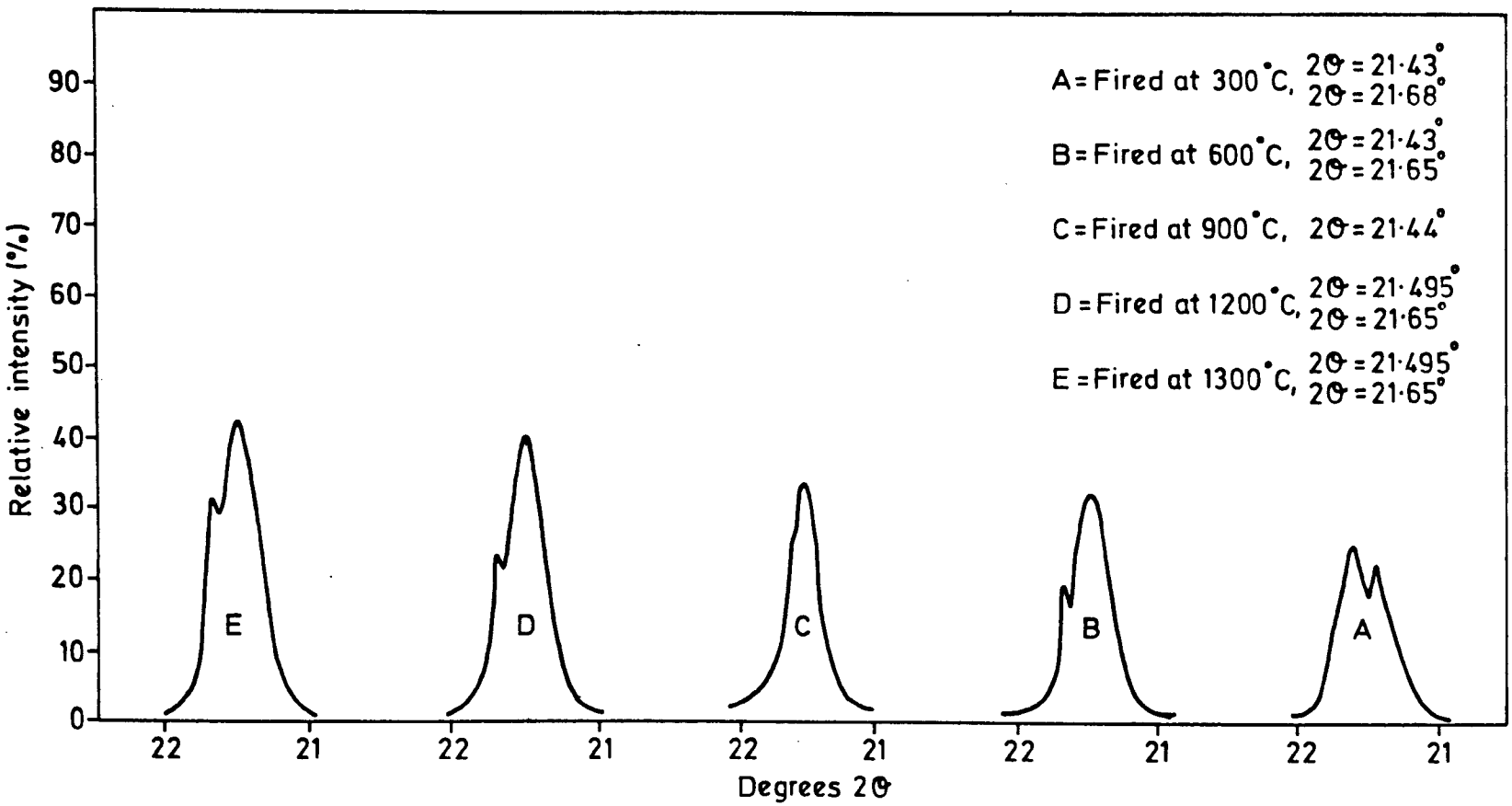

Fig. 4.7: X-ray diffractometer traces for the composition α-Al_2O_3 + 10% H_3PO_4, hot-pressed under 207 MNm^{-2} pressure, at 300°C, for 30 minutes, and fired at various temperatures. Traces near the 2θ value corresponding to main peak of tridymite and cristobalite forms of $AlPO_4$.

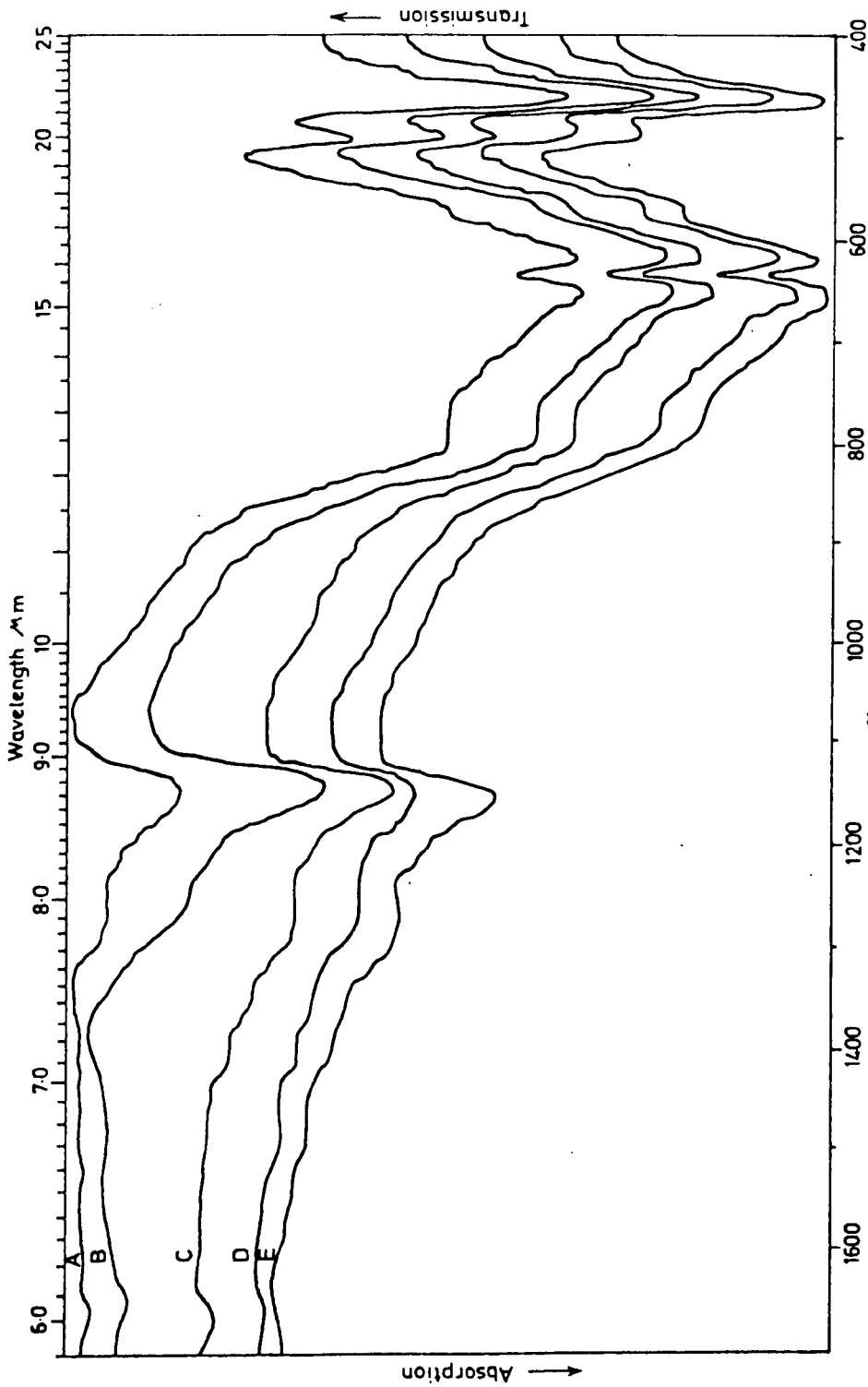

Fig. 4.8: Infra-red spectra of the mixture α-Al_2O_3 + 10% H_4PO_4, hot-pressed under 207 MNm^{-2} pressure, at 300°C for 30 minutes, then fired at (A) 300°C, (B) 600°C, (C) 900°C, (D) 1200°C, (E) 1300°C.

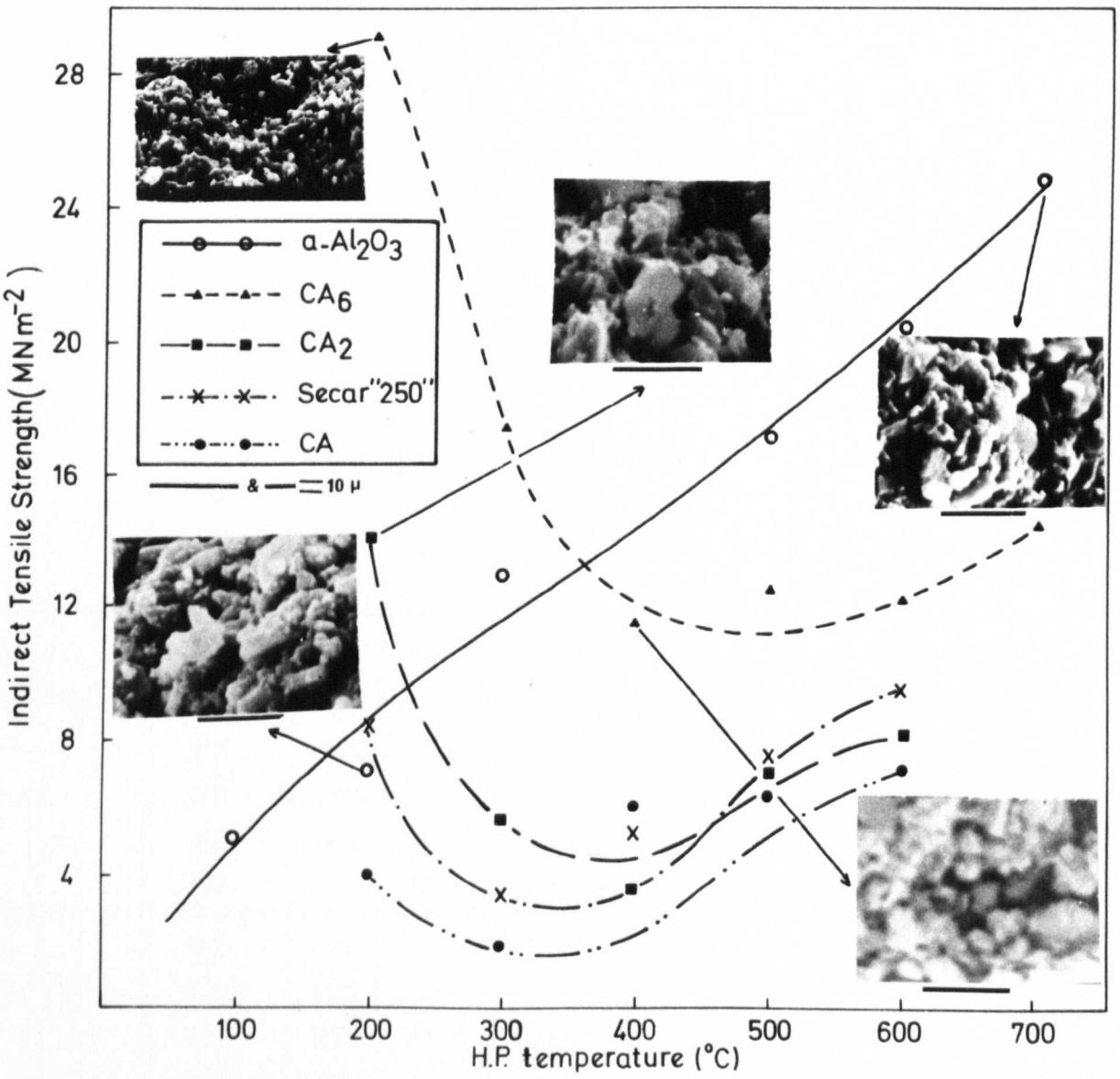

Fig. 4·9 Dependence of strength of α-Al_2O_3, CA_6, CA_2, CA and Secar '250' cement mixed with 10% H_3PO_4 upon H.P. temperature.

Mixture	Hot-pressing parameters			w/s ratio	Density g.cc	Indirect tensile strength (MNm^{-2})	Porosity (%)
	Pressure (MNm^{-2})	Temp. (°C)	Time (min)				
α -Al_2O_3 + 10% H_3PO_4	207	50	30	.08	2.78	2.72	27.72
	207	100	30	.08	2.787	5.35	27.60
	207	200	30	.08	2.774	6.94	27.8
	207	300	30	.08	2.814	12.94	26.9
	207	400	30	.08	2.827	14.58	26.57
	207	500	30	.08	2.84	17.3	26.3
	207	600	30	.08	2.85	20.56	26.06
	207	700	30	.08	2.885	25.58	25.26
CA_6 + 10% H_3PO_4	207	200	30	.08	2.783	29.5	24.58
	207	300	30	.08	2.67	17.8	27.69
	207	400	30	.08	2.59	11.52	29.86
	207	500	30	.08	2.57	12.7	30.41
	207	600	30	.08	2.565	12.00	30.5
	207	700	30	.08	2.603	14.3	29.46
CA_2 + 10% H_3PO_4	207	200	30	.08	2.158	14.00	24.68
	207	300	30	.08	2.0886	5.8	27.1
	207	400	30	.08	2.09	6.13	27.00
	207	500	30	.08	2.094	6.37	26.91
	207	600	30	.08	2.09	8.2	27.00
	207	700	30	.08	2.054	4.1	28.30
CA + 10% H_3PO_4	207	200	30	.08	2.0706	4.00	29.81
	207	300	30	.08	2.050	2.11	30.50
	207	400	30	.08	2.115	5.8	28.3
	207	500	30	.08	2.119	6.34	28.17
	207	600	30	.08	2.124	7.12	28.00
	207	700	30	.08	2.08	5.5	29.49
Secar "250" + 10% H_3PO_4	207	200	30	.08	2.093	8.43	26.56
	207	300	30	.08	2.0693	3.39	27.39
	207	400	30	.08	2.054	5.1	27.9
	207	500	30	.08	2.0976	7.72	26.4
	207	600	30	.08	2.129	9.4	25.29
	207	700	30	.08	2.0437	4.3	28.17

Table 4.3: Mechanical properties and related physical properties of α-Al_2O_3, CA_6, CA_2, CA and Secar "250" cement, mixed with 10% H_3PO_4, hot-pressed under constant pressure (207 MNm^{-2}) for constant time (30 mins.) at different temperatures.

Fig. 4.10

SEM Micrographs of α-Al_2O_3 mixed with 10% H_3PO_4, hot-pressed under 207 MNm^{-2} pressure for 30 minutes at:

(a) 100°C

(b) 200°C

(c) 300°C

(d) 700°C

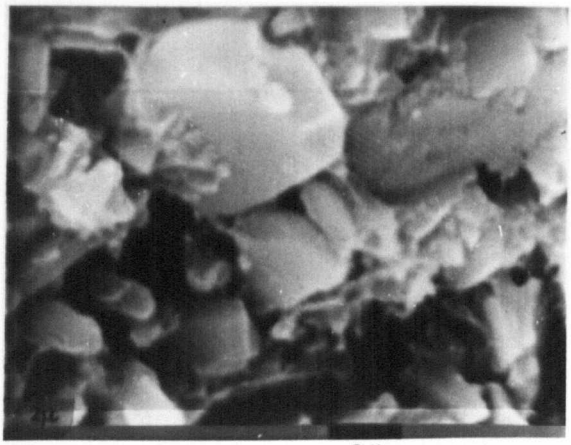

2 μ

a

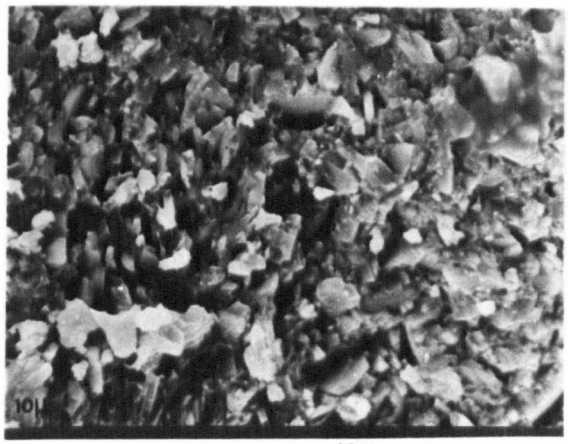

10 μ

a

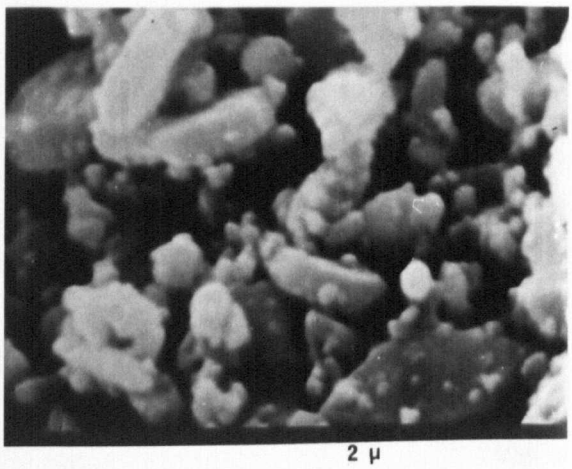

2 μ

b

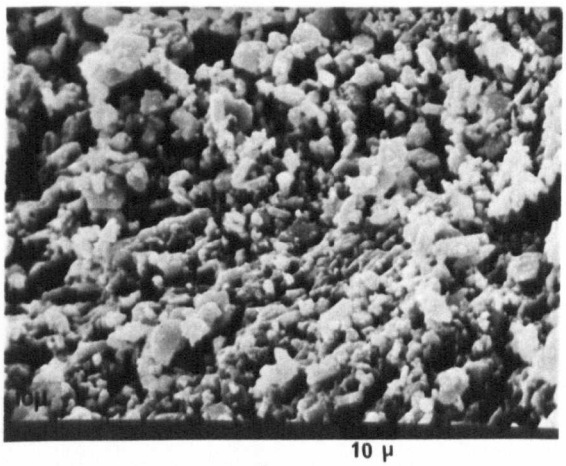

10 μ

b

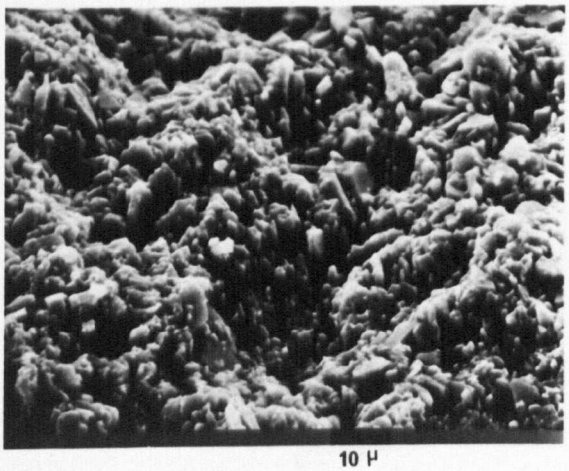

10 μ

d

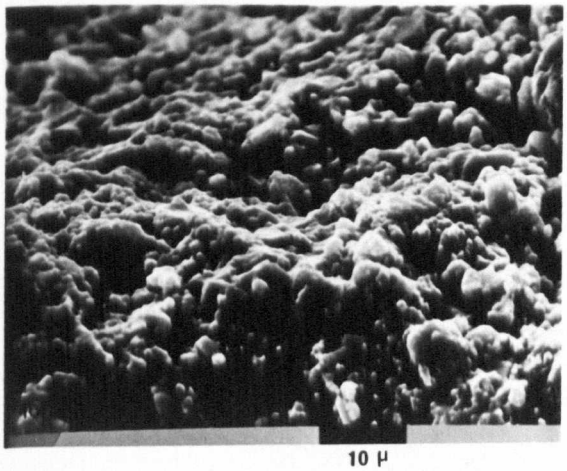

10 μ

c

Fig. 4.11A

S.E.M. Micrographs of α-Al_2O_3 mixed with 10% H_3PO_4, room temperature casting, fired at 1300°C for 24 hours.

Fig. 4.11B

S.E.M. Micrographs of α-Al_2O_3 mixed with 10% H_3PO_4, hot-pressed under 207 MNm^{-2} pressure for 30 minutes at 300°C, fired at 1300°C for 24 hours.

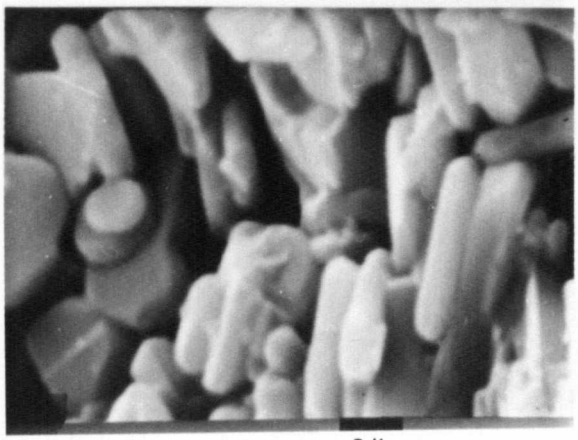

2 μ

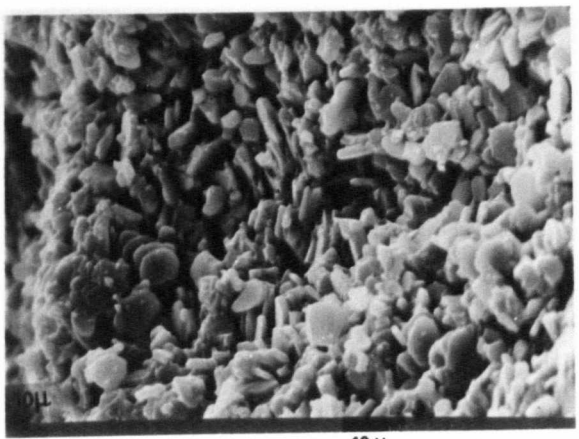

10 μ

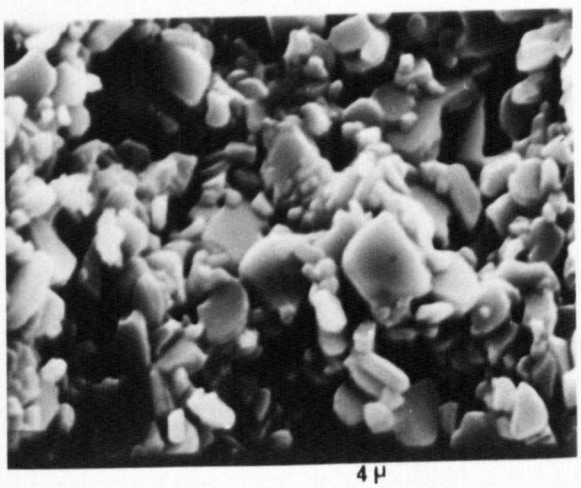

4 μ

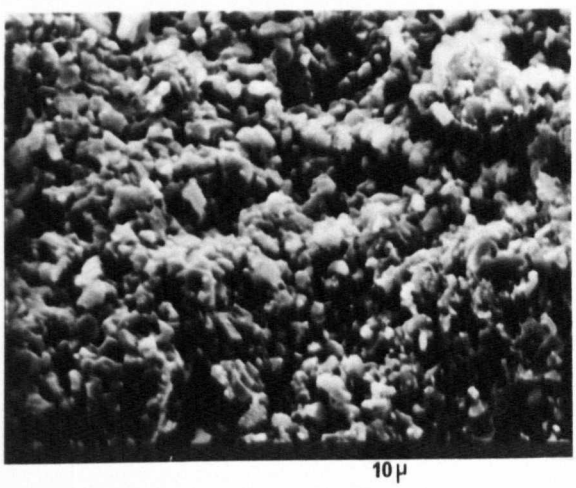

10 μ

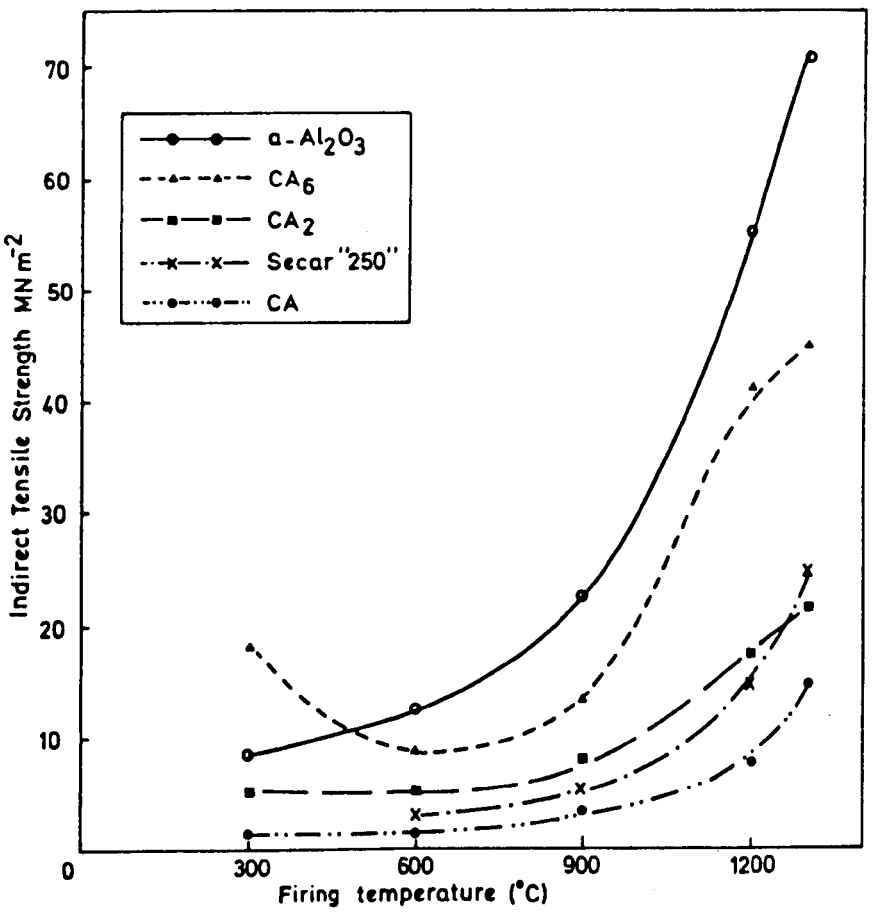

Fig. 4.12: Dependence of strength upon firing temperatures. Samples mixed with 10% H_3PO_4, hot-pressed under 207 MNm^{-2} pressure, at 300°C, for 30 minutes, and fired for 24 hours.

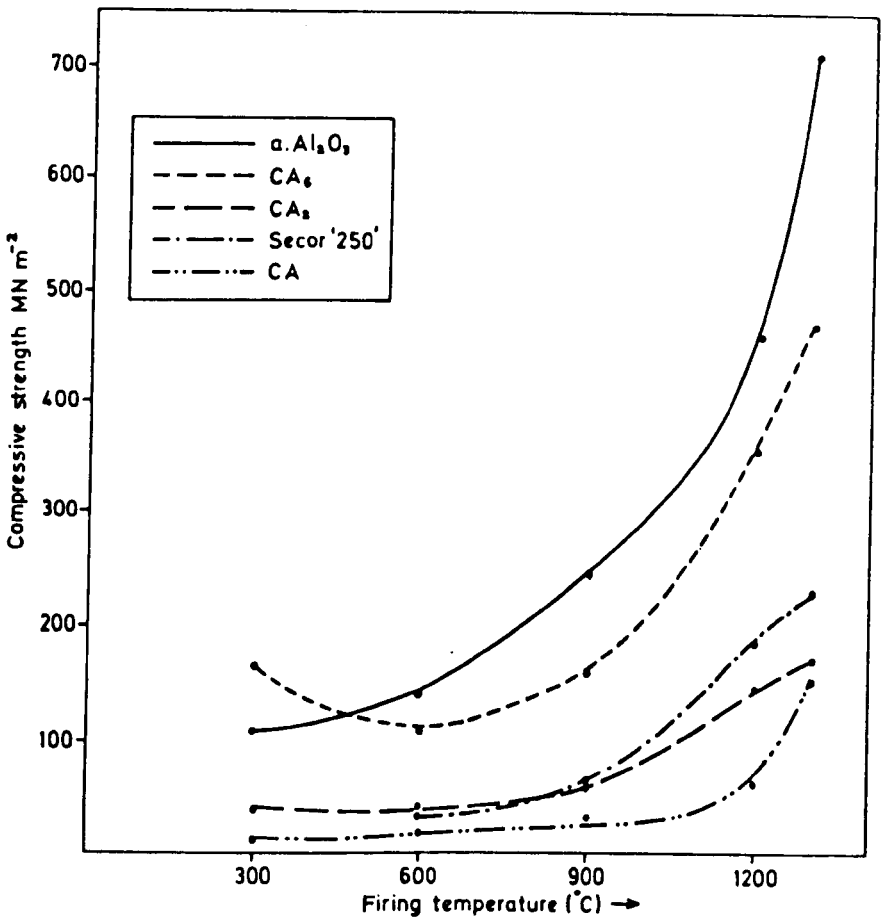

Fig. 4.13: Dependence of strength upon firing temperatures. Samples mixed with 10% H_3PO_4, hot-pressed under 207 MNm^{-2} pressure, at 300°C for 30 minutes, and fired for 24 hours.

Mixture	Hot-Pressing parameters			w/s ratio	Firing Conditions		% Change		Density g.cc	Strength (MNm^{-2})		Porosity (%)
	Pressure (MNm^{-2})	Temp. (°C)	Time (min)		Temp. (°C)	Time (hrs)	wt.	vol.		Tensile	Compressive	
α-Al_2O_3 + 10% H_3PO_4	207	300	30	.08	300	24	-0.74	No change	2.77	8.2	103.9	28.19
	207	300	30	.08	600	24	-0.86	+1.364	2.78	12.4	140.12	27.81
	207	300	30	.08	900	24	-0.84	-.668	2.822	22.4	245.95	26.89
	207	300	30	.08	1200	24	-0.98	-3.335	2.89	55.0	462.5	25.129
	207	300	30	.08	1300	24	-1.325	-4.607	2.984	71.32	717.4	22.5
CA_6 + 10% H_3PO_4	207	300	30	.08	300	24	-.64	No change	2.64	17.5	164.7	28.45
	207	300	30	.08	600	24	-.85	+.29	2.60	8.44	108.8	30.08
	207	300	30	.08	900	24	-.98	-.501	2.65	13.07	211.73	28.72
	207	300	30	.08	1200	24	-.74	-1.64	2.7045	41.6	359.42	27.1
	207	300	30	.08	1300	24	-1.85	-3.18	2.76	44.6	472.03	25.4
CA_2 + 10% H_3PO_4	207	300	30	.08	300	24	-2.26	No change	1.997	5.00	39.5	30.29
	207	300	30	.08	600	24	-2.52	+0.829	2.023	5.11	41.9	29.4
	207	300	30	.08	900	24	-2.65	-1.95	2.058	7.4	58.46	28.15
	207	300	30	.08	1200	24	-2.75	-3.64	2.09	17.6	146.08	27.30
	207	300	30	.08	1300	24	-3.00	-5.19	2.15	21.6	170.42	25.30

Table 4.4 (Cont.)

Table 4.4 (cont.)

Mixture	Hot-Pressing parameters			w/c ratio	Firing Conditions		% Change		Density g.cc	Strength (MNm^{-2})		Porosity (%)
	Pressure (MNm^{-2})	Temp. (°C)	Time (min)		Temp. (°C)	Time (hrs)	wt.	vol.		Tensile	Compressive	
CA + 10% H_3PO_4	207	300	30	.08	300	24	-2.26	-	1.98	1.5	12.00	32.88
	207	300	30	.08	600	24	-2.52	No change	1.98	1.7	18.7	32.88
	207	300	30	.08	900	24	-2.90	-1.67	2.05	3.6	31.3	30.508
	207	300	30	.08	1200	24	-2.95	-4.45	2.097	7.7	61.45	28.42
	207	300	30	.08	1300	24	-3.25	-6.077	2.124	14.4	153.36	27.00
Secar "250" + 10% H_3PO_4	207	300	30	.08	600	24	-1.75	No change	-	3.00	40.5	-
	207	300	30	.08	900	24	-1.88	-1.92	2.058	4.8	60.3	27.2
	207	300	30	.08	1200	24	-2.54	-3.81	2.140	14.8	187.15	24.9
	207	300	30	.08	1300	24	-3.13	-7.07	2.161	24.7	229.72	23.37

Table 4.4: Mechanical properties and related physical properties of α-Al_2O_3, CA_6, CA_2, CA and Secar "250" mixed with 10% H_3PO_4, hot pressed (under 207 MNm^{-2} pressure, at 300°C, for 30 minutes) and fired at different temperatures for 24 hours.

4.1.1.2 $CA_6 + H_3PO_4$

(a) Samples cast at room temperature, followed by firing

The same procedure previously described (Sections 3.3.1 and 3.3.3) were followed to mix and fire CA_6 with 5, 10 and 20% H_3PO_4 using .25 w/s ratio. D.T.A. for the mix CA_6 + 10% H_3PO_4, Fig. 4.1 and Table 4.1, show an endothermic peak at ~135°C and three exothermic peaks at about 726, 792 and 1271°C. Table 4.5 gives a summary of the XRD results after firing at different temperatures. Dependence of cold crushing strength upon firing temperatures is shown in Fig. 4.3.

(b) Hot-pressing

The same procedure previously described (Section 3.3.2.2) was followed for mixing 10% H_3PO_4 with 90% CA_6 using .08 w/s ratio. Hot-pressing was carried out under constant pressure (207 MNm^{-2}) for constant time (30 minutes) and between the range 100-700°C of temperature.

X-ray analysis of the samples showed that variscite, $AlPO_4.2H_2O$, was formed and was detected in samples hot-pressed at 100°C. By increasing the hot-pressing temperature to 150°C, a small new peak at $2\theta = 26.3^\circ$ was detected, which was stronger in a sample hot-pressed at 200°C (Fig. 4.14). On hot-pressing at 300°C, two peaks were detected at $2\theta = 21.63^\circ$ and 21.52°, which correspond to anhydrous $AlPO_4$. After hot-pressing at 400°C, the peaks were shifted to $2\theta = 21.47^\circ$ and 21.55°. On increasing the hot-pressing temperature to 500°C and above, one peak only was detected: $2\theta = 21.37^\circ$ after 500°C, $2\theta = 21.42^\circ$ after 600°C, and $2\theta = 21.45^\circ$ after 700°C. This kind of displacement was followed by XRD and is given in Fig. 4.15. The I.R. spectra are given in Fig. 4.16.

Samples which were fired after hot-pressing (under 207 MNm^{-2} pressure, at 300°C for 30 minutes) were also examined. For samples fired at 300°C, two peaks were detected at $2\theta = 21.69^\circ$ and 21.81°; after firing at 600°C, only one peak appeared at $2\theta = 21.52^\circ$, and after firing

Mix. No.	Composition (wt%)	Firing Conditions		Phase Identification (relative amount)	Other Observations
		Temp. (°C)	Time (hours)		
1	CA_6 95	300	24	CA_6	
	H_3PO_4 5	600	24	$CA_6 > AlPO_4$ ($2\theta = 21.55°$)	
		900	24	$CA_6 > AlPO_4$ ($2\theta = 21.58°$)	
		1200	24	α-$Al_2O_3 > CA_6 > \beta$-$Ca_3(PO_4)_2$	No $AlPO_4$
		1300	24	α-$Al_2O_3 > \alpha$-$Ca_3(PO_4)_2 > CA_6$	No $AlPO_4$
2	CA_6 90	300	24	CA_6	
	H_3PO_4 10	722	24	$CA_6 > AlPO_4$ ($2\theta = 21.55°$)	
		793	24	$CA_6 > AlPO_4$ ($2\theta = 21.55°$)	
		1270	24	α-$Al_2O_3 > \beta$-$Ca_3(PO_4)_2 > CA_6$	No $AlPO_4$
		1300	24	α-$Al_2O_3 > \alpha$-$Ca_3(PO_4)_2 > CA_6$	No $AlPO_4$
3	CA_6 85	300	24	CA_6	
	H_3PO_4 15	600	24	$CA_6 > AlPO_4$ ($2\theta = 21.55°$)	
		1200	24	α-$Al_2O_3 > \beta$-$Ca_3(PO_4)_2 > CA_6 > AlPO_4$(traces)	
4	CA_6 80	300	24	$CA_6 > AlPO_4$ ($2\theta = 21.6°$)	
	H_3PO_4 20	600	24	$CA_6 > AlPO_4$ ($2\theta = 21.55°$)	
		1200	24	α-$Al_2O_3 > CA_6 > \beta$-$Ca_3(PO_4)_2 > AlPO_4$ (traces)	

Table 4.5: Summary of XRD Results of $CA_6 + H_3PO_4$ Mixtures

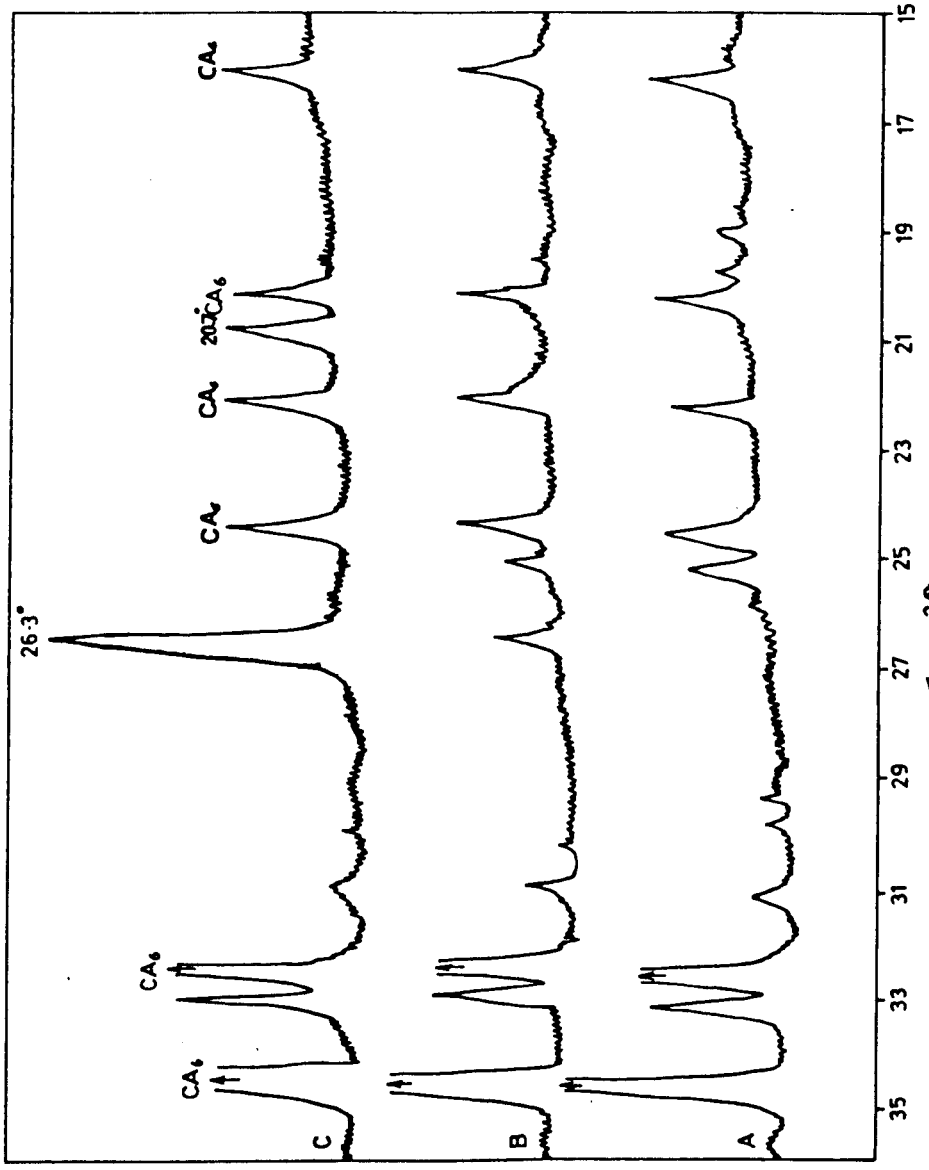

FIG. 4.14: X-ray diffractometer patterns of the mixture CA_6 + 10% H_3PO_4 hot-pressed under 207 MNm^{-2} pressure for 30 minutes at (A) 100°C, (B) 150°C, (C) 200°C.

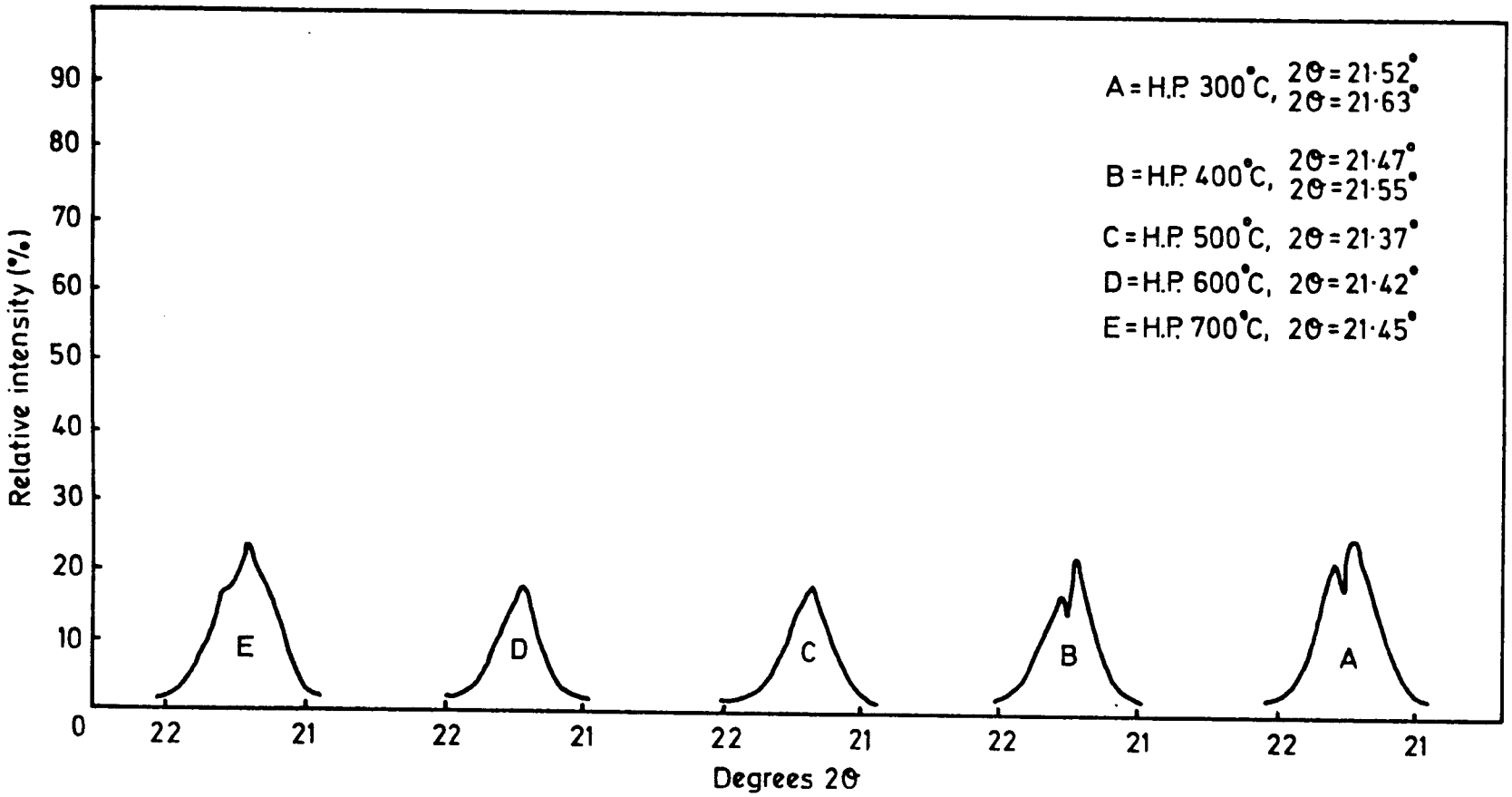

Fig. 4.15: X-ray diffractometer traces of the composition CA_6 + 10% H_3PO_4 hot-pressed at different temperatures under 207 MNm^{-2} pressure. for 30 minutes. Traces near the 2θ values corresponding to main peak of tridymite and cristobalite forms of $AlPO_4$.

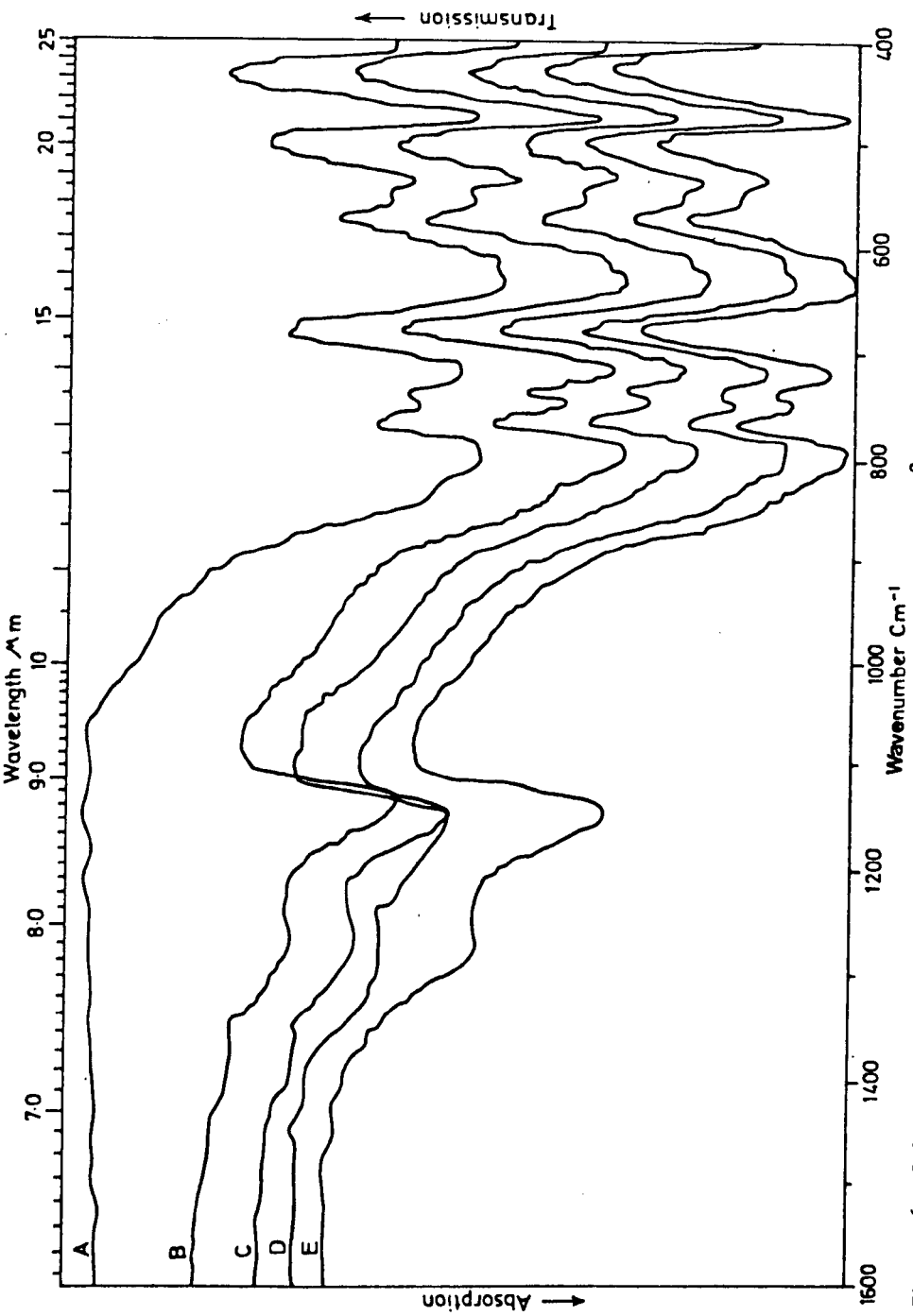

Fig. 4.16: Infra-red spectra of CA_6 + 10% H_3PO_4, hot-pressed under 207 MNm^{-2} pressure for 30 minutes at (A) 100°C, (B) 200°C, (C) 300°C, (D) 500°C, (E) 700°C.

at 900°C, the peak was at 2θ = 21.6°C. After firing at 1200°C, $AlPO_4$ disappeared and was replaced by α-Al_2O_3 as the main product. In the same sample, β-$Ca_3(PO_4)_2$ was detected, and after firing at 1300°C, α-$Ca_3(PO_4)_2$ was found. These results are given in Figs. 4.17 and 4.18.

Dependence of strength upon hot-pressing temperature is given in Fig. 4.9. A high strength value for those samples hot-pressed at 200°C followed by decrease up to 400°C, which gives the minimum value, and then a slight increase in the strength by increasing hot-pressing temperature was observed. Changes in microstructure induced by different hot-pressing or firing temperatures are shown in Fig. 4.19. In samples which were previously hot-pressed and fired, strength was slightly decreased from 300 to 600°C, but from 600 to 1300°C strength was increased (Figures 4.12 and 4.13). The physical and mechanical properties of these mixtures are given in Tables 4.3 and 4.4.

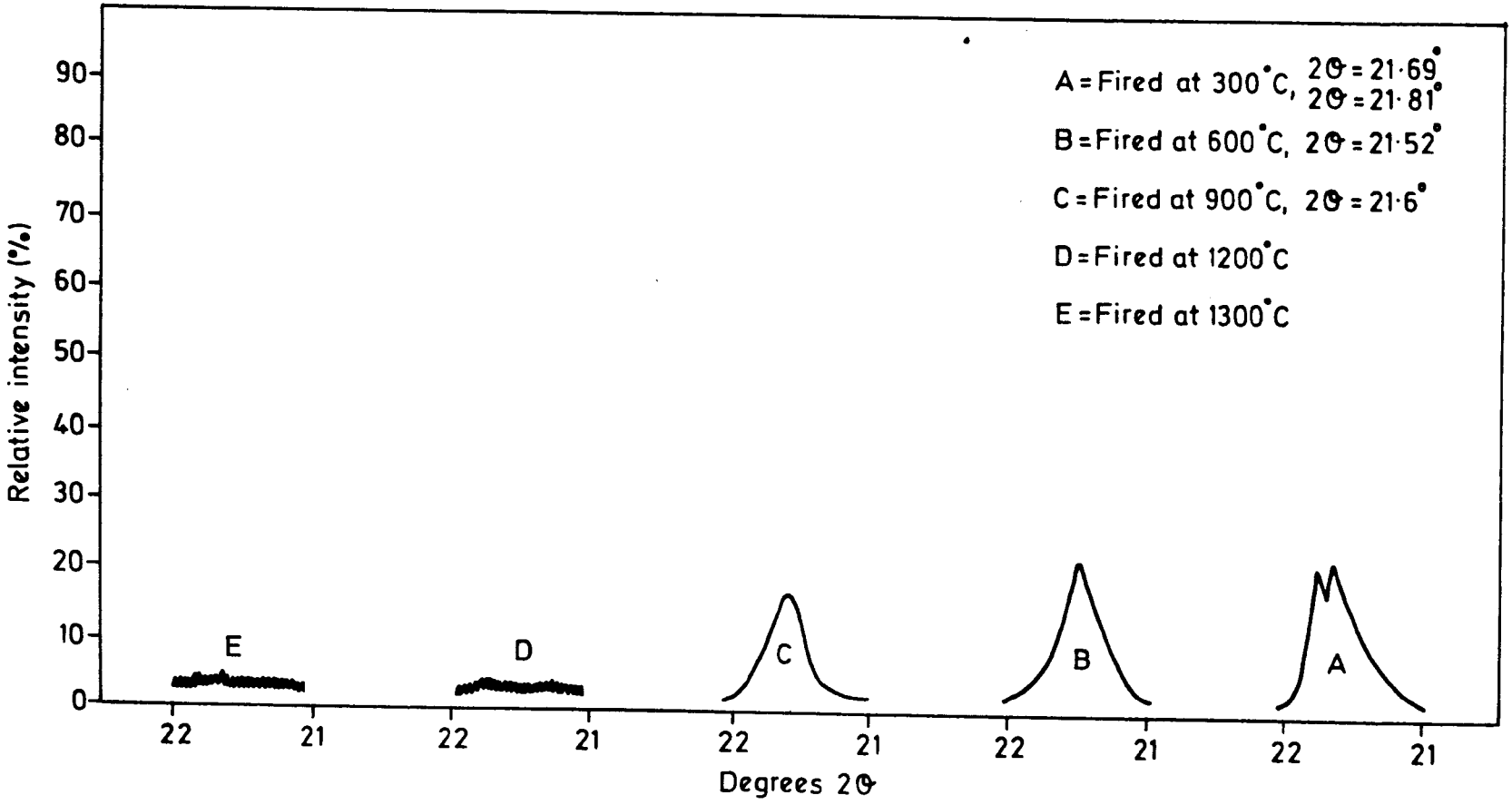

Fig. 4.17: X-ray diffractometer traces for the composition CA_6 + 10% H_3PO_4, hot-pressed under 207 MNm^{-2} pressure, at 300°C for 30 minutes, followed by firing at different temperatures for 24 hours. Traces near the 2θ value corresponding to main peaks of tridymite and cristobalite forms of $AlPO_4$.

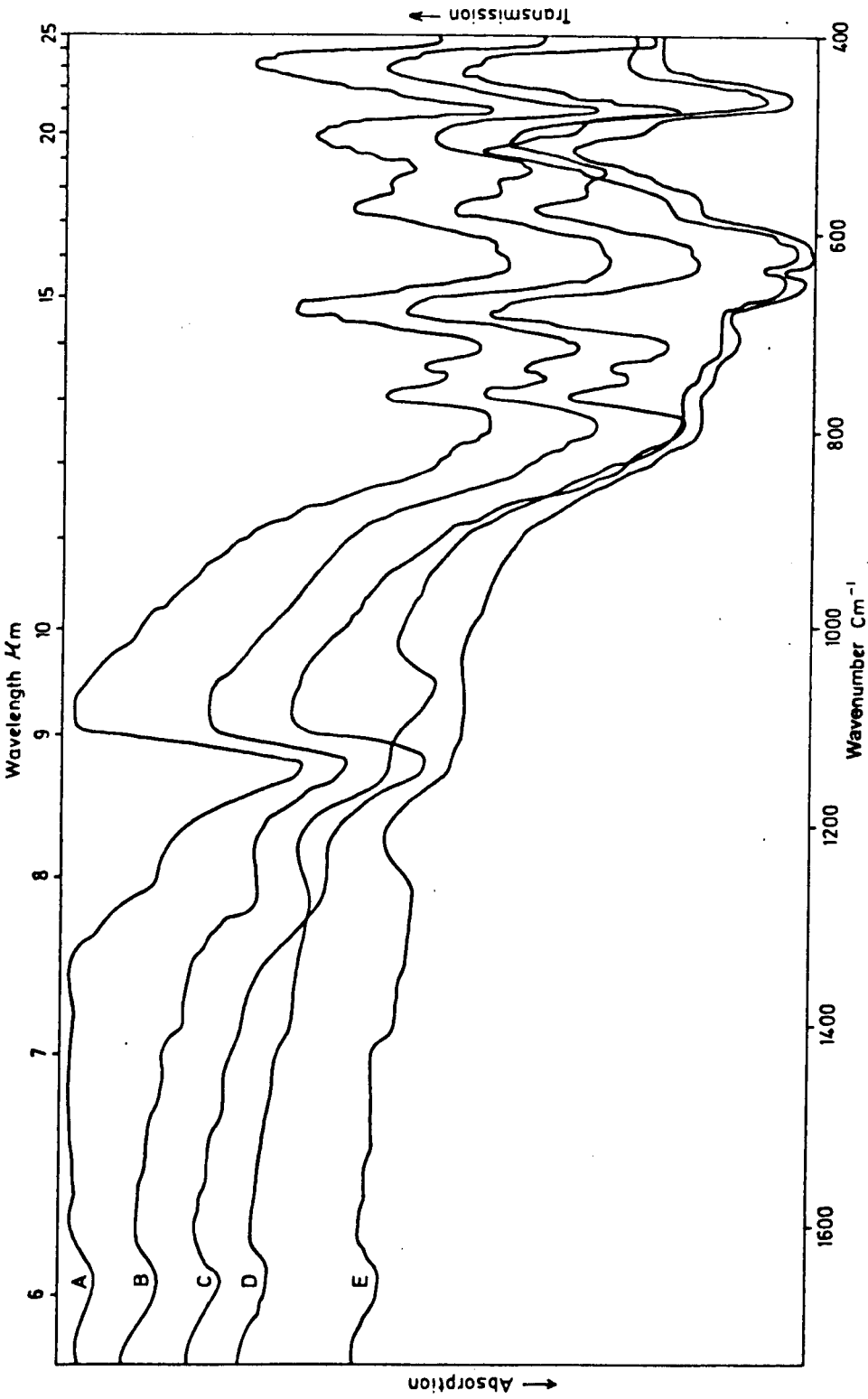

FIG. 4.18: Infra-red spectra of the mixture CA_6 + 10% H_3PO_4, hot-pressed under 207 MNm^{-2} pressure, at 300°C for 30 minutes, followed by firing at (A) 300°C, (B) 600°C, (C) 900°C, (D) 1200°C, (E) 1300°C.

Fig. 4.19A

SEM Micrographs of CA_6 mixed with 10% H_3PO_4, hot-pressed under 207 MNm^{-2} pressure for 30 minutes at:

(a) 200°C

(b) 400°C.

Fig. 4.19B

SEM Micrographs of CA_6 mixed with 10% H_3PO_4:

(a) Hot-pressed under 207 MNm^{-2} pressure, for 30 minutes at 300°C, fired at 1300°C for 24 hours.

(b) Room-temperature casting, fired at 1300°C for 24 hours.

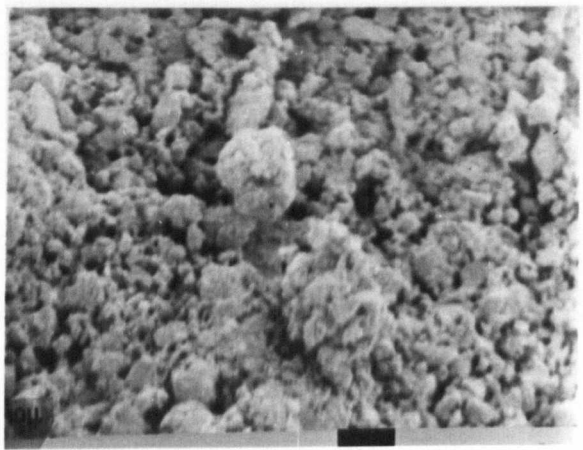

b

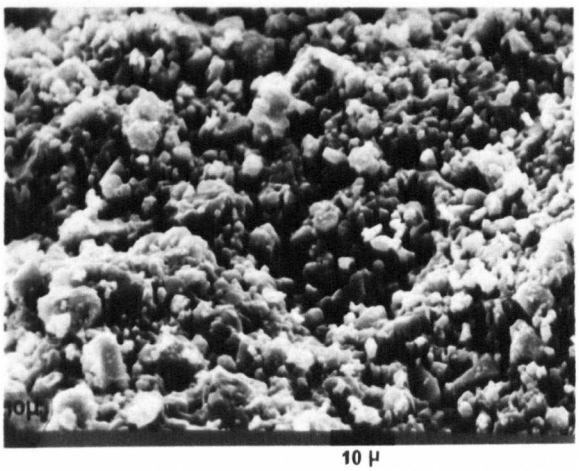

a

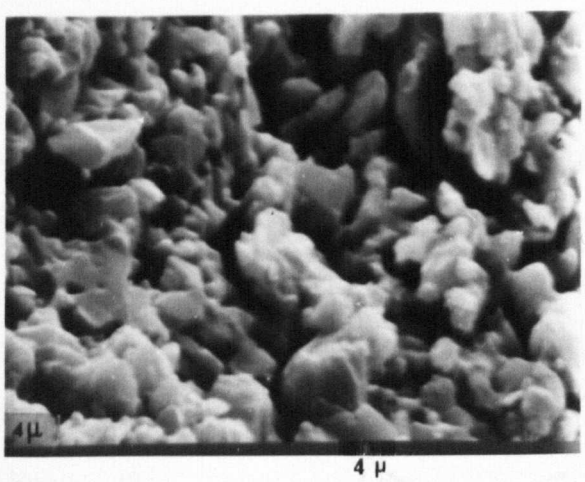

b

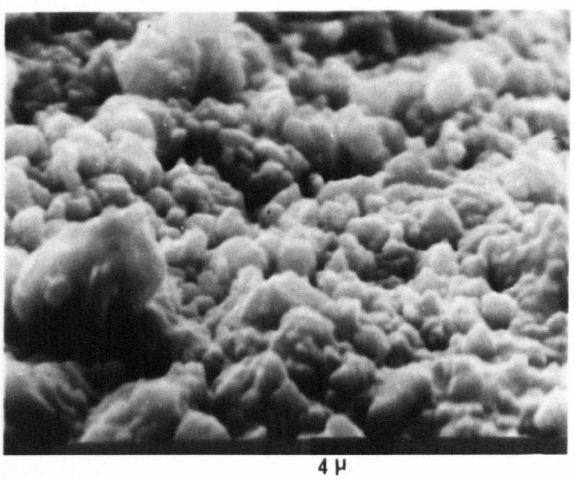

a

4.1.1.3 $CA_2 + H_3PO_4$

(a) Samples cast at room temperature, followed by firing

Calcium dialuminate (CA_2) was mixed with 5, 10, 15 and 20 wt% phosphoric acid using 0.25 w/c ratio, as previously described (Sections 3.3.1 and 3.3.3). D.T.A. of the mix CA_2 + 10% H_3PO_4 showed an endothermic peak at ~120°C, and three exothermic peaks at about 656, 682 and 1080°C (Fig. 4.1 and Table 4.1). The relationship between strength and firing temperatures is given in Fig. 4.3. Table 4.6 gives a summary of the different phases obtained after firing at different temperatures.

(b) Hot-pressing

A mixture of 90% CA_2 and 10% H_3PO_4 was made as previously described (Section 3.3.2.2) using .08 w/c ratio. Samples were hot-pressed under constant pressure (207 MNm^{-2}) for constant time (30 minutes) using a temperature range of 200-700°C. Below 200°C, it was found that it was difficult to extract the sample from the die without cracking. X-ray analysis of the hot-pressed samples showed that no reaction took place after hot-pressing at 200°C, whereas after hot-pressing at 300°C a small peak appeared at $2\theta = 26.3^\circ$. Hot-pressing at 400°C produced a peak at $2\theta = 21.52^\circ$ which represented anhydrous $AlPO_4$. By increasing the hot-pressing temperature up to 500, 600 and 700°C, the intensity of the above peak was increased, with a small shift to $2\theta = 21.55^\circ$ at 700°C. This can be seen in XRD pattern given in Fig. 4.20. The I.R. spectra are shown in Fig. 4.21.

X-ray analysis of the fired samples, which had been hot-pressed under 207 MNm^{-2} pressure, at 300°C for 30 minutes, showed only one peak at $2\theta = 26.3^\circ$ after firing at 300°C, whereas after firing at 600°C a weak peak at $2\theta = 21.52^\circ$ appeared. This same peak was found to be much stronger in those samples fired at 900°C. After further heating at 1200°C and 1300°C, the anhydrous $AlPO_4$ peak disappeared and peaks representing

Mix No.	Composition (wt%)	Firing Conditions		Phase Identification (relative amount)	Other observations
		Temp. (°C)	Time (hours)		
1	CA_2 95	300	24	CA_2	
	H_3PO_4 5	600	24	CA_2 > $AlPO_4$ (s.a.)	
		900	24	CA_2 > $AlPO_4$ (2θ = 21.55°C	
		1200	24	CA_2 > β-$Ca_3(PO_4)_2$	No $AlPO_4$
		1300	24	CA_2 > α-$Ca_3(PO_4)_2$ > CA_6	No $AlPO_4$
2	CA_2 90	300	24	CA_2	
	H_3PO_4 10	600	24	CA_2 > $AlPO_4$ (2θ = 21.55°)(s.a.)	
		900	24	CA_2 > $AlPO_4$ (2θ = 21.65°)	
		1080	24	CA_2 > β-$Ca_3(PO_4)_2$	
		1200	24	CA_2 > β-$Ca_3(PO_4)_2$	No $AlPO_4$
		1300	24	CA_2 > α-$Ca_3(PO_4)_3$ > CA_6	No $AlPO_4$
3	CA_2 85	300	24	CA_2 > $AlPO_4$ (2θ = 21.55°)	
	H_3PO_4 15	600	24	CA_2 > $AlPO_4$ (2θ = 21.55°)	
		900	24	CA_2 > $AlPO_4$ (2θ = 21.62°)	
		1200	24	CA_2 > $AlPO_4$ (2θ = 21.78°) β-$Ca_3(PO_4)_2$	CA_6 (s.a.)
		1300	24	CA_2 > α-$Ca_3(PO_4)_3$	$AlPO_4$ (s.a.) α-Al_2O_3 (s.a.)
4	CA_2 80	300	24	CA_2 > $AlPO_4$ (2θ = 21.55°)	
	H_3PO_4 20	600	24	CA_2 > $AlPO_4$ (2θ = 21.55°)	
		900	24	CA_2 > $AlPO_4$ (2θ = 21.65°)	
		1200	24	CA_2 > β-$Ca_3(PO_4)_2$ α-Al_2O_3	$AlPO_4$ (s.a.)

s.a. = small amount

Table 4.6: Summary of XRD results of CA_2 + H_3PO_4 mixtures

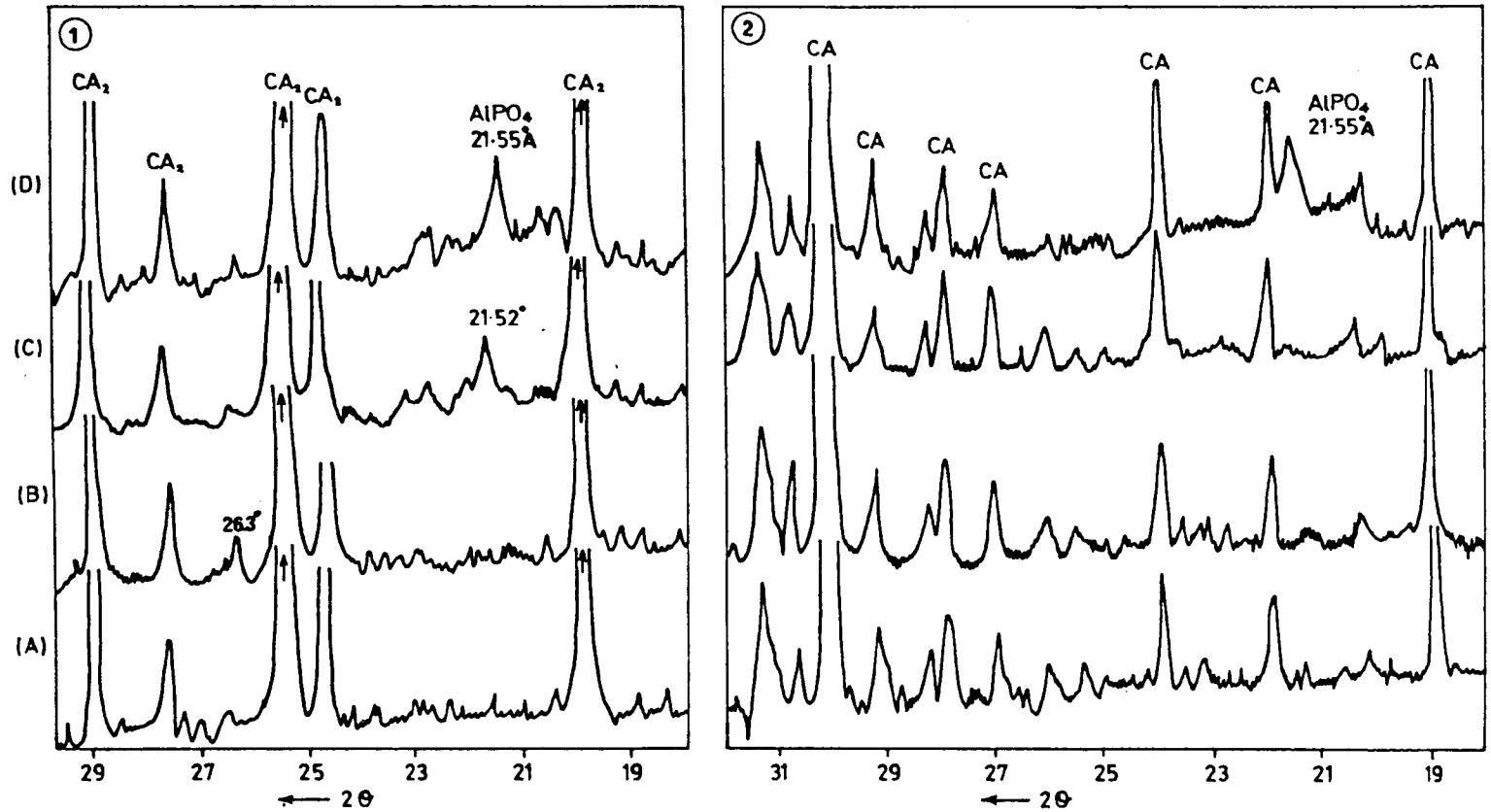

Fig. 4.20: X-ray diffractometer patterns of the mixtures (1) CA_2 + 10% H_3PO_4, (2) CA + 10% H_3PO_4, hot-pressed under 207 MNm^{-2} pressure for 30 minutes at (A) 200°C, (B) 300°C, (C) 400°C, (D) 700°C.

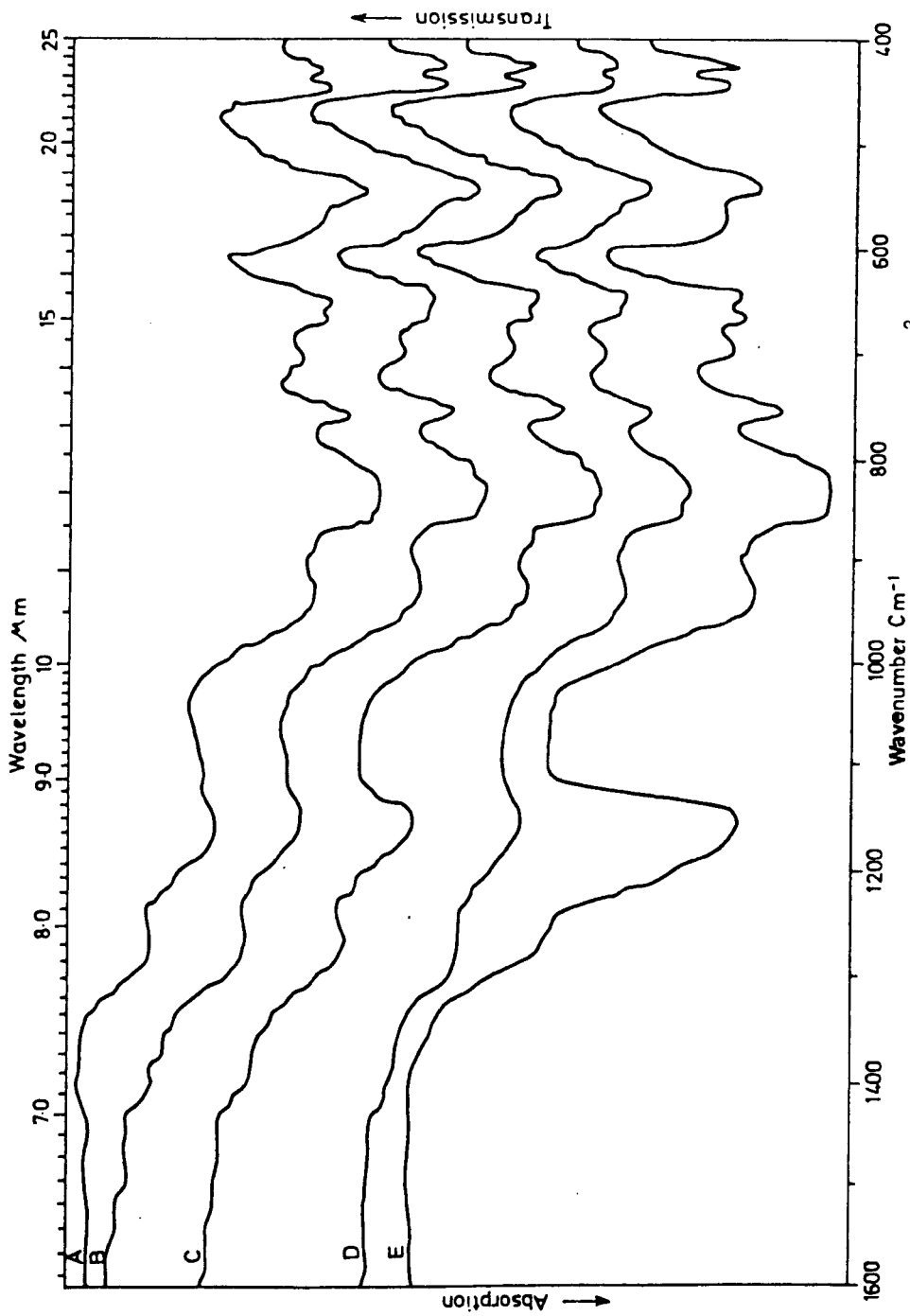

Fig. 4.21: Infra-red spectra of the mixture CA_2 + 10% H_3PO_4, hot-pressed under 207 Mm^{-2} pressure for 30 minutes at (A) 200°C, (B) 300°C, (C) 400°C, (D) 500°C, (E) 700°C.

α-$Ca_3(PO_4)_2$, CA_6 and α-Al_2O_3 appeared. Infra-red spectra are shown in Fig. 4.22.

The dependence of strength upon hot-pressing temperature is given in Fig. 4.9 and Table 4.3, which indicate that this mix behaves approximately like the CA_6 + 10% H_3PO_4 mix, where the strength is decreased from 200 - 300°C and then increases with increasing hot-pressing temperatures up to 700°C. The changes in the microstructures with hot-pressing temperatures and with firing temperatures are given in Fig. 4.23. The strength of fired samples, previously hot-pressed (Figures 4.12 and 4.13) shows an increase with increasing firing temperature from 300 - 1300°C. Physical and mechanical properties of these mixtures are given in Table 4.4.

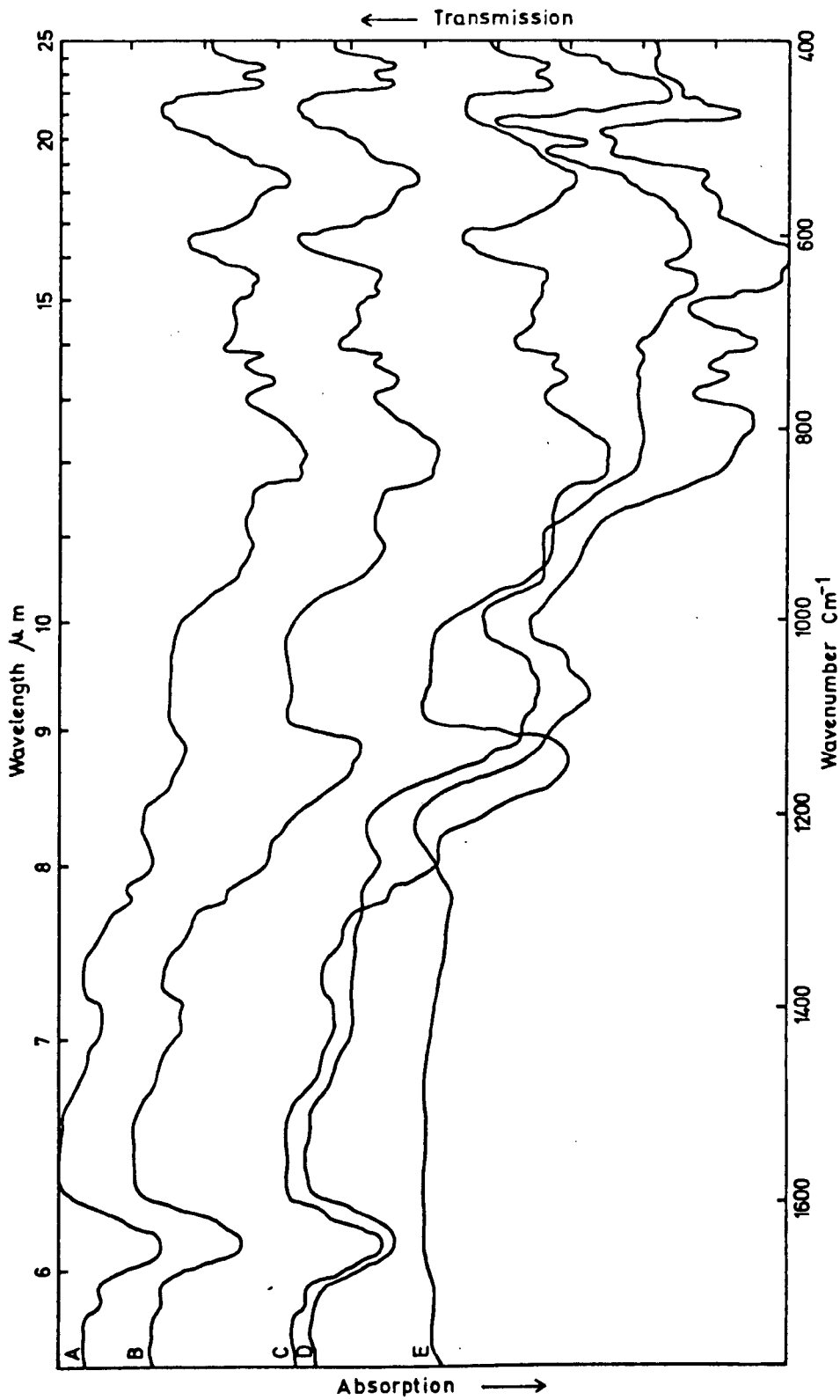

Fig. 4.22: Infra-red spectra of the mixture CA_2 + 10% H_3PO_4, hot-pressed under 207 MNm^{-2} pressure, at 300°C for 30 minutes, fired for 24 hours at (A) 300°C, (B) 600°C, (C) 900°C, (D) 1200°C, (E) 1300°C.

Fig. 4.23A

SEM Micrographs of CA_2 mixed with 10% H_3PO_4, hot-pressed under 207 MNm^{-2} pressure for 30 minutes at:

(a) 200°C

(b) 400°C.

Fig. 4.23B

SEM Micrographs of CA_2 mixed with 10% H_3PO_4:

(a) Hot-pressed under 207 MNm^{-2} pressure for 30 minutes at 300°C, fired at 1300°C for 24 hours.

(b) Room-temperature casting, fired at 1300°C for 24 hours.

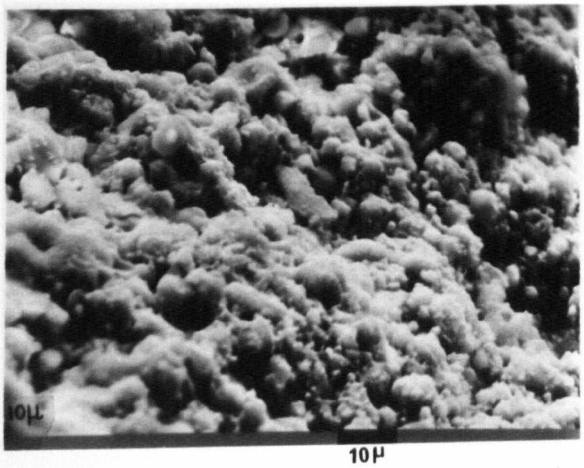

b

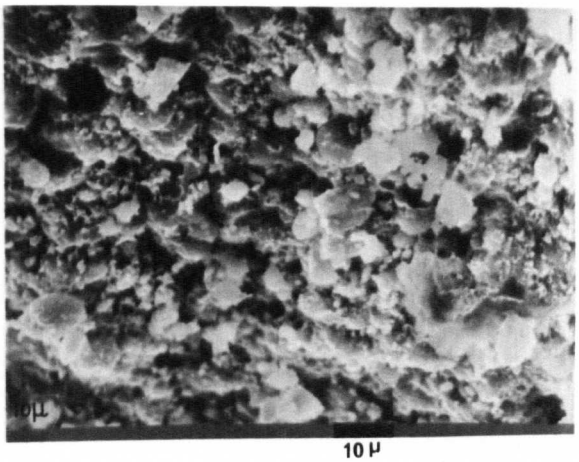

a

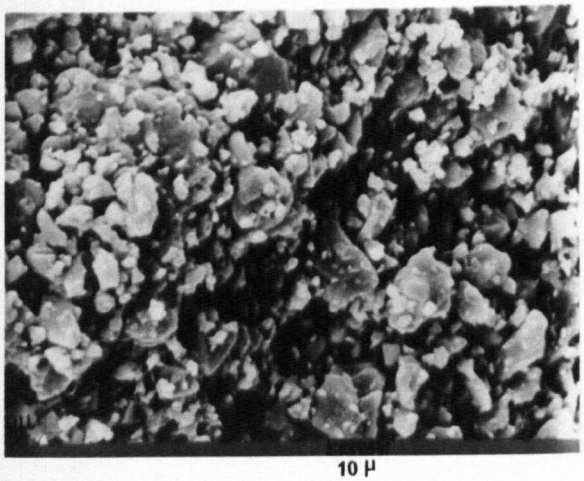

b

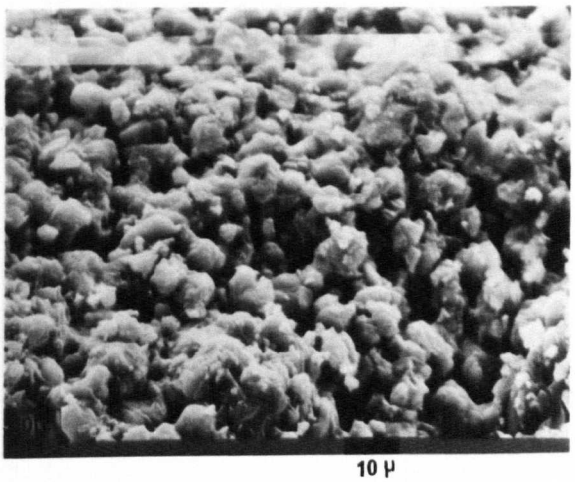

a

4.1.1.4 $CA + H_3PO_4$

(a) Samples cast at room temperature, followed by firing

Calcium monoaluminate was mixed with 5, 10, 15 and 20 wt% phosphoric acid as previously described (Sections 3.3.1 and 3.3.3) using .25 w/c ratio. D.T.A. of the mix CA + 10% H_3PO_4 shows an endothermic peak at about 120°C and two exothermic peaks at about 675 and 925°C as shown in Fig. 4.1, and Table 4.1. Table 4.7 gives a summary of the qualitative analysis of the different phases after firing at different temperatures. Dependence of strength upon firing temperature is shown in Fig. 4.3.

(b) Hot-pressing

Calcium monoaluminate was mixed with 10% H_3PO_4 using .08 w/c ratio and hot-pressing was carried out as previously stated (Section 3.3.2.2) under constant pressure (207 MNm^{-2}) for constant time (30 minutes) in the range of temperature 200-700°C. X-ray analysis showed no sign of reaction after hot-pressing between 200 and 600°C. After hot-pressing at 700°C, the sample showed two peaks at $2\theta = 20.3^\circ$ and 21.55°. The XRD of these mixtures are given in Fig. 4.20 and I.R. spectra are given in Fig. 4.24. For those samples which were fired after hot-pressing, X-ray analysis showed that after firing at 300°C, no change occurred, whereas after firing at 600°C, two weak peaks at $2\theta = 21.55^\circ$ and 20.3° were observed. These two peaks were slightly decreased in intensity after firing at 900°C, and they completely disappeared after firing at 1200 and 1300°C. In samples fired at this latter temperature, α-$Ca_3(PO_4)_2$ was detected with some peaks representing calcium dialuminate (CA_2). The I.R. spectra are shown in Fig. 4.25. Dependence of strength upon hot-pressing temperature is given in Fig. 4.9 and Table 4.3; it can be noted that the mixture behaves almost like the previous calcium aluminate + phosphoric acid mixtures. The cold crushing strength of samples subjected to firing after hot-pressing showed an increase in

Mix No.	Composition (wt%)	Firing Conditions		Phase identification (relative amount)	Other observations
		Temp. (°C)	Time (hours)		
1	CA 95 H_3PO_4 5	300	24	CA only	
		600	24	CA, $AlPO_4$ (s.a.)	
		900	24	CA > $AlPO_4$ ($2\theta = 21.5^o$) + traces of CA_2	
		1200	24	CA > CA_2, traces of $Ca_3(PO_4)_2$	No $AlPO_4$
		1300	24	CA > CA_2, traces of $Ca_3(PO_4)_2$	No $AlPO_4$
2	CA 90 H_3PO_4	300	24	CA	
		600	24	CA, $AlPO_4$ (s.a.)	
		900	24	CA > $AlPO_4$, CA_2 (s.a.)	
		1200	24	CA > CA_2 > β-$Ca_3(PO_4)_2$	No $AlPO_4$
		1300	24	CA > CA_2 > $Ca_3(PO_4)_2$	No $AlPO_4$
3	CA 85 H_3PO_4 15	300	24		
		600	24	CA > γ-$Ca_2P_2O_5$ > $AlPO_4$	
		900	24	CA > $AlPO_4$ > β-$Ca_2P_2O_5$	CA_2 (s.a.)
		1200	24	CA > CA_2 > $\beta Ca_3(PO_4)_2$	No $AlPO_4$
		1300	24	CA > CA_2 > $\alpha Ca_3(PO_4)_2$	No $AlPO_4$
4	CA 80 H_3PO_4	300	24	CA, $CaHPO_4$ (s.a.)	
		600	24	CA > $AlPO_4$ > γ-$Ca_2P_2O_7$	
		900	24	CA > $AlPO_4$ > β-$Ca_2P_2O_7$	CA_2 (s.a.)
		1200	24	CA > $AlPO_4$ > CA_2 > α-$Ca_2P_2O_5$	
		1300	24	CA > CA_2 > $Ca_3(PO_4)_2$	No $AlPO_4$

s.a. = small amount

Table 4.7: Summary of XRD results of CA + H_3PO_4 mixtures.

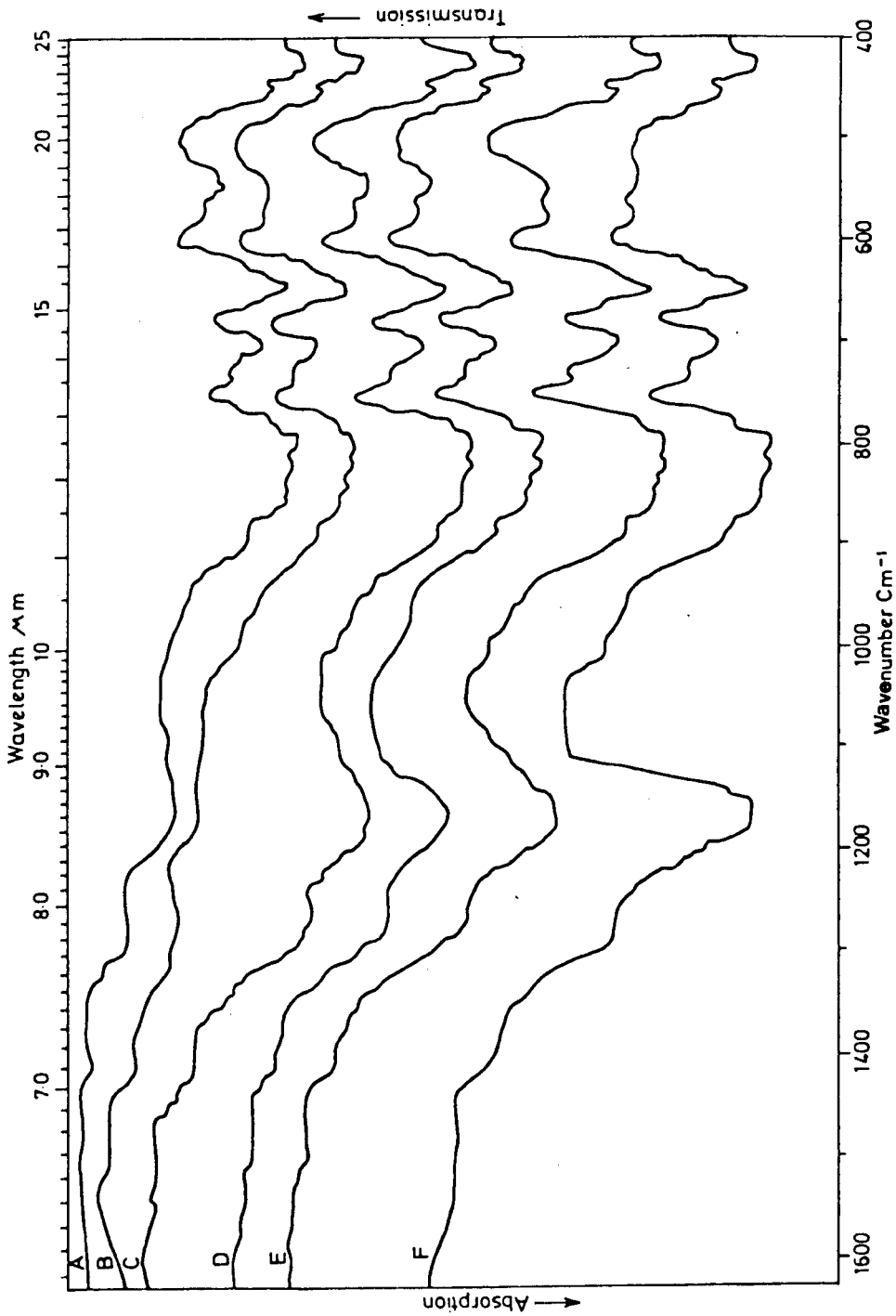

Fig. 4.24: Infra-red spectra of CA mixed with 10 wt% H_3PO_4 and hot-pressed at (A) 200°C, (B) 300°C, (C) 400°C, (D) 500°C, (E) 600°C, (G) 700°C, under constant pressure (2^{07} tTn^{-2}) for constant time ($_{30}$ mins.)

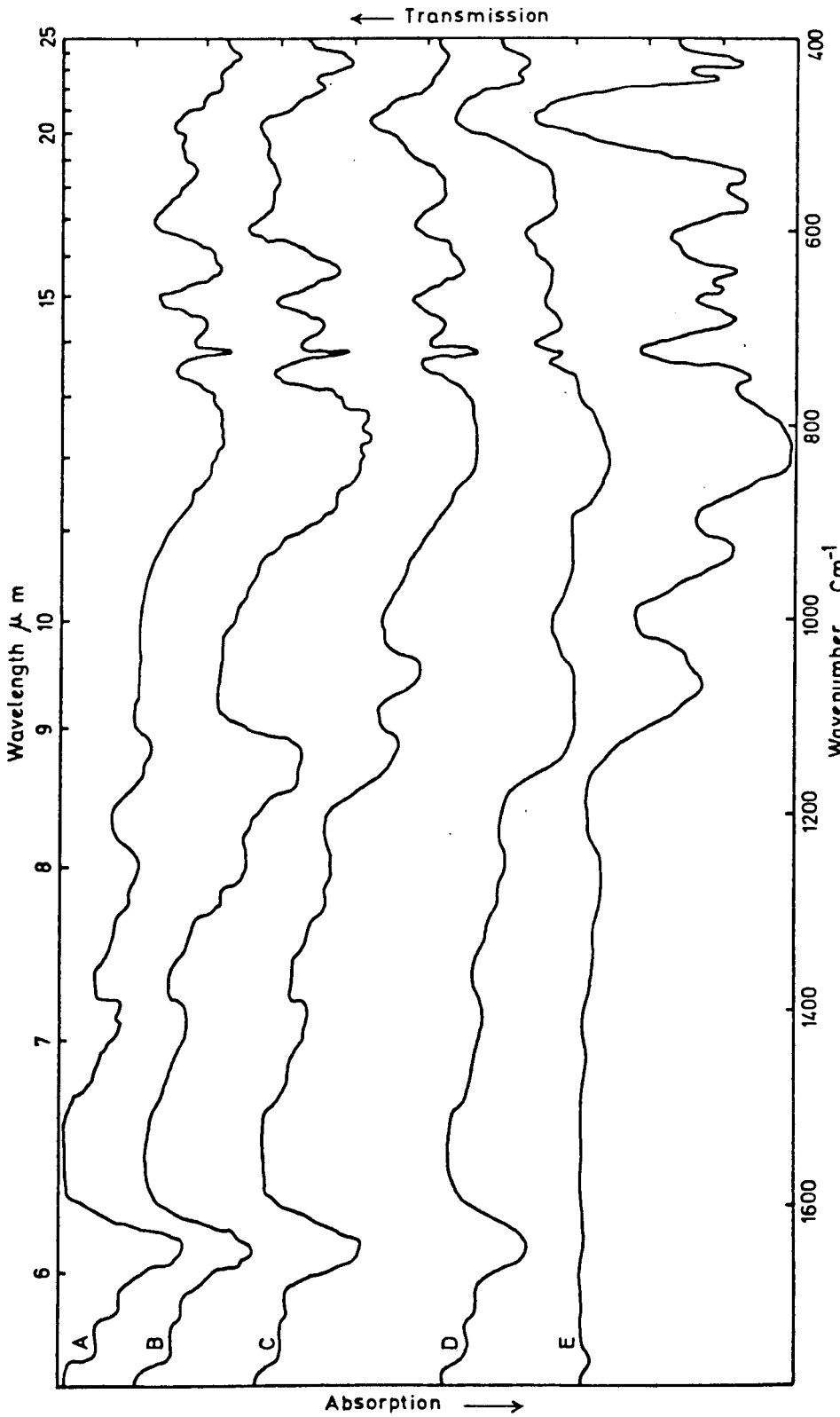

Fig. 4.25: Infra-red spectra of the mixture CA + 10% H_3PO_4, hot-pressed under 207 MNm^{-2} pressure, at 300°C, for 30 minutes, and fired for 24 hours at (A) 300°C, (B) 600°C, (C) 900°C, (D) 1200°C, (E) 1300°C.

Fig. 4.26A

SEM Micrographs of CA mixed with 10% H_3PO_4, hot-pressed under 207 MNm^{-2} pressure for 30 minutes at:

(a) 200°C

(b) 400°C.

Fig. 4.26B

SEM Micrographs of CA mixed with 10% H_3PO_4:

(a) Hot-pressed under 207 MNm^{-2} pressure for 30 minutes, at 300°C, fired at 1300°C for 24 hours.

(b) Room temperature casting, fired at 1300°C for 24 hours.

10 µ

b

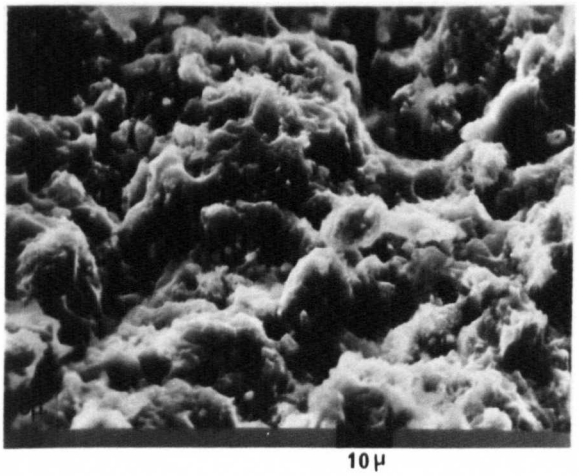

10 µ

a

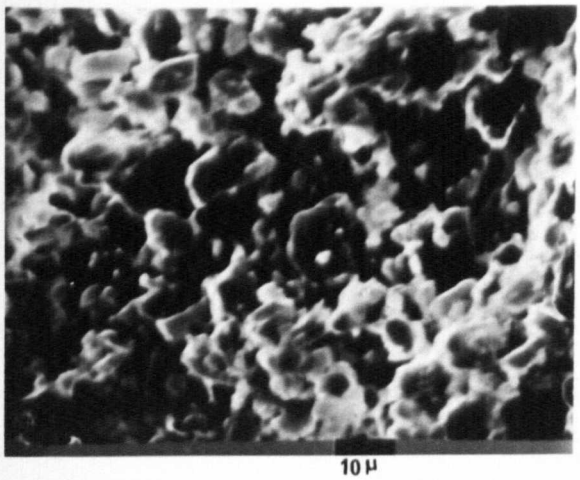

10 µ

b

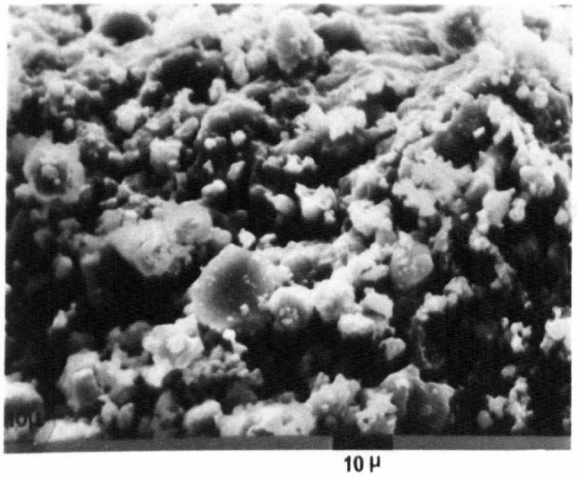

10 µ

a

the strength with increasing firing temperatures (Figs. 4.12 and 4.13). The changes in the microstructures with hot-pressing temperatures and after firing at 1300°C are shown in Fig. 4.26. Physical and mechanical properties are summarised in Table 4.4.

4.1.1.5 Secar "250" cement + H_3PO_4

Secar "250" cement, which can be considered as a mixture of CA and CA_2, was mixed with 10% H_3PO_4, and samples were hot-pressed under constant pressure (207 MNm^{-2}) for constant time (30 minutes) over the range of temperatures 200-700°C. The same procedure previously described (Section 3.3.2.2) was followed, using .08 w/c ratio.

The D.T.A. results of the mixture Secar "250" + 10% H_3PO_4 (Fig. 4.1 and Table 4.1) show an endothermic peak at about 125°C and two exothermic peaks at approximately 692 and 1047°C (Fig. 4.1 and Table 4.1).

X-ray analysis showed that no reaction occurred in the hot-pressed samples at 200 and 300°C, whereas at 400°C two peaks appeared at 2θ = 20.3° and 21.55° (Fig. 4.27). After further hot-pressing at 500, 600 and 700°C a small increase in the intensity of the above peaks was observed. Samples which were fired after hot-pressing were also examined. X-ray analysis showed that the above two peaks (2θ = 20.3° and 21.55°) were detected after firing at 600 and 900°C. In addition, after firing at higher temperatures (i.e. 1200 and 1300°C) mainly CA_2 and a small amount of CA as well as with traces of α-Al_2O_3 and α-$Ca_3(PO_4)_2$ were detected. Infra-red spectra after firing at different temperatures are shown in Fig. 4.28.

Dependence of strength upon hot-pressing temperatures is shown in Fig. 4.9. The relationship between strength and firing temperatures is given in Figs. 4.12 and 4.13. The change in the microstructures either with hot-pressing temperature or after firing at 1300°C are shown in Fig. 4.29. The mechanical properties and related physical properties are given in Tables 4.3 and 4.4.

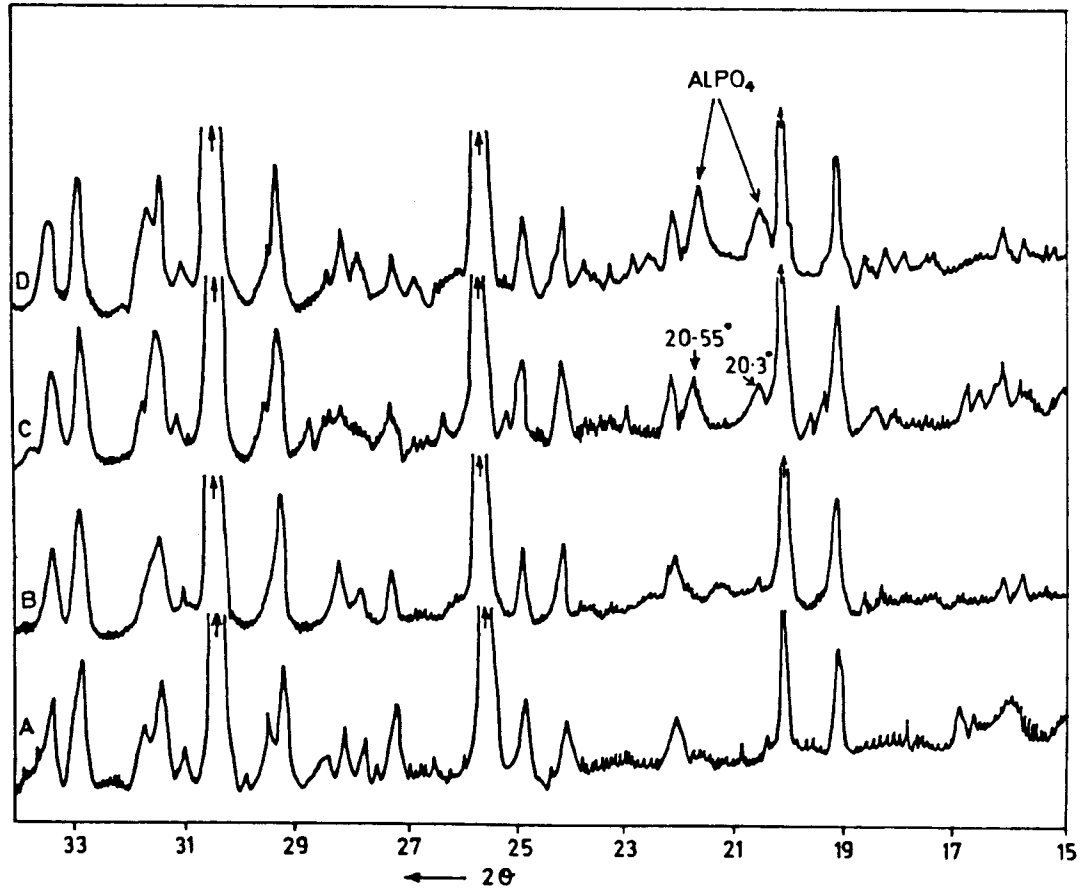

Fig. 4.27: X-ray diffractometer patterns of Secar "250" mixed with 10% H_3PO_4 and hot-pressed under 207 MNm^{-2} pressure for 30 minutes at (A) 200°C, (B) 300°C, (C) 400°C, (D) 700°C.

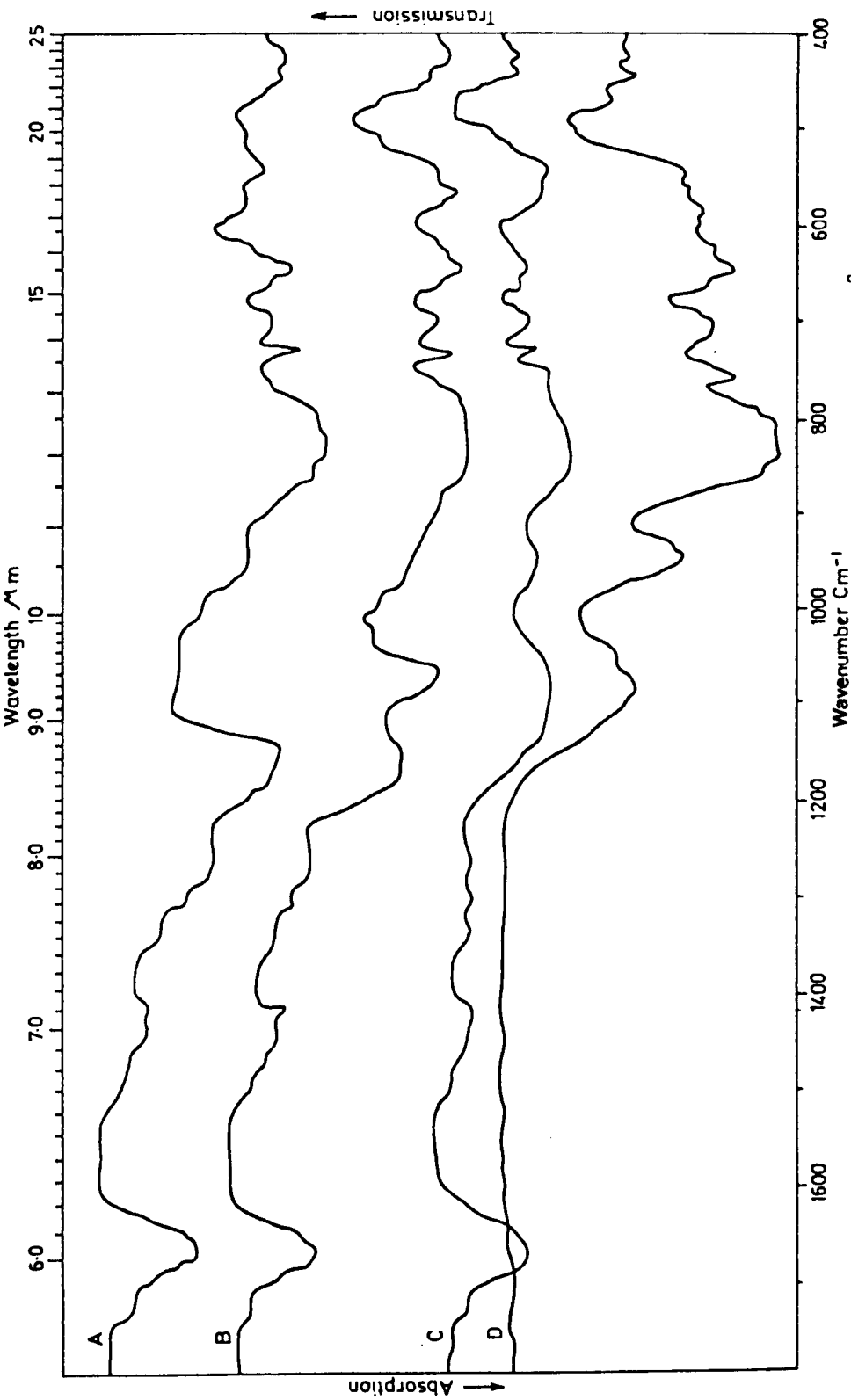

Fig. 4.28: Infra-red spectra of the mixture Secar "250" cement + 10% H_3PO_4, hot-pressed under 207 MNm^{-2} pressure at 300°C for 30 minutes, and fired at (A) 600°C, (B) 900°C, (C) 1200°C, (D) 1300°C.

Fig. 4.29

SEM Micrographs of Secar "250" cement, mixed with 10% H_3PO_4, hot-pressed under 207 MNm^{-2} pressure for 30 minutes at:

(a) 200°C

(b) 400°C

(c) 300°C, followed by firing at 1300°C for 24 hours.

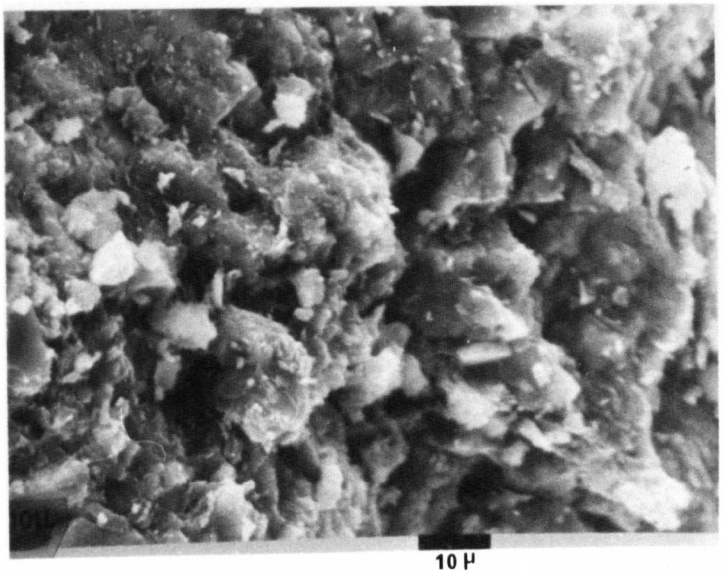

a

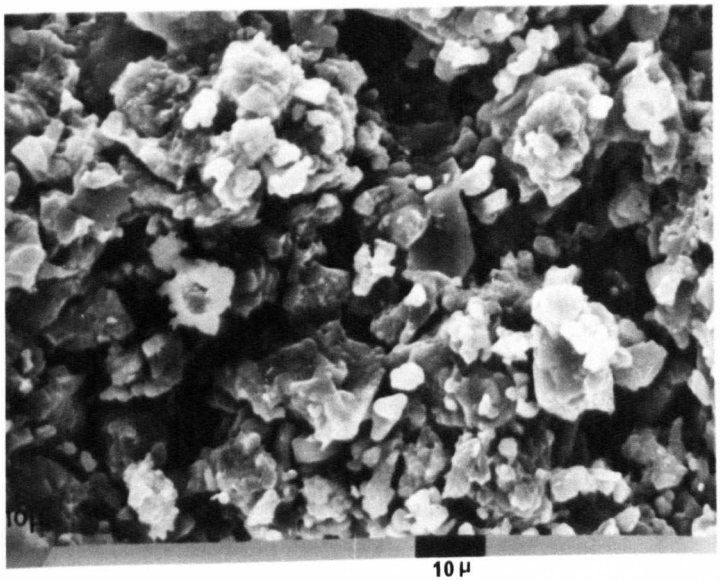

b

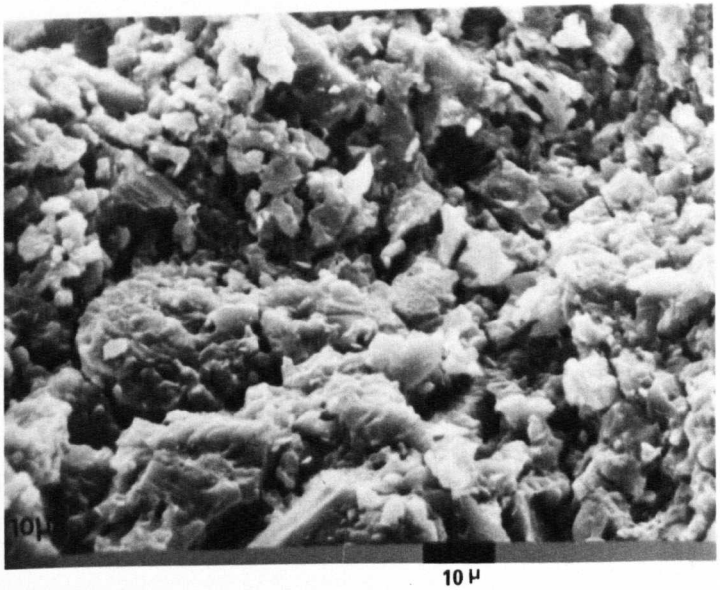

c

4.2 Aluminum Phosphate

The effect of aluminum phosphate (cristobalite form) as a bonding material on some calcium aluminate phases was studied. Room temperature casting followed by firing at different temperatures together with hot-pressing under constant pressure (207 MNm^{-2}) for constant time (30 minutes) at constant temperature (300°C) followed by firing were applied.

4.2.1 Results

(a) Samples cast at room temperature, followed by firing

Calcium mono- and dialuminate were mixed with 5 and 10 wt% aluminum phosphate, previously prepared (Section 3.2) using .25 w/c ratio. The procedures previously described (Sections 3.3.1 and 3.3.3) were followed for mixing and firing.

XRD results of the above mixtures are summarised in Table 4.8. Strength of samples prepared at room temperature was not measured because the samples were not hard enough, even after firing.

The DTA traces of the mixtures CA_6, CA_2, CA and Secar "250" + 10% $AlPO_4$ are shown in Fig. 4.30 and the results are summarised in Table 4.9.

Mixture	Exothermic Reaction			ΔT °C	Peak Area deg.S.mg^{-1}
	Start °C	Peak °C	End °C		
CA + 10% $AlPO_4$	985	1140	1191	0.227	1.36
CA_2 + 10% $AlPO_4$	1015	1135	1169	0.227	1.21
CA_6 + 10% $AlPO_4$	1184	1225	1277	0.367	1.40
Secar "250" + 10% $AlPO_4$	1015	1122	1224	0.245	0.937

Table 4.9: Summary of DTA Results in Fig. 4.30

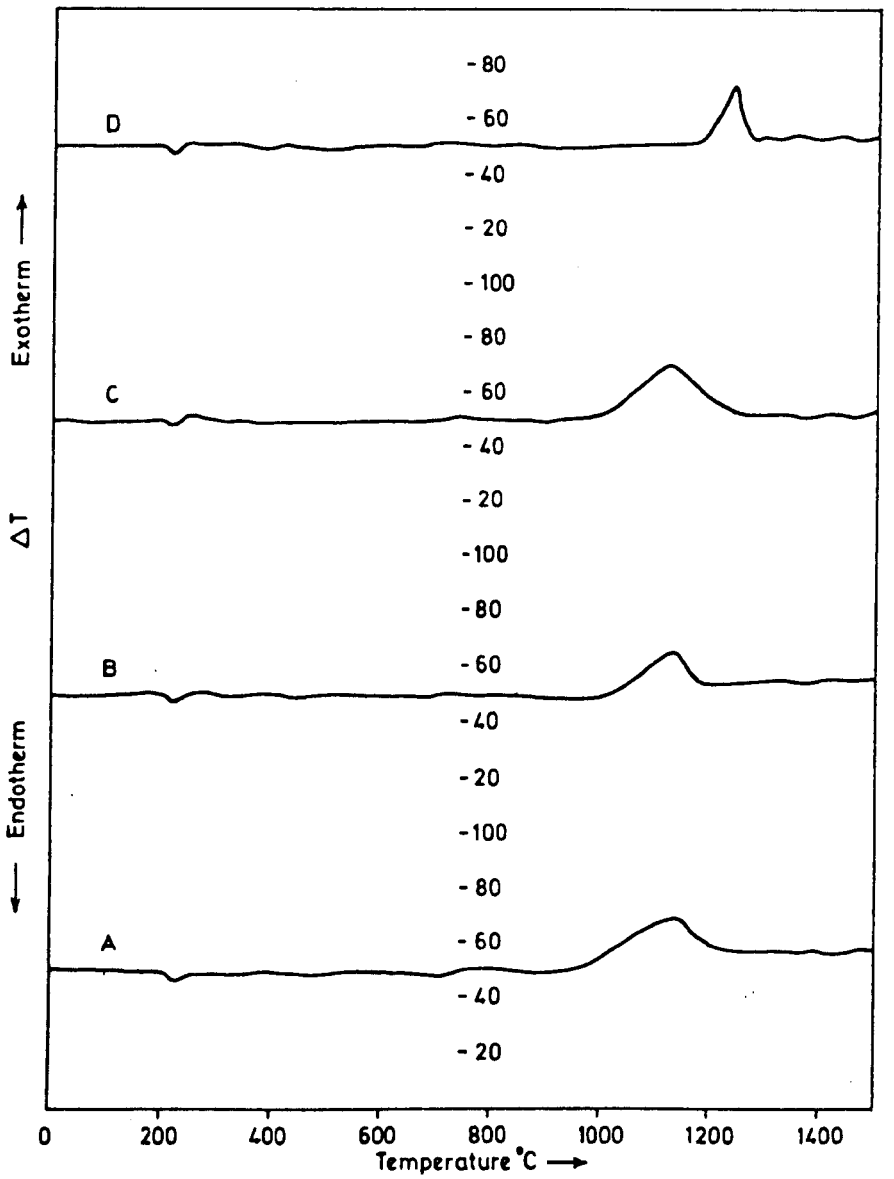

Fig. 4.30: Typical differential thermal analysis curves of (A) CA, (B) CA_2, (C) Secar "250", (D) CA_6, (E) α-Al_2O_3 + 10 wt% $AlPO_4$ (cristobalite form).

Composition (wt%)	Firing Conditions		Phase identification (relative amount)	Other observations
	Temp. (°C)	Time (hours)		
CA 95 $AlPO_4$ 5	300	24	CA > $AlPO_4$	
	600	24	CA	$AlPO_4$ (s.a.)
	900	24	CA > CA_2	No $AlPO_4$
	1200	24	CA > CA_2	No $AlPO_4$
	1300	24	CA > CA_2	$Ca_3(PO_4)_2$ (s.a.)
CA 90 $AlPO_4$ 10	300	24	CA > $AlPO_4$	
	600	24	CA	$AlPO_4$ (s.a.)
	900	24	CA > CA_2	No $AlPO_4$
	1200	24	CA > CA_2	
	1300	24	CA > CA_2	$Ca_3(PO_4)_2$ (s.a.)
CA_2 95 $AlPO_4$ 5	300	24	CA_2 > $AlPO_4$	
	600	24	CA_2 > $AlPO_4$	
	900	24	CA_2	
	1200	24	CA_2 > α-Al_2O_3	No $AlPO_4$
	1300	24	CA_2 > α-Al_2O_3 > CA_6	α-$Ca_3(PO_4)_2$ (s.a.)
CA_2 90 $AlPO_4$ 10	300	24	CA_2 > $AlPO_4$	
	600	24	CA_2 > $AlPO_4$	
	900	24	CA_2	$AlPO_4$ (s.a.)
	1200	24	CA_2 > α-Al_2O_3 > CA_6	No $AlPO_4$
	1300	24	CA_2 > α-Al_2O_3 > CA_6	$Ca_3(PO_4)_2$ (s.a.)

Table 4.8: Summary of XRD data of CA and CA_2 mixed with 5 and 10 wt% $AlPO_4$, cast at room temperature, before firing.

(b) Hot-pressing

Calcium monoaluminate, calcium dialuminate and Secar "250" were mixed with 5% $AlPO_4$ using 0.1 w/c ratio, and hot-pressed under 207 MNm^{-2} pressure at 300°C for 30 minutes. After hot-pressing, samples were fired in air between 300 - 1300°C for 24 hours.

XRD results of the above mixtures are summarised in Table 4.10. An improvement in the strength was observed, for samples hot-pressed before firing, as shown in Fig. 4.31. Mechanical properties and related physical properties are given in Table 4.11.

In general the above results support the conclusion drawn by Gitzen et al.[122], that aluminum phosphate does not behave like a cementitious material when added in prefabricated form. The presence of calcium oxide increases the decomposition rate of aluminum phosphate to α-Al_2O_3 and P_2O_5, which consequently decreases its thermal stability. The formation of $Ca_3(PO_4)_2$ is due to the reaction between P_2O_5 liberated from the decomposition of $AlPO_4$ and CaO. The slight increase in strength and density, however, was probably due to sintering processes.

Composition (wt%)	Firing Conditions		Phase identification (relative amount)	Other observations
	Temp. (°C)	Time (hrs)		
CA 95 $AlPO_4$ 5	300	24	CA > $AlPO_4$	
	600	24	CA	$AlPO_4$ (s.a.)
	900	24	CA > CA_2	No $AlPO_4$
	1200	24	CA > CA_2 - $Ca_3(PO_4)_2$	Mixture α & β
	1300	24	CA > CA_2 > α-$Ca_3(PO_4)_2$	
CA_2 95 $AlPO_4$ 5	300	24	CA_2 > $AlPO_4$	
	600	24	CA_2 > $AlPO_4$ (s.a.)	
	900	24	CA_2	$AlPO_4$ (s.a.)
	1200	24	CA_2 > CA_6 > α-Al_2O_3 > $Ca_3(PO_4)_2$	Mixture α & β $Ca_3(PO_4)_2$
	1300	24	CA_2 > CA_6 > α-Al_2O_3 > α-$Ca_3(PO_4)_2$	
Secar "250" 95 $AlPO_4$ 5	300	24	CA_2 > CA > $AlPO_4$	
	600	24	CA > CA_2 > $AlPO_4$ (s.a.)	
	900	24	CA > CA_2	No $AlPO_4$
	1200	24	CA_2 > CA > β-$Ca_3(PO_4)_2$	
	1300	24	CA_2 > CA	α-$Ca_3(PO_4)_2$ (s.a.)

s.a. = small amount

Table 4.10: Summary of XRD data of CA, CA_2 and Secar "250" + 5 wt% $AlPO_4$, hot-pressed under 207 MNm^{-2} pressure, at 300°C for 30 minutes, and fired for 24 hours.

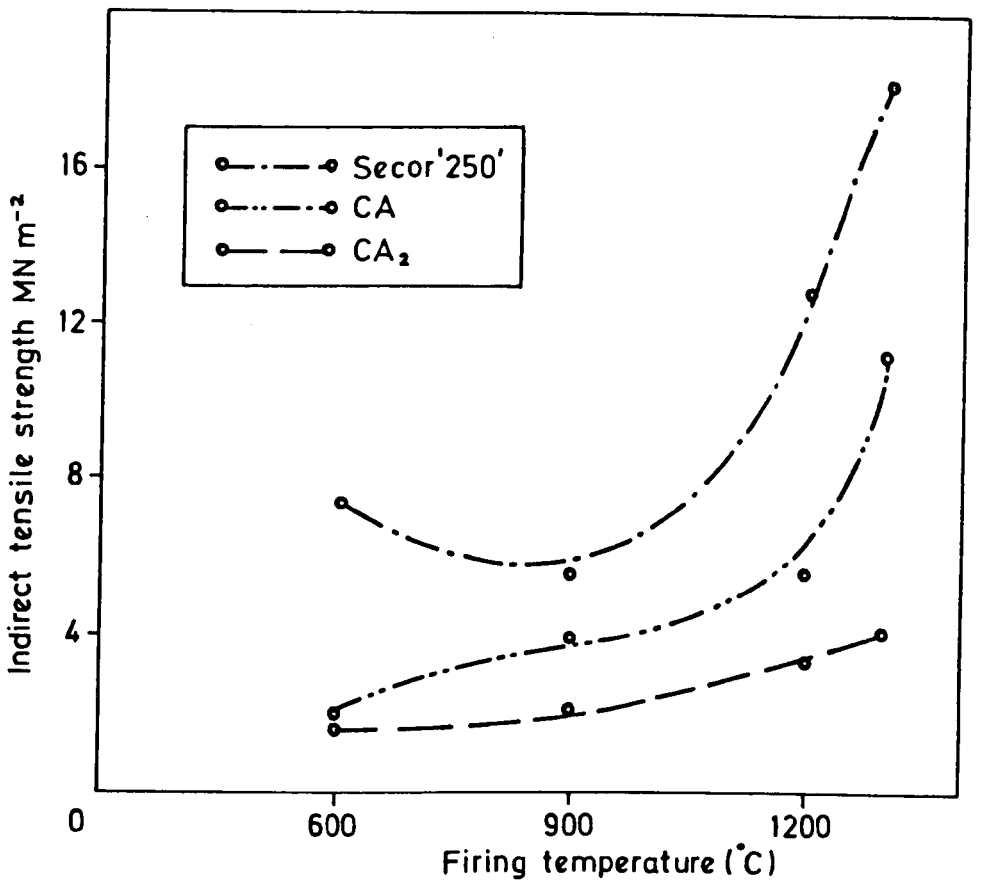

Fig. 4.31: Dependence of strength upon firing temperatures. Samples mixed with 5% $AlPO_4$, hot-pressed under 207 MNm^{-2} pressure, at 300°C for 30 minutes, and fired for 24 hours.

Mixture	Hot-pressing parameters			w/c ratio	Firing conditions		% Change		Density g.cc	Strength MNm^{-2}		Porosity (%)
	Pressure MNm^{-2}	Temp. °C	Time min.		Temp. °C	Time hrs.	wt.	vol.		Compressive	Tensile	
CA + 5% $AlPO_4$	207	300	30	0.1	-	-	-	-	2.12	-	-	-
	207	300	30	0.1	600	24	-2.63	No change	2.066	-	2.09	29.96
	207	300	30	0.1	900	24	-2.706	-.302	2.08	-	3.93	29.50
	207	300	30	0.1	1200	24	-2.90	-1.82	2.12	-	5.5	28.135
	207	300	30	0.1	1300	24	-2.17	-2.94	2.15	-	11.3	27.12
CA_2 + 5% $AlPO_4$	207	300	30	0.1	-	-	-	-	1.94	-	-	-
	207	300	30	0.1	600	24	-1.48	No change	1.93	-	1.8	32.51
	207	300	30	0.1	900	24	-1.59	-.232	-	-	2.00	-
	207	300	30	0.1	1200	24	-2.612	-1.57	1.98	-	3.2	30.77
	207	300	30	0.1	1300	24	-1.78	-2.82	2.014	-	3.9	29.58
Secar "250" + 5% $AlPO_4$	207	300	30	0.1	-	-	-	-	2.105	-	-	-
	207	300	30	0.1	600	24	-1.94	-	2.085	-	7.3	26.84
	207	300	30	0.1	900	24	-2.05	-.579	2.072	-	5.5	27.30
	207	300	30	0.1	1200	24	-3.8	-2.6	2.11	-	12.8	26.00
	207	300	30	0.1	1300	24	-2.5	-3.62	2.15	-	18.1	24.56

Table 4.11: Mechanical properties and related physical properties of CA, CA_2 and Secar "250" mixed with 5 wt% $AlPO_4$ (cristobalite form). Samples hot pressed under 207 MNm^{-2} pressure, at 300°C for 30 minutes, and fired at different temperatures.

4.3 Discussion

(a) Samples cast at room temperature, followed by firing

Phosphoric acid acts as a bonding material, and as stated before (Section 2.4) the addition of aluminum oxide will increase the strength whereas the presence of calcium oxide will decrease its effectiveness as a bonding material[46].

Figure 4.32 confirms the above suggestion, whereas the higher the $\frac{C}{C+A}$ ratio, the lower the strength at all firing temperatures. This may be due to:

(1) In the case of α-Al_2O_3 + H_3PO_4 mixtures, XRD quantitative analysis shows that there is an increase in the amount of $AlPO_4$ formed *in situ* with increasing firing temperatures, Table 4.2. By plotting the percentage of $AlPO_4$ against strength and firing temperatures, Fig. 4.33, it is obvious to notice that the increase of strength is associated with an increase of the percentage of $AlPO_4$ bonding material.

(2) In the case of different calcium aluminate mixtures, with phosphoric acid (Fig. 4.32), the percentage of $AlPO_4$ formed *in situ* decreases with increasing the $\frac{C}{C+A}$ ratio.

(3) The microstructure is more dense with the lower $\frac{C}{C+A}$ ratio, but it is more open with the higher $\frac{C}{C+A}$ ratio (Figures 4.11A & B, 4.19B, 4.23B and 4.26B).

(4) The mixture α-Al_2O_3 + H_3PO_4 does not show any decomposition of $AlPO_4$ when fired up to 1300°C for 24 hours, whereas in calcium aluminate mixtures with phosphoric acid, $AlPO_4$ completely decomposed after firing at 1200°C to Al_2O_3 and P_2O_5.

(5) Owing to the decomposition of $AlPO_4$ in higher temperature range (i.e. 1200 and 1300°C), $Ca_3(PO_4)_2$ was formed in calcium aluminate mixtures. Therefore, the thermal decomposition of $AlPO_4$ is assisted by CaO.

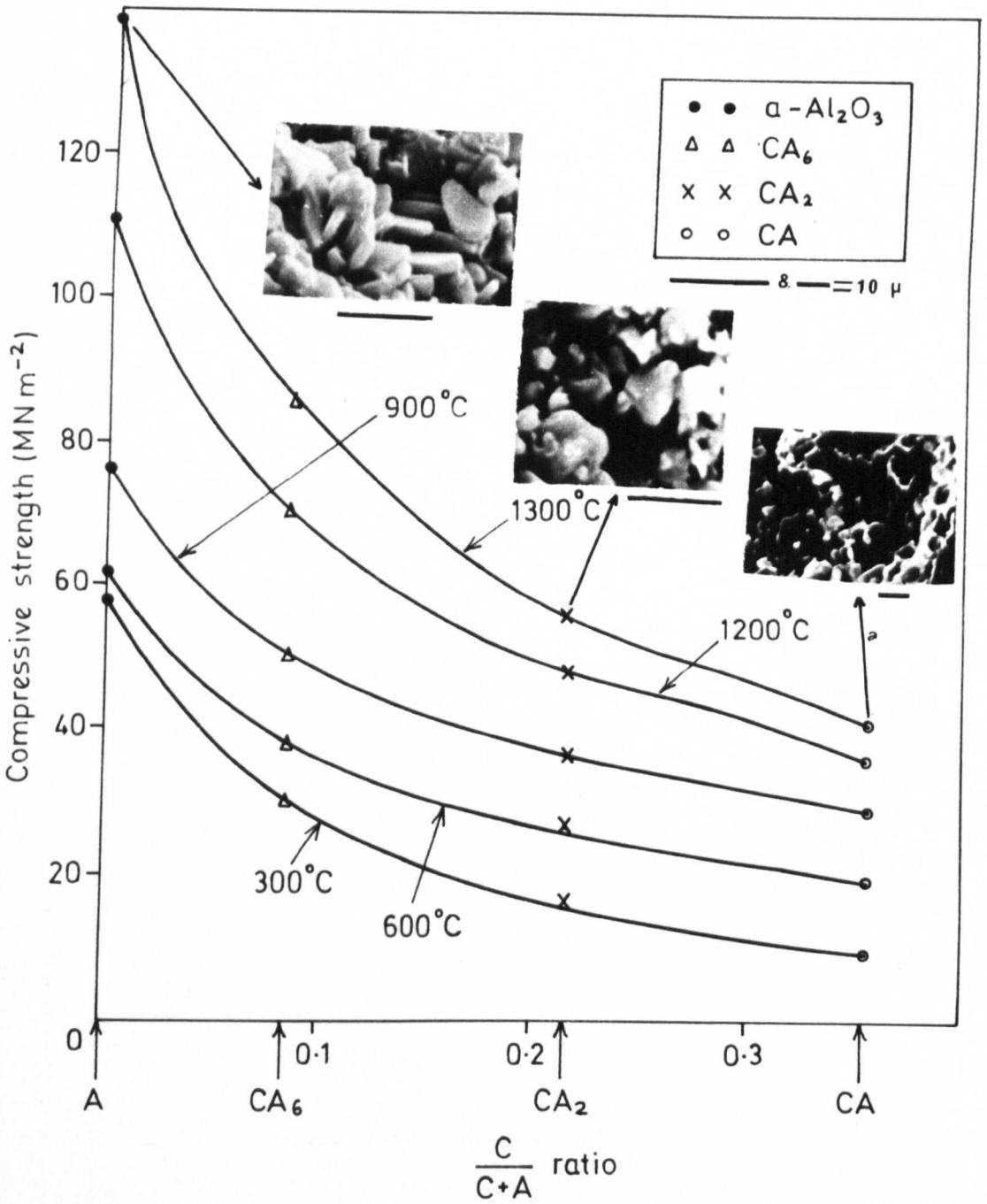

Fig.4·32 Relationship between compressive strength and $\frac{C}{C+A}$ ratio. Sample mixed with 10% H_3PO_4 and fired at various temperatures.

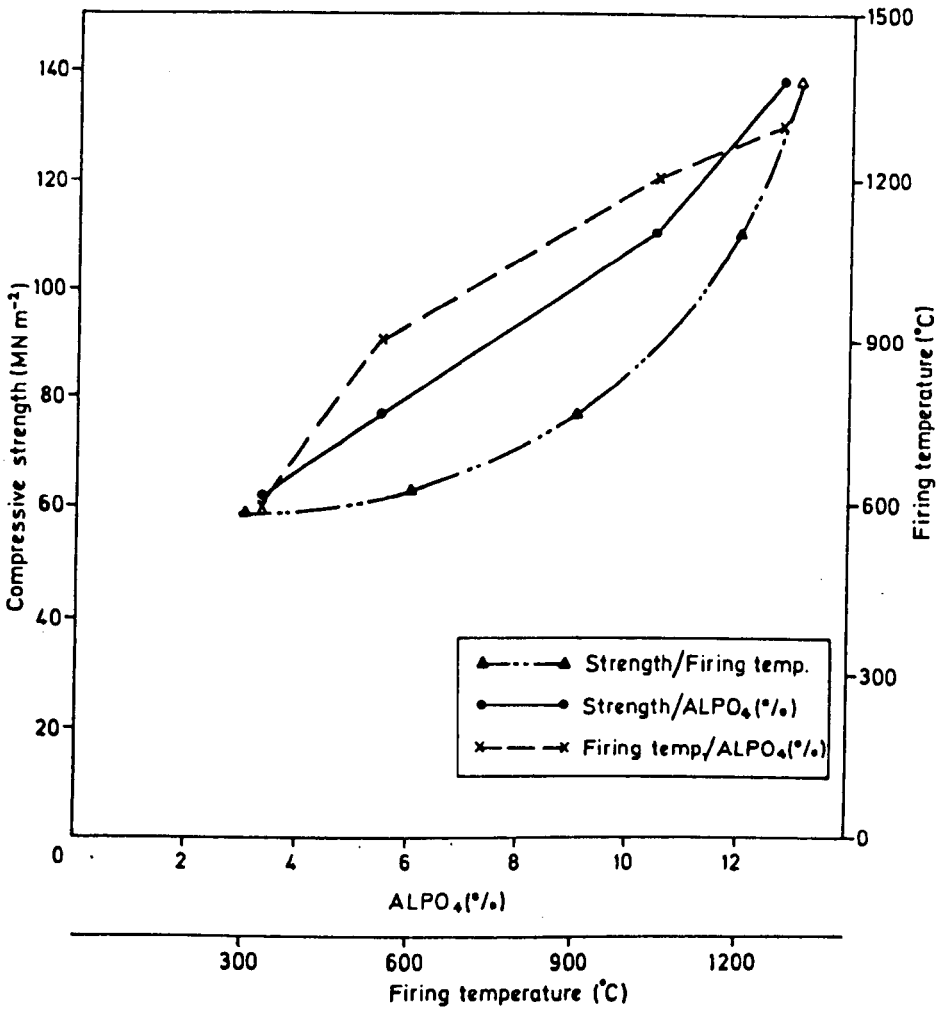

Fig. 4.33: Dependence of strength upon firing temperatures and the percentage of $AlPO_4$.

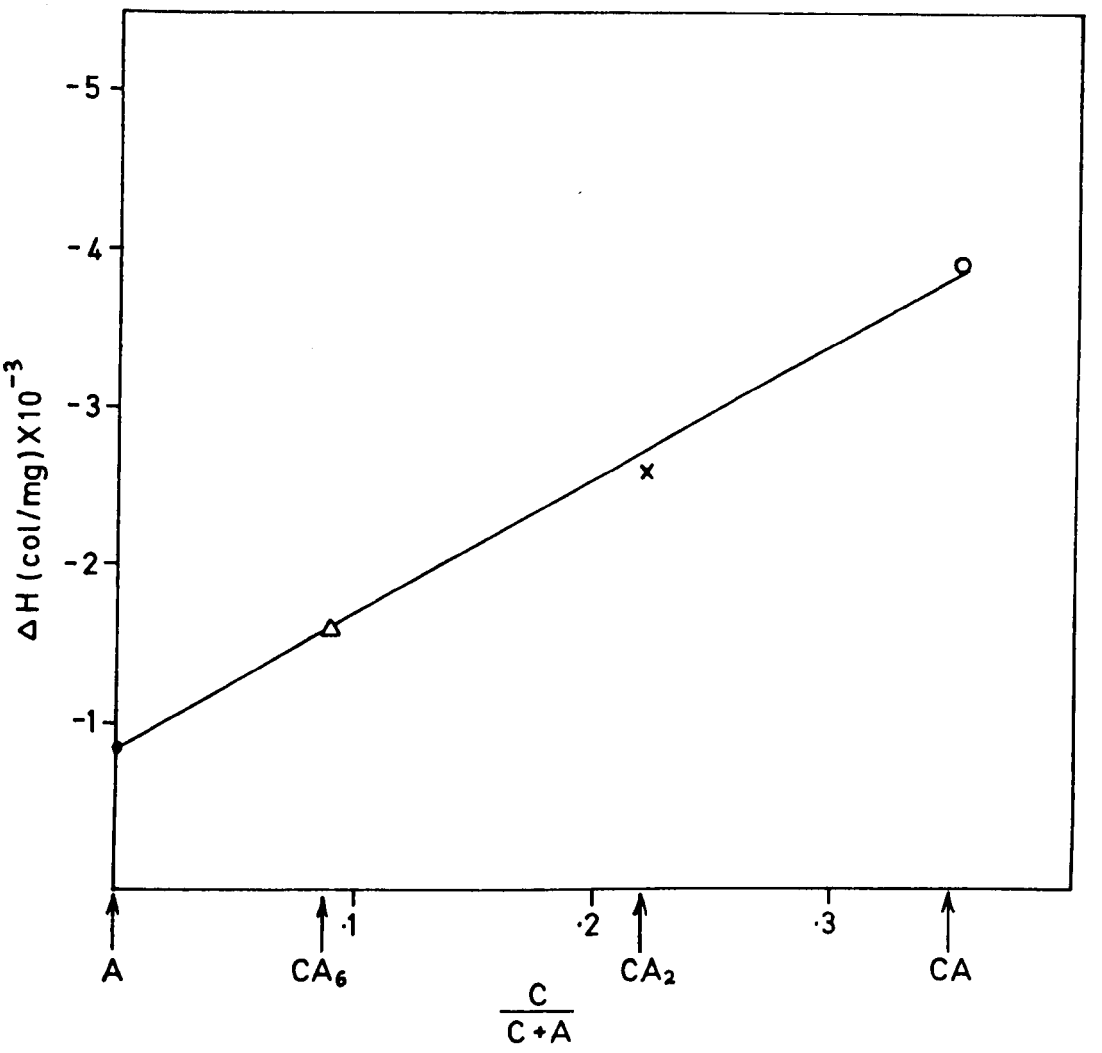

FIG. 4.34: The relationship between ΔH and $\frac{C}{C+A}$ ratio. Samples mixed with 10% H_3PO_4.

From DTA results, Fig. 4.1 and Table 4.1, the first exothermic reaction is due to the formation of crystalline $AlPO_4$. A relationship between the $\frac{C}{C+A}$ ratio and heat of reaction (ΔH^o) in each mixture is shown in Fig. 4.34. It was found that ΔH is increased with increasing the $\frac{C}{C+A}$ ratio.

(b) Hot Pressing

The results of this work, carried out under hot-pressing conditions, show that the reaction between the different starting materials and phosphoric acid takes place at relatively low temperatures compared with reactions in section (a) above. Hot-pressing in this work can be considered as involving a chemical reaction. Figure 4.4 shows that α-Al_2O_3 and H_3PO_4 react to form $AlPO_4$, cristobalite form, at 200°C. It has been found also that there is a relationship between the hot-pressing temperature at which crystalline $AlPO_4$ is formed *in situ* and the $\frac{C}{C+A}$ ratio, under constant pressure (207 MNm^{-2}) for constant time (30 minutes). This relationship is given in Fig. 4.35 which shows that by increasing the CaO content, the minimum hot-pressing temperature at which anhydrous $AlPO_4$ was formed is raised. Table 4.12 gives the quantitative analysis of the different mixtures for the percentage of $AlPO_4$ at different hot-pressing temperatures. It is of interest to note that the percentage of $AlPO_4$ in the mixture α-Al_2O_3+H_3PO_4 did not significantly increase from hot-pressing at 200 up to 700°C (from 9.3-10.7%), Fig. 4.36A. As a result of the present study it is proposed that the reaction is almost complete at a temperature as low as 200°C. In addition, in the case of CA_6 + H_3PO_4 mixture, there is a great similarity whereas hot-pressing at 300°C produces about 8% $AlPO_4$.

However, in calcium di- and monoaluminate, the reaction takes place at about 400 and 700°C respectively. The percentage of $AlPO_4$ formed *in situ* in these two mixtures is small as expected, due to the relatively high

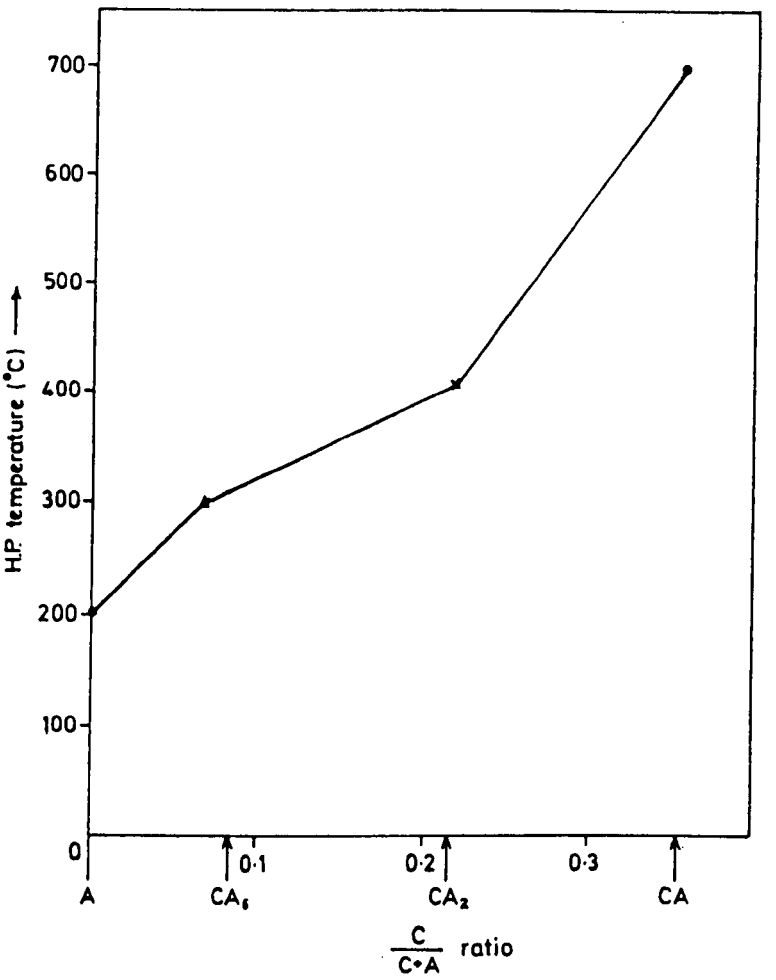

Fig. 4.35: Relationship between $\frac{C}{C+A}$ ratio and the minimum H.P. temperature at which anhydrous $AlPO_4$ is formed.

Hot-pressing Temp. °C	% of crystalline $AlPO_4$ formed in situ by mixing 10 wt% H_3PO_4 with:			
	α-Al_2O_3	CA_6	CA_2	CA
200	9.3	-	-	-
300	8.9	8	-	-
400	9.2	7	1.8	-
500	8.93	5.38	traces	-
600	10.5	5.30	traces	-
700	10.25	7.23	3.8	2.5

Table 4.12: Dependence of the percentage of $AlPO_4$ upon hot-pressing temperatures.

Firing Temp. °C	% of crystalline $AlPO_4$ formed in situ by mixing 10 wt% H_3PO_4 with:			
	α-Al_2O_3	CA_6	CA_2	CA
300	9.99	9.6	not detected	not detected
600	12.00	9.1	traces	traces
900	11.2	7.8	3.2	2.2
1200	12.12	-	-	-
1300	14.00	-	-	-

Table 4.13: Dependence of the percentage of $AlPO_4$ on firing temperature. Samples were previously hot-pressed (under 207 MNm^{-2} for 30 minutes at 300°C).

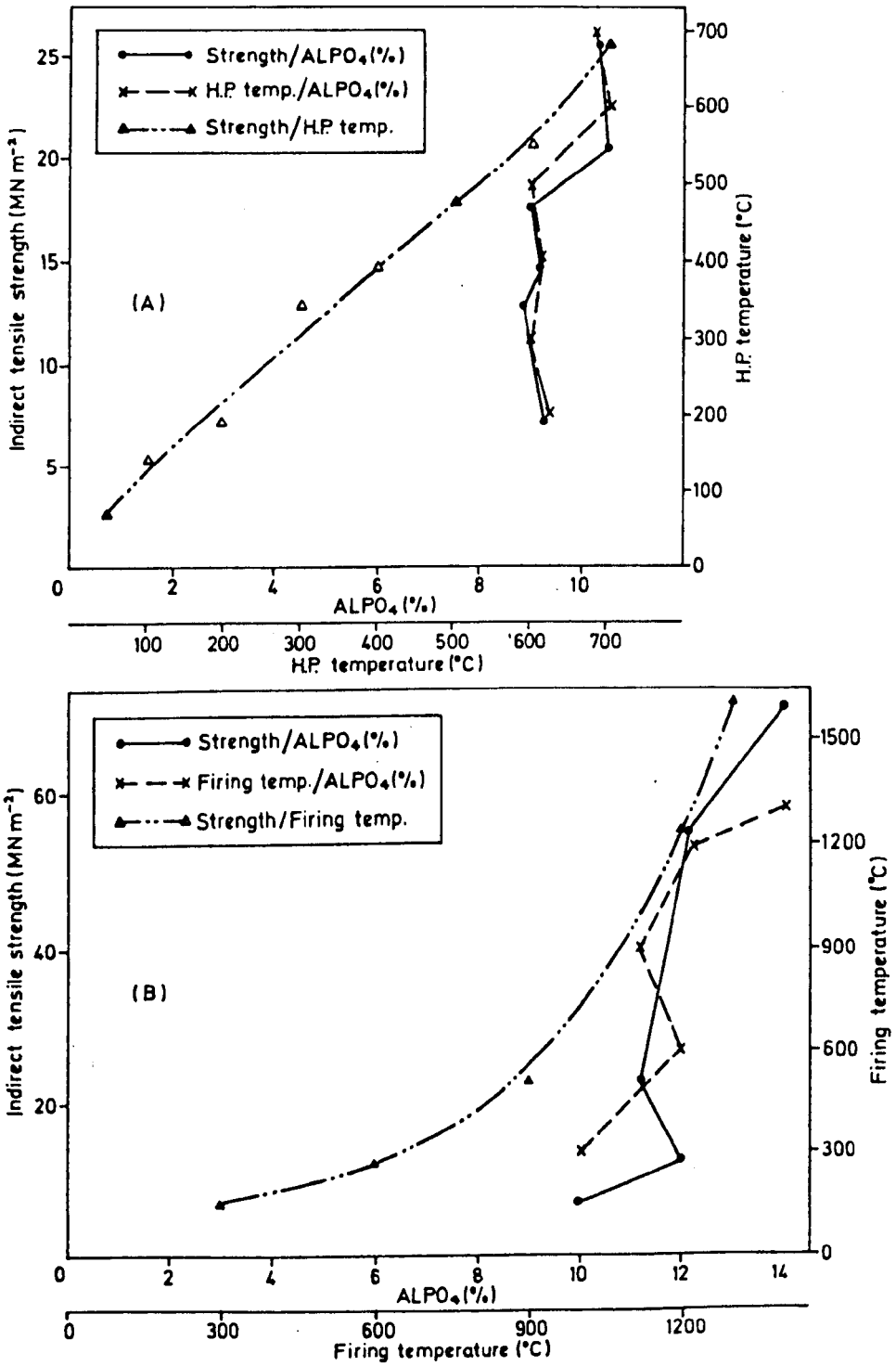

Fig. 4.36: Dependence of strength on (A) hot-pressing temperatures and the percentage of $AlPO_4$, (B) firing temperatures and the percentage of $AlPO_4$.

content of CaO compared with the above two mixtures (i.e. α-Al_2O_3 and CA_6 mixtures).

Quantitative analysis of $AlPO_4$ in the fired samples (previously hot pressed) (Table 4.13 and Fig. 4.36B) confirmed that the reaction which had taken place for 30 minutes under hot-pressing conditions was nearly complete. Table 4.13 shows that in the case of α-Al_2O_3 + H_3PO_4 mixture, a small increase in the percentage of $AlPO_4$ was noticed between those samples which had been hot-pressed at 300°C for only 30 minutes, and those which were fired after that at 300°C in air for 24 hours (8.9-9.9%). However, the overall difference in the percentage of $AlPO_4$ between samples hot-pressed at 300°C for 30 minutes and samples fired after that at 1300°C is also relatively small (i.e. 8.9-14%).

The noticeable phenomenon in the hot-pressed group is the shifting in the position of the main $AlPO_4$ peak ($2\theta = 21.77°$), which may signify a change in the volume of the cell.

In the case of CA_6 mixture, slight changes of unit cell dimensions of $AlPO_4$ were also observed.

Comparing room temperature casting followed by firing, with hot-pressing followed by firing, for α-Al_2O_3 + 10% H_3PO_4 mixes (Tables 4.2 and 4.4), a number of changes are evident:

(1) In the former mix there is a fourfold increase in the percentage of $AlPO_4$ produced by firing in the range 600- 1300°C (3.16 - 12.78%).

(2) If samples are hot-pressed before firing, the increase of the percentage of $AlPO_4$ is very small over the same range of temperatures (12.2 - 14%).

(3) In the latter mix, the samples showed about four times higher strength values and the microstructure is more compact than in the former mix.

It seems unlikely from these results (Figures 4.33 and 4.36) that the gain in strength of the hot-pressed samples is related to the amount

of $AlPO_4$ formed. Decreased porosity is in fact more likely to be responsible.

The achievement of theoretical density, i.e. zero porosity, was not the aim of this work, but as expected, all the hot-pressed samples were less porous and had higher densities than the room-temperature cast samples (Figures 4.11B, 4.19B, 4.23B and 4.26B). The minimum porosity in this group was about 22.5% and the higher density was 77.5% of theoretical. During the firing process after hot-pressing there was a decrease in the porosity especially at higher temperatures. The sintering process could also take place more easily than in those samples which were cast at room temperature.

From X-ray analyses, it was found that, when calcium hexa-aluminate mixture was hot-pressed at 200°C, two new peaks appeared, a strong one at $2\theta = 26.3°$ and a medium one at 20.7° (Fig. 4.14). These peaks may indicate the presence of one of the polymorphic forms of aluminium phosphate (possibly berlinite form) and this was further suggested by I.R. analysis (Fig. 4.16). By increasing hot-pressing temperature to 300°C, the two peaks above disappeared, whereas another two peaks at $2\theta = 21.63°$ and 21.52° were detected (Fig. 4.15). The latter peaks may represent a mixture of tridymite and cristobalite forms of aluminium phosphate, but mainly cristobalite. On the other hand, by increasing hot-pressing temperatures up to 700°C, and after firing in air up to 900°C, X-ray analysis showed that the main peak representing cristobalite predominated with a small shift of position which may signify a change in the volume of the cell figures (Figures 4.15 and 4.17).

These observations may lead to a suggestion that under hot-pressing conditions, the reconstructive change in the polymorphic forms of aluminium phosphate formed <u>in situ</u> can take place at <u>low temperatures</u>.

One of the interesting phenomena, which was observed in calcium

aluminate mixtures with H_3PO_4 (in particular calcium hexa- and dialuminate mixtures) is the decrease in strength values by increasing hot-pressing temperature from 200–600°C (Fig. 4.9). This decrease in strength was accompanied by an increase in the porosity (Table 4.3). Porosity in calcium hexa-aluminate and calcium dialuminate mixtures was found to increase by about 19.4 and 8.6% respectively in the range of hot-pressing between 200–600°C. Furthermore, samples of calcium hexa-aluminate and calcium dialuminate mixtures hot-pressed at 200°C show a lower porosity than those corresponding samples fired in air at 1300°C for 24 hours, previously hot-pressed (under 207 MNm^{-2}, at 300°C for 30 minutes).

This noticeable increase in porosity can be explained on the basis of the theory for movement of pores through a solid which has been discussed by a number of authors[123,124]. Porosity is apparent both on the grain boundaries (intergranular) and within the grain (intragranular). Porosity within the grain causing failure gives a lower porosity dependence, while porosity around the grains gives high porosity effects. Kingery and Francois[123] reported that examination of micrographs of porous sintered UO_2 shows that pores are present almost entirely at the grain corners (intergranular). This means that, in contrast to particulate inclusions, pores on the grain boundaries may be left behind by the moving boundary or migrate with the boundary gradually agglomerating at grain corners. Nichols[124] has discussed this phenomena, considering two gas-filled bubbles in a solid matrix with radii r_1 and r_2 with $r_1 < r_2$. He divided the ensuing process into two stages. Coalescence stage, in which the two bubbles in contact combine into one bubble of radius approximately r_3 ($r_3^3 = r_1^3 + r_2^3$) which then increases in size to a final radius r_4 ($r_4^2 = r_1^2 + r_2^2$) with a continuous decrease in free energy and a net increase in volume. Volume adjustment stage, which may be required to re-establish equilibrium. The author shows that for all practical cases, the

coalescence will occur first and the volume adjustment may then occur over a relatively much longer time.

On the other hand, hot-pressing of calcium aluminate mixtures (especially CA_6 mixture) can be considered as a reaction hot-pressing, i.e. formation of some compounds in situ. The results show that the chemical reaction is greatly dependent on the hot-pressing temperature. Therefore, the decrease of porosity with increasing hot-pressing temperature may be due to liberation of some gases which cause swelling.

Present results show that in the presence of phosphoric acid, some CA_2 is present in the mixture $CA + H_3PO_4$ after firing at only 900°C. In addition CA_2 goes to CA_6 + some α-Al_2O_3 and CA_6 goes to α-Al_2O_3. Infra-red data (Figures 4.18, 4.22, 4.25 and 4.28) showed the transformation of CA to CA_2 and CA_6 to α-Al_2O_3 at higher temperatures. The reference spectra for pure materials used in this study are shown in Fig. 4.37.

Commercial material which was also used in this study, Secar "250" cement, behaved like a mixture of $CA + CA_2$. The dependence of strength upon the bulk density is given in Fig. 4.38. Generally the higher the bulk density, the higher is the strength. The percentage of weight loss during firing is given in Fig. 4.39, which indicates that the higher the CaO, the higher is the weight loss. Infra-red analysis given in Figures 4.6, 4.16, 4.21 and 4.24 confirms the formation of $AlPO_4$ in the above mixtures during hot-pressing, but it is difficult to differentiate by I.R. between the various forms of anhydrous $AlPO_4$ (especially tridymite and cristobalite) in particular when they are formed in situ, because the characteristic wavenumbers are very close[125].

(c) Strength-porosity relationship

The major structural effects in most ceramics arise from porosity, which in turn affects mechanical properties. Pores obviously decrease the cross-sectional area on which the load is applied, but also act as

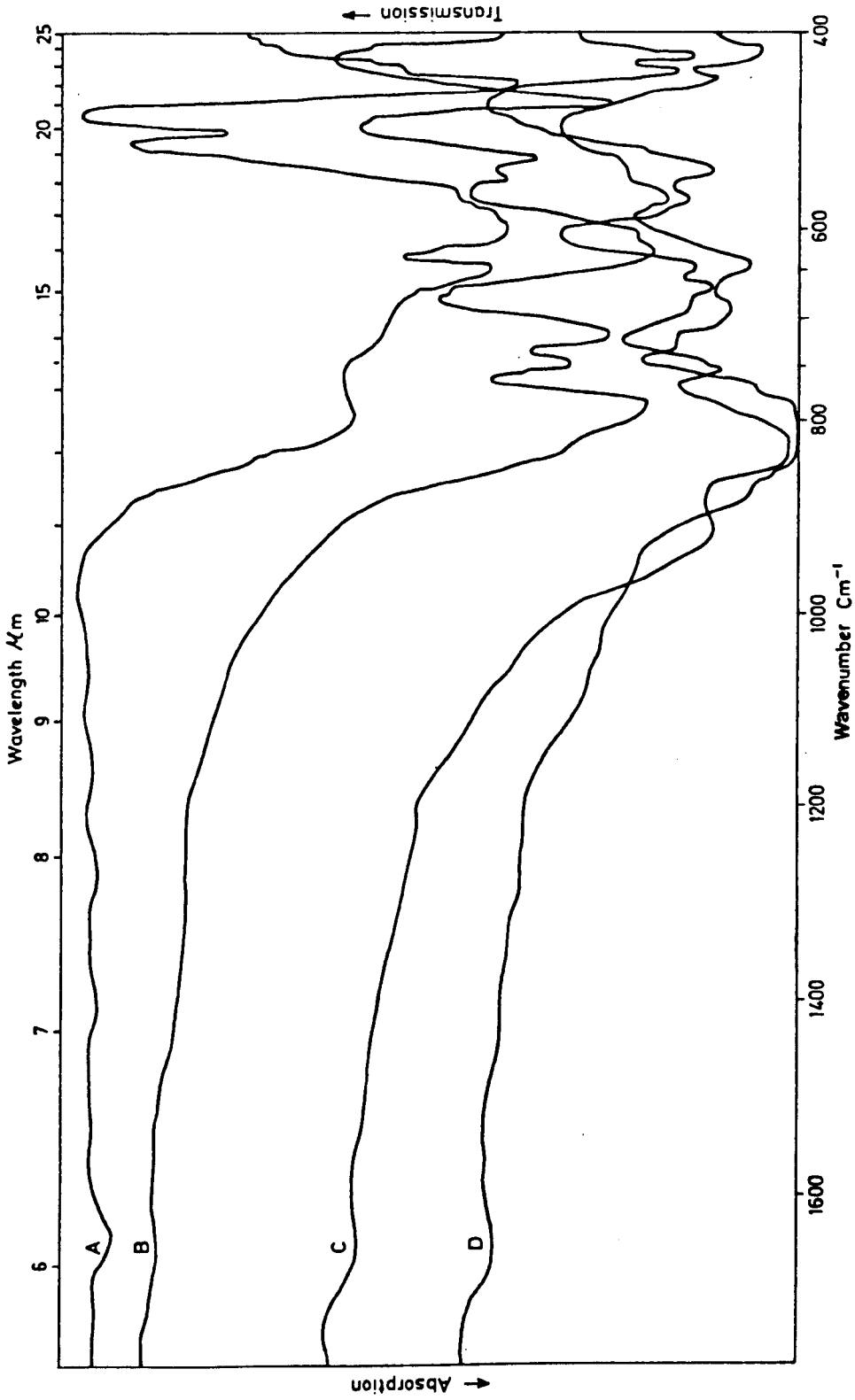

Fig. 4.37: Infra-red spectra of the starting materials (A) α-Al_2O_3, (B) CA_6, (C) CA_2, (D) CA.

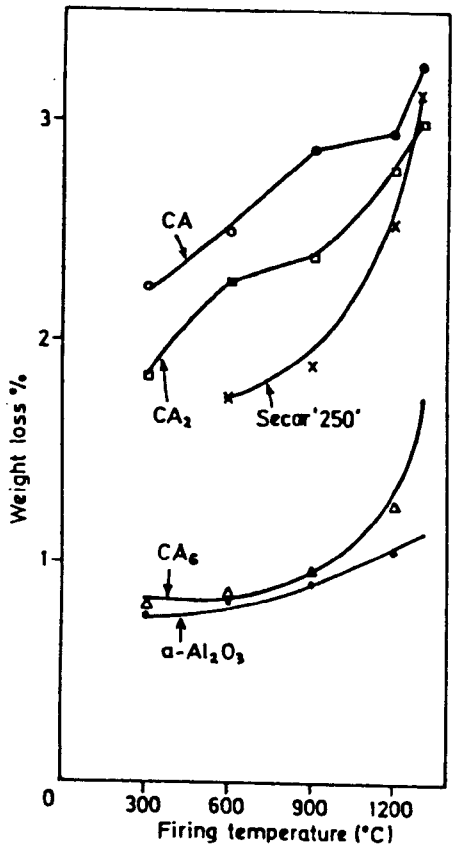

FIG. 4.39: Loss-on-heating curves. Samples mixed with 10% H_3PO_4 previously hot-pressed (under 207 MNm^{-2} pressure for 30 minutes at 300°C) before heating.

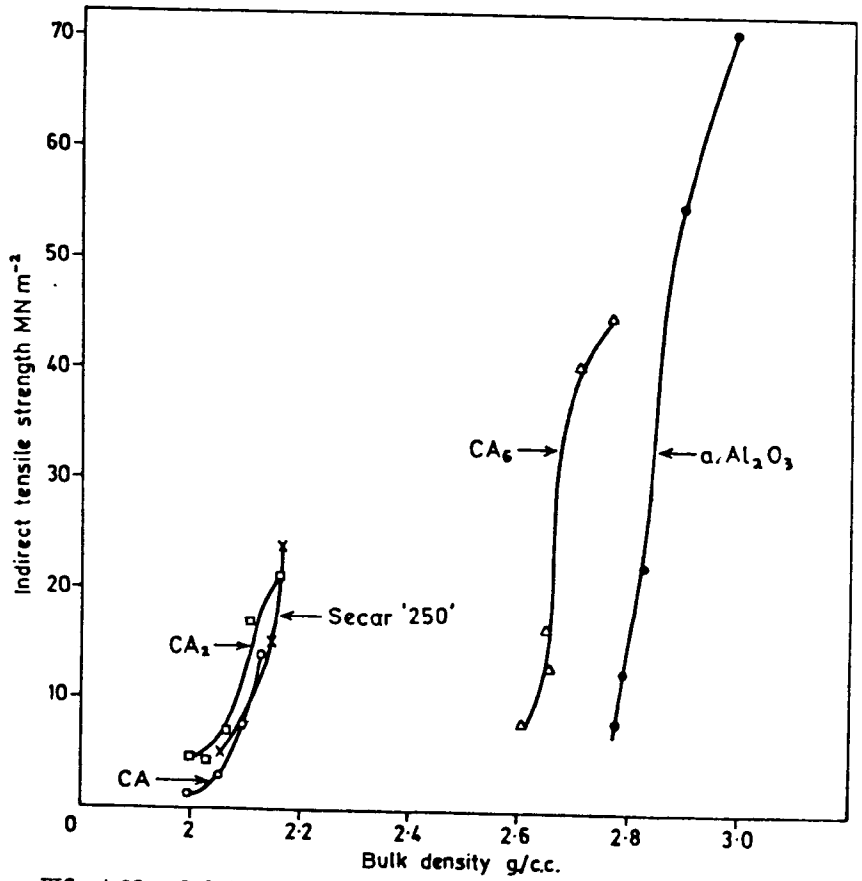

FIG. 4.38: Relationship between bulk density and strength. Samples mixed with 10% H_3PO_4 previously hot-pressed (under 207 MNm^{-2} pressure for 30 minutes at 300°C).

stress concentration points[126]. On the other hand, high porosity reduces Young's Modulus (E) and the effective surface energy for fracture initiation (γ_i) and increases the size of the largest inherent surface flaw (C), all of which reduce strength[127]. Fracture is seen to originate from large, not small, pores in a body having both types of pores[128]. Hasselman[129] has considered some aspect of pores as flaws, whereas Evans and Davidge[127] were major developers of this concept for large pores. Recently, Rice[128] has extended his concept of pores as integral part of flaw by adapting it to pores of essentially all sizes and locations. He concludes that uniform distributions of different types of pores will have similar strength-porosity trends, which will follow the exponential relation, but (n) values will depend on pore location, size and shape. There has generally been no attempt to specifically derive a theory of the porosity dependence of compressive strength, whereas the exponential relation was first empirically applied to compressive strength data[128].

Compressive strength-porosity relationships for fired samples previously hot-pressed (under 207 MNm^{-2} for 30 minutes at 300°C) have been elucidated using some empirical equations. Figure 4.40 shows this relationship plotted on the basis of equation 2.7[108] and Figure 4.41 on the basis of equation 2.8[109]. From the figures, it can be observed that all the materials obtain high values of (n) in equation 2.7 and high slope values in equation 2.8. This, as previously discussed by many investigators[128,130], may be due to inhomogeneous porosity. In addition, it can also be noted that the difference in the starting materials affects the porosity to some extent. This may be why the data in both graphs fit more than one line. However, α-Al_2O_3 and CA_6 mixtures showed a great similarity to each other in this relationship, whereas other calcium aluminate mixtures behave approximately the same.

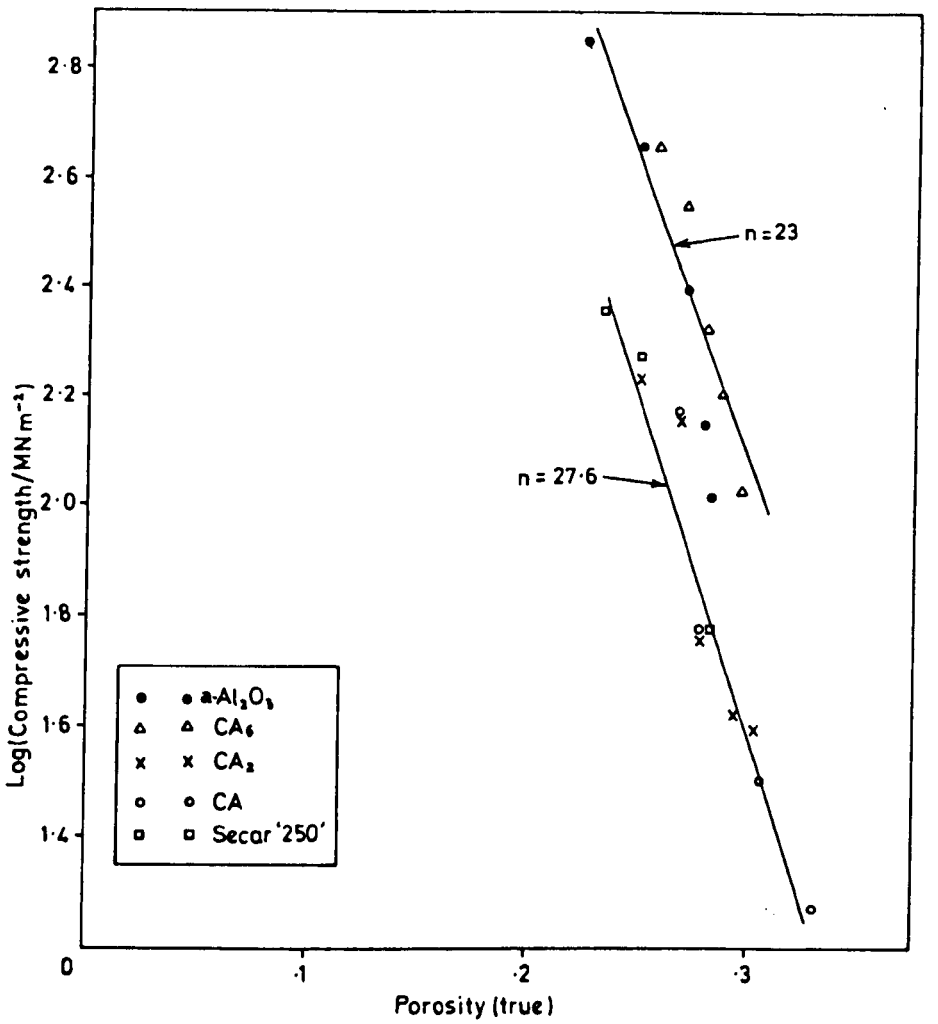

Fig. 4.40: Log strength-porosity relationship; data plotted on the basis of equation (2.7).

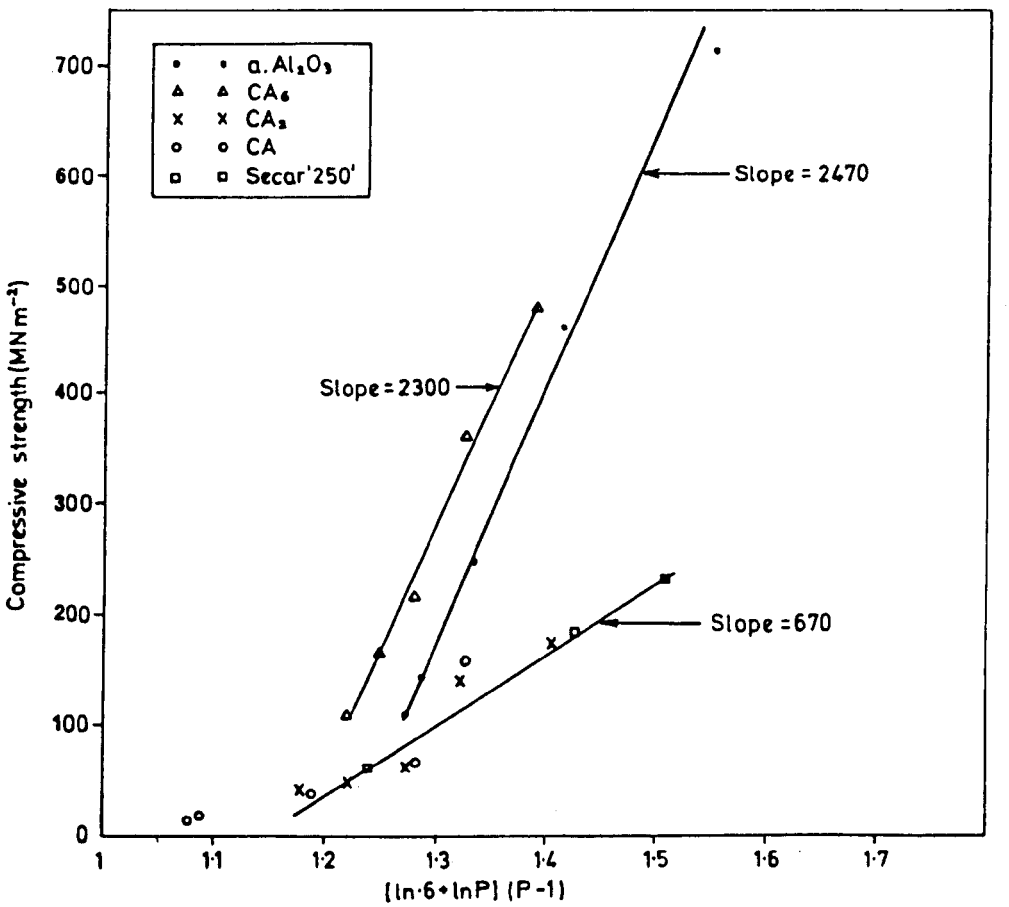

Fig. 4.41: Strength-porosity relationship; data plotted on the basis of equation (2.8).

Another important aspect is the effect of additives or impurities on strength. Additives can either aid or retard densification and hence influence the amount of porosity. They may also influence the shape and size of pores present[128].

Present results show that the addition of phosphoric acid (H_3PO_4) to the different starting materials leads to the formation of aluminium phosphate ($AlPO_4$) in situ, whereas the amount and perhaps the distribution are dependent on the $\frac{C}{C+A}$ ratio. Consequently, it can be suggested that the presence of aluminium phosphate ($AlPO_4$) in the structure may also play a part in influencing the porosity. This may explain the similarity between α-Al_2O_3 and CA_6 mixtures (relatively high $AlPO_4$ content) and the similarity between the other calcium aluminate mixtures (relatively low $AlPO_4$ content). In addition, this may also explain why, for similar porosity, the α-Al_2O_3 and CA_6 mixtures show higher strength than the other calcium aluminate mixtures. Furthermore, based on different location, size and shape of pores, a considerable range of strength behaviour can occur for different bodies over the same porosity range[128].

On the other hand, as stated before (Chapter 1), the effect of grain size on strength was minimised by keeping the specific surface area of all the starting materials nearly the same except for α-Al_2O_3 (Table 3.1). Generally it has been considered that strength increases with decreasing grain size. The present results are consistent with the generally observed behaviour in that the smaller grain size α-Al_2O_3 mixtures exhibit higher strengths than the larger grain size calcium aluminate mixtures.

CHAPTER 5

PHOSPHORIC ACID + BORIC ACID MIXTURE AND PREFABRICATED BORON PHOSPHATE ADDITIVES

5.1 Phosphoric Acid + Boric Acid Mixture

A stoichiometric mixture of phosphoric and boric acid was used as a bonding agent. Throughout the present work 5 and 10% of this mixture was reacted with α-Al_2O_3, whereas only 5% was added to the other calcium aluminate phases. The three different techniques of sample preparation, previously stated in Chapter 4, were applied.

5.1.1 Results

5.1.1.1 α-Al_2O_3 + (H_3PO_4 + H_3BO_3)

(a) Samples cast at room temperature, followed by firing

The same procedures previously described (Sections 3.3.1 and 3.3.3) were followed to mix and fire α-Al_2O_3 with 5 and 10% (H_3PO_4 + H_3BO_3) using .25 w/s ratio.

DTA (Fig. 5.1 and Table 5.1) shows that α-Al_2O_3 + 10% (H_3PO_4+H_3BO_3) mixture produced two endothermic peaks at about 120 and 145°C and two exothermic peaks at about 740 and 1030°C. X-ray analyses, Fig. 5.2, showed that the binary crystalline phases $AlPO_4$ and $9Al_2O_3.2B_2O_3$ were the only two compounds to be detected in the range of firing, i.e. 300-1300°C.

Dependence of strength upon the percentage of the mixture "H_3PO_4 + H_3BO_3" used and upon firing temperatures is shown in Fig. 5.3. The results indicated that 5% "H_3PO_4+H_3BO_3" gave higher strength values than mixing with 10%, especially above 600°C. However, there was a decrease in the strength after firing both mixes above 900°C, but above 1200°C the strength increased rapidly.

Boric oxide (B_2O_3) was also mixed with phosphoric acid in the same stoichiometric ratios, and the mixtures were used as bonding agents with α-Al_2O_3. X-ray analyses showed that there was no significant difference in using B_2O_3 instead of H_3BO_3. Cold crushing strength (Fig. 5.3) using

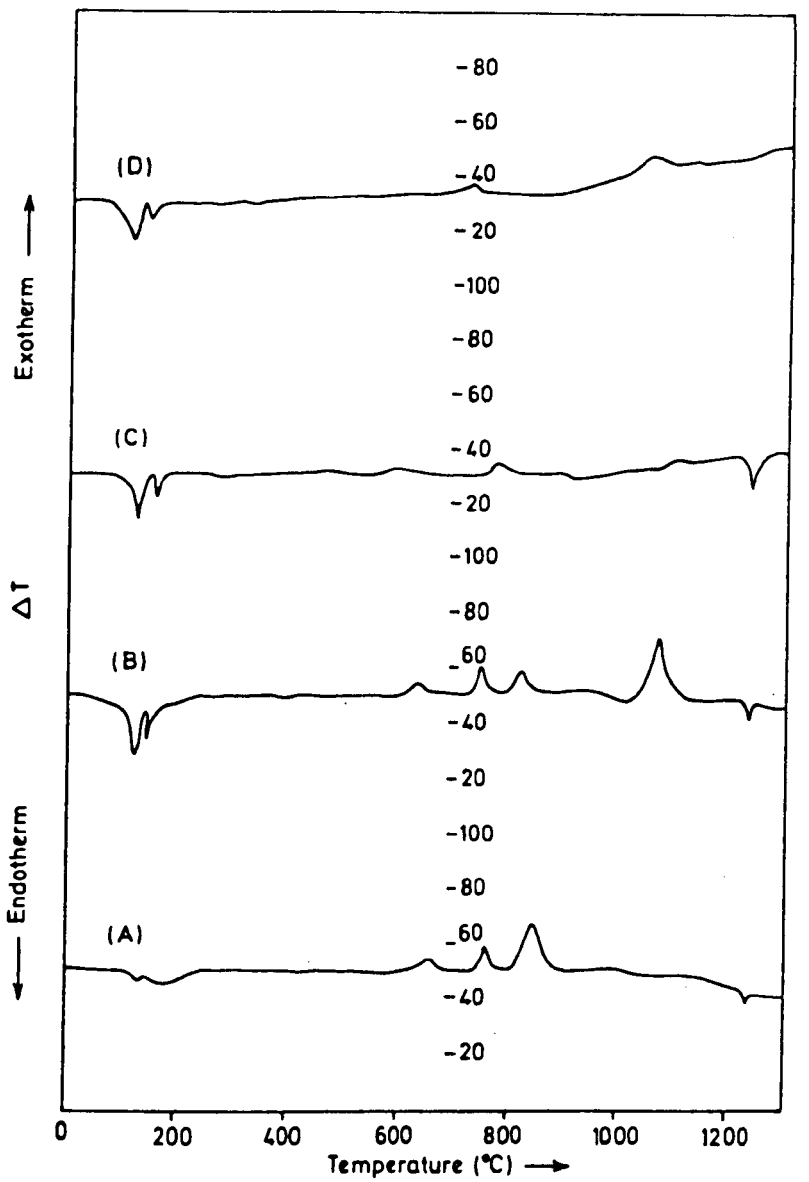

FIG. 5.1: DTA traces of (A) CA + 10% (H_3PO_4+H_3BO_3)
(B) CA_2 + " " "
(C) CA_6 + " " "
(D) α-Al_2O_3 + " "

Mixture	Exothermic reaction			ΔT (°C)	Peak Area A deg.s.mg^{-1}	Endothermic reaction			ΔT (°C)	Peak Area A deg.s.mg^{-1}
	Start °C	Peak °C	End °C			Start °C	Peak °C	End °C		
α-Al_2O_3 + 10% (H_3PO_4+H_3BO_3)	709 1028	726 1050	743 1096	0.045 0.060	0.033 0.135					
CA_6 + 10% (H_3PO_4+H_3BO_3)	755 1075	775 1110	804 1133	0.080 0.070	0.120 0.1575	1225	1240	1256	0.219	0.198
CA_2 + 10% (H_3PO_4+H_3BO_3)	710 776 1030	755 820 1070	776 840 1148	0.44 0.26 0.96	0.468 0.66 2.304	1220	1240	1252	0.102	0.0968
CA + 10% (H_3PO_4+H_3BO_3)	628 705 806	658 755 848	674 782 880	0.067 0.32 0.64	0.084 0.67 1.34	1220	1241	1248	0.0525	0.0415

Table 5.1: Summary of DTA Results in Fig. 5.1.

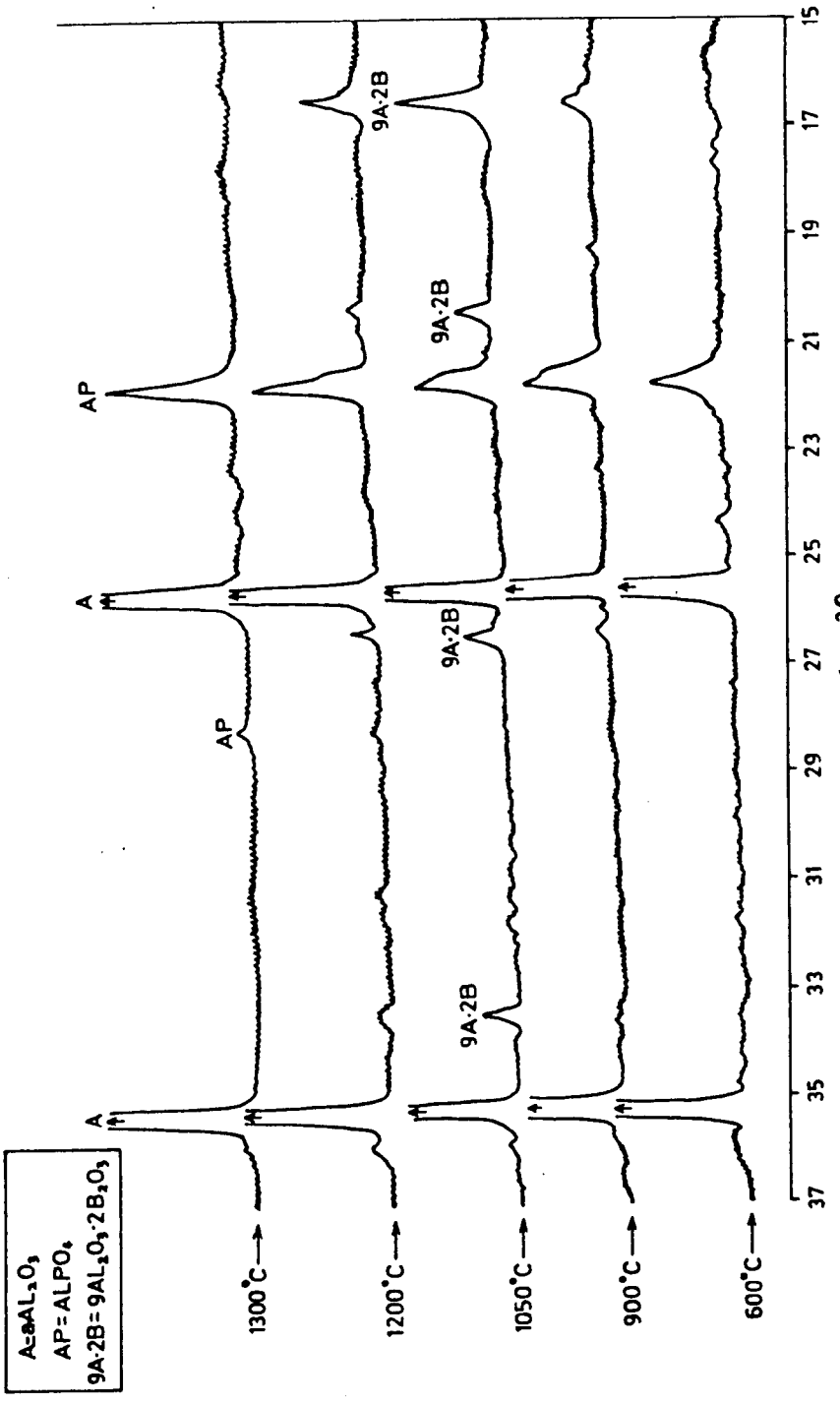

Fig. 5.2: X-ray diffractometer traces of the mixture α-Al_2O_3 + 10% (H_3PO_4 + H_3BO_3); room temperature casting, fired at different temperatures for 24 hours.

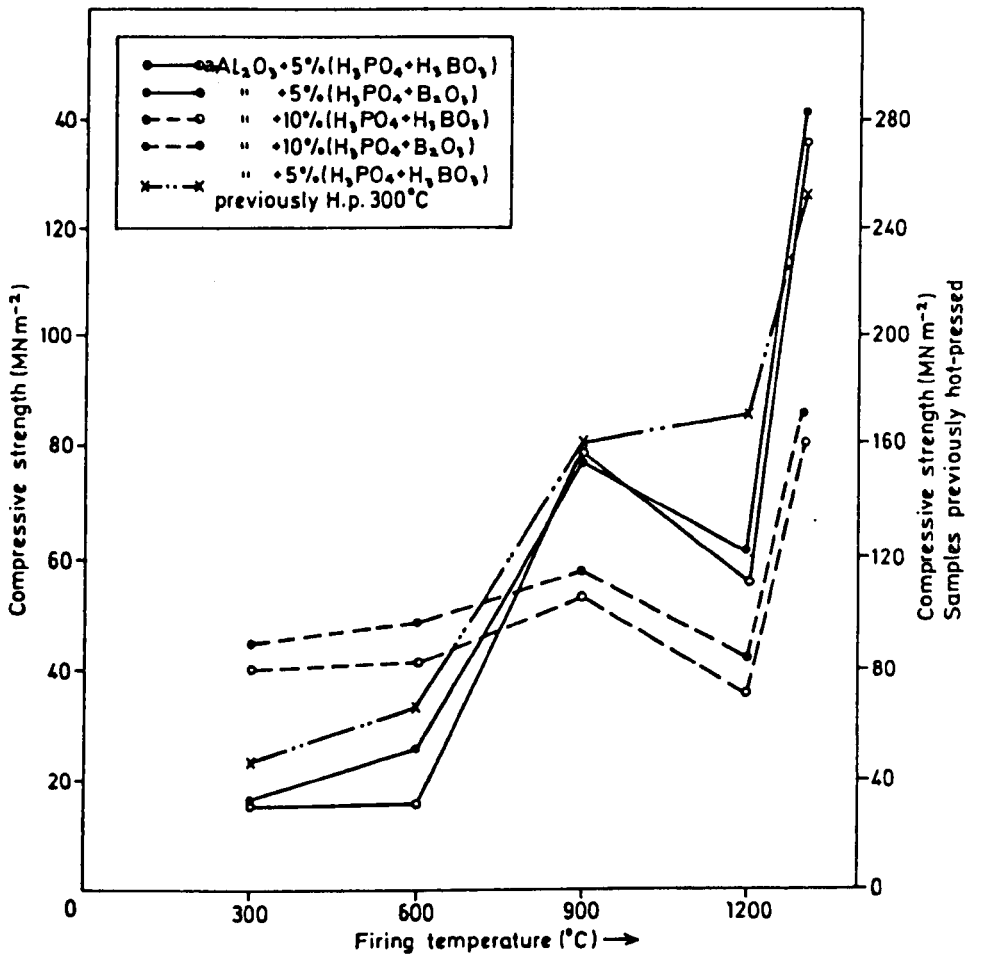

Fig. 5.3: Dependence of strength upon firing temperatures.

Firing Temp. (°C) (24 hrs)	α-Al_2O_3 + 5% (H_3PO_4 + H_3BO_3)					α-Al_2O_3 + 5% (H_3PO_4 + H_3BO_3)*					α-Al_2O_3 + 5% (H_3PO_4 + B_2O_3)				
	AP (%)	9A2B (%)	BD	P (%)	Comp. St.	AP (%)	9A2B (%)	BD	P (%)	Comp. St.	AP (%)	9A2B (%)	BD	P (%)	Comp. St.
300	-	-	2.14	44.5	16.15	-	-	2.52	34.7	47.8	-	-	2.17	43.7	16.56
600	2.6	n.d.	2.125	44.9	15.9	3.2	2.10	2.56	33.7	67.5	2.2	n.d.	2.17	43.5	25.3
900	2.8	1.8	2.19	43.3	78.3	3.45	2.45	2.627	31.4	158.6	2.65	Traces	2.21	42.6	76.0
1200	2.98	2.8	2.26	41.3	55.0	3.20	2.68	2.648	30.85	169.5	2.89	2.8	2.27	41.0	61.3
1300	3.4	-	2.475	35.37	136.75	3.17	-	2.742	28.4	253.7	3.2	-	2.486	35.1	141.0

AP = $AlPO_4$ n.d. = not detected

9A2B = $9Al_2O_3.2B_2O_3$

BD = Bulk density (g.cc)

P = Porosity

Comp.St. = Compressive strength (MNm^{-2})

*Samples previously hot-pressed (under 207 MNm^{-2} pressure, at 300°C for 30 minutes), before firing.

Table 5.2 (Cont.)

Table 5.2 (Cont.)

Firing Temp. (°C) (24 hours)	α-Al_2O_3 + 10% (H_3PO_4 + H_3BO_3)					α-Al_2O_3 + 10% (H_3PO_4 + B_2O_3)				
	AP (%)	9A2B (%)	BD	P (%)	Comp. St.	AP (%)	9A2B (%)	BD	P (%)	Comp. St.
300	-	-	2.12	45.1	40.0	-	-	2.15	44.4	44.9
600	5.8	n.d.	2.12	45.1	41.5	4.95	n.d.	2.15	44.3	48.3
900	6.2	2.27	2.11	44.9	53.6	6.4	3.1	2.14	44.1	57.4
1200	7.1	5.4	2.16	43.5	35.0	7.25	6.8	2.18	43.0	42.3
1300	7.4	-	2.30	39.9	80.0	7.51	-	2.32	39.4	85.3

n.d. = not detected

AP = $AlPO_4$

9A2B = $9Al_2O_3.2B_2O_3$

BD = Bulk density (g.cc)

P = Porosity

Comp.St. = Compressive strength (MNm^{-2})

Table 5.2: Mechanical properties, physical properties and quantitative analysis of the mixtures α-Al_2O_3 + 5 and 10% (H_3PO_4+H_3BO_3), room temperature casting, and previously hot-pressed, fired at different temperatures for 24 hours.

the two additives $[(H_3PO_4+H_3BO_3)$ or $(H_3PO_4+B_2O_3)]$ shows a great similarity. Strength, porosity, density and quantitative analysis of the $AlPO_4$ and $9Al_2O_3.2B_2O_3$ content of all these mixtures after firing in the range 300 -1300°C are given in Table 5.2. Microstructures of some of these samples are shown in Fig. 5.4A & B.

(b) Hot-pressing

A combination of 5% "$H_3PO_4 + H_3BO_3$" and 95% α-Al_2O_3 was mixed using 0.1 w/s ratio. The mixture was hot-pressed under constant pressure (207 MNm^{-2}) for constant time (30 minutes) in the temperature range 200 - 700°C. The procedure which was previously described (Section 3.3.2.2) was followed. In addition, samples prepared under hot-pressing conditions (207 MNm^{-2} pressure, for 30 minutes at 300°C) were also fired in air for 24 hours in the same range of temperatures, i.e. 300 -1300°C.

X-ray analyses of samples prepared at different hot-pressing temperatures show that the reaction took place at about 600°C. Aluminum phosphate, $AlPO_4$, and the compound $9Al_2O_3.2B_2O_3$ were detected after hot-pressing at this temperature. On increasing the hot-pressing temperature to 700°C, no significant change in phase compositions was observed, but the strength was found to increase. Mechanical properties and related physical properties are given in Table 5.3. On the other hand, X-ray analyses of previously hot-pressed samples (Fig. 5.5) showed that $AlPO_4$ and $9Al_2O_3.2B_2O_3$ were present after firing at 600°C. By increasing the firing temperatures up to 1200°C, no significant change in the percentage of $AlPO_4$ or $9Al_2O_3.2B_2O_3$ was observed, Table 5.2. However, a change in the position of 2θ of the main peak of $AlPO_4$ was detected; after firing at 600 and 900°C, 2θ = 21.45°, whereas after 1200°C and 1300°C, 2θ = 21.65°. Mechanical properties and related physical properties are given in Table 5.4. Dependence of strength upon firing temperatures is given in Fig. 5.3. Microstructures of some of these samples are shown in Fig. 5.4C.

Fig. 5.4(A): SEM Micrographs of α-Al_2O_3 mixed with 5% (H_3PO_4 + H_3BO_3), room temperature casting, fired for 24 hours at:

(a) 900°C

(b) 1200°C

(c) 1300°C

Fig. 5.4(B): SEM Micrographs of α-Al_2O_3 mixed with 10% (H_3PO_4 + H_3BO_3), room temperature casting, fired for 24 hours at:

(d) 1300°C

Fig. 5.4(C): SEM Micrographs of α-Al_2O_3 mixed with 5% (H_3PO_4 + H_3BO_3), hot-pressed under 207 MNm^{-2} pressure, for 30 minutes at 300°C, fired for 24 hours at:

(e) 900°C

(f) 1200°C

(g) 1300°C.

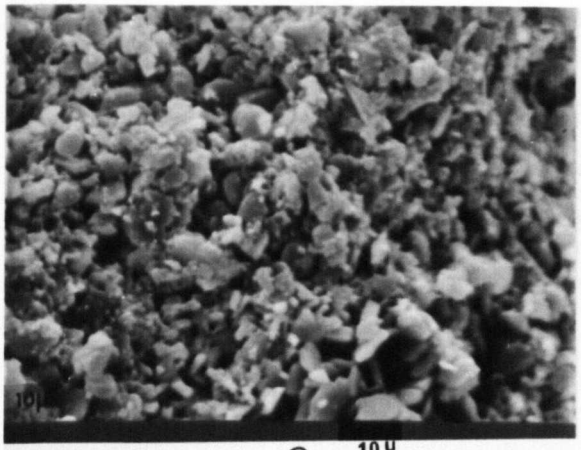

e 10 µ

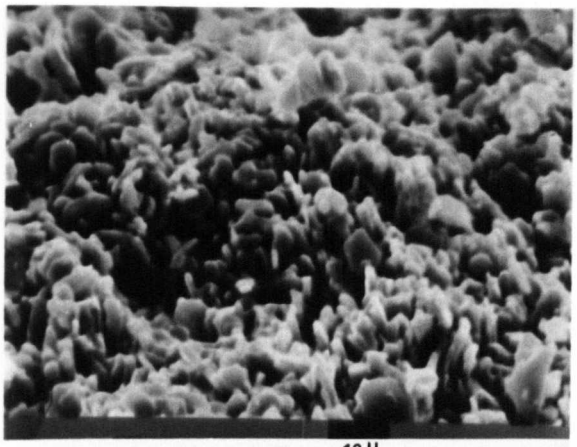

a 10 µ

f 10 µ

b 10 µ

g 10 µ

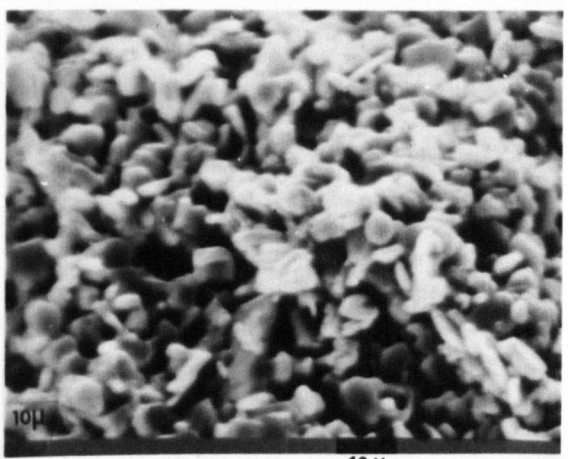

c 10 µ

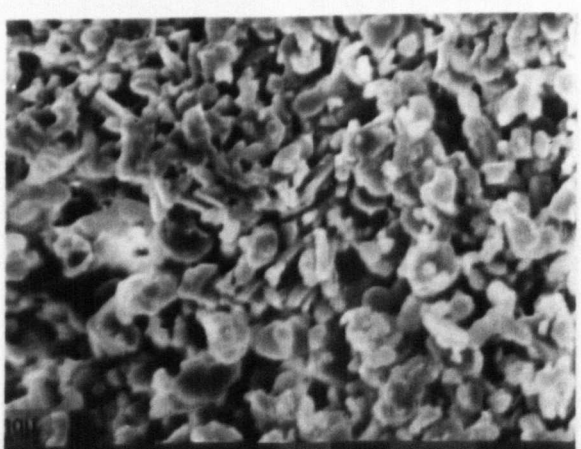

d 10 µ

Mixture	Hot-pressing parameters			w/s ratio	Density g.cc	Tensile strength MNm^{-2}	Porosity (%)
	Pressure (MNm^{-2})	Temp. (°C)	Time (min)				
α-Al_2O_3 + 5% (H_3PO_4+H_3BO_3)	207	300	30	0.1	2.57	4.9	33.25
	207	400	30	0.1	2.59	5.87	32.727
	207	500	30	0.1	2.62	6.77	31.948
	207	600	30	0.1	2.62	7.14	31.948
	207	700	30	0.1	2.64	9.2	31.428
CA_6 + 5% (H_3PO_4+H_3BO_3)	207	300	30	0.1	2.39	1.86	35.23
	207	400	30	0.1	2.40	2.6	34.96
	207	500	30	0.1	2.42	3.2	34.4
	207	600	30	0.1	2.43	3.85	34.15
	207	700	30	0.1	2.46	5.82	33.33
CA_2 + 5% (H_3PO_4+H_3BO_3)	207	400	30	0.1	1.95	1.2	31.93
	207	500	30	0.1	1.953	1.18	31.83
	207	600	30	0.1	1.969	1.26	31.27
	207	700	30	0.1	2.0535	3.2	28.32
CA + 5% (H_3PO_4+H_3BO_3)	207	300	30	0.1	2.04	1.90	30.847
	207	400	30	0.1	2.06	1.80	30.169
	207	500	30	0.1	2.04	2.03	30.84
	207	600	30	0.1	2.08	2.6	29.49
	207	700	30	0.1	2.10	3.7	28.81
Secar "250" + 5% (H_3PO_4+H_3BO_3)	207	300	30	0.1	2.009	1.12	29.508
	207	400	30	0.1	2.04	1.6	28.42
	207	500	30	0.1	2.02	1.8	29.12
	207	600	30	0.1	2.08	2.9	27.25
	207	700	30	0.1	2.06	2.9	27.70

Table 5.3: Mechanical properties and related physical properties of α-Al_2O_3, CA_6, CA_2, CA and Secar "250" mixed with 5% (H_3PO_4+H_3BO_3), hot-pressed under 207 MNm^{-2} pressure, for 30 min. at different temperatures.

Mixture	Hot-pressing parameters			w/s ratio	Firing Conditions		% Change		Density g.cc	Strength MNm^{-2}		Porosity (%)
	Pressure (MNm^{-2})	Temp. (°C)	Time (min)		Temp. (°C)	Time (hrs)	wt	vol.		Tensile	Compressive	
α-Al_2O_3 + 5% (H_3PO_4+H_3BO_3)	207	300	30	0.1	300	24	-	No change	2.52	5.4	47.8	34.7
	207	300	30	0.1	600	24	-1.476	-	2.56	6.4	67.5	33.7
	207	300	30	0.1	900	24	-2.236	-0.31	2.627	18.1	158.6	31.4
	207	300	30	0.1	1200	24	-2.433	-2.32	2.648	20.2	169.5	30.85
	207	300	30	0.1	1300	24	-2.635	-6.70	2.742	30.8	253.7	28.4
CA_6 + 5% (H_3PO_4+H_3BO_3)	207	300	30	0.1	300	24	-	No change	2.36	3.1	28.7	36.00
	207	300	30	0.1	600	24	-1.76	" "	2.434	5.2	54.8	34.04
	207	300	30	0.1	900	24	-2.48	-0.468	2.469	8.7	102.7	33.09
	207	300	30	0.1	1200	24	-3.638	-1.70	2.493	16.5	147.0	32.7
	207	300	30	0.1	1300	24	-3.869	-4.4	2.549	21.5	188.7	31.2
CA_2 + 5% (H_3PO_4+H_3BO_3)	207	300	30	0.1	300	24	-1.42	No change	-	2.1	17.4	-
	207	300	30	0.1	600	24	-1.60	" "	1.89	4.2	28.9	34.00
	207	300	30	0.1	900	24	-1.58	-0.532	2.034	6.7	41.8	29.00
	207	300	30	0.1	1200	24	-2.477	-16.4	2.444	18.5	165.7	14.98
	207	300	30	0.1	1300	24	-2.704	-21.00	2.558	24.57	218.0	11.03

Table 5.4 (Cont.)

Table 5.4 (Cont.)

Mixture	Hot-pressing parameters			w/c ratio	Firing Conditions		% Change		Density g.cc	Strength MNm^{-2}		Porosity (%)
	Pressure (MNm^{-2})	Temp. (°C)	Time (min)		Temp. (°C)	Time (hrs)	wt.	vol.		Tensile	Compressive	
CA + 5% (H_3PO_4+H_3BO_3)	207	300	30	0.1	300	24	-	No change	-	1.9	17.00	-
	207	300	30	0.1	600	24	-1.66	" "	2.002	2.8	21.7	32.13
	207	300	30	0.1	900	24	-1.49	-2.05	2.187	7.96	66.86	26.1
	207	300	30	0.1	1200	24	-2.18	-17.2	2.576	24.56	210.13	12.96
	207	300	30	0.1	1300	24	-2.85	-21.94	2.678	33.57	307.7	9.75
Secar "250" + 5% (H_3PO_4+H_3BO_3)	207	300	30	0.1	300	24	-	No change	-	1.29	-	-
	207	300	30	0.1	600	24	-1.426	" "	-	2.3	24.308	-
	207	300	30	0.1	900	24	-1.48	-.3115	2.023	3.26	36.675	29.07
	207	300	30	0.1	1200	24	-1.68	-17.689	2.48	20.94	188.06	12.98
	207	300	30	0.1	1300	24	-3.54	-21.986	2.57	30.39	253.75	9.95

Table 5.4: Mechanical properties and related physical properties of α-Al_2O_3, CA_6, CA_2, CA and Secar "250" samples mixed with 5% (H_3PO_4+H_3BO_3), hot-pressed under 207 MNm^{-2} pressure, at 300°C for 30 min., and fired at different temperatures for 24 hours.

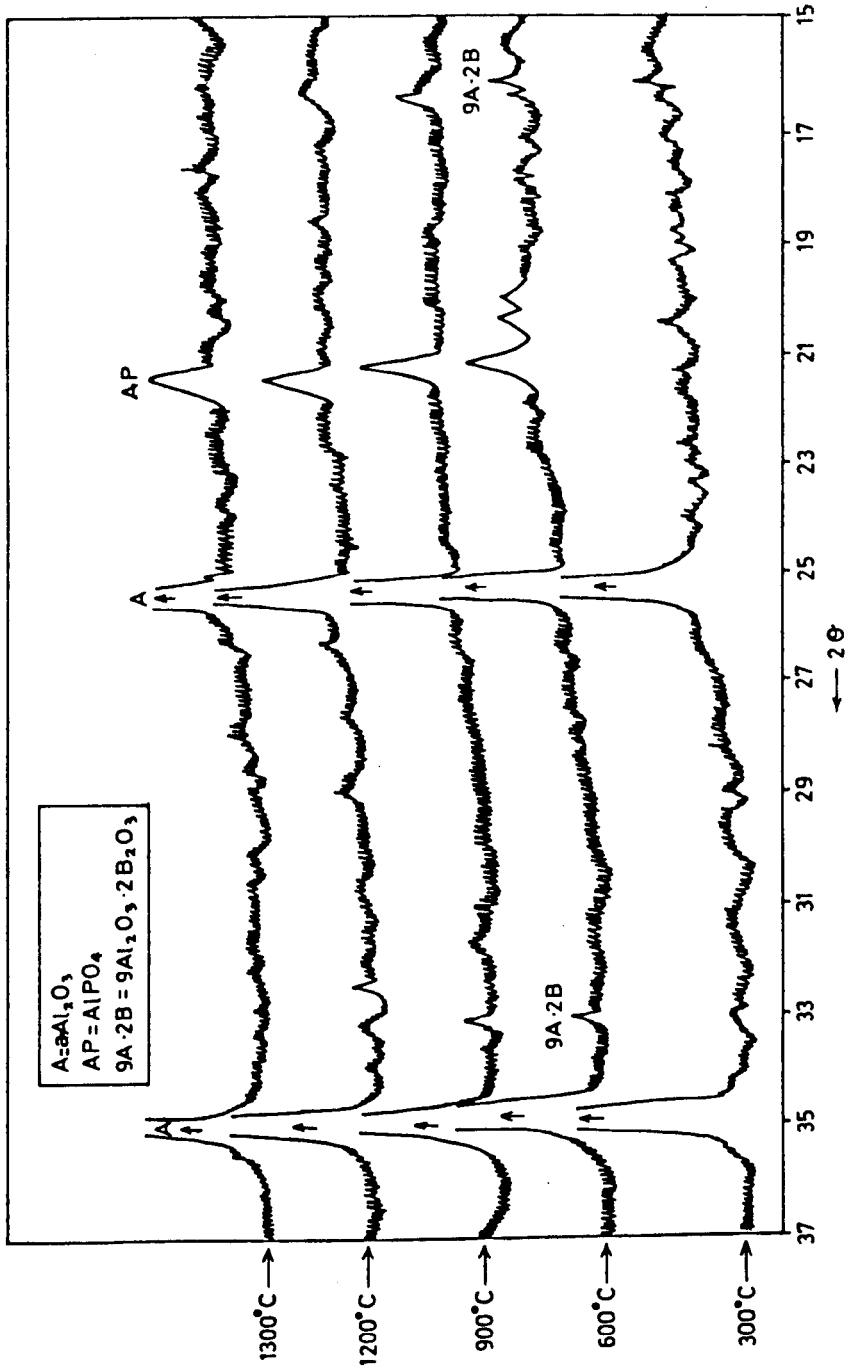

Fig. 5.5: X-ray diffractometer traces of the mixture α-Al_2O_3 + 5% (H_3PO_4 + H_3BO_3). Samples previously hot-pressed (under 207 Mm^{-2} pressure, for 30 minutes at 300°C) and fired at different temperatures for 24 hours.

5.1.1.2 Calcium aluminates + (H_3PO_4 + H_3BO_3)

(a) Samples cast at room temperature, followed by firing

The same procedures previously described (Sections 3.3.1 and 3.3.3) were followed to mix and fire calcium mono-, di- and hexa-aluminate with 5% (H_3PO_4 + H_3BO_3).

The DTA results, Fig. 5.1 and Table 5.1, showed that the reaction in the case of CA_6 produced two exothermic peaks at about 750 and 1110°C. In the case of CA_2, three exothermic peaks were detected at about 755, 820 and 1070°C, and with CA three exothermic peaks at about 658, 755 and 848°C. On the other hand all the above mixtures were produced a small endothermic peak at about 1240°C.

X-ray analysis showed that $AlPO_4$ could be detected after firing at 900°C. The compound $9Al_2O_3.2B_2O_3$ could be detected only as traces above 900°C. Generally, the above two compounds could be detected easily in the CA_6 mixtures, but the quantity was less in the CA_2 mixtures, and only traces could be found in the CA mixtures. After firing at 1200°C, the above two phases could not be detected, but β-$Ca_3(PO_4)_2$ was found. The amount of the latter increased as the calcium content of the mixes increased. In addition, new peaks especially in the CA and CA_2 mixtures were detected at the characteristic 2θ = 32°, 33.3° and 34° (Fig. 5.6).

On the other hand, α-Al_2O_3 was detected in the CA_6 mix, CA_6 in the CA_2 mix, and CA_2 in the CA mix after firing at higher temperatures.

Some samples (especially CA mixes), after firing at high temperatures (i.e. 1200 and 1300°C) were found to have some cracks. However, slow rates of heating and cooling ($\sim$ 3°C/min) were used to prevent the formation of most of these cracks.

Generally calcium hexa-aluminate mixes show a great similarity to α-Al_2O_3 mixes and strength values increased with increasing firing temperatures up to 900°C. Above this temperature, the strength values decreased, but increased again if fired above 1200°C. In addition,

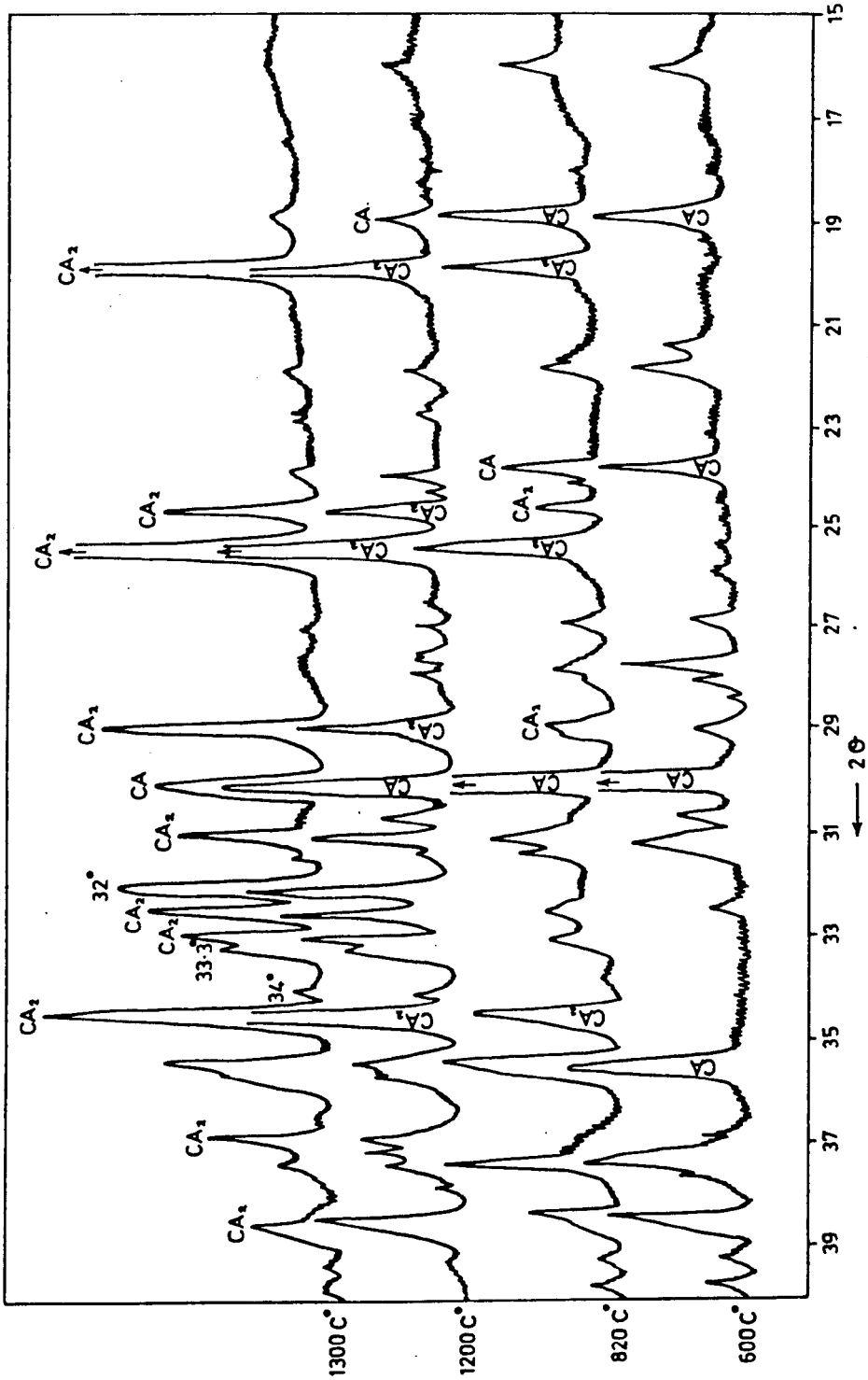

Fig. 5.6: X-ray diffractometer traces of the mixture CA+5%(H_3PO_4 + H_3BO_3). Room temperature casting, fired at different temperatures for 24 hours.

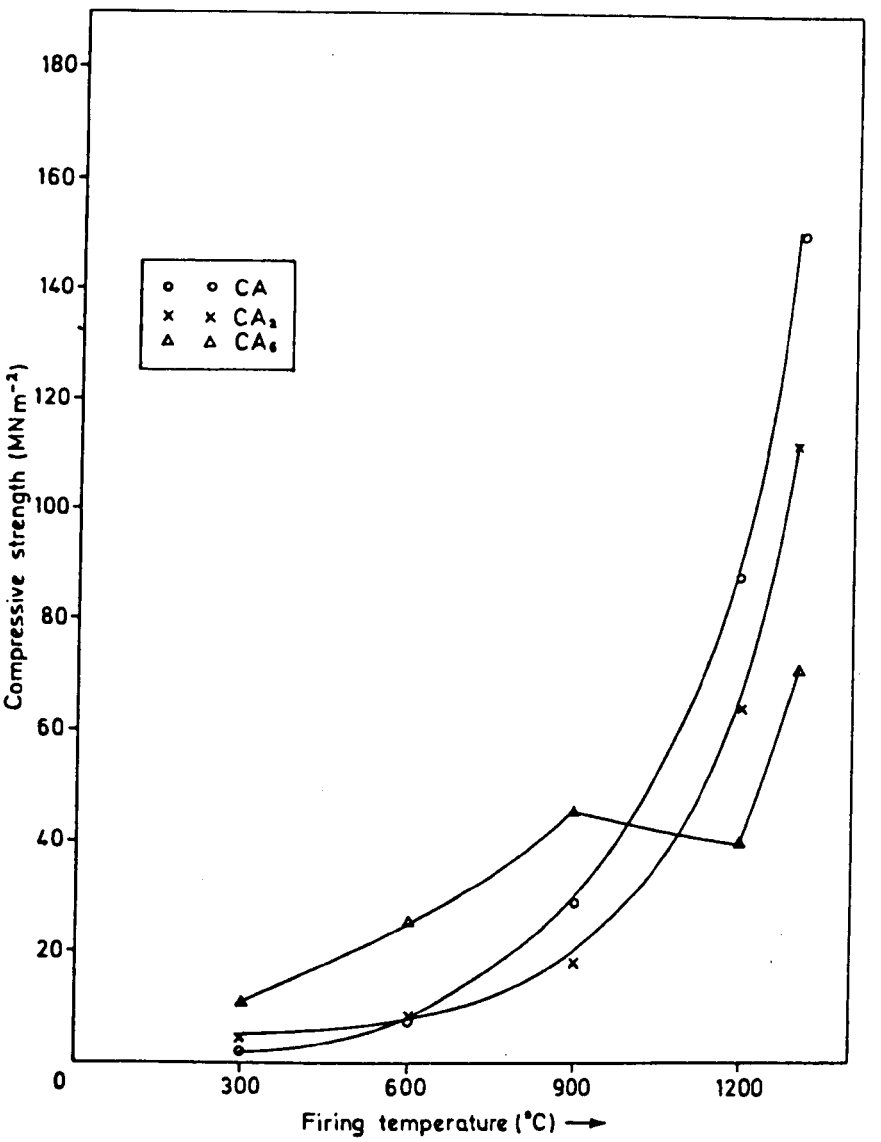

Fig. 5.7: Dependence of strength upon firing temperature. Samples mixed with 5% (H_3PO_4 + H_3BO_3), room temperature casting, fired for 24 hours.

strength values of calcium mono- and di-aluminate showed an increase with increasing firing temperatures without exception (Fig. 5.7). Microstructures of some of the above samples are shown in Figures 5.8(A), 5.9(A), 5.10(A) & (B).

(b) Hot-pressing

A combination of 5% "H_3PO_4+H_3BO_3" and 95% CA_6, CA_2, CA and Secar "250" cement were mixed using 0.1 w/c ratio. The mixtures were hot-pressed under constant pressure (207 MNm^{-2}) for constant time (30 minutes) in the range of temperatures 200 - 700°C using the same procedure previously described (Section 3.3.2.2). At the same time, samples were prepared under hot-pressing conditions (under 207 MNm^{-2} pressure, for 30 minutes at 300°C), fired in air for 24 hours in the range 300-1300°C.

X-ray analysis showed that, in samples hot-pressed at different temperatures, the reaction took place in the case of CA_6 mix at about 700°C to produce some $AlPO_4$ and trace of $9Al_2O_3.2B_2O_3$. However, in the other three mixes (i.e. CA, CA_2 and Secar "250"), no reaction took place up to 700°C. X-ray analysis of the fired samples previously hot-pressed showed a great similarity to those samples fired after casting at room temperature (Fig. 5.11). Generally, strength values of these samples were higher than samples fired after room temperature casting (Fig. 5.12). In addition, no cracks were observed in these samples after firing at high temperatures. Also, these samples were found to have a good surface finish. Microstructures of some of the above samples are shown in Figures 5.8(B), 5.9(B) and 5.10(C). Mechanical properties and related physical properties are given in Tables 5.3 and 5.4.

Fig. 5.8(A): SEM Micrographs of CA mixed with 5% (H_3PO_4+H_3BO_3), room temperature casting, fired for 24 hours at:

(a) 900°C
(b) 1200°C

Fig. 5.8(B): SEM Micrographs of CA mixed with 5% (H_3PO_4+H_3BO_3), hot-pressed under 207 MNm^{-2} pressure, for 30 minutes at 300°C, fired for 24 hours at:

(c) 900°C
(d) 1200°C
(e) 1300°C.

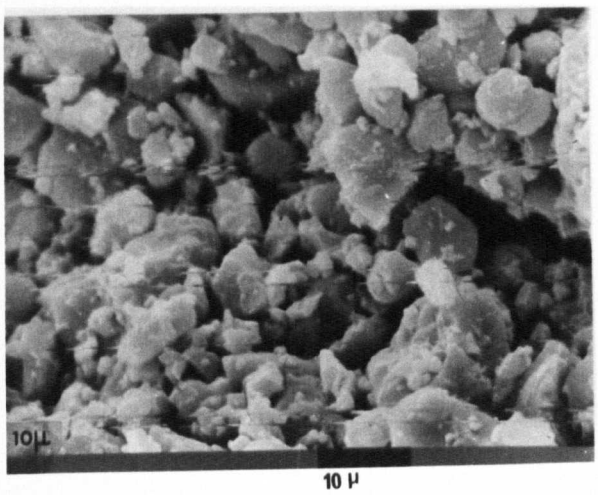

a

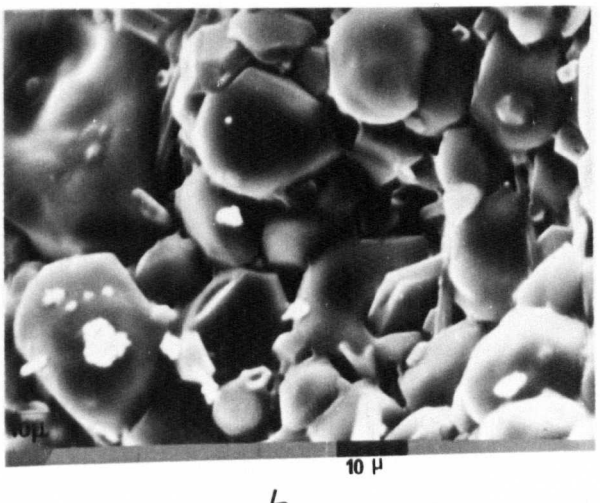

b

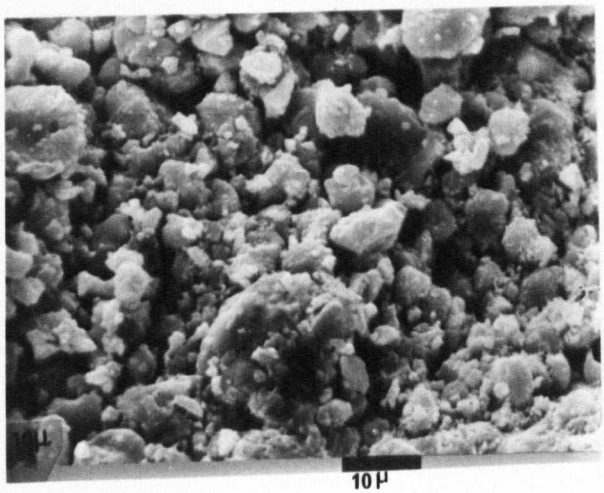

c

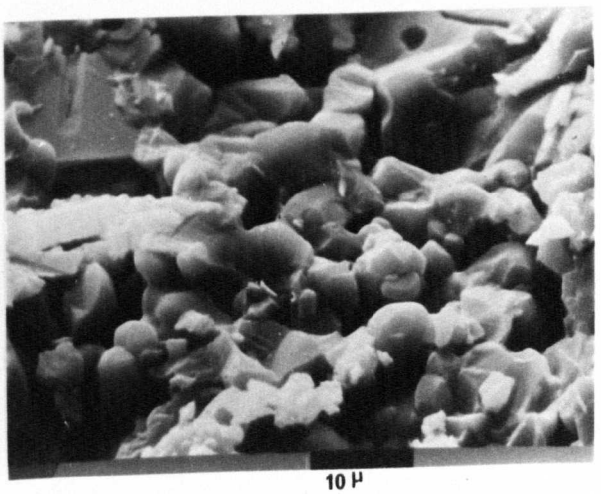

d

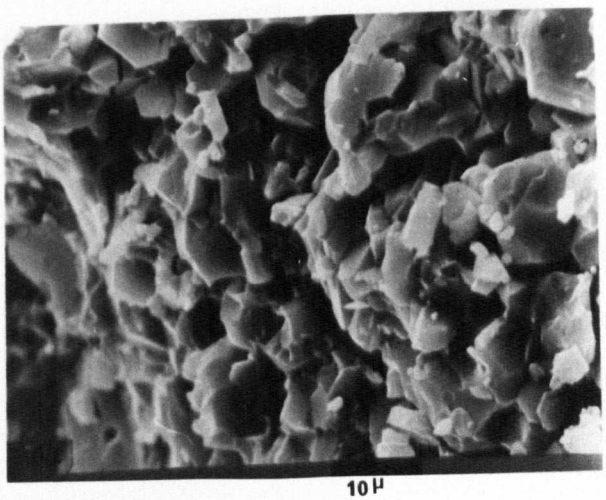

e

Fig. 5.9(A): SEM Micrographs of CA_2 mixed with 5% (H_3PO_4+H_3BO_3), room temperature casting, fired for 24 hours at:

(a) 900°C
(b) 1200°C
(c) 1300°C

Fig. 5.9(B): SEM Micrographs of CA_2 mixed with 5% (H_3PO_4+H_3BO_3), hot-pressed under 207 MNm^{-2} pressure, at 300°C for 30 minutes, fired for 24 hours at:

(d) 900°C
(e) 1200°C
(f) 1300°C.

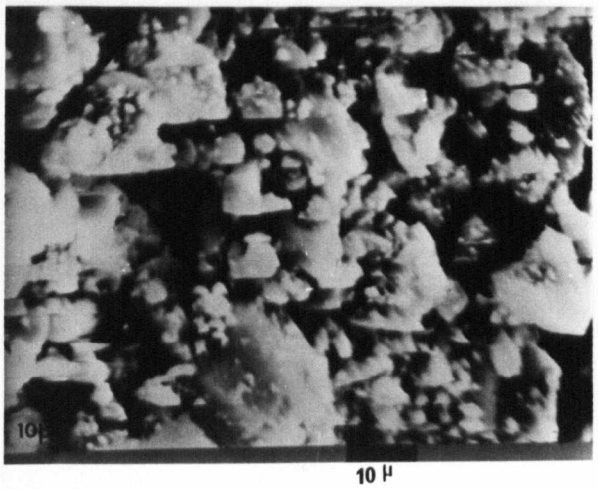

a

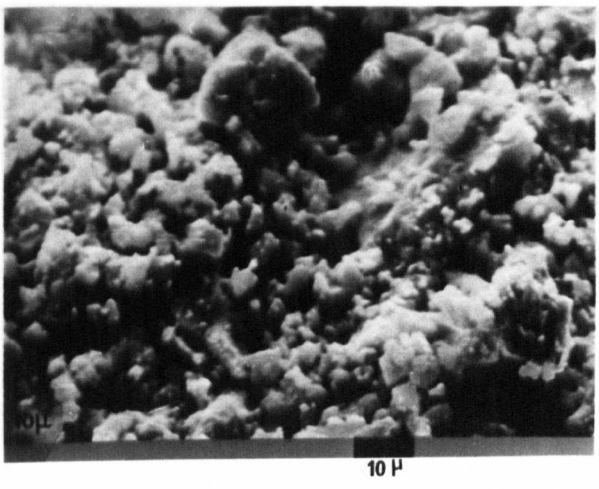

d

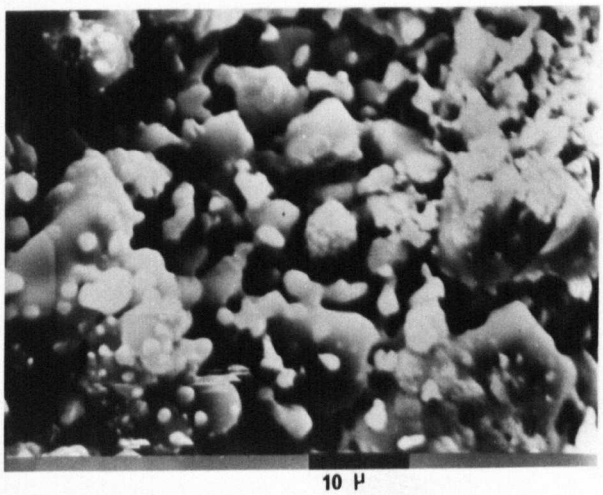

b

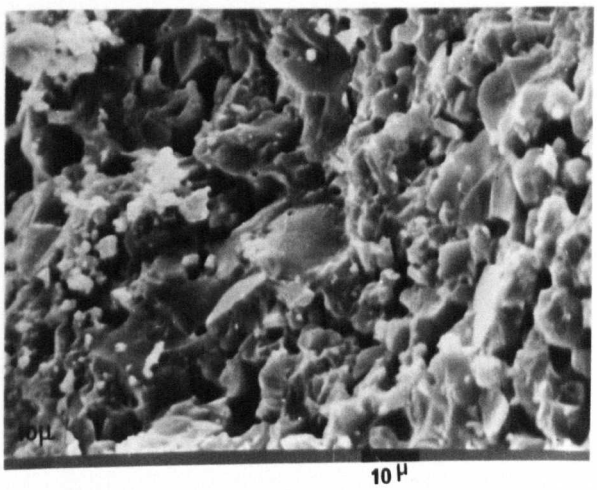

e

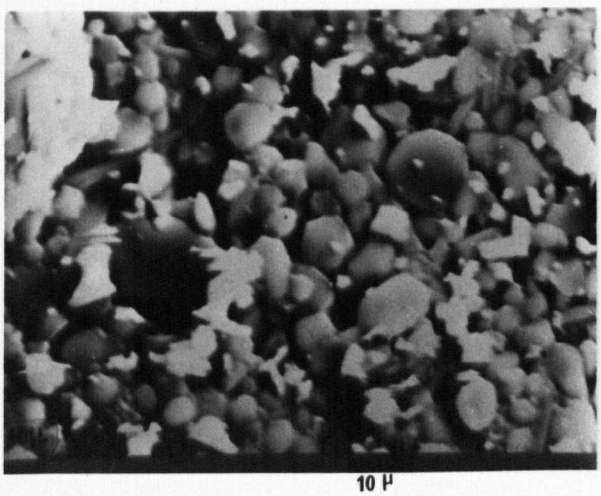

c

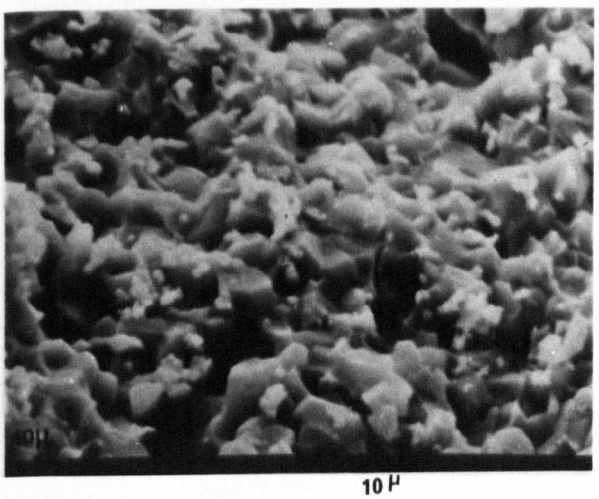

f

Fig. 5.10(A): SEM Micrographs of CA_6 mixed with 5% (H_3PO_4+H_3BO_3), room temperature casting, fired for 24 hours at:

(a) 900°C
(b) 1200°C

Fig. 5.10(B): SEM Micrographs of CA_6 mixed with 10% (H_3PO_4+H_3BO_3), room temperature casting, fired for 24 hours at:

(c) 900°C
(d) 1200°C

Fig. 5.10(C): SEM Micrographs of CA_6 mixed with 5% (H_3PO_4+H_3BO_3), hot-pressed under 207 MNm^{-2} pressure, at 300°C for 30 minutes, followed by firing at:

(e) 900°C
(f) 1200°C
(g) 1300°C.

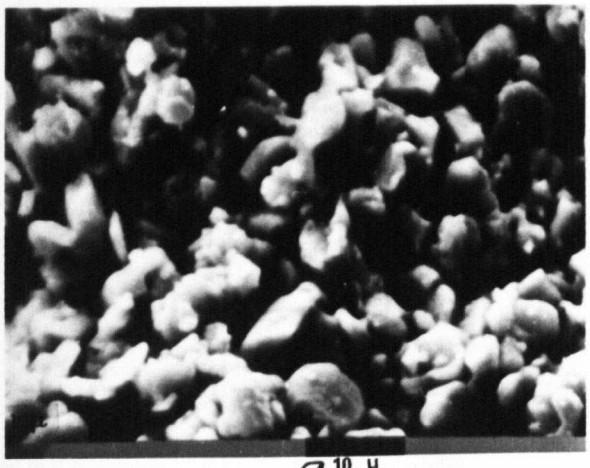

a

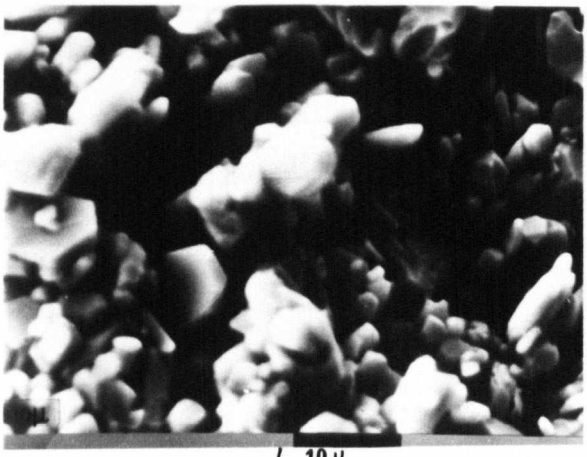

b

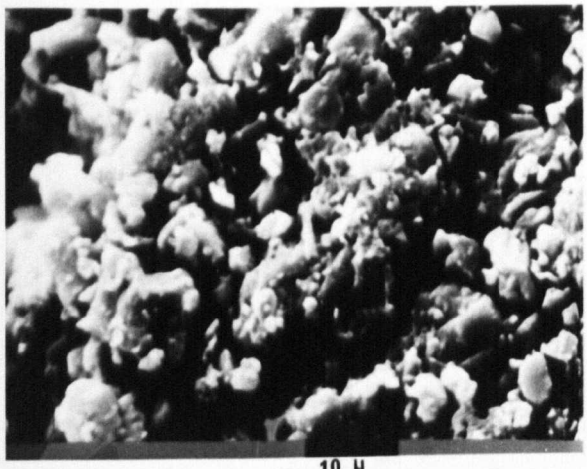

c

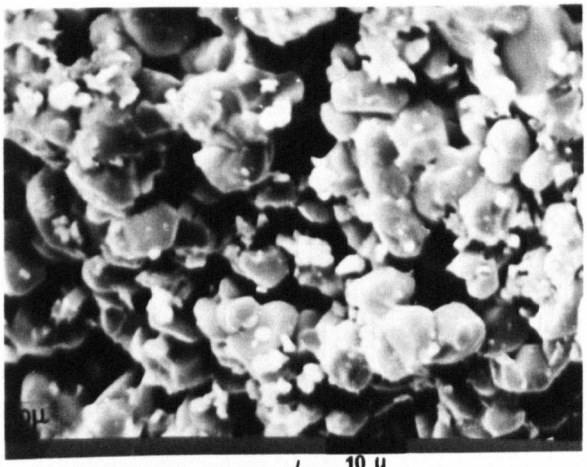

d

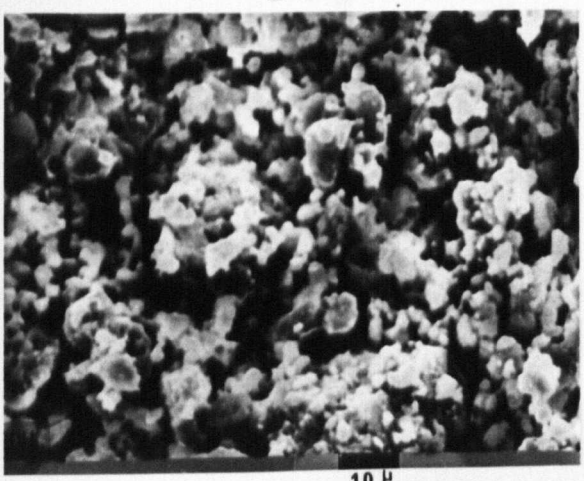

e

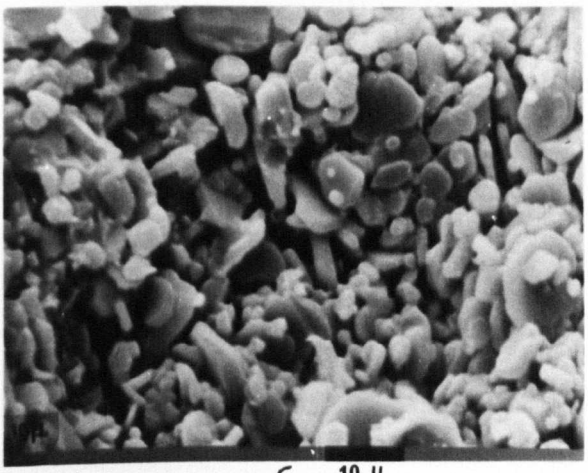

f

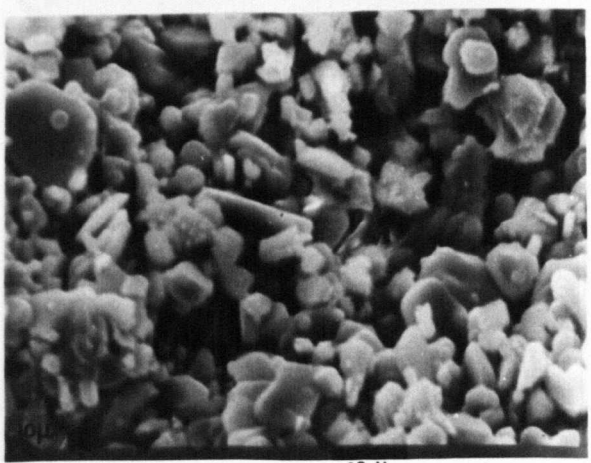

g

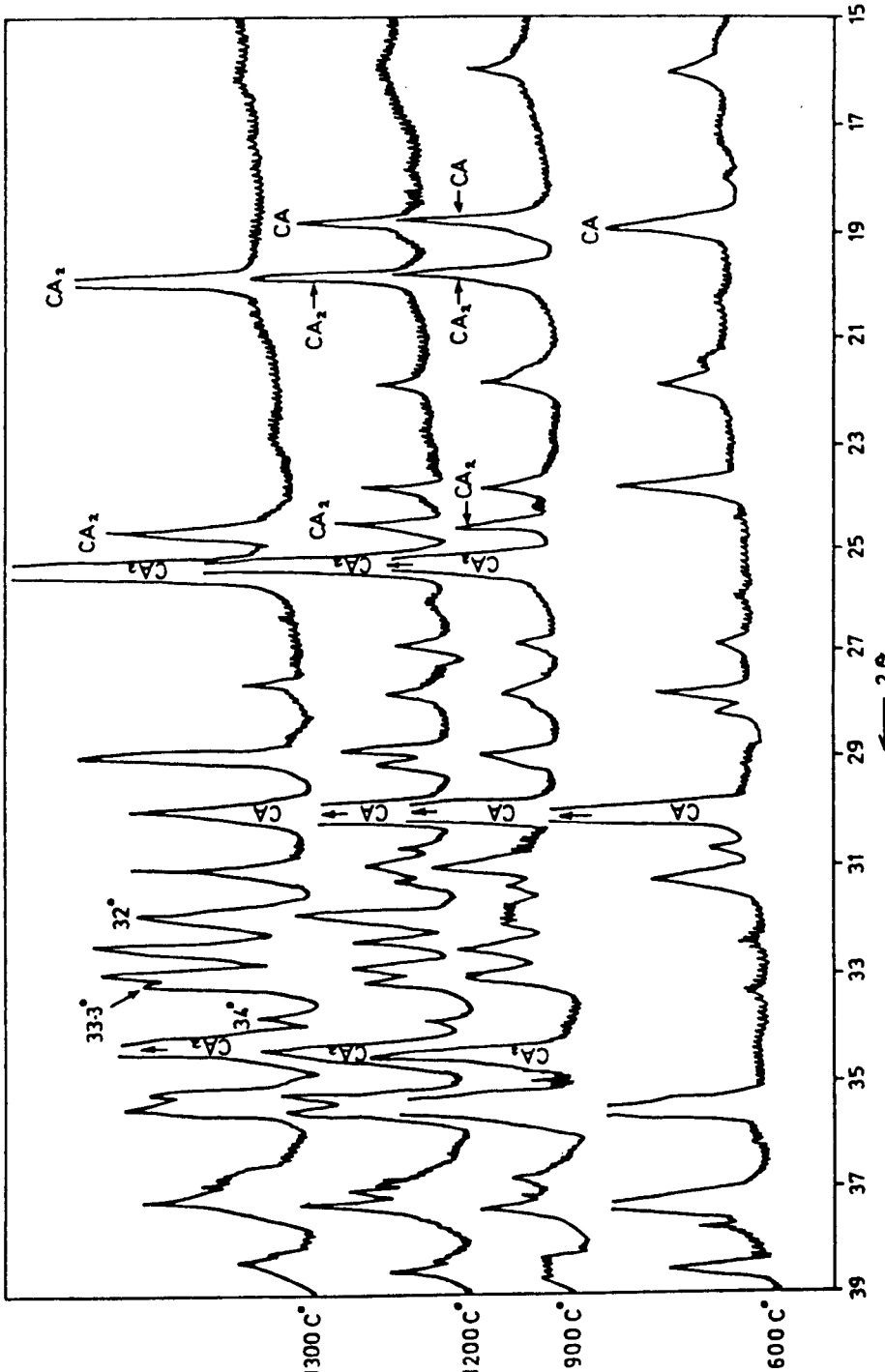

Fig. 5.11: X-ray diffractometer traces of the mixture CA + 5% (H_3PO_4 + H_3BO_3). Samples hot-pressed (under 207 MNm^{-2} pressure, at 300°C for 30 minutes), before firing at different temperatures for 24 hours.

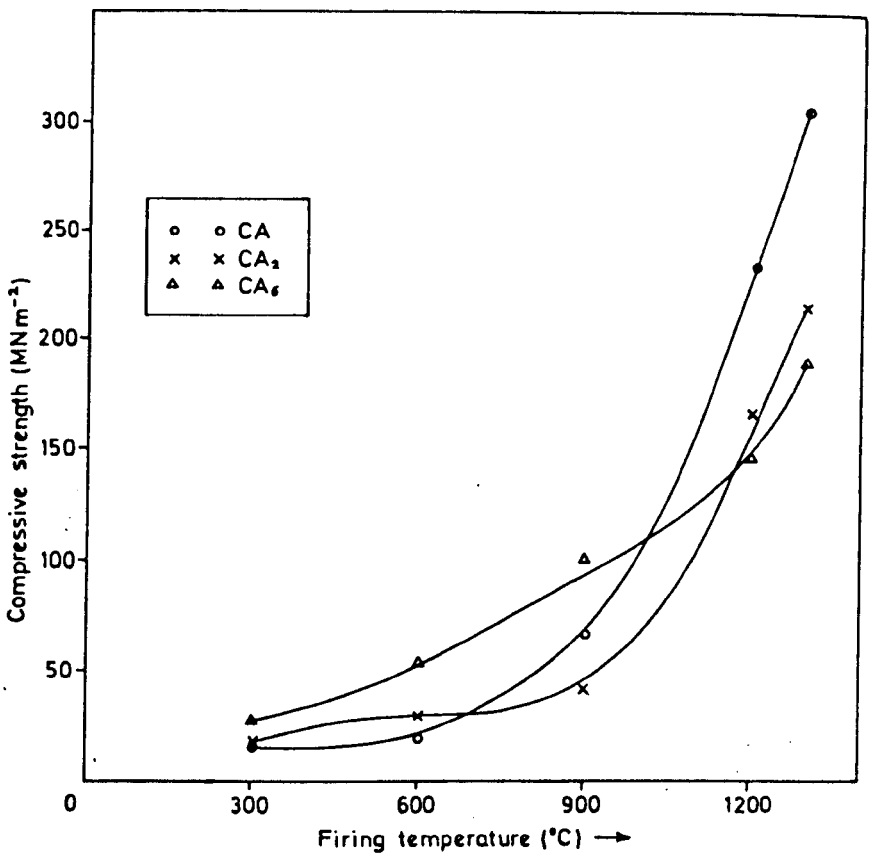

Fig. 5.12: Dependence of strength upon firing temperatures. Samples mixed with 5% (H_3PO_4 + H_3BO_3), hot-pressed (under 207 MNm^{-2} pressure, at 300°C for 30 min.), fired at different temperatures for 24 hours.

5.2 Boron Phosphate

The effect of boron phosphate, BPO_4, cristobalite form (previously prepared as in Section 3.2) as a bonding agent on the calcium aluminate phases, aluminum oxide, and the commercial material Secar "250" cement was studied. The three different methods of sample preparation previously stated in Chapter 4 were applied.

5.2.1 Results

(a) Samples cast at room temperature, followed by firing

Calcium monoaluminate (CA), calcium dialuminate (CA_2) and calcium hexa-aluminate (CA_6) were mixed with 5 and 10% dry powder boron phosphate using .25 w/c ratio. The same procedures previously described (Sections 3.3.1 and 3.3.3) were followed for mixing and firing. The DTA results of the mixtures CA, CA_2, CA_6 and α-Al_2O_3 + 10% BPO_4 are shown in Fig. 5.13 and Table 5.5. The reaction in the mixture "CA + 10% BPO_4" produced two exothermic peaks at about 825 and 1004°C and two endothermic peaks at about 1083 and 1240°C. On the other hand the mixture "CA + 5% BPO_4" produced only one exothermic peak at about 825°C and one endothermic peak at about 1240°C. Calcium dialuminate mixture with 10% BPO_4 produced three exothermic peaks, two of them are small at about 804 and 992°C, and the third is medium at about 1075°C. The mixture CA_2 + 5% BPO_4 showed only two exothermic peaks at about 804 and 1075°C. The mixtures CA_6 and α-Al_2O_3 + 10% BPO_4 showed a great similarity, and each one produced only one small exothermic peak at about 1056°C.

X-ray analyses of the mixtures CA + 5 and 10% BPO_4 show that above 825°C, calcium dialuminate is formed. By increasing the firing temperatures up to 1300°C, increases in the intensities of the CA_2 peaks and decreases in the CA peaks were recorded, Fig. 5.14. Aluminum phosphate was detected as a trace after firing at 900°C, but $9Al_2O_3.2B_2O_3$ was not detected. In addition, new peaks (previously recorded,

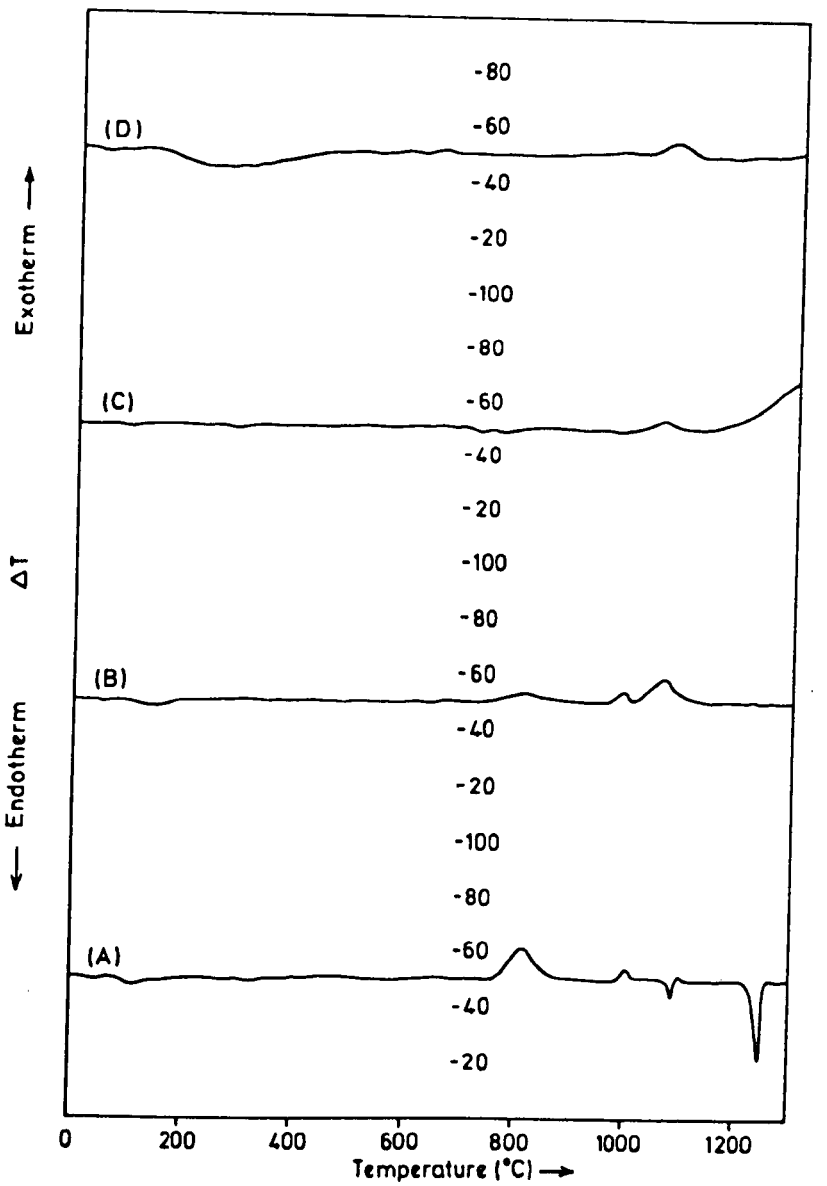

Fig. 5.13: D.T.A. traces of (A) CA + 10% BPO_4, (B) CA_2 + 10% BPO_4 (C) CA_6 + 10% BPO_4, (D) α-Al_2O_3 + 10% BPO_4.

Mixture	Exothermic reactions					Endothermic reactions				
	Peak temperature °C			ΔT °C	Peak area A deg.s.mg^{-1}	Peak temperature °C			ΔT °C	Peak area A deg.s.mg^{-1}
	Start	Peak	End			Start	Peak	End		
CA+10% BPO_4	788	825	890	0.42	1.584	1067	1083	1096	0.28	0.294
	992	1004	1022	0.159	0.1669	1212	1241	1256	1.0675	1.1208
CA+5% BPO_4	782	825	892	0.23	0.858	1213	1240	1256	0.5775	0.60637
CA_2+10% BPO_4	755	804	884	0.06	0.243					
	969	992	1007	0.0937	0.1405					
	1015	1075	1140	0.290	1.177					
CA_2+5% BPO_4	772	809	870	0.03	0.102					
	1015	1062	1112	0.1675	0.5625					
CA_6+10% BPO_4	1015	1056	1104	0.075	0.1687					
αAl_2O_3+10% BPO_4	1037	1056	1089	0.075	0.135					

Table 5.5: Summary of DTA results of the mixtures CA, CA_2, CA_6 & α-Al_2O_3 + 10% BPO_4 and CA and CA_2 + 5% BPO_4.

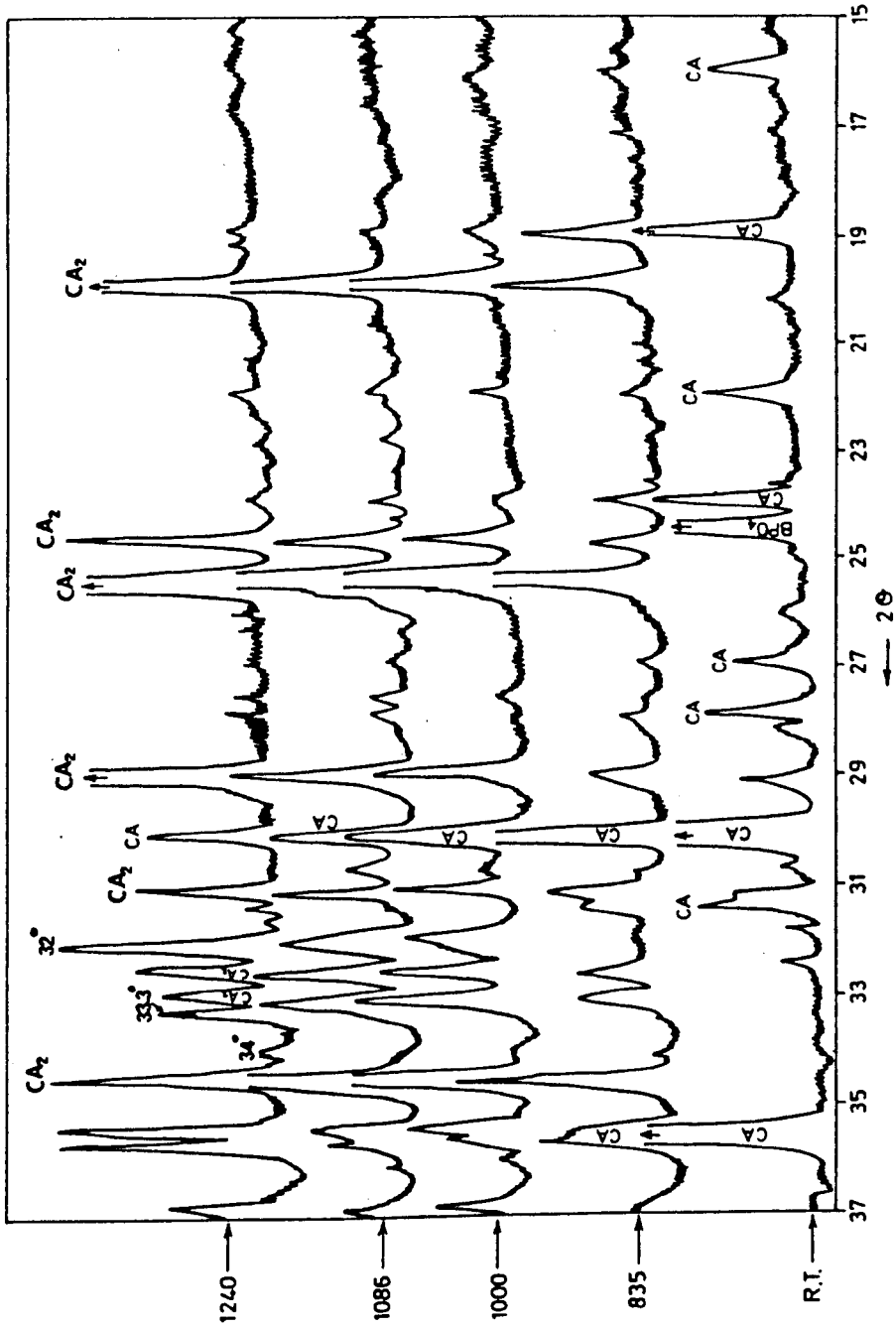

Fig. 5.14: X-ray diffractometer traces of the mixture CA + 10% BPO_4, room temperature casting, fired at different temperatures for 24 hours.

Section 5.1.1.2(a)) at $2\theta = 32^{\circ}$, 33.3° and 34° were detected after firing at higher temperatures (1200 and 1300°C).

X-ray analyses of the mixtures CA_2 + 5 and 10% BPO_4 show that above 900°C, traces of CA_6 and α-Al_2O_3 can be detected. Increasing the firing temperature up to 1300°C resulted in an increase of the CA_6 and α-Al_2O_3 content with decrease in the CA_2 content. In addition small amounts of $AlPO_4$ and $9Al_2O_3.2B_2O_3$ were detected after firing at 900°C. The compound β-$Ca_3(PO_4)_2$ was also detected after firing at 1200°C. Analysis of the mixture CA_6 + 10% BPO_4 using X-ray technique showed that $AlPO_4$ is formed first after firing at 900°C. Above that temperature the compound $9Al_2O_3.2B_2O_3$ was detected. Firing at higher temperatures (i.e. 1200 and 1300°C) showed the formation of α-Al_2O_3 and a small amount of α- and β-$Ca_3(PO_4)_2$. Microstructures of some of the above samples are shown in Figures 5.15(A), 5.16(A) and 5.17(A). Dependence of strength of the above mixtures upon firing temperatures is given in Figs. 5.18(A) and (B). From these figures it is obvious to notice that up to 900°C the strength values are in the sequence $CA_6 > CA_2 > CA$, whereas above that temperature (900°C) the strength values are in the sequence $CA > CA_2 > CA_6$. In addition, adding 10% BPO_4 was slightly better from the strength point of view than 5%.

Fig. 5.15(A): SEM Micrographs of CA mixed with 10% BPO_4, room temperature casting, fired for 24 hours at:

(a & b) 1200°C

Fig. 5.15(B): SEM Micrographs of CA mixed with 10% BPO_4, hot-pressed under 207 MNm^{-2} pressure, for 30 minutes at 300°C, fired for 24 hours at:

(c) 900°C

(d) 1200°C.

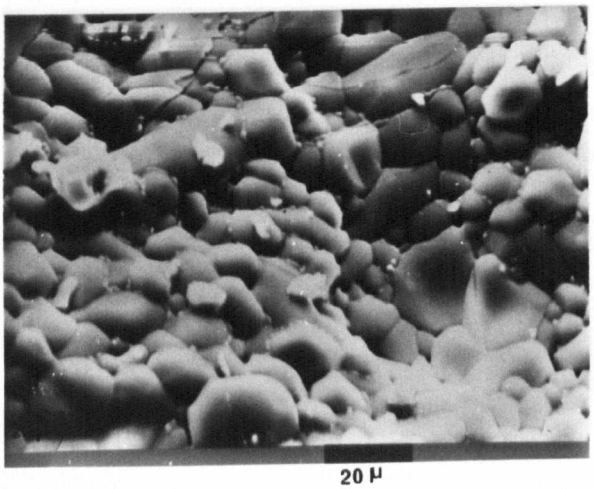

a

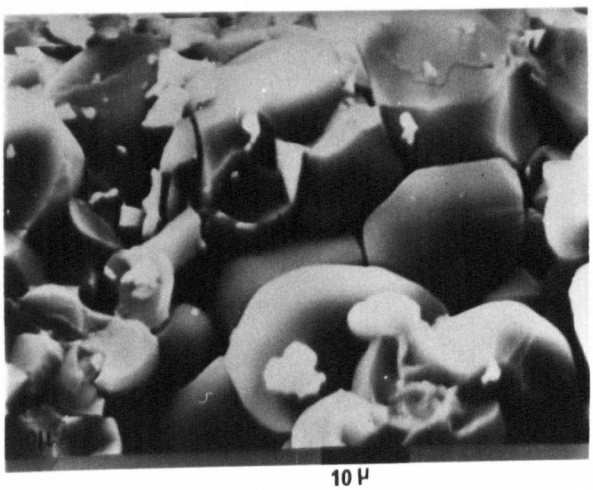

b

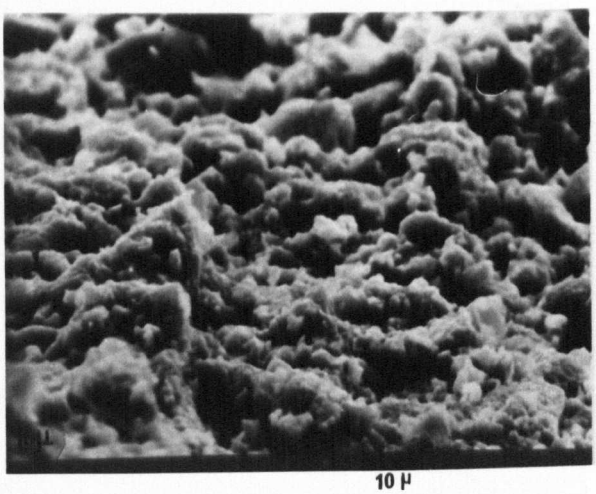

c

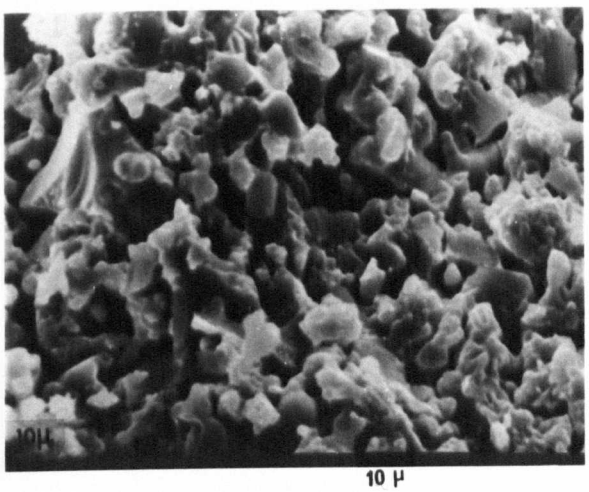

d

Fig. 5.16(A): SEM Micrographs of CA_2 mixed with 5% BPO_4, room temperature casting, fired for 24 hours at:

(a) 900°C
(b) 1200°C

Fig. 5.16(B): SEM Micrographs of CA_2 mixed with 10% BPO_4, room temperature casting, fired for 24 hours at:

(c) 900°C
(d) 1200°C

Fig. 5.16(C): SEM Micrograph of CA_2 mixed with 5% BPO_4, hot-pressed under 207 MNm^{-2} pressure, at 300°C for 30 minutes, fired for 24 hours at:

(e) 1200°C.

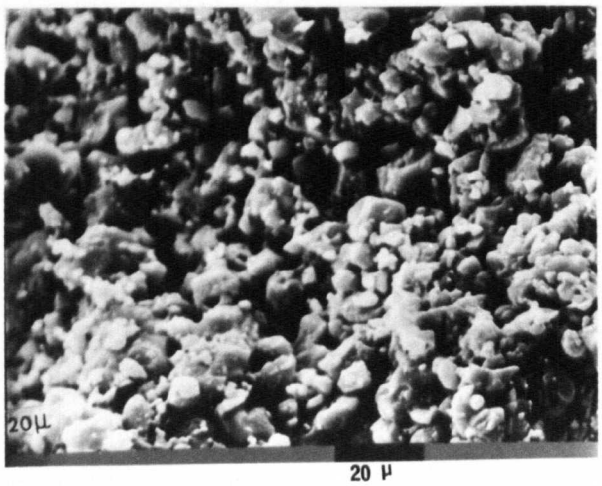

a

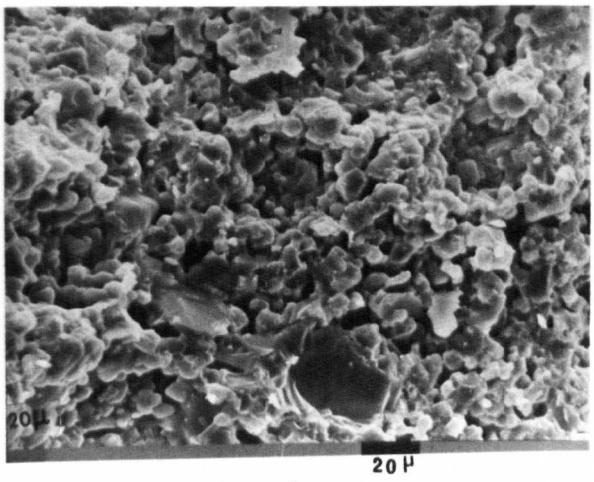

b

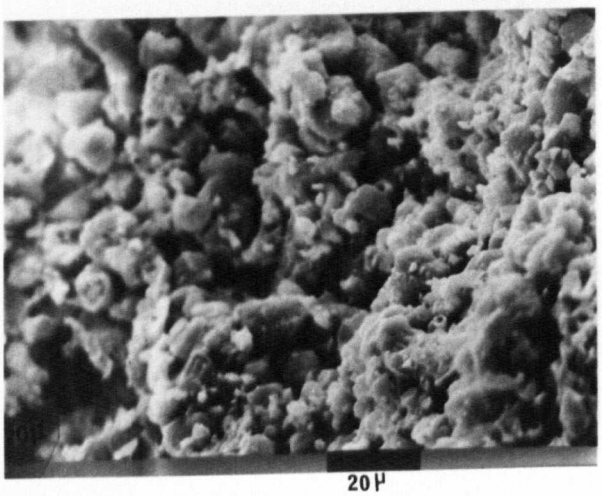

c

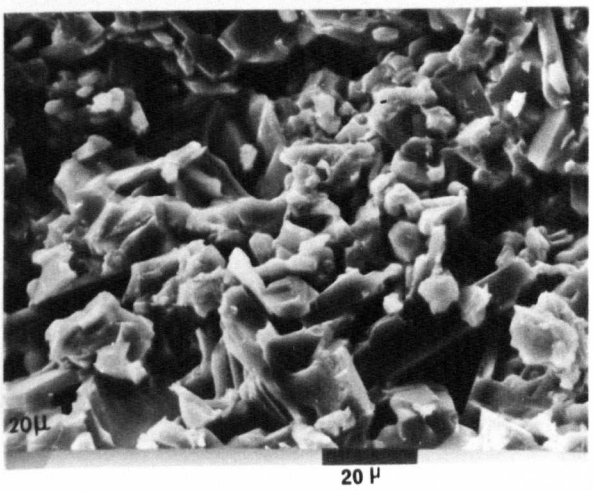

d

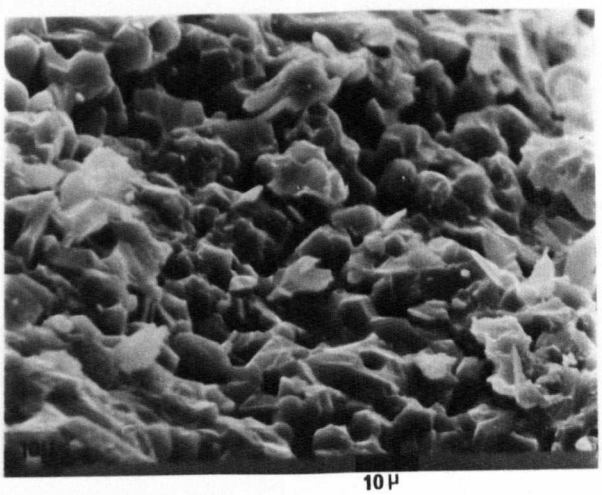

e

Fig. 5.17(A): SEM Micrographs of Al_6 mixed with 5% BPO_4, room temperature casting, fired for 24 hours at:

(a) 900°C
(b) 1200°C

Fig. 5.17(B): SEM Micrographs of Al_6 mixed with 5% BPO_4, hot-pressed under 207 MNm^{-2} pressure, for 30 minutes at 300°C, fired for 24 hours at:

(c) 900°C
(d) 1200°C.

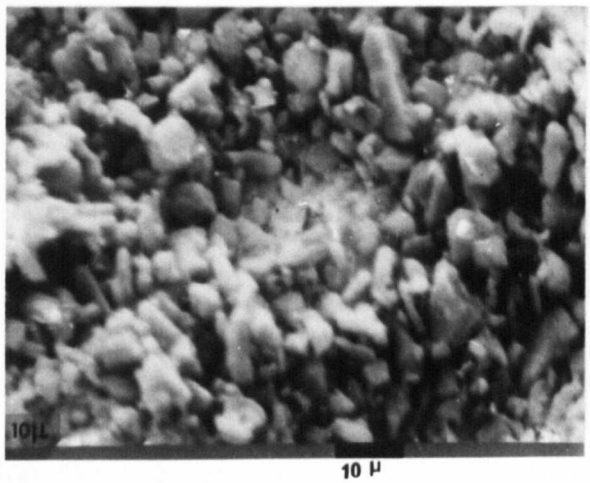

a

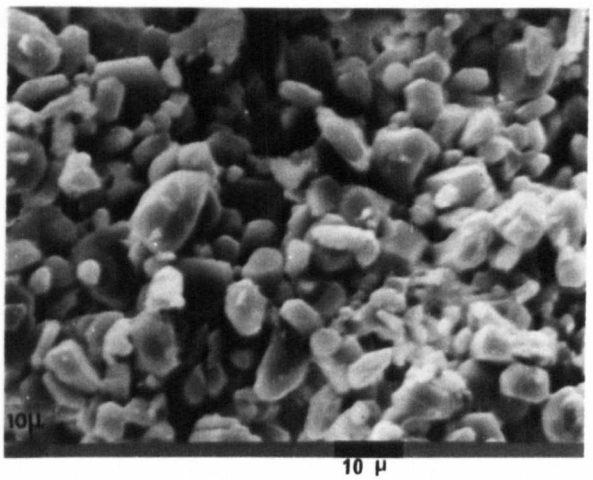

b

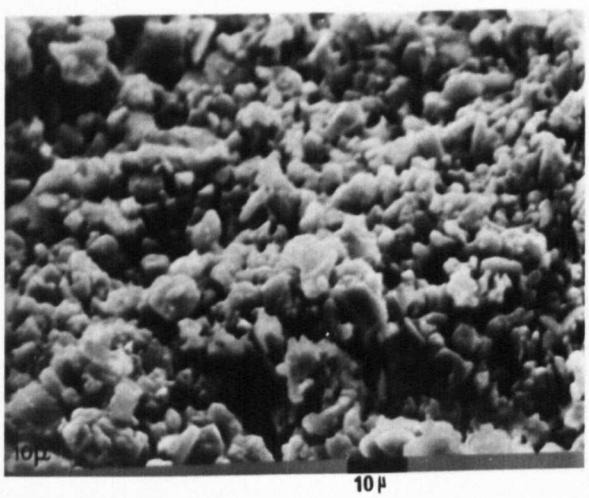

c

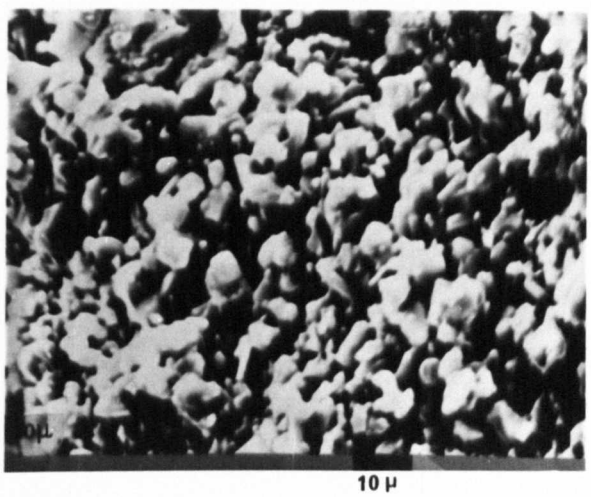

d

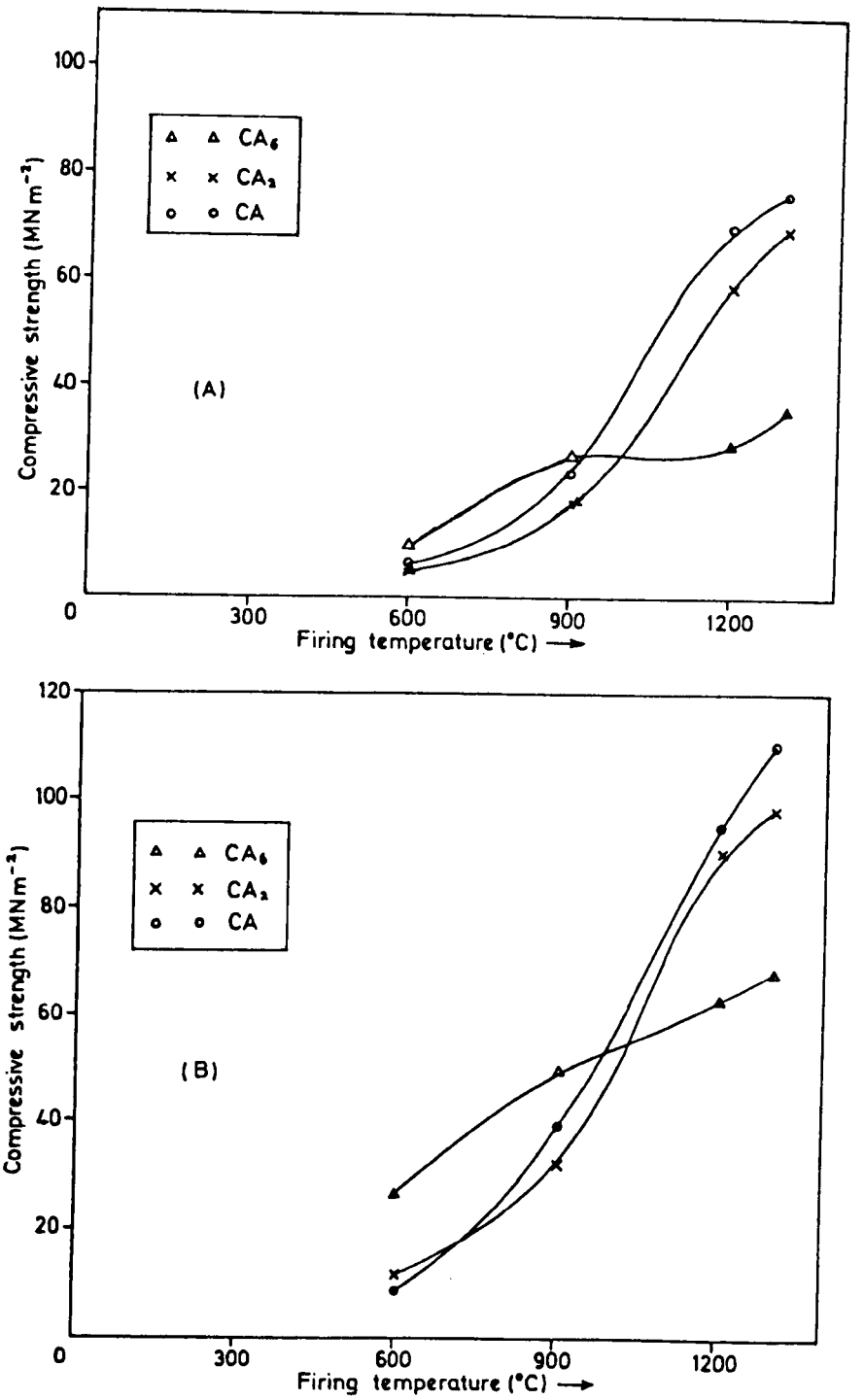

Fig. 5.18: Dependence of strength upon firing temperatures. Samples mixed with (A) 5% BPO_4, (B) 10% BPO_4, room temperature casting, fired for 24 hours.

(b) Hot-pressing

The hot-pressing technique was applied to the preparation of samples, by mixing the same starting materials previously employed in room temperature casting (CA, CA_2 and CA_6) as well as α-Al_2O_3 and the commercial material Secar "250" with 5% BPO_4. In addition, a combination between 90% CA and 10% BPO_4 was also studied. The procedure which was previously described (Section 3.3.2.2) was followed using 0.1 w/s ratio. Samples prepared under hot-pressing conditions (under 207 MNm^{-2} pressure, at 300°C for 30 minutes) were also fired in air for 24 hours in the same range of temperatures (i.e. 300-1300°C).

(1) α-Al_2O_3 + BPO_4

X-ray analysis of this mix, hot-pressed at different temperatures up to 700°C, showed that no reaction took place up to 600°C. After hot-pressing at that temperature, anhydrous aluminum phosphate was detected. On increasing the hot-pressing temperatures to 700°C, an increase in the $AlPO_4$ content was obtained. Mechanical properties and related physical properties of this mix are given in Table 5.6. X-ray analyses of previously hot-pressed samples, Fig. 5.19, show that $AlPO_4$ could be detected after firing at 600°C. On increasing the firing temperature to 900°C, $9Al_2O_3.2B_2O_3$ was detected. However, after firing at 1200°C an increase in the $AlPO_4$ and a small increase in the $9Al_2O_3.2B_2O_3$ content was observed. Finally, after firing at 1300°C, only $AlPO_4$ was detected at $2\theta = 21.58°$ and a small peak at $2\theta = 21.45°$, with traces of $9Al_2O_3.2B_2O_3$. Microstructures of some of the above samples are shown in Fig. 5.20. Dependence of strength upon firing temperatures is given in Fig. 5.21. Mechanical properties and related physical properties are given in Table 5.7.

Mixture	Hot-pressing parameters			w/s ratio	Density g.cc	Tensile strength MNm^{-2}	Porosity (%)
	Pressure (MNm^{-2})	Temp. (°C)	Time (min)				
α-Al_2O_3 + 5% BPO_4	207	300	30	0.1	2.54	4.8	34.02
	207	400	30	0.1	2.56	5.1	33.50
	207	500	30	0.1	2.57	6.3	33.25
	207	600	30	0.1	2.60	6.3	32.46
	207	700	30	0.1	2.611	6.8	32.18
CA_6 + 5% BPO_4	207	300	30	0.1	-	-	-
	207	400	30	0.1	2.36	1.48	36.04
	207	500	30	0.1	2.36	2.4	36.00
	207	600	30	0.1	2.39	3.2	35.23
	207	700	30	0.1	2.40	4.8	34.9
CA_2 + 5% BPO_4	207	300	30	0.1	1.96	-	31.588
	207	400	30	0.1	1.92	-	32.98
	207	500	30	0.1	1.95	-	31.94
	207	600	30	0.1	1.99	-	30.54
	207	700	30	0.1	-	-	-
Secar "250" +5% BPO_4	207	300	30	0.1	1.99	-	30.175
	207	400	30	0.1	1.98	1.7	30.526
	207	500	30	0.1	2.029	1.6	28.92
	207	600	30	0.1	2.06	3.2	27.719
	207	700	30	0.1	2.08	5.07	27.017
CA + 5% BPO_4	207	300	30	0.1	2.00	2.00	32.20
	207	400	30	0.1	1.99	2.02	32.54
	207	500	30	0.1	2.01	2.3	31.86
	207	600	30	0.1	2.04	3.0	30.847
	207	700	30	0.1	2.07	3.04	29.83
CA + 10% BPO_4	207	300	30	0.1	2.00	1.8	32.20
	207	400	30	0.1	2.028	2.02	31.254
	207	500	30	0.1	2.039	2.1	30.88
	207	600	30	0.1	2.067	3.1	29.93
	207	700	30	0.1	2.08	4.2	29.49

Table 5.6: Mechanical properties and related physical properties of α-Al_2O_3, CA_6, CA_2, CA and Secar "250" cement. Samples mixed with 5% BPO_4 (5 and 10% in the case of CA), hot-pressed under constant pressure (207 MNm^{-2}) for constant time (30 minutes) at different hot-pressing temperatures.

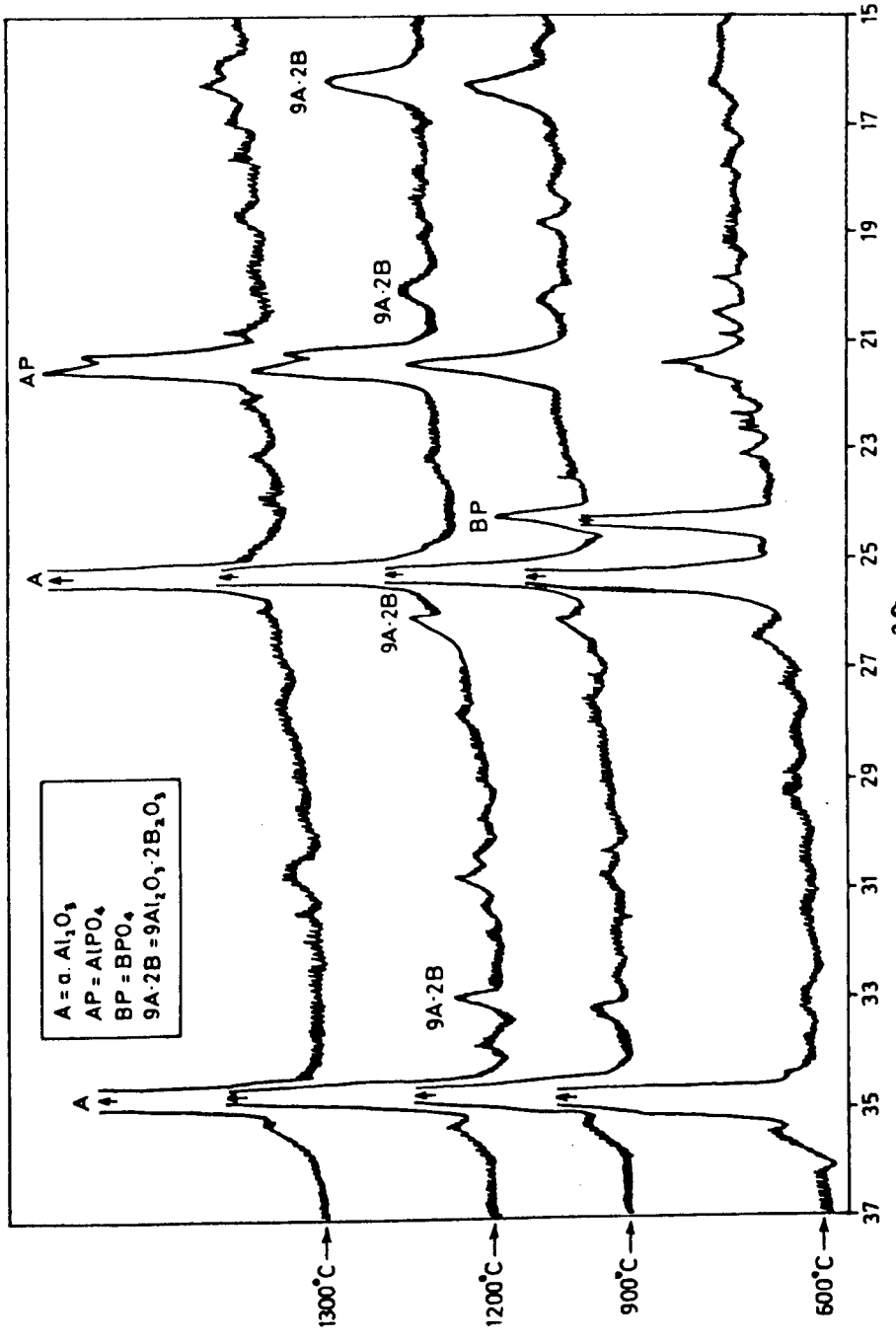

Fig. 5.12: X-ray diffractometer traces of the mixture α-Al_2O_3 + 5% BPO_4, hot-pressed (under 207 Mm^{-2} pressure, at 300°C for 30 minutes), fired at different temperatures for 24 hours.

Fig. 5.20: SEM Micrographs of α-Al_2O_3 mixed with 5% BPO_4, hot-pressed under 207 MNm^{-2} pressure, for 30 minutes, at 300°C, and fired for 24 hours at:

(a) 900°C

(b) 1300°C.

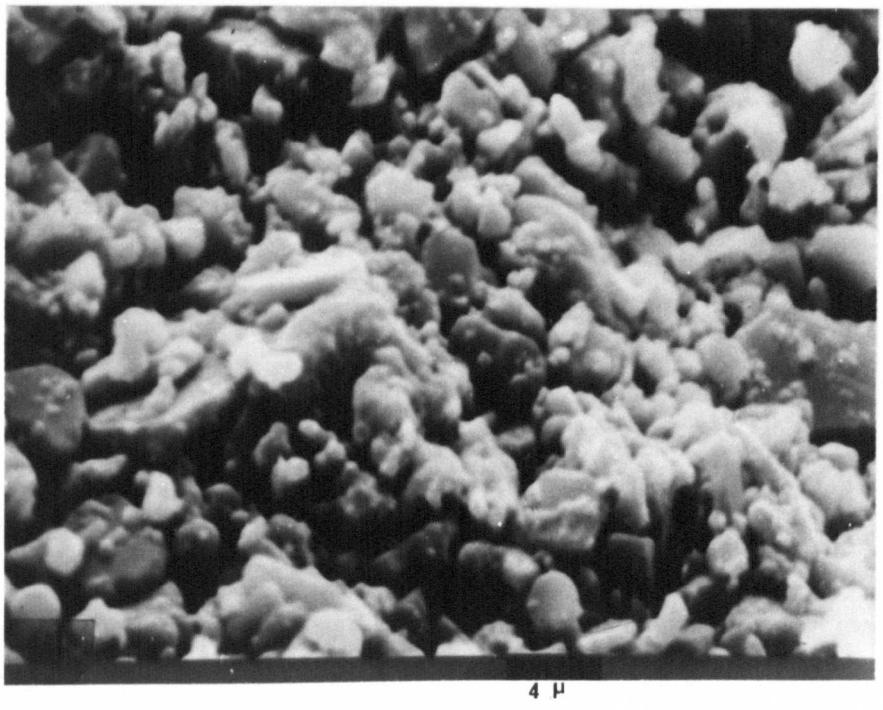

a

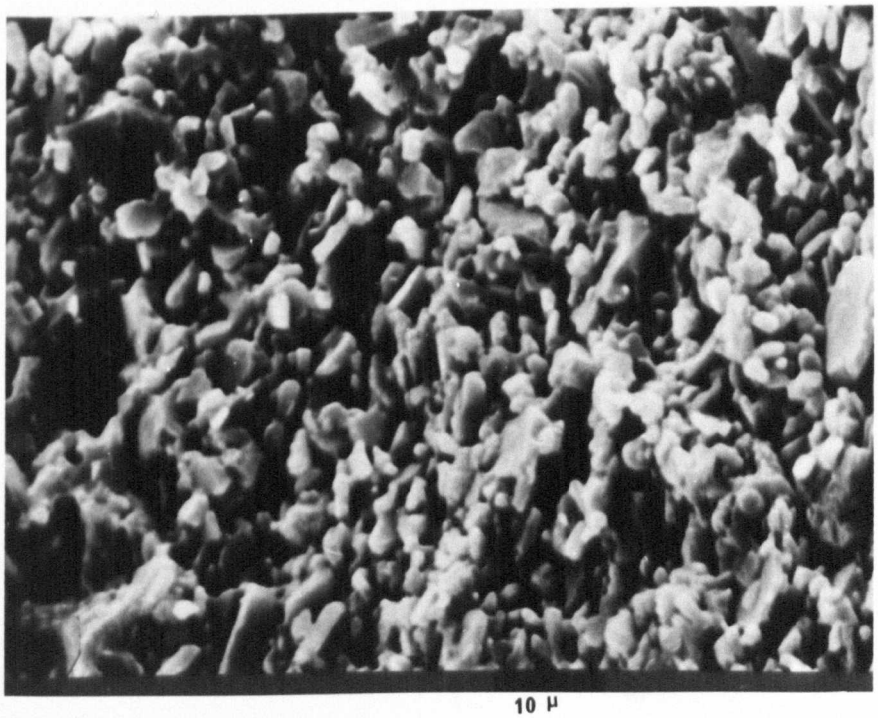

b

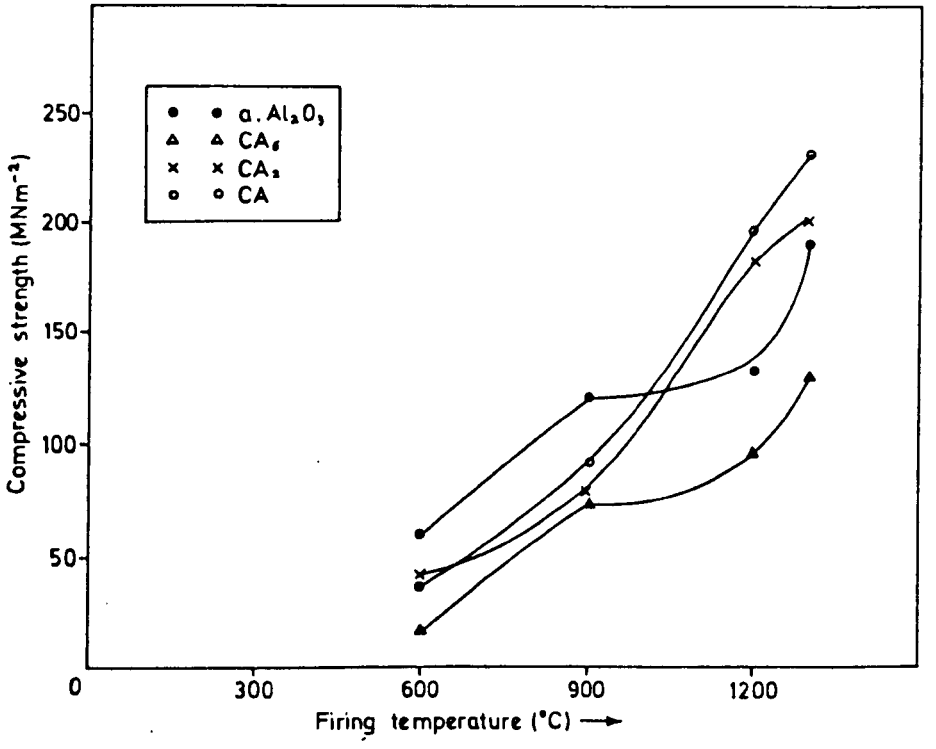

Fig. 5.21: Dependence of strength upon firing temperatures. Samples mixed with 5% BPO_4, hot-pressed (under 207 MNm^{-2} pressure, at 300°C for 30 min.), and fired at various temperatures for 24 hours.

Mixture	Hot-pressing parameters			w/s ratio	Firing Conditions		% Change		Density g.cc	Strength MNm^{-2}		Porosity (%)
	Pressure (MNm^{-2})	Temp. (°C)	Time (min)		Temp. (°C)	Time (hrs)	wt.	vol.		Tensile	Compressive	
α -Al_2O_3 + 5%	207	300	30	0.1	300	24	-1.35	No change	-	3.3	-	-
BPO_4	207	300	30	0.1	600	24	-1.34	" "	2.509	7.8	60.6	34.657
	207	300	30	0.1	900	24	-1.55	" "	2.5708	12.2	120.63	33.05
	207	300	30	0.1	1200	24	-2.60	-1.54	2.603	13.7	127.7	32.03
	207	300	30	0.1	1300	24	-2.88	-4.8	2.663	20.8	187.02	30.46
CA_6 + 5%	207	300	30	0.1	300	24	-	No change	-	-	-	-
BPO_4	207	300	30	0.1	600	24	-	" "	2.3169	2.3	16.5	37.21
	207	300	30	0.1	900	24	-1.89	" "	2.430	6.8	72.2	34.12
	207	300	30	0.1	1200	24	-2.37	-1.12	2.4605	12.2	99.1	33.50
	207	300	30	0.1	1300	24	-2.85	-2.6	2.5202	14.4	126.86	32.07
CA_2 + 5%	207	300	30	0.1	300	24	-	No change	-	-	-	-
BPO_4	207	300	30	0.1	600	24	-1.32	" "	-	3.3	39.64	-
	207	300	30	0.1	900	24	-1.50	-0.35	2.0607	7.8	75.05	28.07
	207	300	30	0.1	1200	24	-2.311	-12.48	2.45	18.8	150.5	15.05
	207	300	30	0.1	1300	24	-2.458	-20.08	2.525	23.7	200.1	12.55

Table 5.7 (Cont.)

Table 5.7 (Cont.)

Mixture	Hot-pressing parameters			w/c ratio	Firing Conditions		% Change		Density g.cc	Strength MNm^{-2}		Porosity (%)
	Pressure (MNm^{-2})	Temp. (°C)	Time (min)		Temp. (°C)	Time (hrs)	wt.	vol.		Tensile	Compressive	
Secar "250" + 5% BPO_4	207	300	30	0.1	300	24	-	-	-	-	-	-
	207	300	30	0.1	600	24	-	No change	2.02	2.8	30.00	29.2
	207	300	30	0.1	900	24	-1.34	-0.46	2.06	6.4	54.6	27.72
	207	300	30	0.1	1200	24	-1.44	-16.82	2.49	20.7	177.20	12.63
	207	300	30	0.1	1300	24	-1.63	-18.95	2.54	24.5	195.70	10.88
CA + 5% BPO_4	207	300	30	0.1	300	24	-	No change	-	-	-	-
	207	300	30	0.1	600	24	-	" "	1.997	3.2	36.0	32.3
	207	300	30	0.1	900	24	-1.267	-1.29	2.142	9.8	78.8	27.49
	207	300	30	0.1	1200	24	-1.19	-14.48	2.564	21.7	194.7	13.58
	207	300	30	0.1	1300	24	-1.68	-20.17	2.665	26.5	230.5	10.19
CA + 10% BPO_4	207	300	30	0.1	300	24	-1.420	No change	-	3.07	-	-
	207	300	30	0.1	600	24	-1.48	" "	-	8.04	-	-
	207	300	30	0.1	900	24	-1.634	-1.8	2.128	10.78	-	27.37
	207	300	30	0.1	1200	24	-1.788	-17.1	2.592	27.7	-	11.53
	207	300	30	0.1	1300	24	-2.599	-22.3	2.690	34.92	-	8.19

Table 5.7: Mechanical properties and related physical properties of α-Al_2O_3, CA_6, CA_2, CA and Secar "250" cement samples, mixed with 5% BPO_4 (5 and 10% in case of CA), hot-pressed under 207 MNm^{-2} pressure, at 300°C for 30 minutes, and fired at different temperatures for 24 hours.

(2) $\underline{CA_6 + BPO_4}$

X-ray analysis of CA_6 + 5% BPO_4 mixture, hot-pressed at different temperatures, showed that no reaction took place up to 600°C. After hot-pressing at 700°C, a weak peak representing $AlPO_4$ could be detected. In addition, X-ray analysis of previously hot-pressed samples showed a great similarity to those samples fired after room temperature casting. In the range 900 - 1200°C, $AlPO_4$ and $9Al_2O_3.2B_2O_3$ were detected. At higher temperatures (i.e. 1300°C) α-Al_2O_3 could be clearly detected accompanied with a noticeable decrease in the intensities of the CA_6 peaks. Microstructures of some of these samples are shown in Fig. 5.17(B). Dependence of strength upon firing temperatures is shown in Fig. 5.21. Mechanical properties and related physical properties are given in Tables 5.6 and 5.7.

(3) $\underline{CA_2 + BPO_4}$

X-ray analysis showed that no reaction occurred on hot-pressing this mixture at different temperatures up to 700°C. On the other hand, X-ray analysis of previously hot-pressed samples showed that small amounts of $AlPO_4$ could be detected after firing at 900°C. A trace of $9Al_2O_3.2B_2O_3$ could also be detected after firing at 900 and 1200°C. At higher temperatures (i.e. 1200 and 1300°C), calcium hexa-aluminate together with α-Al_2O_3 were clearly detected. Microstructures of some of these samples are shown in Fig. 5.16(C). Dependence of strength upon firing temperatures is given in Fig. 5.21. Strength, porosity and other physical properties are given in Tables 5.6 and 5.7.

(4) $\underline{CA + BPO_4}$

X-ray analysis of these mixtures, hot-pressed at different temperatures up to 700°C, showed that no reaction took place either by using 5% or 10% BPO_4. In addition, X-ray analysis of previously hot-pressed

samples showed that traces of $AlPO_4$ could be detected after firing at 900°C. Calcium dialuminate was detected and this increased markedly at the higher temperatures used (Fig. 5.22). In addition, a group of peaks previously observed (Section 5.1.1.2) at $2\theta = 32$, 33.3 and 34° were also detected after firing at high temperatures (i.e. 1200-1300°C). At higher temperatures a ceramic-type bond is formed, transforming the material rapidly into a dense refractory body. Dependence of strength upon firing temperatures is given in Fig. 5.21. Microstructures of some of these samples are shown in Fig. 5.15(B). Mechanical properties and related physical properties are given in Tables 5.6 and 5.7.

(5) Secar "250" + BPO_4

The commercial material Secar "250" was found to behave exactly like a mixture of CA + CA_2. At higher temperatures (i.e. 1200 and 1300°C) mainly CA_2 was detected, but hardly any CA. After firing at 1200 and 1300°C, the material was transforming rapidly into a dense material. Mechanical properties and related physical properties are given in Tables 5.6 and 5.7.

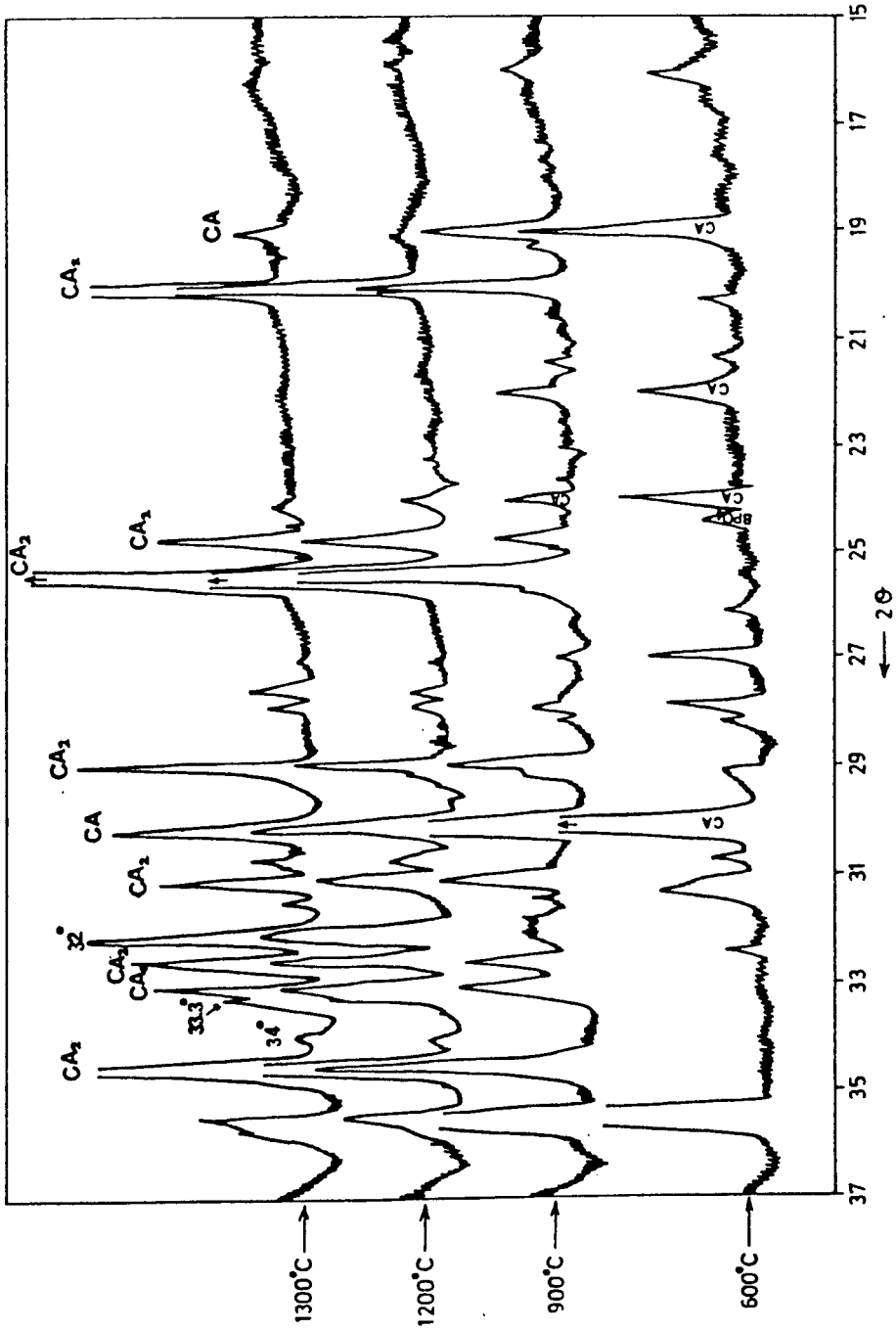

Fig. 5.22: X-ray diffractometer traces of the mixture CA + 10% BPO_4, hot-pressed (under 207 MNm^{-2} pressure, at 300°C for 30 min.), fired at different temperatures for 24 hours.

5.3 Discussion

Only a limited amount of information on the phase relationships in the ternary system B_2O_3-Al_2O_3-P_2O_5 has been reported in the literature[67]. Primary interest in the system has been centred on its glass-forming properties[131,132]. Ternary phase relations in the system CaO-B_2O_3-P_2O_5 have not been studied in detail[133]. On the other hand, there has been no report in the literature of phase or property studies in the quaternary system B_2O_3-CaO-Al_2O_3-P_2O_5.

(a) Samples cast at room temperature, followed by firing

From the present DTA and XRD results of the mixtures α-Al_2O_3 + 5 or 10% (H_3PO_4+H_3BO_3) (Figures 5.1, 5.2), it has been found that the binary crystalline phases $AlPO_4$ and $9Al_2O_3$-$2B_2O_3$[126,134,135] are the only two compounds formed in the range of firing up to 1300°C. Therefore, it is believed that the strength properties of the above mixtures will depend mainly on these two components. The role of aluminum phosphate as a cementitious material has been previously discussed (Section 4.3), where it was established that in room temperature casting followed by firing, the strength increased with the percentage of $AlPO_4$ formed *in situ*. This can explain the increase in the strength up to 900°C (Fig. 5.3), but not the sudden decrease between 900 and 1200°C. On the other hand, the compound $9Al_2O_3.2B_2O_3$ was detected after firing at 900°C and above, the amount increasing with temperature up to 1200°C (Fig. 5.2 and Table 5.2). Therefore, it may be suggested that the decrease in the strength may be due to the formation of the compound $9Al_2O_3.2B_2O_3$. Above 1200°C, the strength increased rapidly and this may be due either to the increase of the $AlPO_4$ content or to the decrease of the amount of $9Al_2O_3.2B_2O_3$ and the formation of the ceramic-type bond. On the other hand, all of these factors may be important.

Comparing the two mixtures α-Al_2O_3 + 10% (H_3PO_4+H_3BO_3) and α-Al_2O_3 + 5% (H_3PO_4+H_3BO_3) (Fig. 5.3 and Table 5.2), it can be noted that:

(1) With low temperature fired samples (300 -600°C), the 10% mixture has a higher strength value than the 5% mixture. This may be explained on the basis of the higher percentage of $AlPO_4$ which has been formed *in situ* in the former than in the latter.

(2) Between 900 -1200°C, the strength values of the 10% mixture are lower than those of the 5%. This may be due to the higher amount of $9Al_2O_3.2B_2O_3$ which has been formed *in situ* in the 10% mixture.

From the above evidence, it appears that the compound $9Al_2O_3.2B_2O_3$ does not function as a cementitious material when formed *in situ*. This result is supported by the work carried out recently by Baranova et al.[136] in their investigation of the influence of boric anhydride upon the physicomechanical properties of corundum ceramics. They found that mechanical flexure strength is decreased noticeably when the boric anhydride content is increased from ~1-2.9%. The authors also suggested the reduction in strength may be due to crystal growth and the partial dissolution of corundum crystals in the liquid phase, which in turn weakens the contact points between the various phases and grains. It was also noted that when calcium hexa-aluminate is mixed with (H_3PO_4 + H_3BO_3), it behaves approximately like α-Al_2O_3 mixtures. Therefore, the above explanation may serve in the case of the CA_6 mixtures.

The DTA results (Fig. 5.1 and Table 5.1) show that CA_6, CA_2 and CA, when mixed with 10% (H_3PO_4+H_3BO_3), all produce an endothermic peak at about 1240°C. This was reported by Rickles[87] as the sublimation temperature of BPO_4 at atmospheric pressure. A small amount of boron phosphate may thus be formed from the above mixtures, but it is evidently too small to be detected by XRD (Fig. 5.6). A DTA peak at 1240°C was not however detected when α-Al_2O_3 was used instead of a calcium aluminate phases. This was probably due to BPO_4/$AlPO_4$ solid solution formation,

and is in accordance with the work of Hern[67] who concluded that a complete series solid solution of this type can be attained above 1200°C. On the other hand it was also reported[67] that $AlPO_4$-$9Al_2O_3$-$2B_2O_3$ was a binary system with partial solid solution at both ends.

Calcium monoaluminate, calcium dialuminate and Secar "250" mixtures showed an increase in strength with increasing firing temperatures without exception. This may be due to:

(1) The formation of $AlPO_4$ *in situ* at 300-900°C.

(2) The presence of only small amounts or the entire absence of $9Al_2O_3.2B_2O_3$.

(3) A high degree of densification taken place between 900-1300°C. (Particles were deformed[137], Fig. 5.8A, 5.9A and 5.15A).

In addition, the phase composition and especially the CA/CA_2 ratio was found to affect the strength of the fired samples. Any decrease in this ratio would increase the strength as shown in Fig. 5.23. This is consonsurate with contemporary published work[138]. On the other hand the unknown peaks (2θ = 32°, 33.3° and 34°) which were detected in the CA mixtures after firing at higher temperatures represent uncharacterized compound.

(b) Hot-pressing

The dependence of strength upon firing temperatures of the mixture α-Al_2O_3 + 5% (H_3PO_4+H_3BO_3) (previously hot-pressed under 207 MNm^{-2} pressure, at 300°C for 30 minutes) showed a great similarity to the room temperature casting mixture except between 900 and 1200°C. In this mixture, the strength values are (as expected) approximately twice those of the room temperature casting. At the same time, there is no decrease in the strength between 900°C and 1200°C. This may be due to:

(1) The formation of $9Al_2O_3.2B_2O_3$ at relatively low temperature, (600°C) (Fig. 5.5 and Table 5.2). (No noticeable increase in the

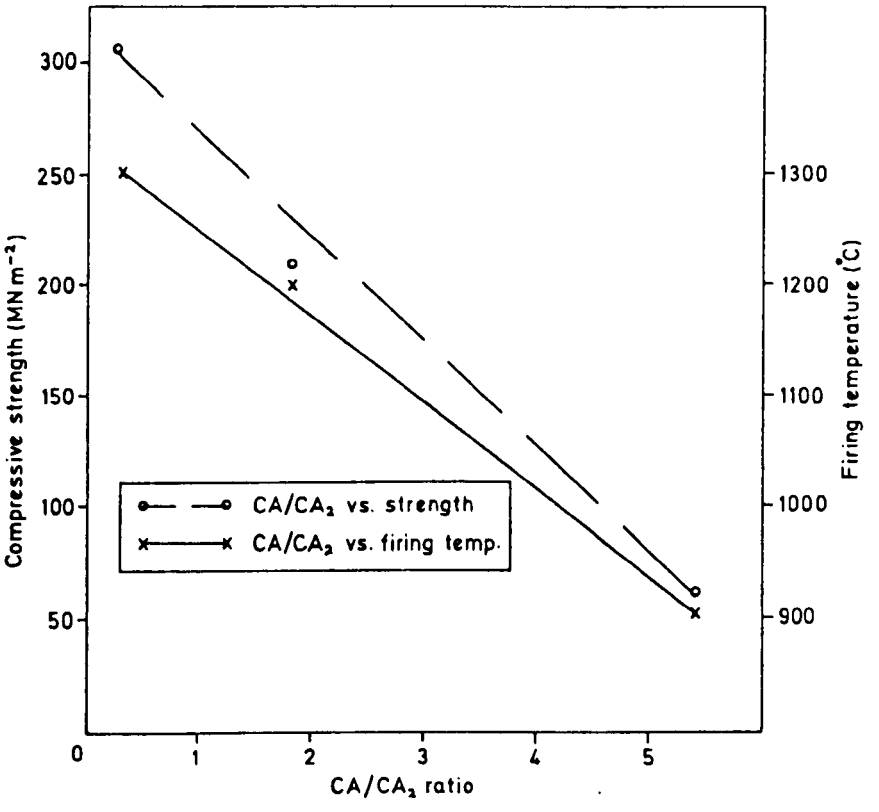

FIG. 5.23: The relationship between CA/CA_2 ratio and the strength and firing temperature of the mixture CA + 5% (H_3PO_4+H_3BO_3), room temperature casting.

$9Al_2O_3 \cdot 2B_2O_3$ content after firing between 600 -1200°C was observed (2-2.4%, Table 5.2)).

(2) Changes of porosity.

The above observations may explain why the strength values in the previously hot-pressed samples did not show the sudden decrease between 900 -1200°C.

The mixture α-Al_2O_3 + 5% BPO_4 showed a great similarity to the above mixture over all the range of firing temperatures. On the other hand, and as expected, CA_6 mixtures with (H_3PO_4+H_3BO_3) or BPO_4 showed a great similarity to the corresponding α-Al_2O_3 mixtures. This is due to the much higher Al_2O_3 content and products similar to those from α-Al_2O_3 mixtures are perhaps more likely.

Fired products of calcium monoaluminate, calcium dialuminate and Secar "250" cement mixtures with (H_3PO_4+H_3BO_3) or BPO_4 showed a great similarity with each other. They all showed an increase in strength with increasing firing temperatures without exception. The factors suggested previously (Section 5.3(a)) are believed to affect the strength here as well. The dependence of strength on $\frac{C}{C+A}$ ratio using (H_3PO_4 + H_3BO_3) or BPO_4 bonding agents are shown in Figures 5.24 and 5.25. A great similarity between both figures can be noticed. This suggests that for each starting material, mixed with (H_3PO_4+H_3BO_3) or BPO_4, nearly the same reaction products and degree of densification took place. It is believed that the most important part of the strength vs firing temperature curve is between 900 -1200°C. In this part, most of the reactions, and densification process, took place. The relationship of strength difference between samples fired at 900 and 1200°C and $\frac{C}{C+A}$ ratio is shown in Fig. 5.26. An increase in this difference with increasing $\frac{C}{C+A}$ ratio is evident. It is believed that the degree of densification is playing the important part in this zone of firing

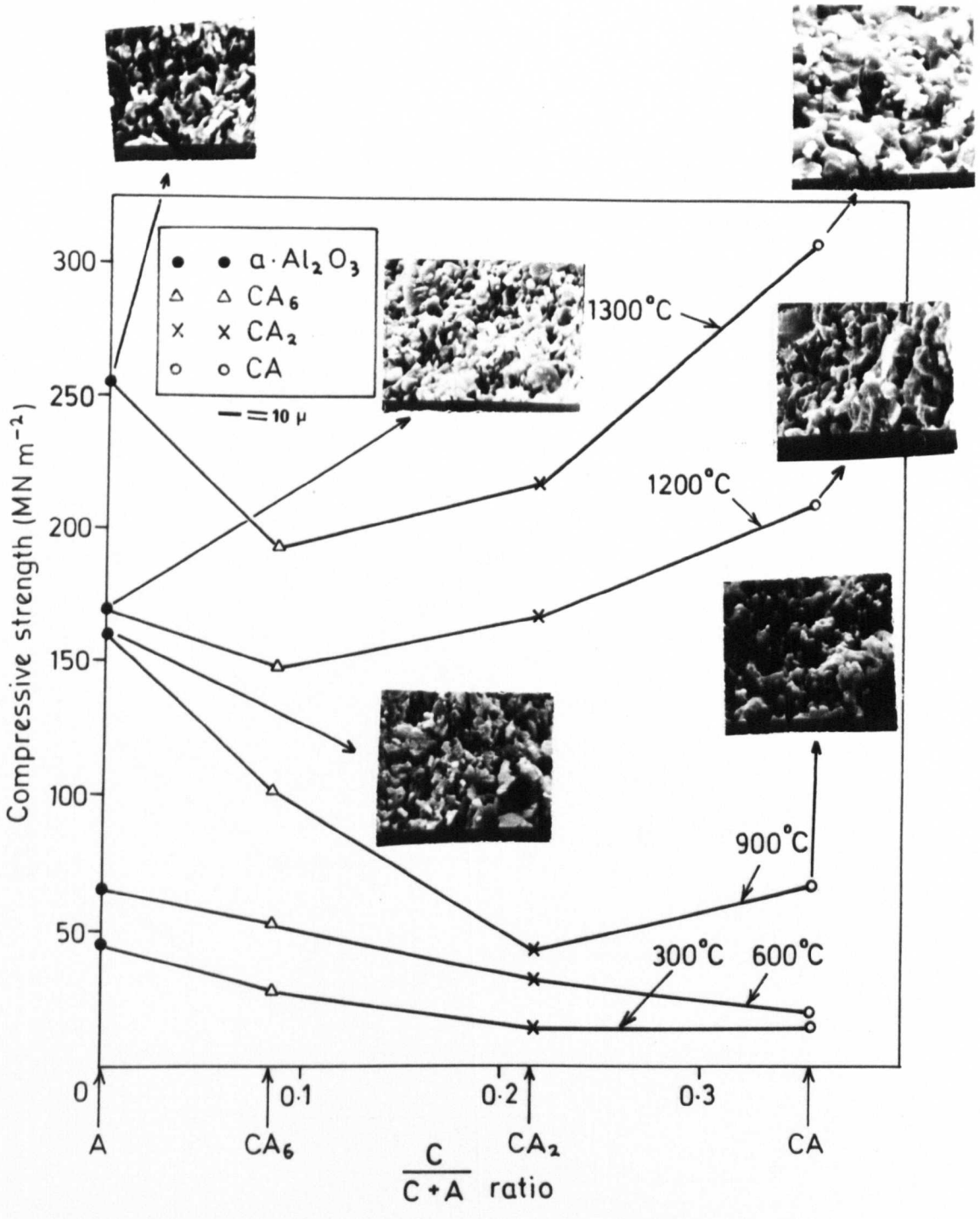

Fig. 5·24 Relationship between compressive strength and $\frac{C}{C+A}$ ratio. Samples mixed with 5% (H_3PO_4 + H_3BO_3), hot-pressed (under 207 MNm^{-2} pressure, at 300°C for 30 minutes) and fired at various temperatures.

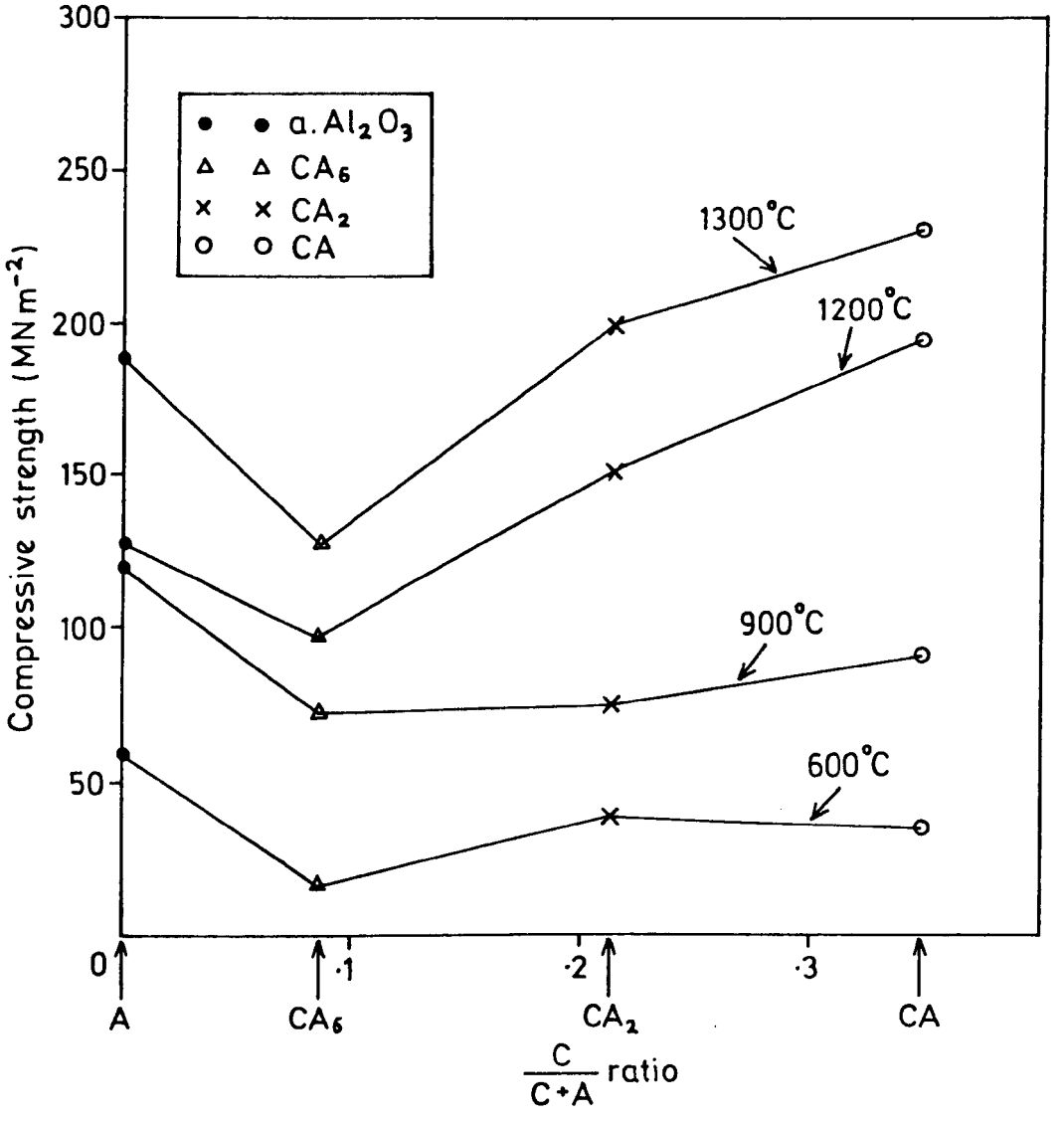

Fig. 5.25: The relationship between compressive strength and $\frac{C}{C+A}$ ratio. Samples mixed with 5% BPO_4, hot-pressed (under 207 MNm^{-2} pressure, at 300°C for 30 min.), and fired at various temperatures for 24 hours.

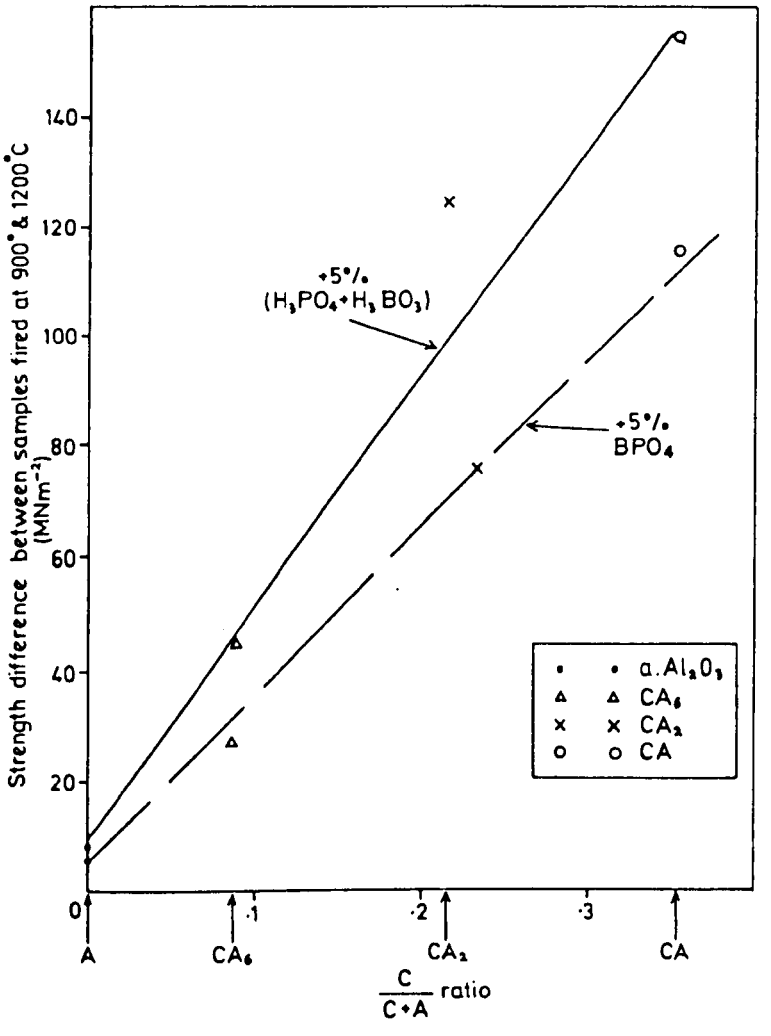

Fig. 5.26: The relationship between strength difference between samples fired at 900°C and 1200°C, and $\frac{C}{C+A}$ ratio. Samples mixed with 5% (H_3PO_4 + H_3BO_3) or 5% BPO_4, previously hot-pressed (under 207 MNm^{-2} pressure, at 300°C for 30 min.) before firing.

temperature and consequently generating the high strength values. However, volumetric shrinkage is one of the important phenomena which occur during sintering processes. The relationships between the percentage of volumetric shrinkage and $\frac{C}{C+A}$ ratio is shown in Fig. 5.27, whereas the relationship between the percentage of volumetric shrinkage and the compressive strength is shown in Fig. 5.28. From these graphs, it was found that the higher the $\frac{C}{C+A}$ ratio, the higher the strength difference between 900 and 1200°C and the higher the volumetric shrinkage in the same range of firing. In addition, it is of interest to notice that there is no great strength difference between samples mixed with $(H_3PO_4+H_3BO_3)$ and those mixed with BPO_4.

The above observations indicate that the results may be divided into two main groups:

(1) The first group includes α-Al_2O_3 and CA_6 mixtures with either "$H_3PO_4+H_3BO_3$" or BPO_4. In this group it is suggested that the strength developed is dependent <u>firstly</u> on the phases produced from the reaction, and <u>secondly</u> on the densification and sintering processes which take place at high temperatures.

(2) The second group includes CA, CA_2 and Secar "250" cement mixtures with "$H_3PO_4+H_3BO_3$" or BPO_4. In this group, it is suggested that the strength is dependent <u>firstly</u> on the densification and sintering processes which take place at higher temperatures and <u>secondly</u> on the phases produced in the reactions.

This may explain why members of the first group have higher strength values than the second group, in the low range of firing temperature, (i.e. 300 -900°C), whereas members of the second group (especially CA) develop the higher strength when fired in the high temperature range (i.e. > 900 -1300°C).

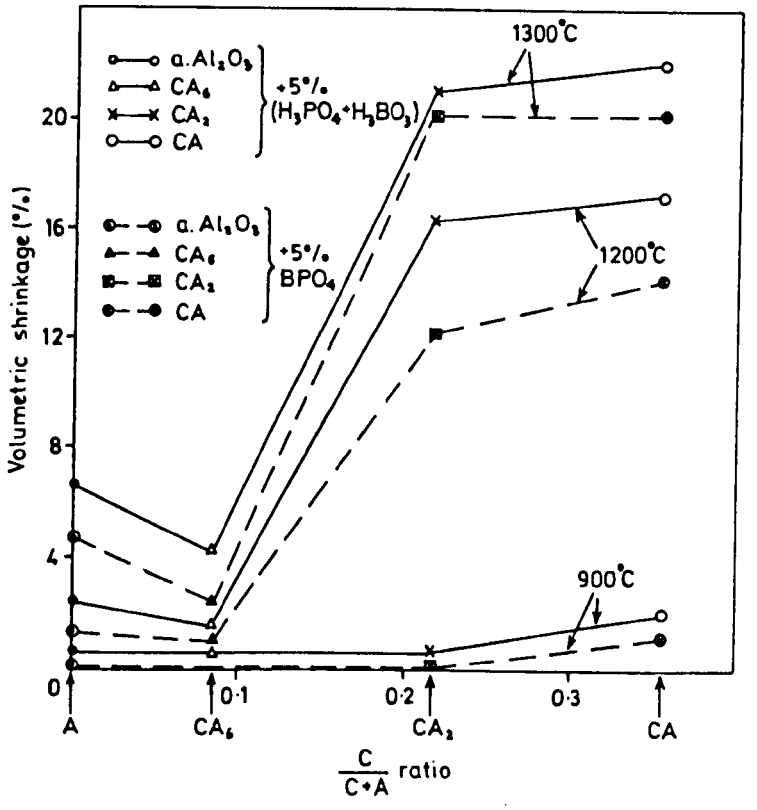

Fig. 5.27: The relationship between % of volumetric shrinkage and $\frac{C}{C+A}$ ratio. Samples previously hot-pressed (under 207 MNm^{-2} pressure, at 300°C for 30 min.) before firing for 24 hours.

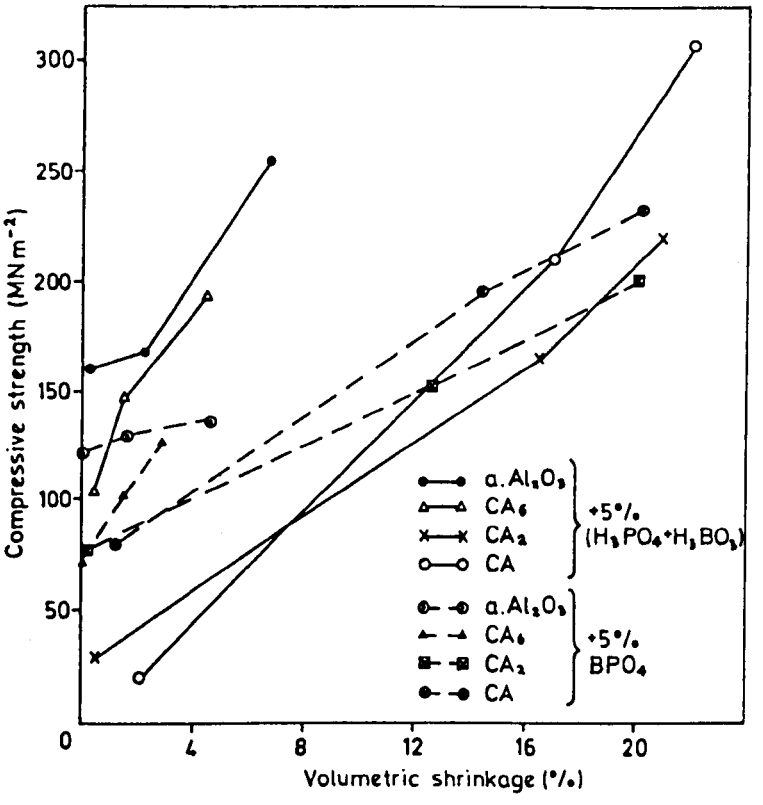

Fig. 5.28: The relationship between compressive strength and % of volumetric shrinkage. Samples were previously hot-pressed (under 207 MNm^{-2} pressure, at 300°C for 30 min.) before firing.

(c) Strength-porosity relationship

Compressive strength-porosity relationships for fired samples previously hot-pressed (under 207 MNm^{-2} pressure, at 300°C for 30 minutes) have been investigated using two different empirical equations. Figure 5.29 shows this relationship plotted on the basis of equation 2.7[108], and Fig. 5.30 on the basis of equation 2.8[109].

From these figures, the following observations can be made:

(1) Calcium monoaluminate, CA, calcium dialuminate, CA_2, and Secar "250" cement mixtures follow the exponential relation in equation 2.7, Fig. 5.29, with an acceptable n value (n = 9). The values of n as discussed before (Section 4.3(c)) will depend on pore location, size and shape. Therefore, it can be suggested that these three mixtures behave approximately the same with regard to those factors which affect n values (pore location, size and shape).

(2) The line representing calcium hexa-aluminate, CA_6, and α-Al_2O_3 mixtures, Fig. 5.29, has a steeper slope (n = ~34) which indicates that for a given decrease of porosity a great increase of strength is obtained. In addition, these two mixtures are also approximately similar to each other but they look quite different to the three mixtures above (CA, CA_2 and Secar "250").

(3) Figure 5.30 shows a good fitting of the data from calcium hexa-aluminate, CA_6, and α-Al_2O_3 mixtures with a high slope value. Moreover, calcium monoaluminate, calcium dialuminate and Secar "250" cement show an acceptable fit as well.

(4) The effect of either (H_3PO_4+H_3BO_3) or BPO_4 as additives can be considered to aid the densification, especially of CA, CA_2 and Secar "250" cement. Therefore, it has a great influence in decreasing the porosity of these mixtures, particularly after firing at higher temperatures.

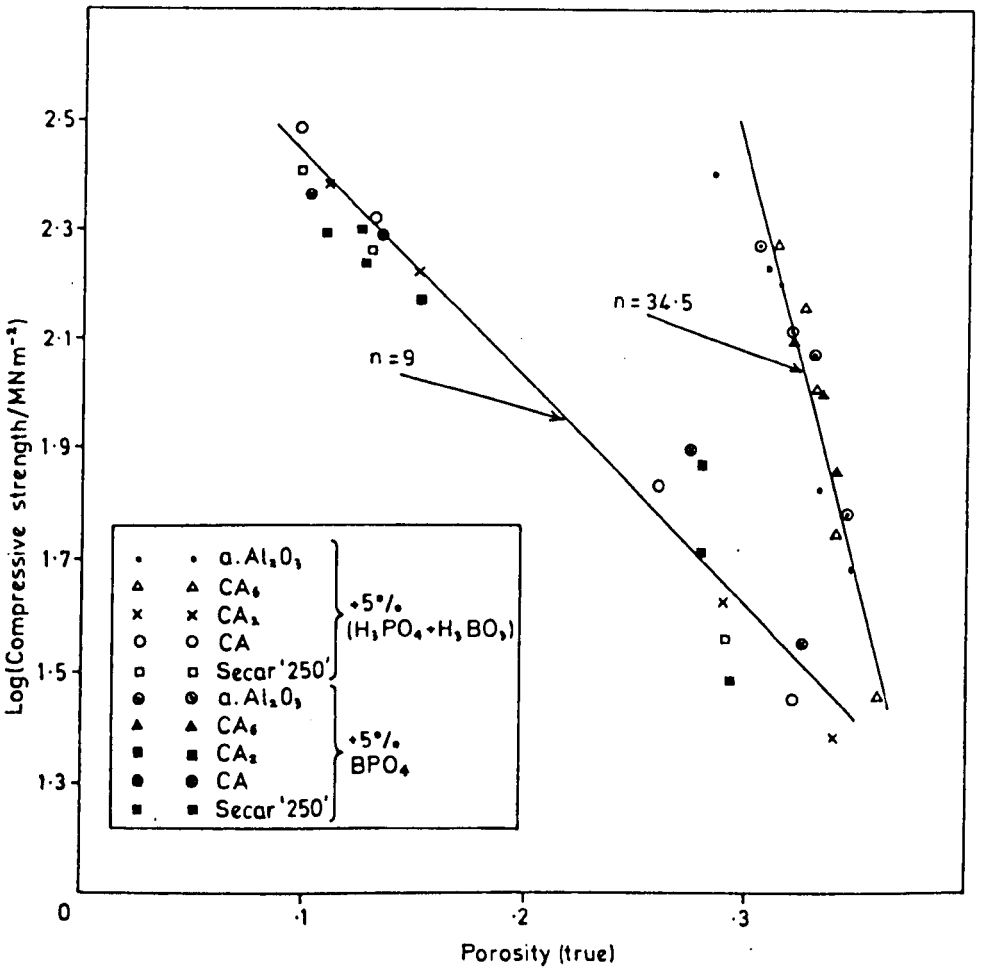

Fig. 5.29: Log strength-porosity relationship; data plotted on the basis of equation (2.7).

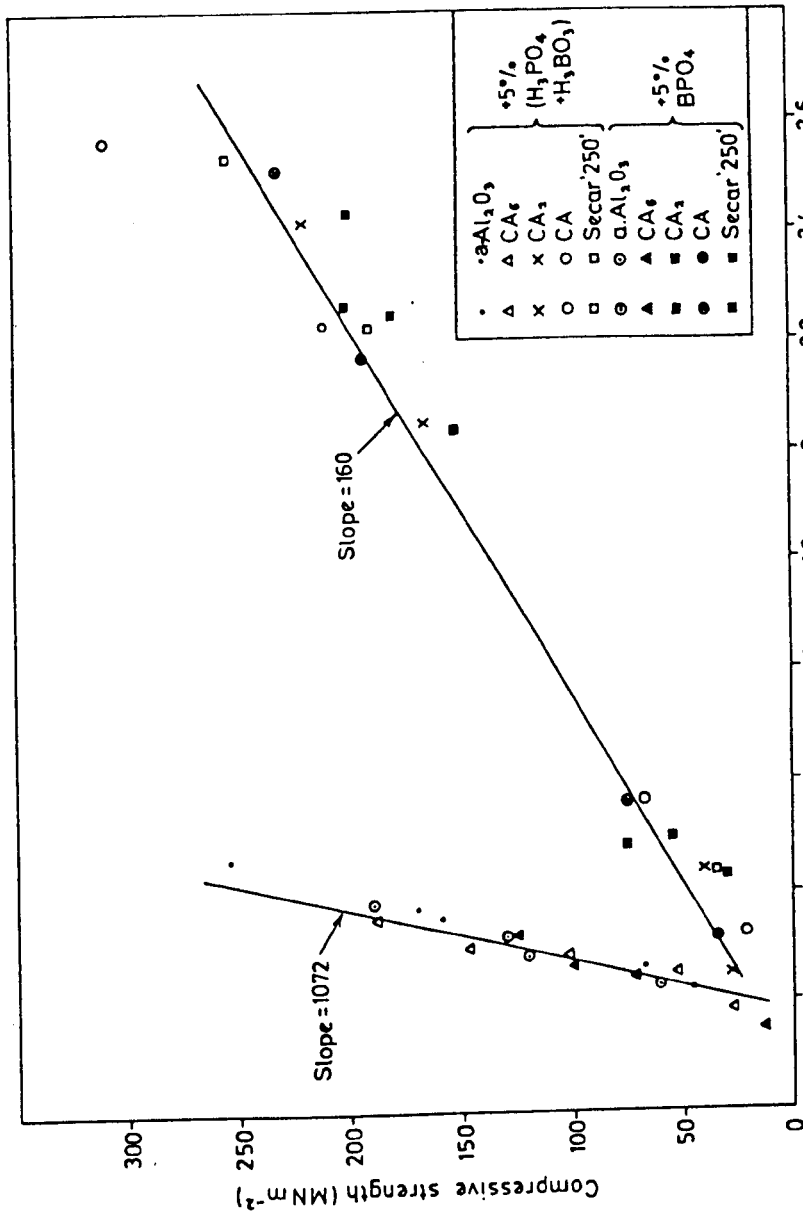

Fig. 5.30: Strength-porosity relationship. Data plotted on the basis of equation (2.8).

(5) It is evident from both graphs that the data will fit in two lines with different n or slope values. Therefore, it is apparent that the difference in starting material is affecting this relationship, especially in the presence of additives.

(6) Generally, both equations, with appropriate n and slope values, show a nearly similar fit to the data. Therefore, this work supports the view of Evans and Tappin[139] that the use of single empirical relationship to represent this dependence could be misleading.

CHAPTER 6

PHOSPHORIC ACID + CHROMIUM TRIOXIDE MIXTURE AND PREFABRICATED CHROMIUM PHOSPHATE ADDITIVES

6.1 Phosphoric Acid + Chromium Trioxide Mixture

A stoichiometric mixture of phosphoric acid (H_3PO_4) and chromium trioxide (CrO_3) was used as a bonding agent. Throughout the present work, 5 and 10% of this mixture was reacted with α-Al_2O_3, CA_6, CA_2, CA and Secar "250" cement. The three different techniques of sample preparation were used (Chapter 4).

6.1.1 Results

6.1.1.1 α-Al_2O_3 + (H_3PO_4 + CrO_3)

(a) Samples cast at room temperature, followed by firing

The same procedures previously described (Sections 3.3.1 and 3.3.3) were followed to mix and fire α-Al_2O_3 with 5 and 10% (H_3PO_4 + CrO_3). X-ray analysis, Fig. 6.1, showed that aluminium phosphate, $AlPO_4$, was the only new crystalline compound to be formed and detected after firing. Dependence of strength upon firing temperatures is shown in Figures 6.2 and 6.3. The results showed that 10% (H_3PO_4 + CrO_3) gave higher strength values than mixing with 5%. However, in both mixtures, there was an increase in the strength values with increasing firing temperatures. Microstructures of some of these samples after firing at 1300°C are shown in Fig. 6.4A & B.

(b) Hot-pressing

A combination of 5% "H_3PO_4 + CrO_3" and 95% α-Al_2O_3 was mixed using $\sim$0.1 w/s ratio, under constant pressure (207 MNm^{-2}), for constant time (30 mins.) and in the range of temperature 150 - 700°C. The procedure previously described (Section 3.3.2.2) was followed. In addition, samples prepared under hot-pressing conditions (207 MNm^{-2} pressure, for 30 minutes

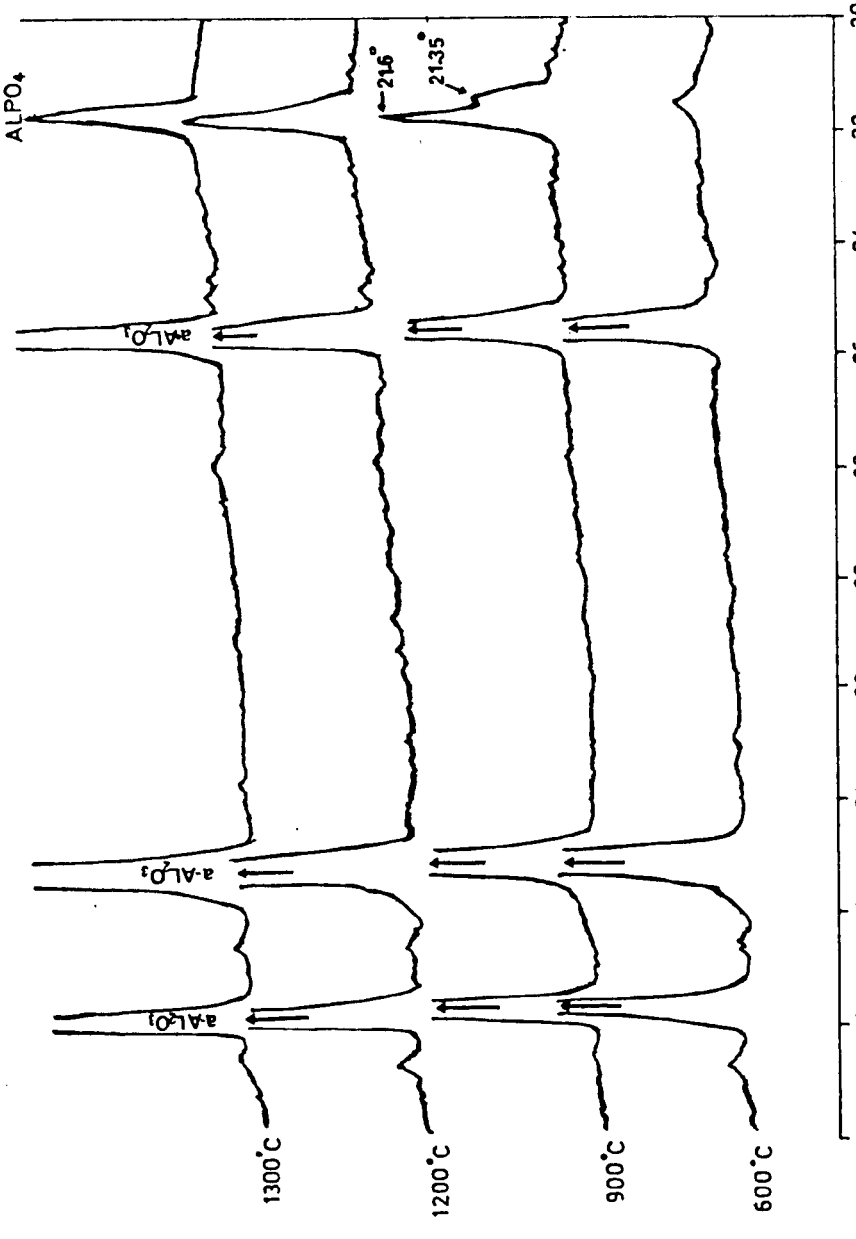

FIG. 6.1: X-ray diffraction patterns of the mixture α-Al_2O_3 + 10% (H_3PO_4 + CrO_3), room temperature casting, followed by firing at different temperatures for 24 hours.

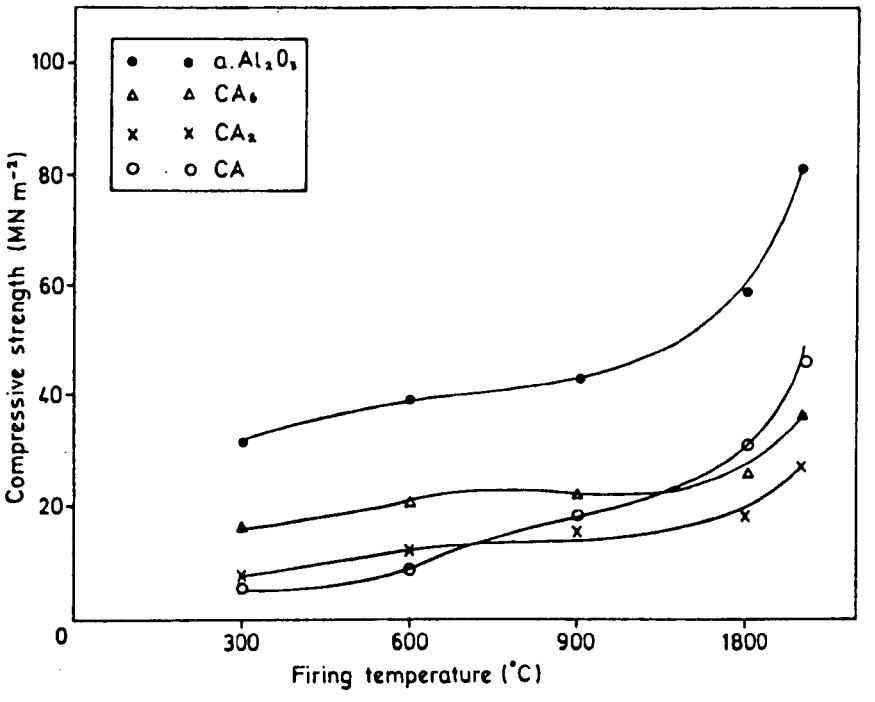

FIG. 6.2: Dependence of strength upon firing temperatures. Samples mixed with 5% (H_3PO_4 + CrO_3), room temperature cast, fired for 24 hours.

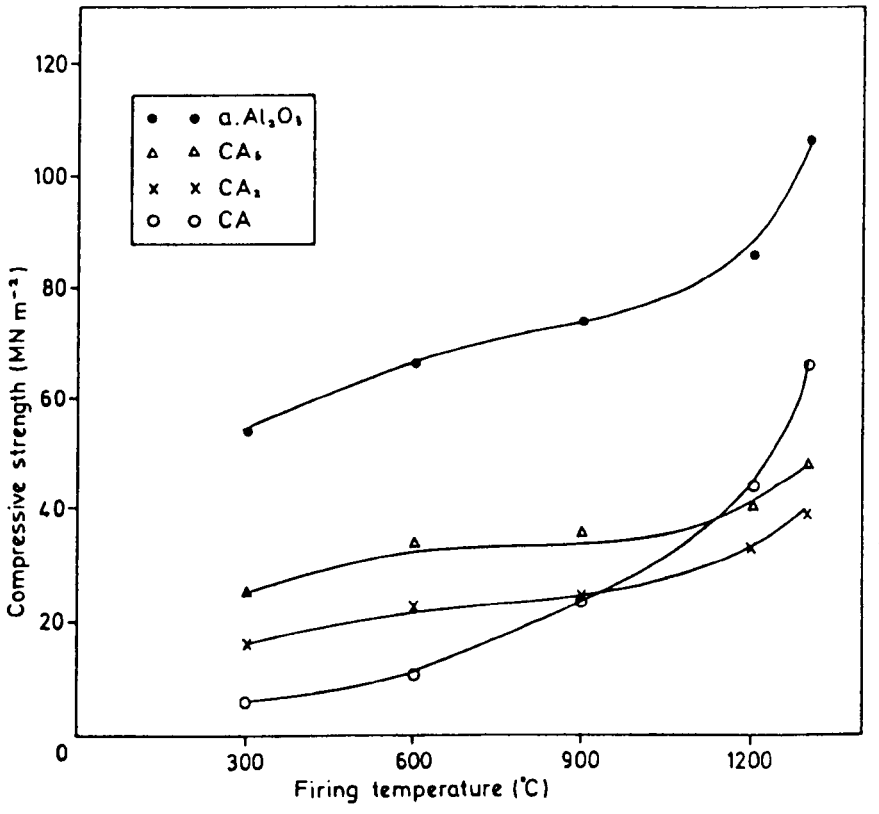

FIG. 6.3: Dependence of strength upon firing temperature. Samples mixed with 10% (H_3PO_4 + CrO_3), room temperature cast, fired for 24 hours.

FIG. 6.4A: SEM Micrographs of α-Al_2O_3 mixed with 5% (H_3PO_4+CrO_3), cast at room temperature, fired for 24 hours at:

(a) 1300°C.

FIG. 6.4B: SEM Micrographs of α-Al_2O_3 mixed with 10% (H_3PO_4+CrO_3), cast at room temperature, fired for 24 hours at:

(b) 1300°C.

FIG. 6.4C: SEM Micrographs of α-Al_2O_3 mixed with 5% (H_3PO_4+H_3BO_3), hot-pressed, under 207 MNm^{-2} pressure at 300°C for 30 mins., fired for 24 hours at:

(c) 900°C

(d) 1200°C

(e) 1300°C.

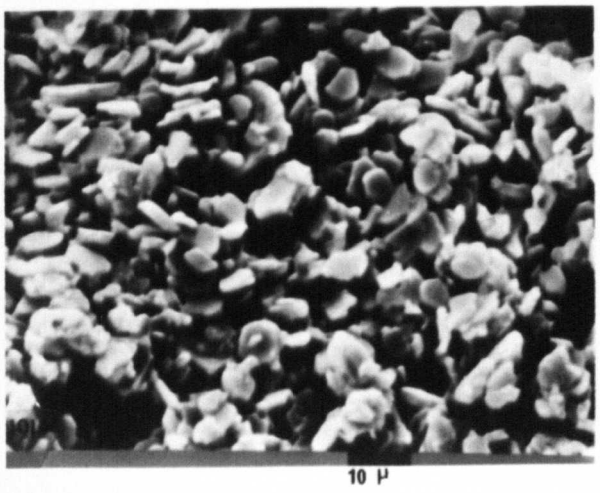

a

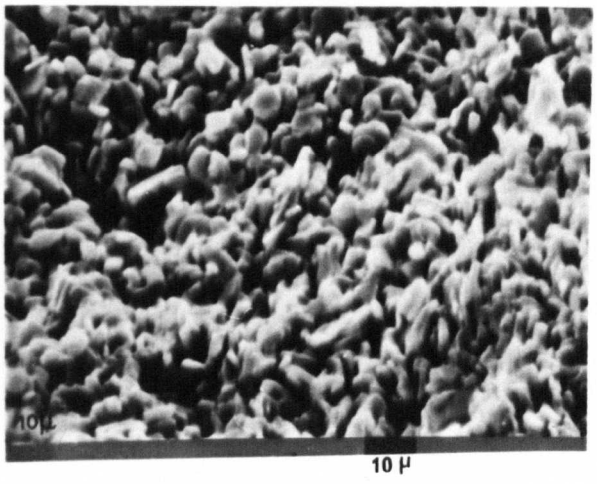

b

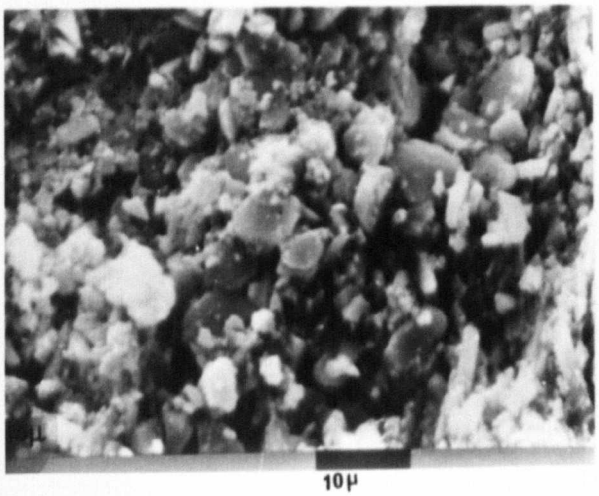

c

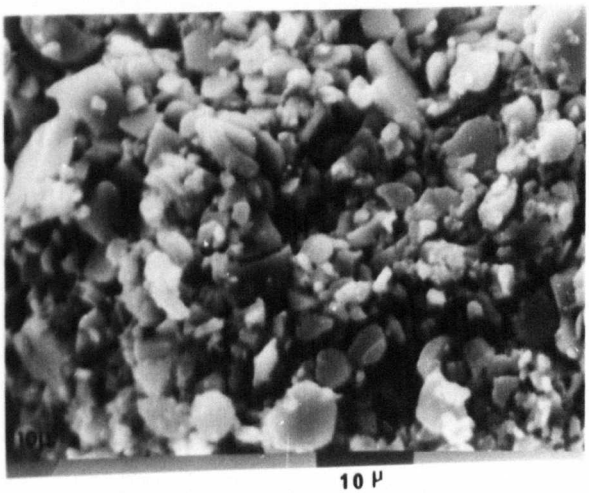

d

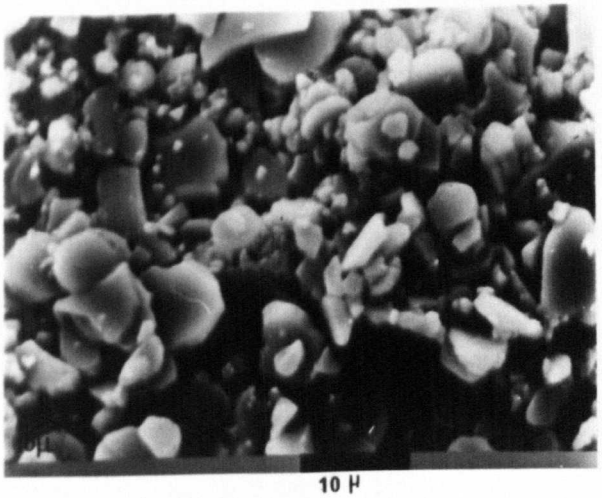

e

at 300°C) were subjected to heat treatment in air in the range 300 - 1300°C for 24 hours.

X-ray analyses of samples hot-pressed at different temperatures show that traces of $AlPO_4$ could be detected only after hot-pressing at 700°C. However, X-ray analyses of fired samples, previously hot-pressed (under 207 MNm^{-2} pressure, for 30 minutes, at 300°C), showed that aluminium phosphate, $AlPO_4$, is the only new phase which could be detected. After firing at 900°C, the peak representing $AlPO_4$ was at $2\theta = 21.35^{\circ}$ (tridymite form), whereas after firing at 1200 and 1300°C the 2θ value is 21.63° (mixture of tridymite + cristobalite forms but mainly the latter). Dependence of strength upon firing temperatures is shown in Fig. 6.5, where a continuous increase in strength with increasing firing temperatures was observed. Mechanical properties of samples hot pressed at different temperatures are given in Table 6.1, whereas mechanical properties and related physical properties of previously hot-pressed samples after firing are given in Table 6.2. Microstructure of some of these samples are shown in Fig. 6.4C.

6.1.1.2 Calcium aluminates + (H_3PO_4 + CrO_3)

(a) Samples cast at room temperature, followed by firing

The same procedures previously described (Sections 3.3.1 and 3.3.3) were followed to mix and fire calcium mono-, di- and hexa-aluminate with 5 and 10% (H_3PO_4+CrO_3) using 0.25 w/c ratio. X-ray analyses show that anhydrous aluminium phosphate could be detected as traces in CA_6 and CA_2 mixtures after firing at 900°C. In addition, calcium monoaluminate mixtures showed the formation of calcium chromate, $CaCrO_4$, after firing at 800°C which was detected by the peaks at 3.62, 2.68 and 1.85 Å. After firing at 900°C, a new compound appeared with the main peak at ~3.77 Å. By increasing firing temperature up to 1500°C, an increase in the intensity of the above peak and the appearance of another group of

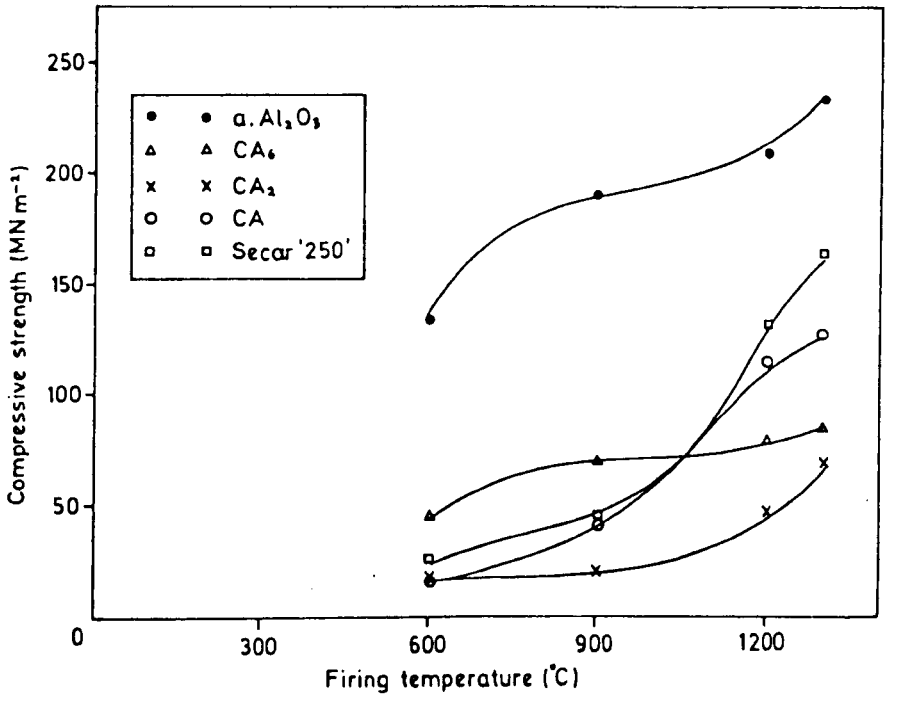

FIG. 6.5: Dependence of strength upon firing temperatures. Samples mixed with 5% (H_3PO_4 + CrO_3), hot-pressed (under 207 MNm^{-2} pressure, at 300°C for 30 minutes) before firing for 24 hours.

Mixture	Hot-pressing Parameters			w/s ratio	Indirect Tensile Strength (MNm^{-2})
	Pressure (MNm^{-2})	Temp. (°C)	Time (min)		
α-Al_2O_3 + 5% (H_3PO_4+CrO_3)	207	150	30	0.1	3.560
	207	300	30	0.1	7.184
	207	400	30	0.1	6.870
	207	500	30	0.1	9.394
	207	600	30	0.1	9.545
	207	700	30	0.1	11.148
CA_6 + 5% (H_3PO_4+CrO_3)	207	150	30	0.1	5.24
	207	300	30	0.1	3.14
	207	400	30	0.1	2.24
	207	500	30	0.1	2.43
	207	600	30	0.1	-
	207	700	30	0.1	2.87
CA_2 + 5% (H_3PO_4+CrO_3)	207	150	30	0.1	2.37
	207	300	30	0.1	-
	207	400	30	0.1	3.25
	207	500	30	0.1	-
	207	600	30	0.1	-
	207	700	30	0.1	2.236
CA + 5% (H_3PO_4+CrO_3)	207	150	30	0.1	1.86
	207	300	30	0.1	-
	207	400	30	0.1	1.93
	207	500	30	0.1	1.688
	207	600	30	0.1	2.046
	207	700	30	0.1	2.14
Secar "250" + 5% (H_3PO_4+ CrO_3)	207	150	30	0.1	5.87
	207	300	30	0.1	-
	207	400	30	0.1	3.78
	207	500	30	0.1	2.45
	207	600	30	0.1	2.75
	207	700	30	0.1	2.99

TABLE 6.1: Mechanical properties of α-Al_2O_3, CA_6, CA_2, CA and Secar "250" cement mixed with 5% (H_3PO_4+CrO_3), hot-pressed under constant pressure (207 MNm^{-2}) for constant time (30 mins.) at different temperatures.

Mixture	Hot-pressing parameters			w/c ratio	Firing Conditions		% Change		Density g.cc	Strength (MNm^{-2})		Porosity (%)
	Pressure (MNm^{-2})	Temp. (°C)	Time (min)		Temp. (°C)	Time (hrs)	wt.	vol.		Tensile	Compressive	
α-Al_2O_3 + 5% (H_3PO_4+CrO_3)	207	300	30	0.1	600	24	-1.26	-	2.76	11.625	134.3	30.303
	207	300	30	0.1	900	24	-1.87	-2.15	2.809	20.4	188	29.06
	207	300	30	0.1	1200	24	-2.407	-4.31	2.85	23.48	209	27.85
	207	300	30	0.1	1300	24	-4.84	-6.58	2.89	27.3	235	26.83
CA_6 + 5% (H_3PO_4+CrO_3)	207	300	30	0.1	600	24	-1.93	-	2.485	5.8	44.2	32.6
	207	300	30	0.1	900	24	-2.07	-0.97	2.53	8.35	70.2	31.44
	207	300	30	0.1	1200	24	-2.13	-1.3	2.56	9.4	77.5	30.7
	207	300	30	0.1	1300	24	-2.19	-4.70	2.58	10.2	88.5	30.08
CA_2 + 5% (H_3PO_4+CrO_3)	207	300	30	0.1	600	24	-1.292	-	1.92	1.8	16.5	32.80
	207	300	30	0.1	900	24	-1.921	-1.6	1.96	2.3	19.3	31.58
	207	300	30	0.1	1200	24	-2.03	-3.2	1.99	5.6	46.2	30.54
	207	300	30	0.1	1300	24	-2.120	-5.4	2.02	8.9	69.8	29.12

Table 6.2 (Cont.)

Mixture	Hot-pressing parameters			w/c ratio	Firing Conditions		% Change		Density g.cc	Strength (MNm^{-2})		Porosity (%)
	Pressure (MNm^{-2})	Temp. (°C)	Time (min)		Temp. (°C)	Time (hrs)	wt.	vol.		Tensile	Compressive	
CA + 5% (H_3PO_4+CrO_3)	207	300	30	0.1	600	24	-1.36	No change	1.98	1.76	16.5	32.88
	207	300	30	0.1	900	24	-1.68	-1.5	2.02	3.9	42.3	30.50
	207	300	30	0.1	1200	24	-1.715	-4.08	2.135	12.46	115.6	27.62
	207	300	30	0.1	1300	24	-1.778	-7.5	2.140	14.56	125	27.45
Secar "250" cement + 5% (H_3PO_4+CrO_3)	207	300	30	0.1	600	24	-1.4	No change	1.98	4.07	25.5	31.00
	207	300	30	0.1	900	24	-1.90	-1.8	2.01	5.8	43	29.84
	207	300	30	0.1	1200	24	-1.98	-3.50	2.08	17.00	133	27.09
	207	300	30	0.1	1300	24	-2.2	-5.85	2.105	20.6	163	26.89

Table 6.2: Mechanical properties and related physical properties α-Al_2O_3, CA_6, CA_2, CA and Secar "250" cement mixed with 5% (H_3PO_4+CrO_3), hot-pressed (under 207 MNm^{-2} for 30 minutes at 300°C), and fired at different temperatures for 24 hours.

peaks were observed (Fig. 6.6).

An attempt was made to separate this compound in a pure state.

A mixture of CA + 5% CrO_3 was fired at 1300°C for 24 hours. The product was then ground in an agate mortar, mixed with excess distilled water and stirred continuously overnight. The solution was then filtered and the filtrate was evaporated on a water bath. Finally, the product was fired in air at 1300°C for 24 hours.

The X-ray pattern of this product is shown in Fig. 6.7. The product was chemically analysed for Ca^{2+}, Al^{3+}, Cr^{3+} and Cr^{6+} as follows[140]:

0.2 gm of finely ground sample was weighed, and about 2 ml of H_3NO_4 (1:1) was added. The solution was then diluted to about 100 ml and heated (~ 80°C) and ammonium hydroxide was added drop by drop, so that all the Al^{3+} and Cr^{3+} were precipitated. The solution was then filtered and the filtrate was kept for the determination of Ca^{2+} and Cr^{6+}. The precipitate was then dried (110°C), ignited and weighed as two mixed oxides of Al and Cr(III).

Calcium was determined by an Atomic Absorption Spectrophotometer (Model EEL 240, Corning-EEL, Essex, England). A calibration curve for Ca^{2+} was prepared using standard $CaCl_2$ solutions, and the calcium content was determined from this.

The amount of hexavalent chromium was determined by adding a 10% solution of barium acetate drop by drop to the filtrate while it was hot. After cooling, the solution was filtered through a sintered glass crucible of porosity grade 4 and the precipitate of $BaCrO_4$ washed with hot water. Finally Cr^{6+} was determined by weighing the sintered glass crucible after drying to a constant weight.

Trivalent chromium was determined on a separate 0.2 gm sample and the procedure described above was repeated until all the Al^{3+} and Cr^{3+} were precipitated. The solution was then filtered and sodium peroxide

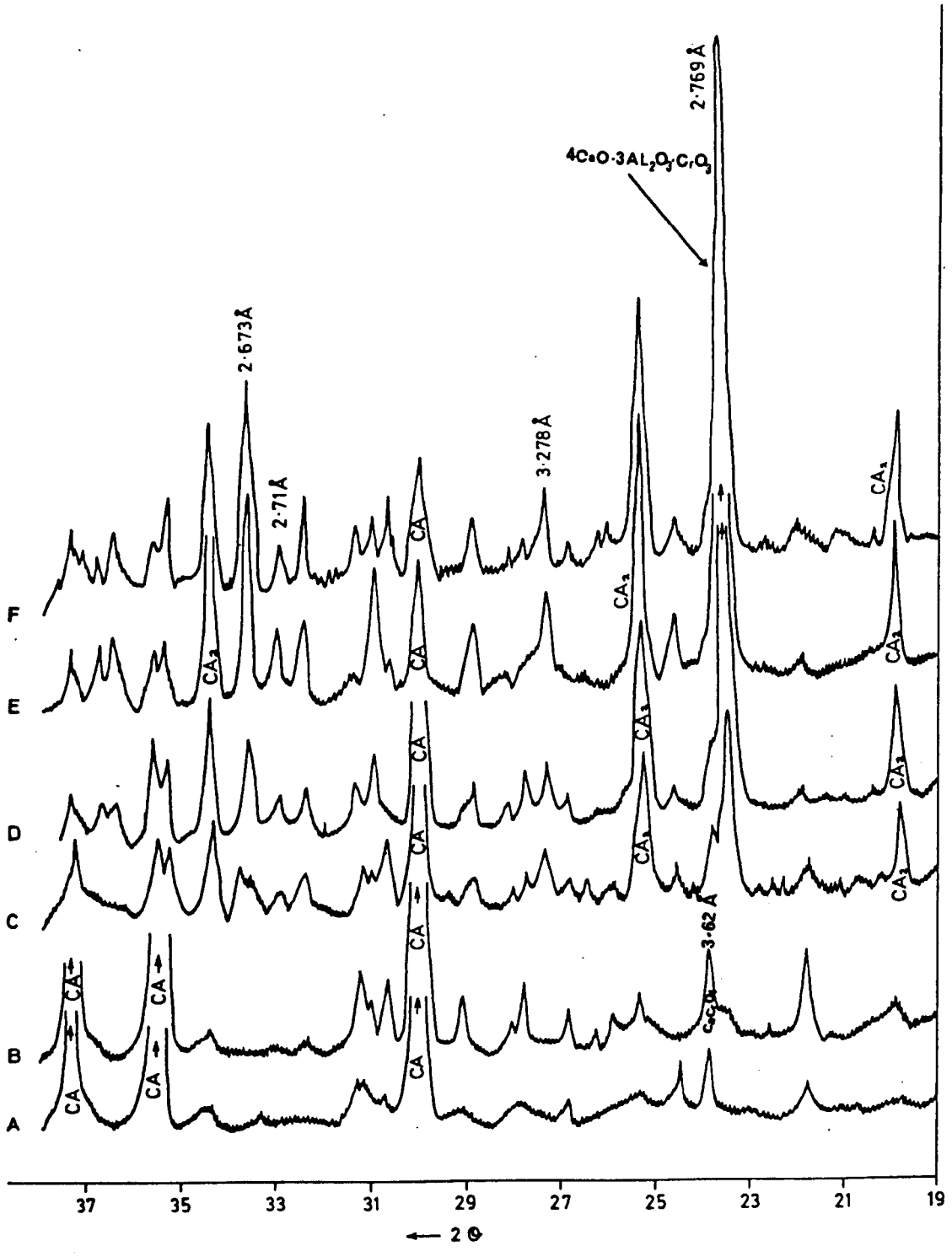

FIG. 6.6: X-ray diffractometer traces of the mixture CA + 10% (H_3PO_4 + CrO_3). Room temperature cast, and fired at: (A) 800°C, (B) 900°C, (C) 1000°C, (D) 1200°C, (E) 1300°C, for 24 hours, and (F) 1500°C for 2 hours.

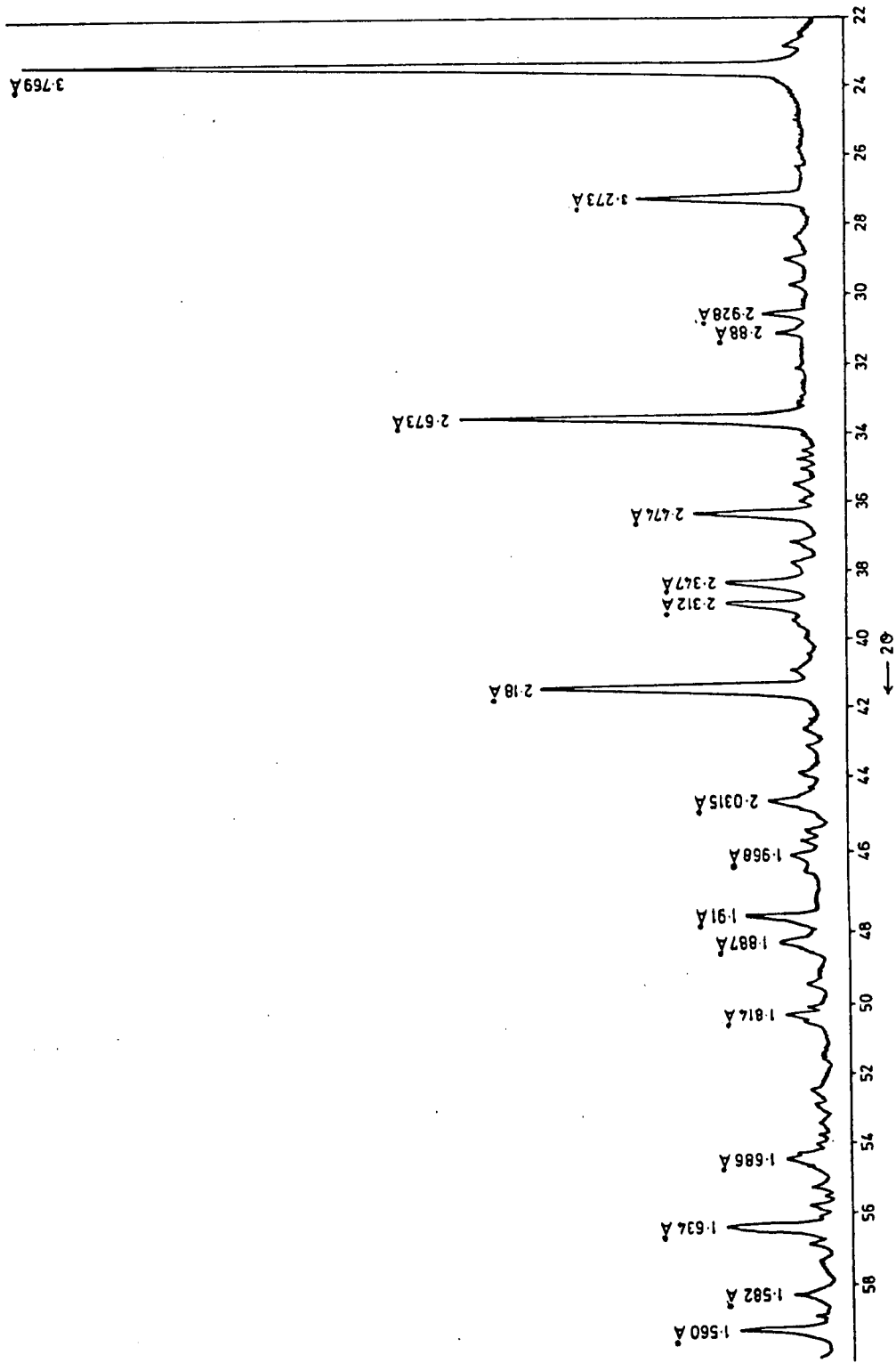

Fig-(6-7): X-ray diffractometer pattern of the compound $4C_2O_3 \cdot 3Al_2O_3 \cdot C_2O_3$

was added carefully to the precipitate until it was dissolved, converting the Cr(III) to sodium chromate. The solution was then diluted to about 40 ml and nitric acid (1:9) was added until the solution was neutral to litmus paper. The solution was then transferred to a 100 ml beaker and a solution of 10% barium acetate was added to the solution whilst it was hot until all the Cr(VI) was precipitated as $BaCrO_4$. After cooling, and allowing the precipitate to settle, the solution was filtered through a sintered glass crucible and washed with hot water. After drying, the sintered glass crucible was weighed and the weight of Cr calculated. By subtracting the weight of Cr^{3+} from the combined weight of the mixed oxides of Al and Cr(III) determined above, the Al^{3+} was found by difference.

The results showed that this compound contains 48.2% Al_2O_3, 35.8% CaO and 15.7% CrO_3. No Cr_2O_3 was detected.

Dependence of strength on firing temperatures is shown in Figures 6.2 and 6.3. In all the mixtures, there was an increase in the strength with increasing firing temperatures. However, it is of interest to note that the strengths after firing between 300 - 900°C were in the sequence $CA_6 > CA_2 > CA$, whereas after firing in the range 900 - 1300°C they were in the sequence $CA > CA_2 > CA_6$.

(b) Hot-pressing

Combinations of 5% (H_3PO_4 + CrO_3) with 95% CA_6, CA_2, CA and Secar "250" cement were mixed using ~0.1 w/c ratio, under constant pressure (207 MNm^{-2}) for constant time (30 minutes) and in the range of temperature 150-700°C. The procedure previously described (Section 3.3.2.2) was followed. In addition, samples prepared under hot-pressing conditions (207 MNm^{-2} pressure, for 30 mins. at 300°C) were subjected to heat treatment in air in the temperature range 300-1300°C.

X-ray analyses of samples hot-pressed at different temperatures

show that no reaction in any of the above mixtures took place up to 700°C. X-ray analyses of fired samples previously hot-pressed show no significant difference to those fired samples cast at room temperature. The new peaks previously detected in CA mixtures, room temperature cast and fired at 900°C, were also detected in CA and Secar "250" mixtures after firing at 900°C (Fig. 6.8). Mechanical properties and related physical properties are given in Tables 6.1 and 6.2. Dependence of strength upon firing temperatures is shown in Fig. 6.5. Between 300 - 900°C, the strength was in the sequence CA_6 > Secar "250" > CA_2 > CA, whereas above 900 - 1300°C, the sequence was Secar "250" > CA > CA_2 > CA_6. Microstructures of some of those samples are shown in Figures 6.9, 6.10 and 6.11.

Calcium monoaluminate and Secar "250" cement both contain the compound analyzed in (a) above, and the X-ray pattern is shown in Fig. 6.7. The above two starting materials were mixed with 2.5 and 5% CrO_3 only. Three different methods of sample preparation were also used (Chapter 4).

X-ray analyses of both mixtures (CA or Secar "250" + CrO_3), either those cast at room temperature or those previously hot-pressed (under 207 MNm^{-2} pressure at 300°C for 30 minutes), revealed that the compound with the characteristic X-ray pattern shown in Fig. 6.7 was formed after firing at 900°C. On the other hand, no reaction took place by hot-pressing between 150-700°C. Dependence of strength on firing temperature, and upon the percentage of CrO_3 added of previously hot-pressed samples is shown in Fig. 6.12. Generally, by increasing the percentage of CrO_3, improvements in the strength values were obtained.

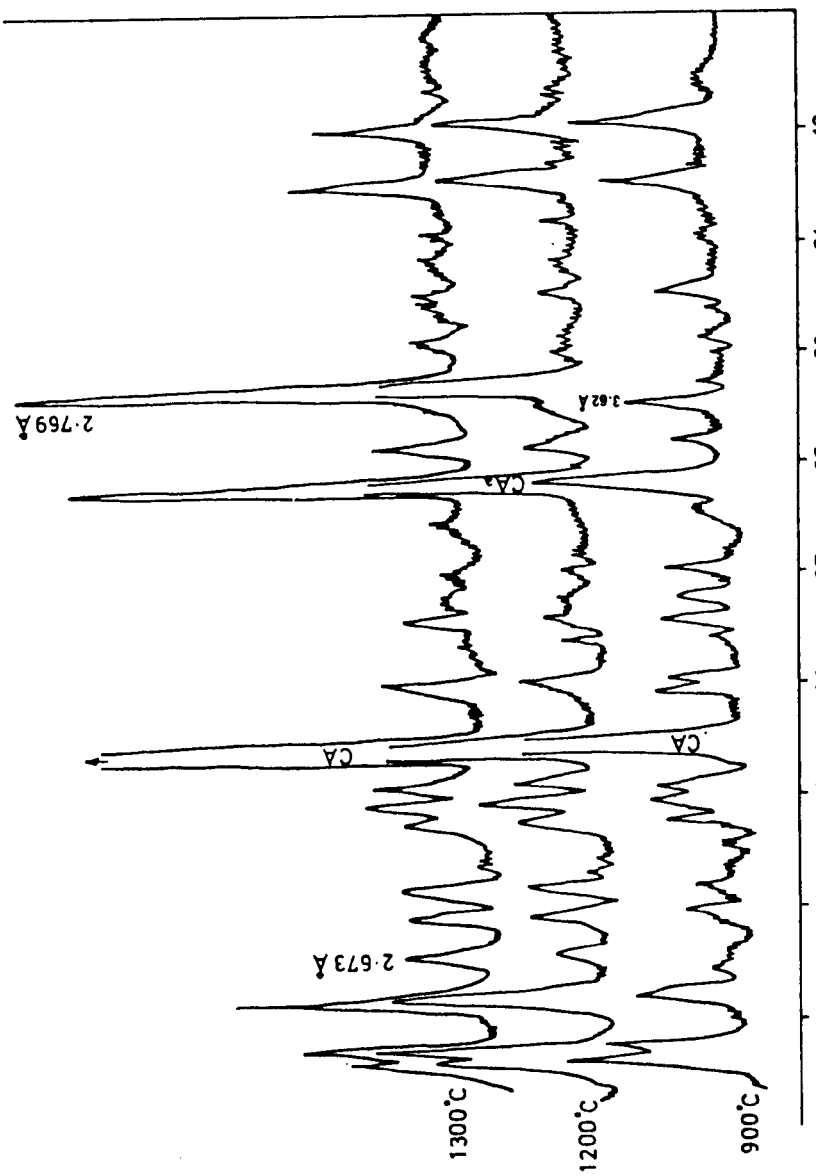

FIG. 6.8: X-ray diffractometer traces of the mixture CA + 5% (H_3PO_4 + CrO_3). Samples hot-pressed (under 207 Mlm^{-2} pressure, at 300°C for 30 minutes), before firing at different temperatures for 24 hours.

FIG. 6.9: SEM Micrographs of CA mixed with 5% (H_3PO_4+CrO_3), hot-pressed under 207 MNm^{-2} pressure at 300°C for 30 minutes, fired for 24 hours at:

(a) 900°C

(b) 1200°C

(c) 1300°C.

a

b

c

FIG. 6.10: SEM Micrographs of CA_2 mixed with 5% (H_3PO_4+CrO_3), hot-pressed under 207 MNm^{-2} pressure for 30 minutes at 300°C, fired for 24 hours at:

(a) 900°C

(b) 1200°C

(c) 1300°C.

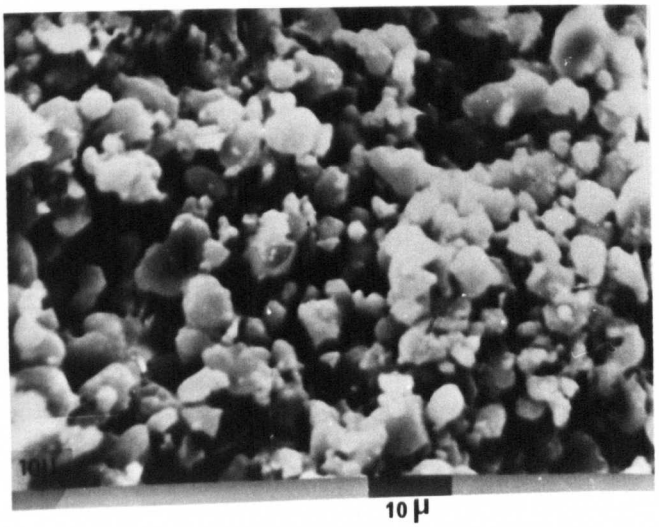

a

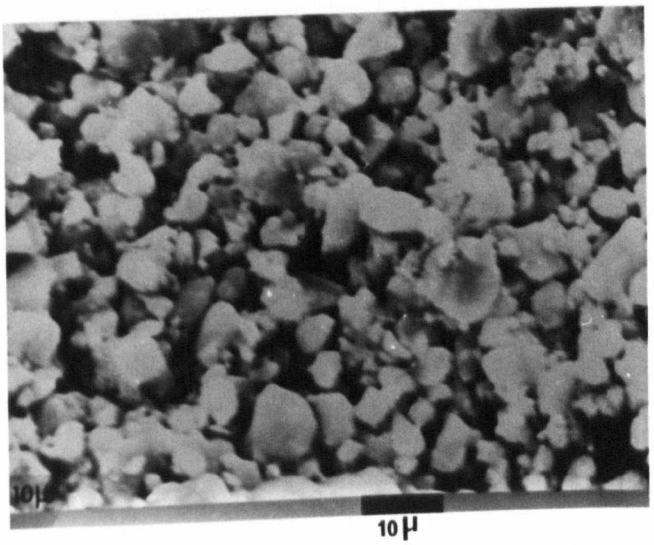

b

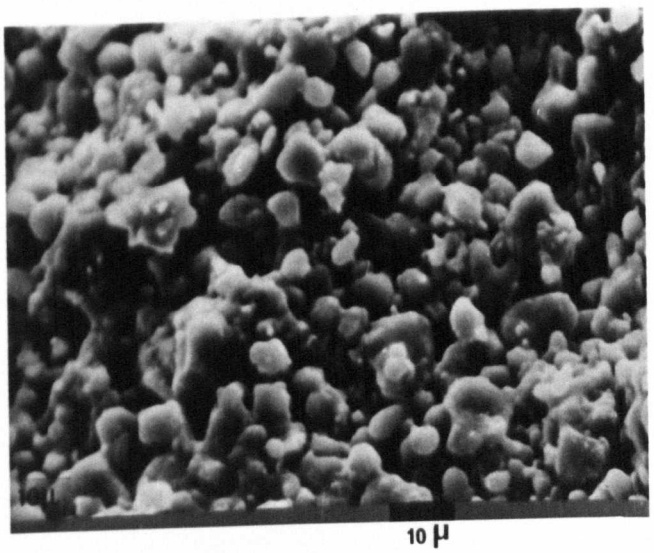

c

FIG. 6.11: SEM Micrographs of CA_6 mixed with 5% (H_3PO_4+CrO_3), hot-pressed under 207 MNm^{-2} pressure for 30 minutes at 300°C, fired for 24 hours at:

(a) 900°C

(b) 1200°C

(c) 1300°C.

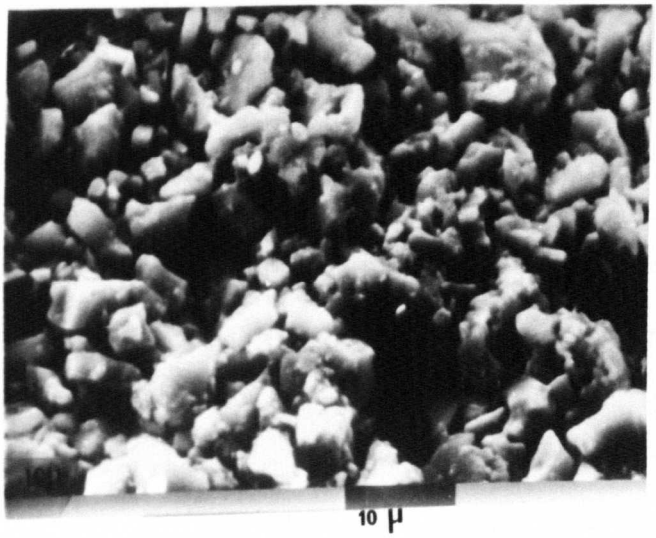

a

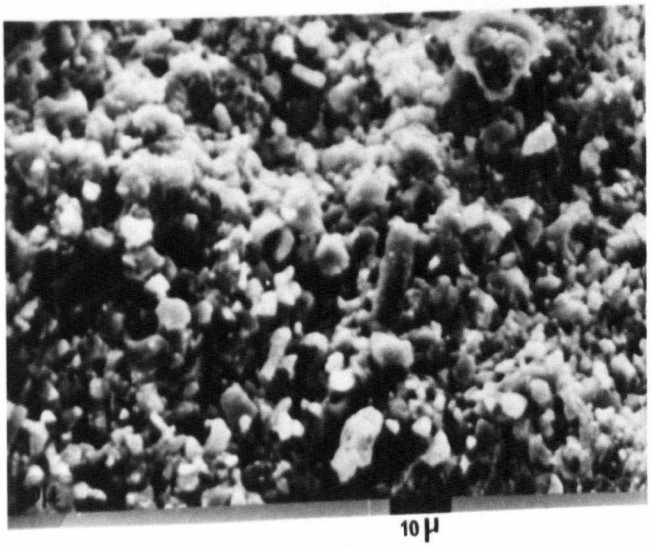

b

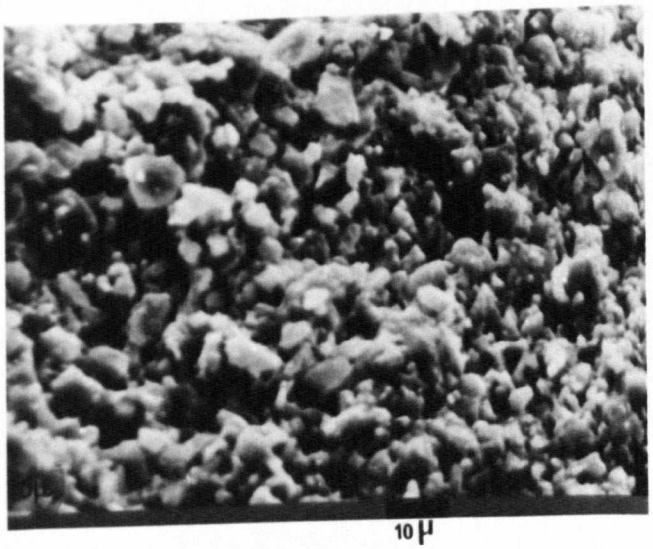

c

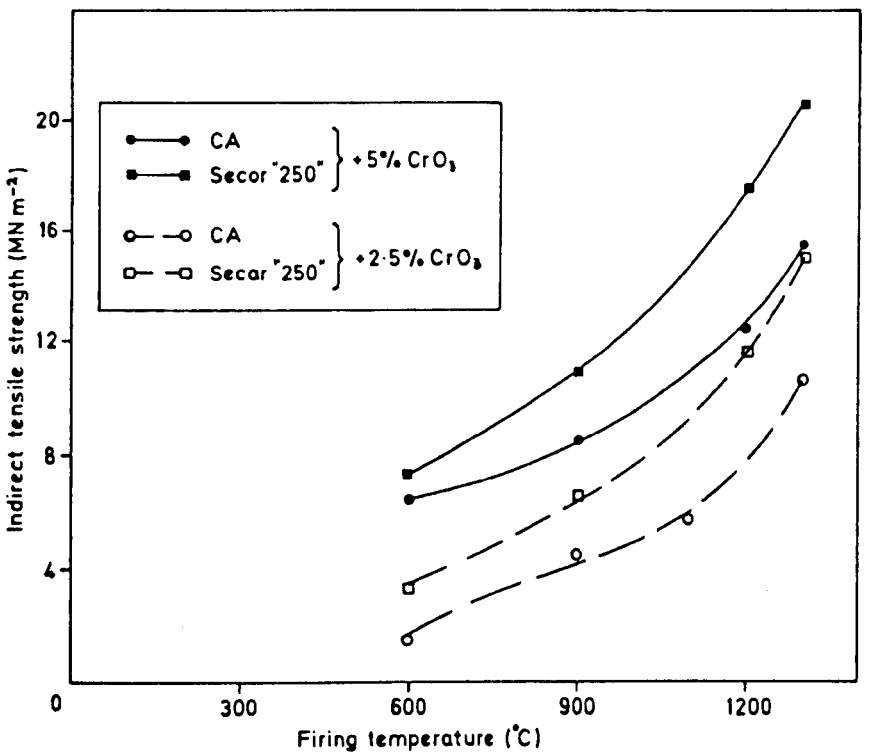

FIG. 6.12: Dependence of strength on firing temperature and upon the percentage of CrO_3 added. Samples hot-pressed (under 207 MNm^{-2} pressure for 30 minutes at 300°C), before firing.

6.2 Chromium Phosphate

Amorphous, α and β chromium phosphate, $CrPO_4$, were used as bonding agents. The two different techniques of sample preparation (room temperature casting, and hot-pressing (under 207 MNm^{-2} pressure at 300°C for 30 minutes) followed by firing, 300-1300°C) were applied.

6.2.1 Results

(a) Samples cast at room temperature, followed by firing

Calcium monoaluminate, calcium dialuminate and calcium hexa-aluminate were mixed with 10% of either α, β or amorphous chromium phosphate. The procedures previously described (Section 3.3.1 and 3.3.3) were followed for mixing and firing using 0.25 w/c ratio. X-ray analyses show that traces of aluminium phosphate were present in the CA_6 mixture, but not in the other two mixtures (CA_2 and CA). On the other hand, CA mixtures showed the appearance of the compound with the X-ray pattern in Fig. 6.7, after firing at ~ 800°C, whereas below that temperature calcium chromate, $CaCrO_4$, was detected, as shown in Fig. 6.13.

The compressive strength values of the above three mixtures were found to be not so promising. However, by using amorphous chromium phosphate, a slight improvement was noticed.

(b) Hot-pressing

Only amorphous chromium phosphate was used as a bonding agent by applying hot-pressing technique. Calcium monoaluminate, calcium dialuminate and Secar "250" cement were selected to bond with 5% amorphous chromium phosphate. The same procedure, previously described (Section 3.3.2.2) was used for sample preparation with ~ 0.1 w/c ratio.

X-ray analyses indicate that there were no significant differences between these samples and those cast at room temperature. The hot-pressed samples did, however, show some improvement in strength. Dependence of strength upon firing temperatures is shown in Fig. 6.14. Mechanical properties and related physical properties are given in Table 6.3.

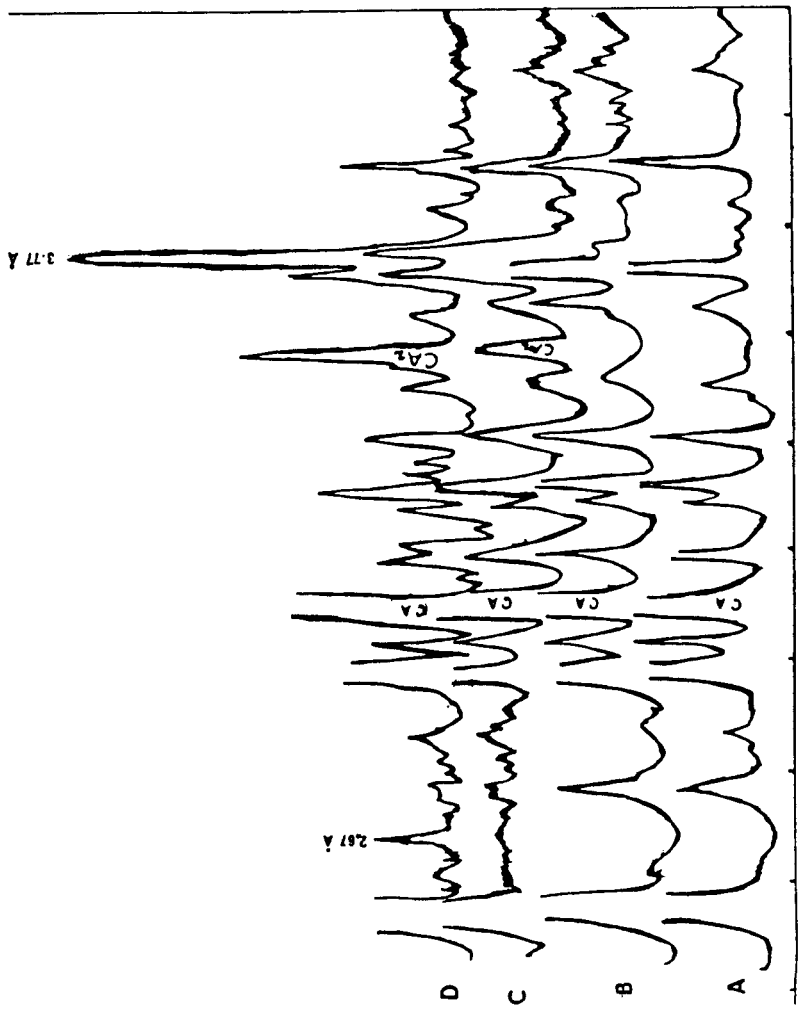

FIG. 6.13: X-ray diffractometer traces of the mixture CA + 5% amorphous $CrPO_4$ cast at room temperature, fired at (A) 600°C, (B) 700°C, (C) 800°C, (D) 900°C for 24 hours.

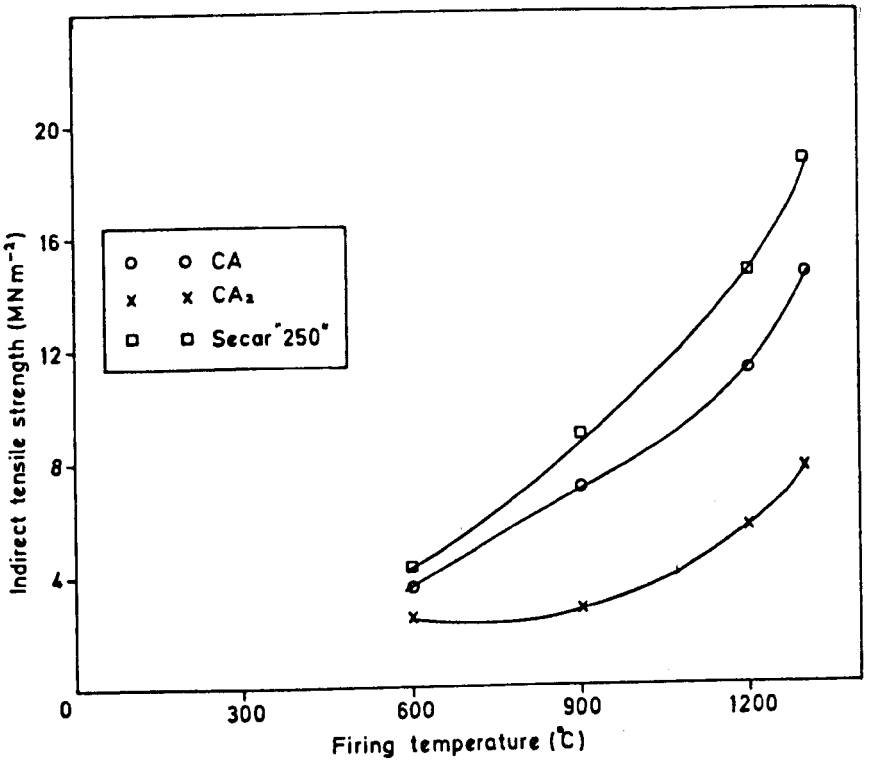

FIG. 6.14: Dependence of strength upon firing temperatures. Samples mixed with 5% amorphous $CrPO_4$, hot-pressed (under 207 MNm^{-2} pressure, at 300°C, for 30 minutes) before firing at different temperatures for 24 hours.

Mixture	Hot-pressing parameters			w/c ratio	Firing Conditions		% Change		Density g.cc	Strength (MNm^{-2})		Porosity (%)
	Pressure (MNm^{-2})	Temp. (°C)	Time (min)		Temp. (°C)	Time (hrs)	wt.	vol.		Tensile	Compressive	
CA + 5% amorphous $CrPO_4$	207	300	30	0.1	-	-	-	-	2.07	-	-	29.59
	207	300	30	0.1	600	24	-1.4	No change	2.07	3.8	-	29.59
	207	300	30	0.1	900	24	-2.08	-0.9	2.085	7.08	-	29.08
	207	300	30	0.1	1200	24	-2.4	-2.94	2.125	11.14	-	27.89
	207	300	30	0.1	1300	24	-3.07	-3.53	2.15	14.6	-	26.87
Secar "250" + 5% amorphous $CrPO_4$	207	300	30	0.1	-	-	-	-	2.04	-	-	28.70
	207	300	30	0.1	600	24	-1.97	-	2.05	4.37	-	28.32
	207	300	30	0.1	900	24	-2.38	-1.05	2.07	8.89	-	27.62
	207	300	30	0.1	1200	24	-2.75	-2.49	2.10	14.7	-	26.60
	207	300	30	0.1	1300	24	-3.17	-3.08	2.108	18.75	-	26.29
CA_2 + 5% amorphous $CrPO_4$	207	300	30	0.1	-	-	-	-	1.94	-	-	32.167
	207	300	30	0.1	600	24	-1.64	-	1.92	2.63	-	32.86
	207	300	30	0.1	900	24	-1.65	No change	1.96	2.93	-	31.46
	207	300	30	0.1	1200	24	-1.74	-1.93	1.98	5.58	-	30.76
	207	300	30	0.1	1300	24	-1.95	-3.31	2.01	7.55	-	29.72

Table 6.3: Mechanical properties and related physical properties of CA, Secar "250" cement and CA_2 mixed with 5% amorphous $CrPO_4$, hot-pressed (under 207 MNm^{-2} pressure, for 30 minutes at 300°C), and fired at different temperatures for 24 hours.

6.3 Discussion

At an early date, Kingery[46] reported that the addition of chromic acid was believed to increase the activity of phosphoric acid. However, the most extensive study using a mixture of CrO_3 and P_2O_5 was carried out by O'Hara et al.[52]. In their investigation they studied the effect of varying the phosphoric to chromic acid ratio on the strength properties of the product. However, it has been reported that the formation of aluminophosphate and aluminum chromium phosphate binders depends mainly on the P_2O_5/Cr_2O_3 molar ratio[141,142].

The $CaO-Cr_2O_3$-$CaO-Al_2O_3$ system was first investigated by Ford and Rees[143]. They suggested the formation of a quaternary phase with the formula $10CaO.8Al_2O_3.2Cr_2O_3.CrO_3$. These authors also established the upper limit of its stability at about 1500°C and the dissociation products α-calcium chromite and calcium monoaluminate, which formed a limited solid solution. Later, in 1964, Nishino and Motoki[144] also observed a ternary compound in the system $CaO-Cr_2O_3-Al_2O_3$ above 1000°C and proposed the formula $8CaO.5Al_2O_3.2CrO_3$. However, the most recent work on the above system was carried out by Klyocharov and Gaenko[145]. These authors have confirmed the existence of a ternary compound in the system $CaO-Al_2O_3-CrO_3$. According to their data, the composition of this compound corresponds to the formula $4CaO.3Al_2O_3.CrO_3$.

From the present study, it has been noticed that, in the mixture $CA + CrO_3$, a new compound was formed on firing at 900°C. X-ray analysis showed that the d-spacing data from this compound agreed to a great extent with the recently published data[145] (Table 6.4). In addition, chemical analysis of this compound (Section 6.1.1.2(a)) indicated that the formula is $4CaO.3Al_2O_3.CrO_3$. It is of interest to note that when calcium dialuminate, CA_2, was mixed with CrO_3, no traces of the above compound were detected.

Present Work			Klyucharov and Gaenko[145]		
2θ	d-Å	I/I_o	2θ	d-Å	I/I_o
23.61	3.769	100	23.60	3.77	100
27.24	3.273	19	27.26	3.27	13
30.53	2.928	5			
31.04	2.88	4			
33.53	2.673	45	33.56	2.67	31
36.31	2.474	15	36.36	2.47	9
38.35	2.347	10			
38.95	2.312	10	38.99	2.31	13
41.42	2.18	35	41.42	2.18	35
44.61	2.0315	6	44.63	2.03	3
46.09	1.968	3	46.05	1.971	4
47.61	1.91	9			
48.22	1.887	5	48.25	1.886	6
50.3	1.814	5	50.4	1.810	8
54.42	1.686	9	54.45	1.685	7
56.30	1.634	13	56.37	1.632	12
58.32	1.582	5	58.32	1.582	6
59.3	1.56	11			
			60.25	1.536	4
62.00	1.497	7	62.00	1.497	7
67.36	1.39	6	67.31	1.391	7
69.35	1.355	7	69.17	1.358	7
70.95	1.328	6	70.84	1.330	5
76.15	1.25	4	75.85	1.254	6

Table 6.4: X-ray diffraction data for the compound $4CaO.3Al_2O_3.CrO_3$

It appears, therefore, that the $\frac{C}{C+A}$ ratio may play a part in the formation of the $4CaO.3Al_2O_3.CrO_3$ compound, which is favoured by increasing CaO content. On the other hand, the formation of this compound can also be explained on the basis of the structure of both CA and CA_2. Calcium monoaluminate was reported to have β-tridymite type structure[19], in which the presence of 6-coordinated Ca^{2+} (by oxygen) causes considerable distortion of the structure. This distortion probably opens the oxygen framework and loosens Al^{3+} in its 4-coordinated positions, thus enabling some Cr^{6+} (ionic radius 0.52 Å) to replace Al^{3+} (ionic radius 0.50 Å). In order to balance the charges it is probable that one Cr^{6+} replaces two Al^{3+}, leaving unoccupied sites. In the calcium dialuminate structure, Ca^{2+} is reported to be 9-coordinated (by oxygen). This may lead to less distortion of the structure and consequent greater retention of the Al^{3+}.

(a) Samples cast at room temperature, followed by firing

It appeared from the XRD analyses that aluminum phosphate was the only new compound in these mixtures. However, it is obvious that its formation *in situ* was favoured by increasing Al_2O_3 content. On the other hand, no aluminum chromium phosphate binders were detected. In addition, it is well known that Cr^{3+} (ionic radius 0.69 Å) and Al^{3+} (ionic radius 0.50 Å) are similar in their chemical properties and their 6-fold coordination by oxygen. Furthermore, it was also reported that the calculated values of the lattice parameters a, c of Cr_2O_3-Al_2O_3 solid solutions showed a linear relationship to the concentration of Cr_2O_3 (Vegard's law)[146]. Moreover, because the ionic radius of Cr^{3+} is much larger (~27 percent) than that of Al^{3+}, the solid solutions have less atomic density and also the crystal lattice is more distorted owing to disturbance of the atomic arrangement[147].

The lattice parameters for the mixture α-Al_2O_3 + 10% (H_3PO_4 + CrO_3) were studied. The interplanar distance d_{hkl} for the reflection 110 and 012 was selected for calculation of a and c, using the equation

$$\left(\frac{1}{d^2}\right) = \frac{4}{3}\left(\frac{h^2 + hk + k^2}{a^2}\right) + \frac{l^2}{c^2}$$

The results show that the a and c axes increased by about 0.42 and 0.77% from the values with pure α-Al_2O_3. This increase is due to the solid solution.

At the same time CA_6 and CA_2 also formed solid solutions with Cr_2O_3.

On the other hand, calcium monoaluminate, CA, was the only compound to react with CrO_3 to form calcium chromate at about 800°C, and the ternary compound $4CaO.3Al_2O_3.CrO_3$ on firing at about 900°C.

Dependence of strength upon firing temperature of these mixtures is shown in Figs. 6.2 and 6.3. It is believed that aluminum phosphate content and porosity are the main factors which affect the strength. From the figures it appears that up to 900°C, the strength was in sequence α-Al_2O_3 > CA_6 > CA_2 > CA. This can be explained on the basis of the $AlPO_4$ content which is decreased by increasing CaO content. However, above 900°C the strength was in the sequence α-Al_2O_3 > CA > CA_6 > CA_2. The large improvement in strength values of calcium monoaluminate may be due to the formation of the compound $4CaO.3Al_2O_3.CrO_3$ on firing at 900°C. This compound is believed to contribute to the strength. In addition, 10% (H_3PO_4 + CrO_3) was found to be better than 5%. This may be due to the observed increase of the $AlPO_4$ and $4CaO.3Al_2O_3.CrO_3$ contents, formed <u>in situ</u> by increasing the percentage from 5 to 10%.

Prefabricated chromium phosphate, α, β and amorphous forms, were found to have limited success as bonding agents. However, the amorphous phase was more effective than the crystalline forms in promoting an increase of strength.

(b) Hot-pressing

Apart from producing more dense and less porous materials, Figures 6.4(c), 6.9, 6.10, 6.11, XRD analysis showed no significant differences in composition between samples cast at room temperature and those which were fired after hot-pressing (under 207 MNm^{-2} pressure at 300°C for 30 minutes). However, the dependence of strengths upon $\frac{C}{C+A}$ ratio is shown in Fig. 6.15. The same behaviour which has been observed in (a) above is evident. The data in Fig. 6.15 indicates that, up to 900°C, the strength was in the sequence α-Al_2O_3 > CA_6 > CA_2 > CA, whereas above 900°C the sequence was α-Al_2O_3 > CA > CA_6 > CA_2. This again may indicate that the compound $4CaO.3Al_2O_3.CrO_3$ may take part in the improvement of the strength properties of CA above 900°C.

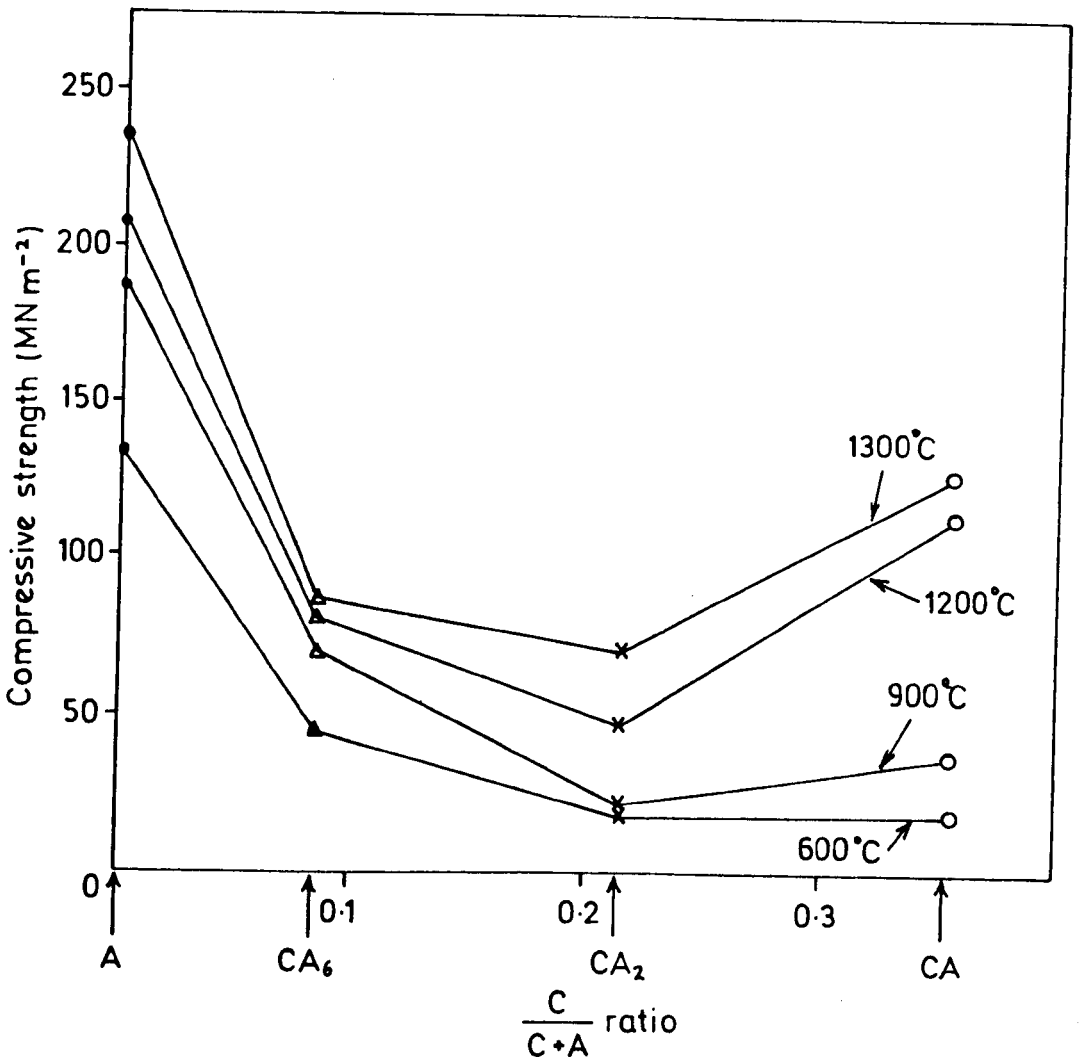

FIG. 6.15. The relationship between strength and $\frac{C}{C+A}$ ratio. Samples mixed with 5% (H_3PO_4+CrO_3), hot-pressed (under 207 MNm^{-2} pressure, at 300°C for 30 minutes) before firing.

(c) Strength-porosity relationship

Compressive strength-porosity relationships for fired samples, mixed with 5% (H_3PO_4 + CrO_3), previously hot-pressed (under 207 MNm^{-2} pressure, at 300°C for 30 minutes), have been investigated on the basis of the empirical equations 2.7[108] and 2.8[109]. These relationships are shown in Figures 6.16 and 6.17.

From the figures, it can be observed that the data fits three different lines, with different n and slope values. Therefore (as discussed in Sections 4.3(c) and 5.3(c)), it is believed that pore location, size and shape are the main factors which affect n and slope values. These results also show the dependence of this relationship on the starting material. At the same time, it has been found that the data from both CA and Secar "250" mixtures fit in one line on both graphs. These are the only mixtures containing the $4CaO.3Al_2O_3.CrO_3$ compound. Therefore, it may be suggested that the pore size, shape and location in both of them are nearly similar. Generally the line which represents these mixtures has a steeper slope in both graphs than the other two lines representing α-Al_2O_3 and CA_6. This indicates that for a given decrease of porosity a great increase in strength is obtained. At the same time, no clear conclusion can be drawn from these results about the effect of the additive on the strength-porosity relationship, whereas it is noticed that CA and Secar "250" cement are clearly reduced in porosity by the formation of the compound $4CaO.3Al_2O_3.CrO_3$ *in situ*.

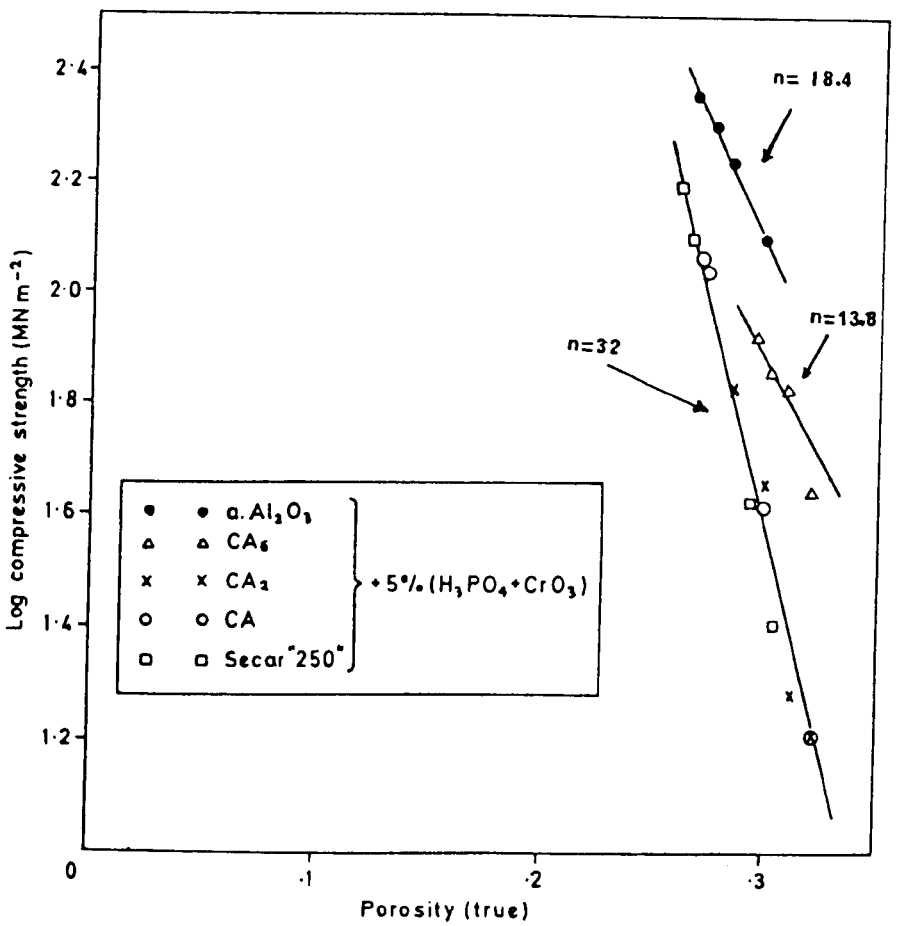

FIG. 6.16: Log strength-porosity relationship; data plotted on the basis of equation 2.7.

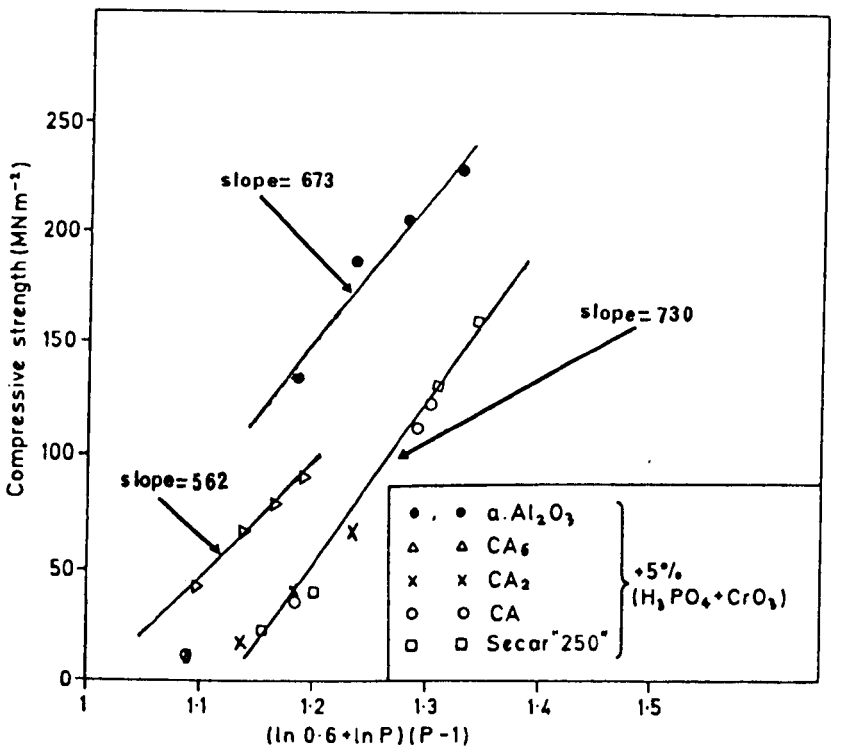

FIG. 6.17: Strength-porosity relationship; data plotted on the basis of equation 2.8.

CHAPTER 7

HOT-PRESSING OF PURE MATERIALS

Pure calcium monoaluminate (CA), calcium dialuminate (CA_2), calcium hexa-aluminate (CA_6), corundum (α-Al_2O_3) and the commercial material Secar "250" cement were studied under hot-pressing conditions. All the experiments were carried out under constant pressure (207 MNm^{-2}), constant time (30 minutes) and in the range of temperatures 50-700°C using 0.1 w/c ratio. Some of the samples hot-pressed at 150°C were cured for 1, 5 and 28 days, and some of them were heated in the range 300-1300°C for 24 hours after curing for 28 days. In addition, samples were also hot-pressed at 300°C and directly heated (without curing) in the same range of temperatures.

Physical and mechanical properties were measured and, in addition, XRD and I.R. analysis, DTA study, and morphological observation by SEM were carried out.

7.1 Results

7.1.1 Hot-pressing at different temperatures

Calcium monoaluminate (CA), calcium dialuminate (CA_2) and Secar "250" cement were selected for study at different hot-pressing temperatures. As shown in Fig. 7.1, as well as in Table 7.1, strengths of all samples increased, when hot-pressing temperatures were raised from 50-150°C, but at 300°C strengths decreased markedly, although there was a subsequent small rise between 500-700°C.

The DTA patterns for CA, CA_2 and Secar "250" cement hot-pressed at different temperatures are shown in Fig. 7.2 and the results summarised in Table 7.2. A small endothermic peak at about 290°C is found in CA hot-pressed at 50°C. This is presumably due to dehydration of $C_2A.aq.$[148] On increasing the hot-pressing temperature to 75°C, two endothermic peaks were found at about 290 and 315°C, which presumably represent $C_2A.aq.$ and C_3AH_6 respectively[148]. By increasing hot-pressing

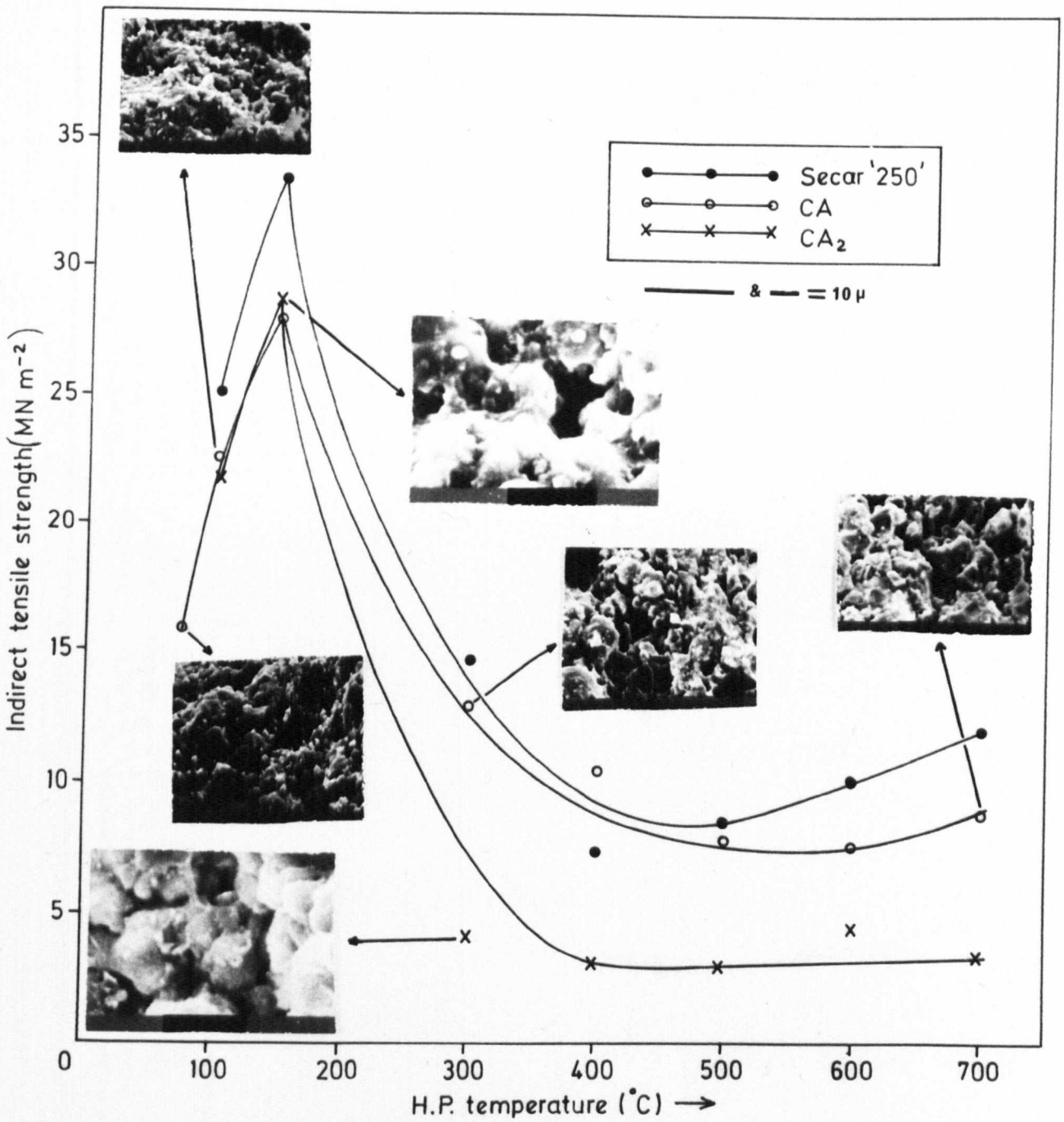

Fig.7·1 Dependence of strength of pure CA, CA_2 and Secar '250' cement upon H.P. temperature.

Material	Hot-pressing parameters			w/c ratio	Density g.cc	Strength MNm^{-2}		Porosity (%)
	Pressure MNm^{-2}	Temp. °C	Time min.			Compressive	Tensile	
Pure CA	207	75	30	0.1	2.38	140.6	15.8	19.322
	207	100	30	0.1	2.46	234	22.5	16.27
	207	150	30	0.1	2.51	253.4	28.00	14.91
	207	300	30	0.1	2.20	113.09	12.6	25.42
	207	400	30	0.1	2.14	-	10.4	27.45
	207	500	30	0.1	2.10	-	8.0	28.81
	207	600	30	0.1	2.11	-	7.4	28.47
	207	700	30	0.1	2.10	-	8.8	28.81
Pure CA_2	207	100	30	0.1	2.35	190.46	21.4	17.83
	207	150	30	0.1	2.49	260.2	28.9	12.94
	207	300	30	0.1	2.05	47.04	4.08	28.32
	207	400	30	0.1	2.05	-	3.16	28.32
	207	500	30	0.1	2.04	-	2.9	28.67
	207	600	30	0.1	2.04	-	4.4	28.67
	207	700	30	0.1	2.02	-	3.2	29.37

Table 7.1 (Cont.)

Table 7.1 (cont.)

Material	Hot-pressing parameters			w/c ratio	Density g.cc	Strength MNm^{-2}		Porosity (%)
	Pressure MNm^{-2}	Temp. °C	Time min.			Compressive	Tensile	
Secar "250"	207	100	30	0.1	2.48	244	25	12.98
	207	150	30	0.1	2.55	310	33.4	10.52
	207	300	30	0.1	2.21	150.8	13.4	22.45
	207	400	30	0.1	2.18	-	6.5	23.51
	207	500	30	0.1	2.20	-	7.7	22.80
	207	600	30	0.1	2.16	-	9.9	24.21
	207	700	30	0.1	2.16	-	12.0	24.21

Table 7.1: Mechanical properties and related physical properties of CA, CA_2 and Secar "250" cement hot-pressed under 207 MNm^{-2} pressure for 30 minutes at different temperatures.

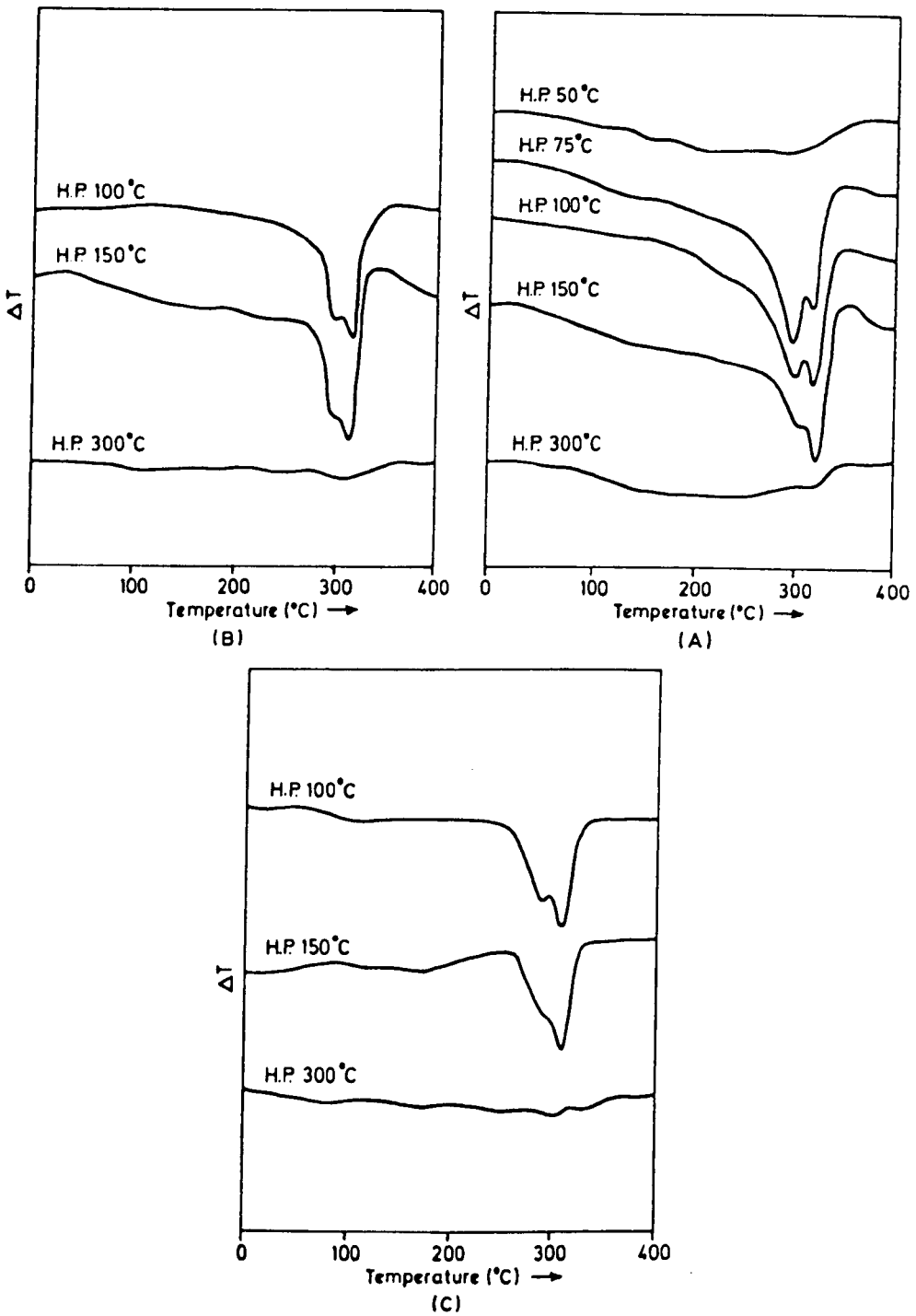

Fig. 7.2: DTA traces of (A) CA, (B) CA_2, (C) Secar "250", hot-pressed under 207 MNm^{-2} pressure for 30 minutes at different temperatures.

H.P. Temp. (°C)	Compound	1st endothermic peak			2nd endothermic peak		
		Peak temp. °C	ΔT °C	Peak area A deg.s.mg^{-1}	Peak temp. °C	ΔT °C	Peak area A deg.s.mg^{-1}
50	CA	290	-	-	-	-	-
75	CA	292	0.675	1.65	315	0.575	1.11
100	CA	290	0.525	1.22	314	0.625	1.17
150	CA	290	0.375	1.068	311	0.70	1.46
300	CA	-	-	-	314	-	-
100	CA_2	292	0.425	0.63	314	0.55	0.96
150	CA_2	295	0.525	0.80	315	0.70	1.685
300	CA_2	-	-	-	-	-	-
100	Secar "250"	290	0.375	0.675	314	0.475	0.78
150	" "	295	0.325	0.4387	315	0.475	0.82
300	" "	-	-	-	-	-	-

TABLE 7.2: Summary of DTA Results in Fig. 7.2.

temperature to 100 and 150°C, a remarkable decrease in the DTA peak at 290°C, and a noticeable increase in the peak at 315°C, was observed. Finally, by hot-pressing at 300°C, a very small trace of a peak at 315°C was detected. The same products were observed either from CA_2 or Secar "250" cement hot-pressed between 100 - 300°C as in Fig. 7.2B & C.

The XRD analysis of the samples are shown in Figures 7.3, 7.4 and 7.5. Tricalcium aluminate hexahydrate (C_3AH_6) was identified by peaks at 5.13, 2.81 and 2.30 Å, and gibbsite (AH_3) was identified by a peak at 4.85 Å; these were the main hydrated products obtained by hot-pressing up to 150°C. By hot-pressing at 300°C, only traces of C_3AH_6 were found from CA samples and it completely disappeared in CA_2 and Secar "250" cement samples.

Infra-red analyses of these samples are shown in Figures 7.6, 7.7 and 7.8. In addition to the usual absorption peaks due to CA, CA_2 and Secar "250" cement, an absorption peak appears at about 530 cm^{-1} which is due to the presence of C_3AH_6 [149]. This peak appeared in samples hot-pressed up to 150°C, whereas it was weaker or completely absent in samples hot-pressed at 300°C.

Morphological observations of the microstructure of these samples are shown in Figures 7.9, 7.10 and 7.11. Samples hot-pressed at 150°C are generally more dense, and less porous, than samples hot-pressed at 300°C.

7.1.2 Hot-pressing, followed by curing

Calcium monoaluminate and secar "250" cement were hot-pressed under 207 MNm^{-2} pressure at 150°C for 30 minutes, then cured for 1, 5 and 28 days.

The results obtained were in good agreement with results published recently [36]. The XRD results are summarised in Table 7.3.

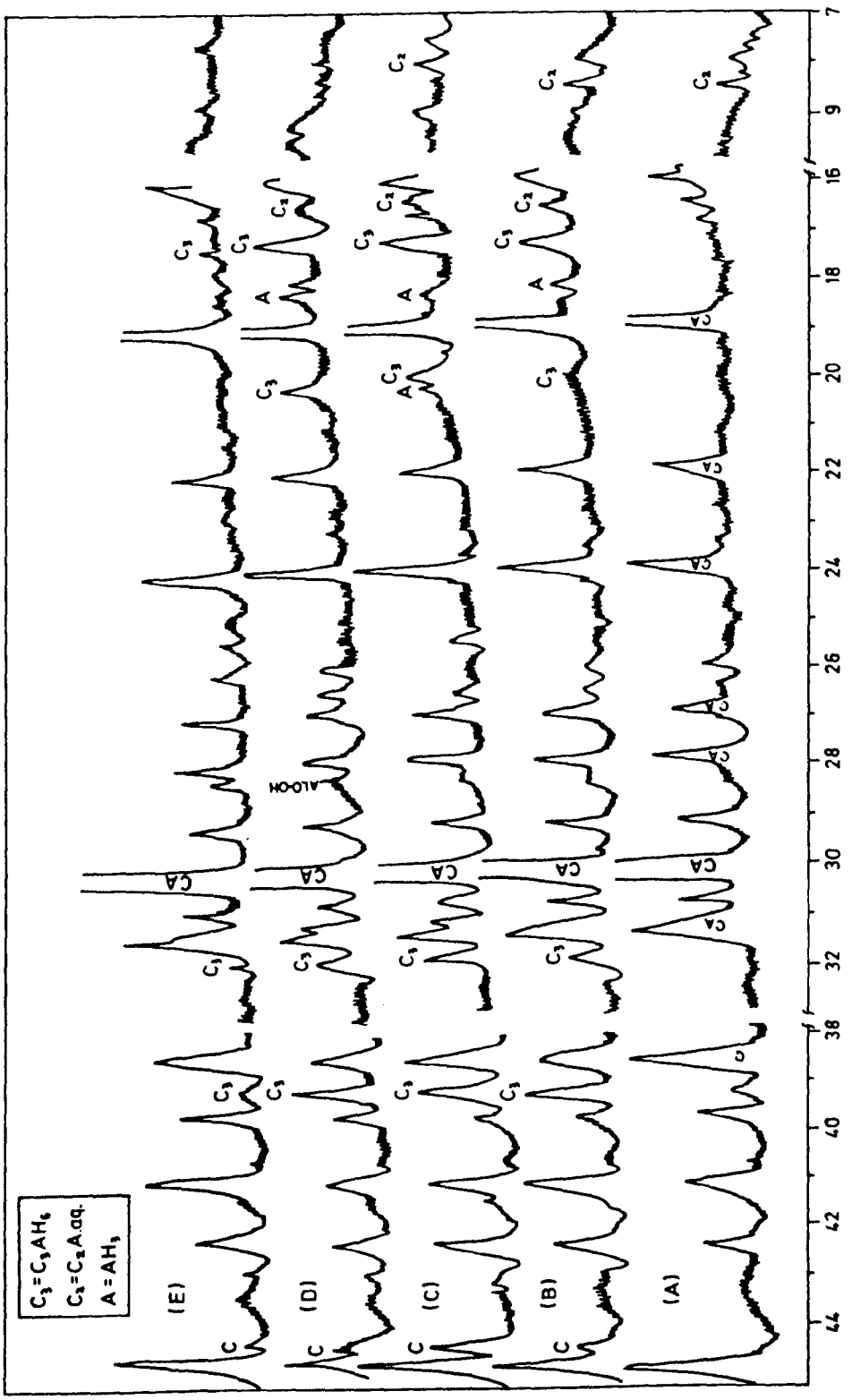

Fig. 7.3: X-ray diffractometer traces of CA, hot-pressed under 207 Mm^{-2} for 30 minutes at (A) 50°C, (B) 75°C, (C) 100°C, (D) 150°C, (E) 300°C.

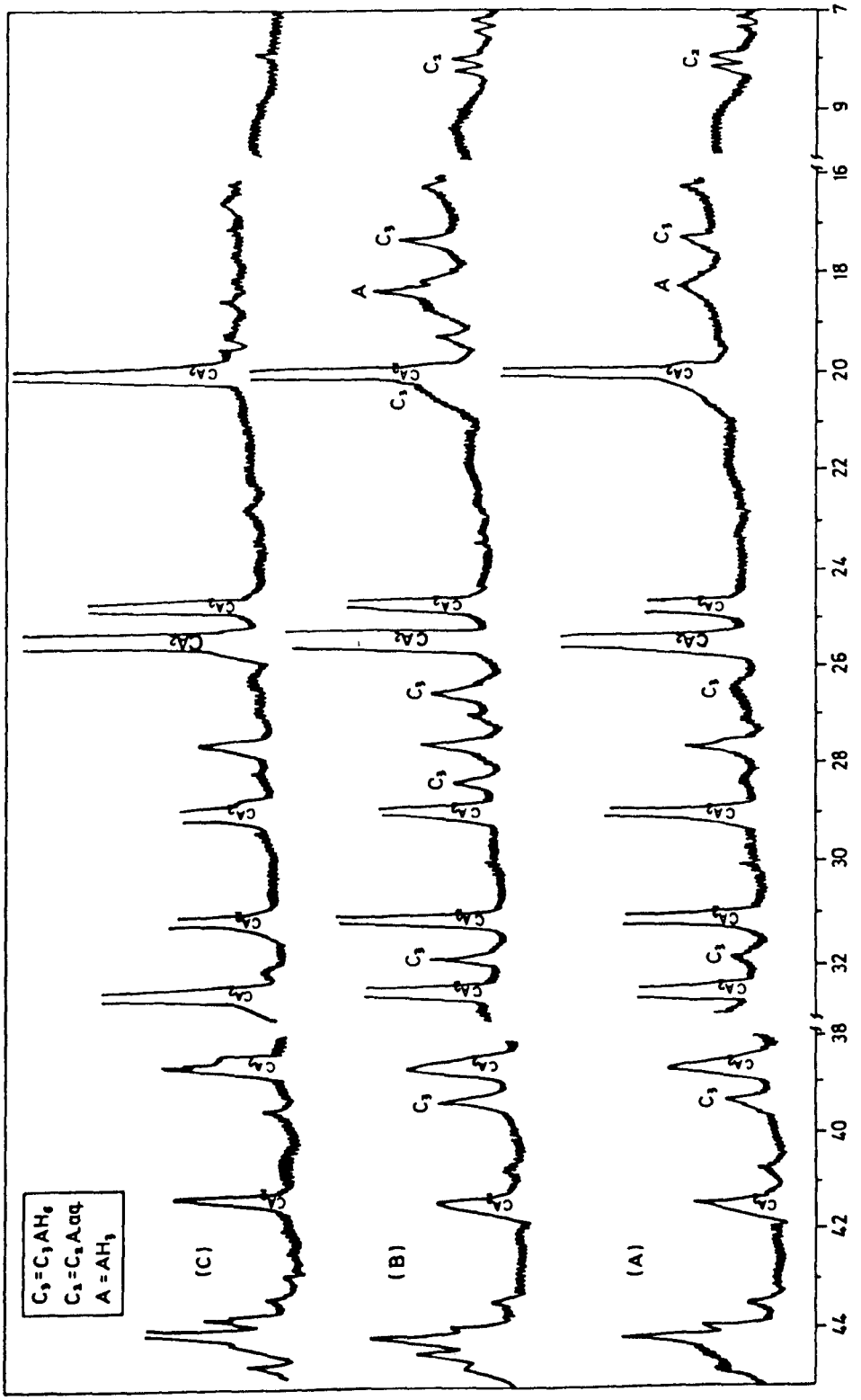

Fig. 7.4: X-ray diffractometer traces of CA_2 hot-pressed under 207 MNm^{-2} for 30 minutes at (A) 100°C, (B) 150°C, (C) 300°C.

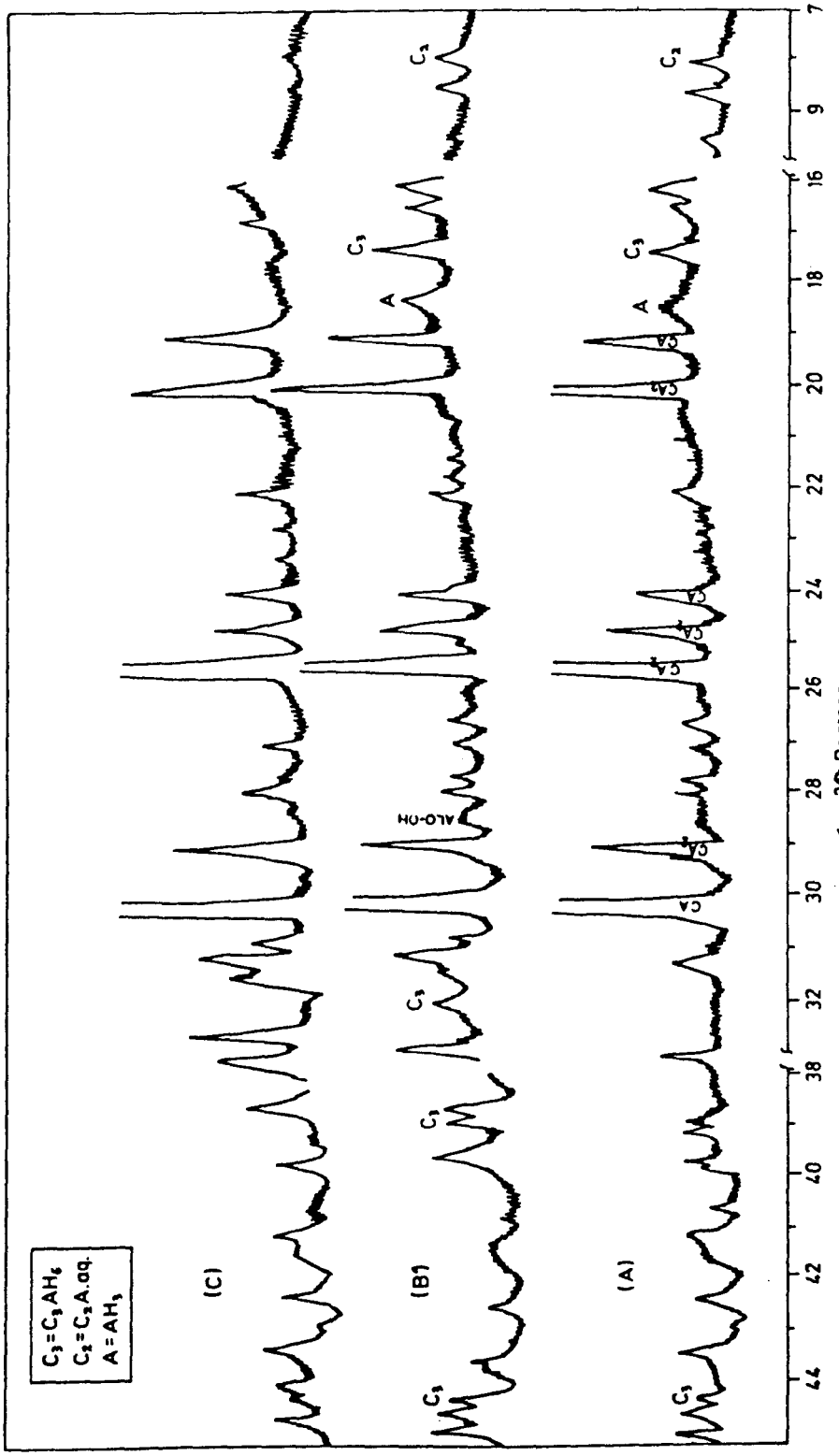

Fig. 7.5: X-ray diffractometer traces of Secar "250" cement, hot-pressed under 207 MNm^{-2} for 30 minutes at (A) 100°C, (B) 150°C, (C) 300°C.

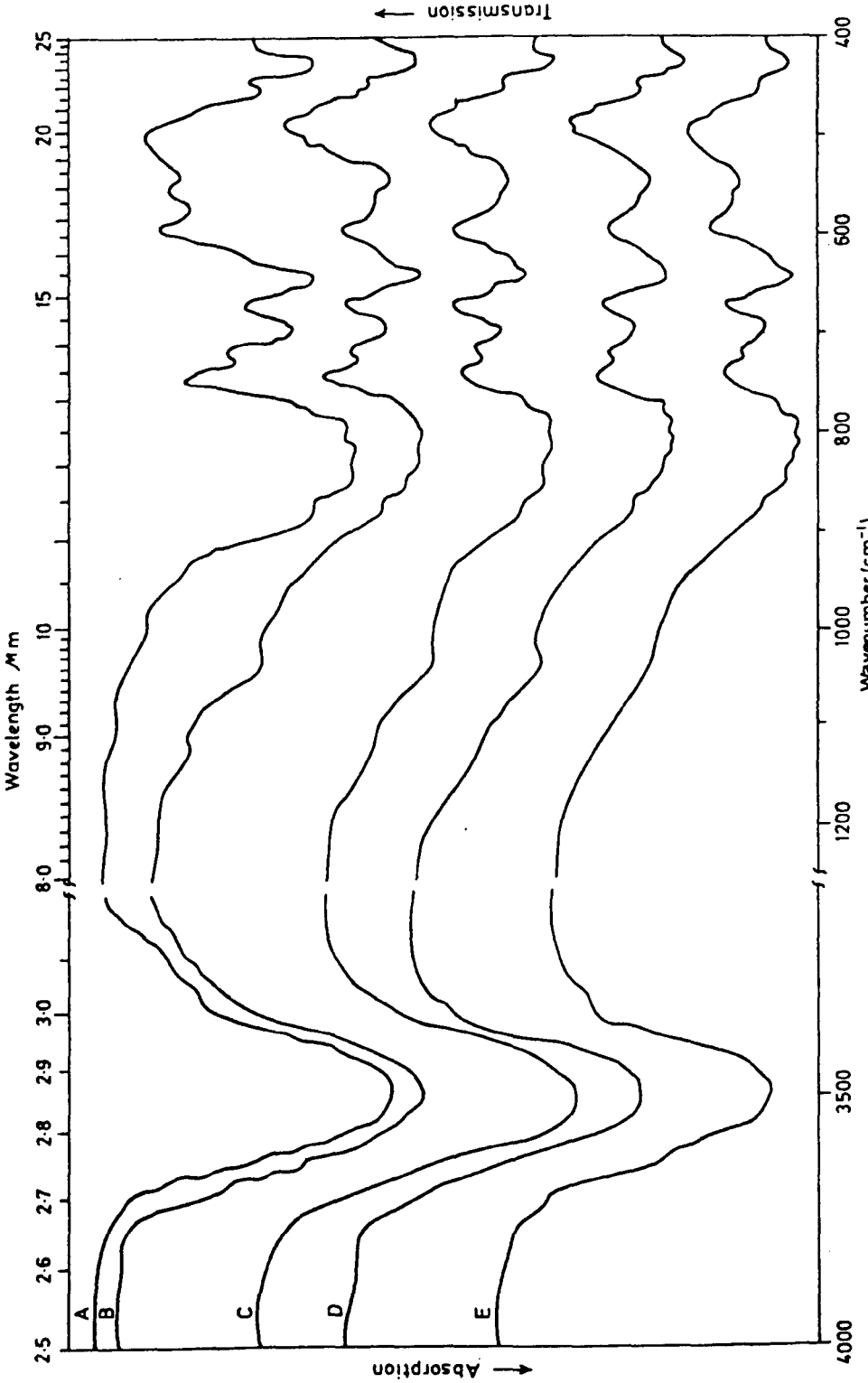

Fig. 7.6: Infra-red spectra of CA hot-pressed under 207 MNm^{-2} for 30 minutes at (A) 50°C, (B) 75°C, (C) 100°C, (D) 150°C, (E) 300°C.

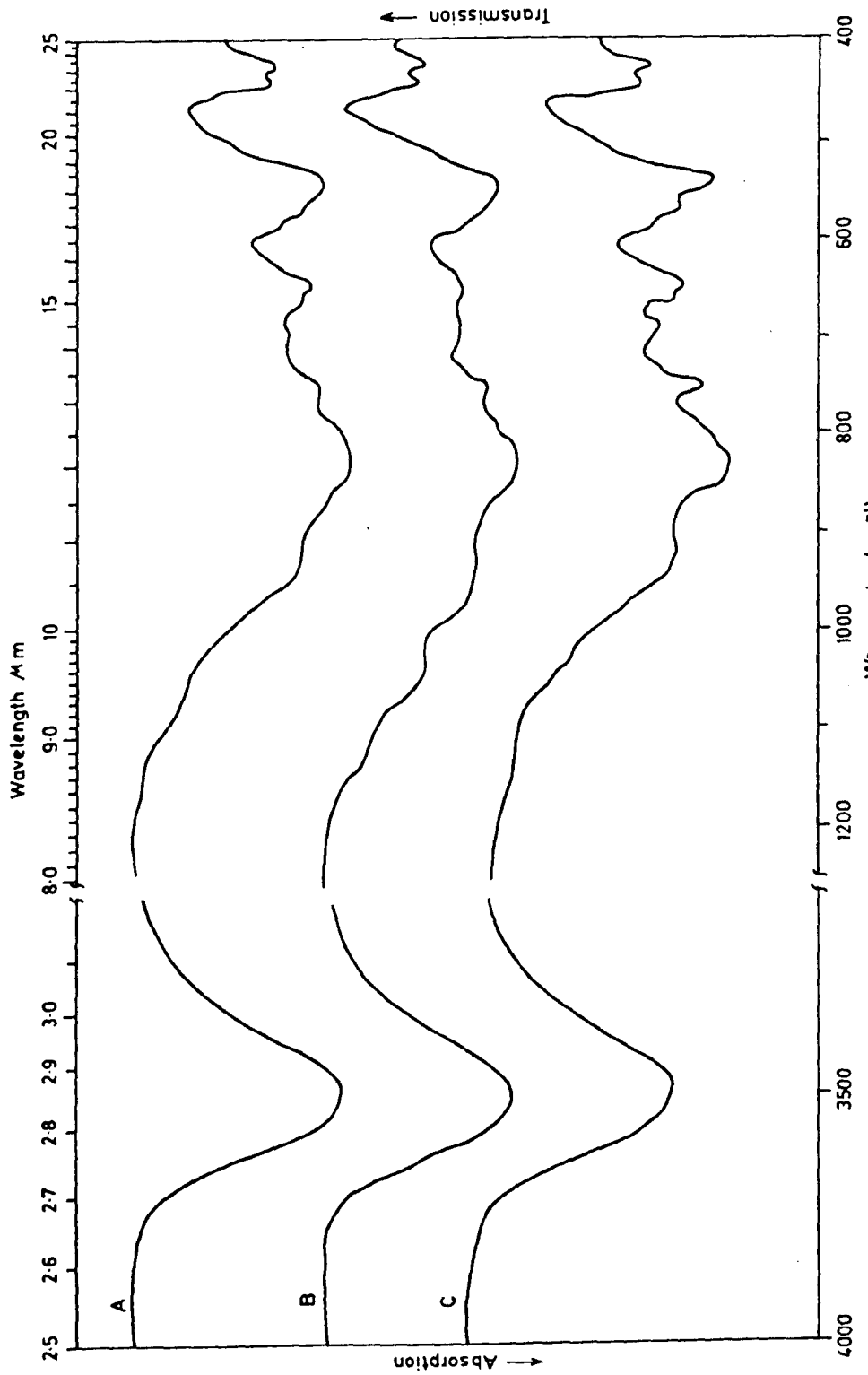

Fig. 7.7: Infra-red spectra of CA_2 hot-pressed under 207 MNm^{-2} pressure, for 30 minutes at (A) 100°C, (B) 150°C, (C) 300°C.

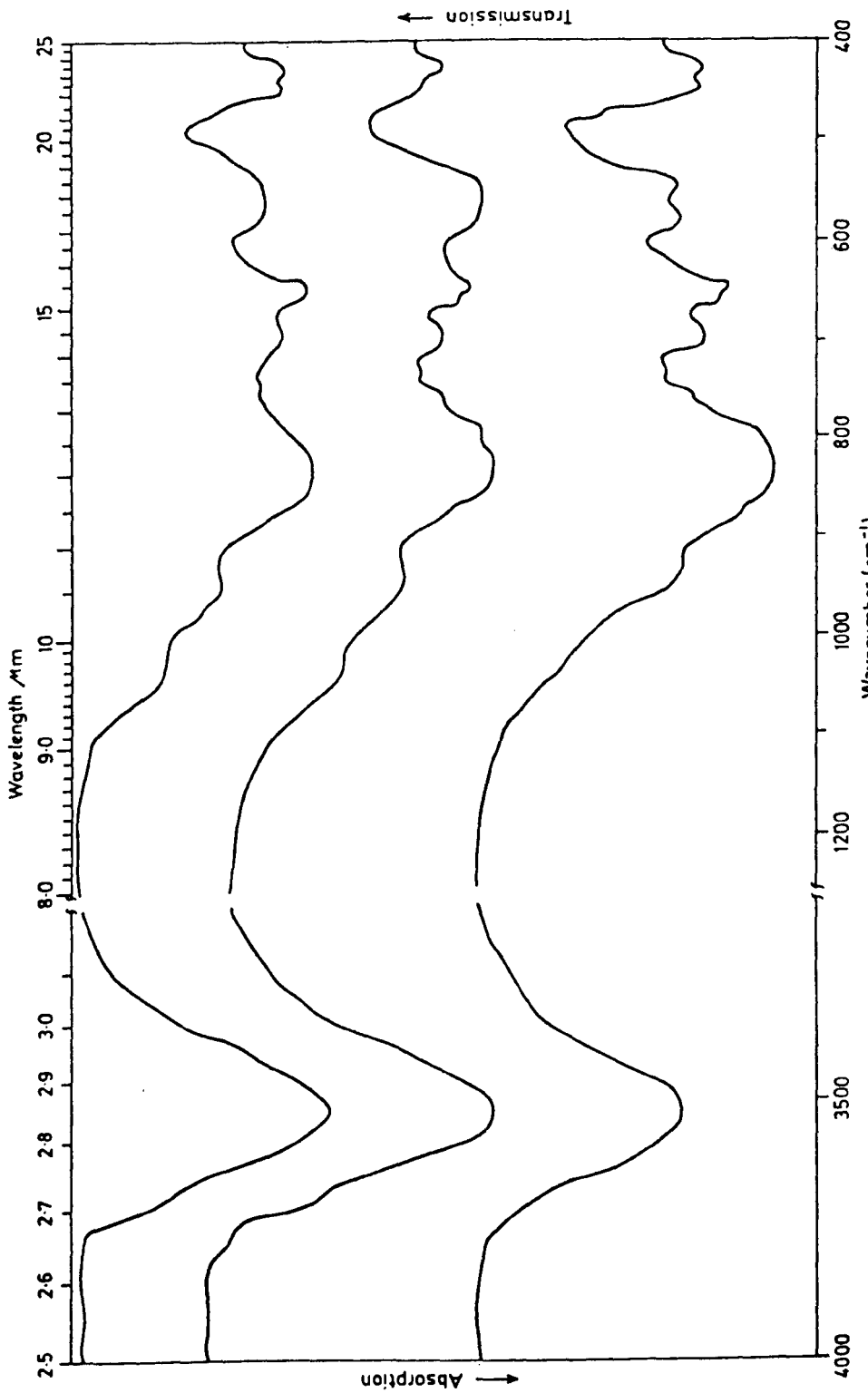

Fig. 7.8: Infra-red spectra of Secar "250" cement, hot-pressed under 207 MNm^{-2} for 30 minutes, at (A) 100°C, (B) 150°C, (C) 300°C.

Fig. 7.9

SEM Micrographs of CA, hot-pressed under 207 MNm^{-2} pressure, for 30 minutes, at:

(a) 75°C
(b) 100°C
(c) 150°C
(d) 300°C
(e) 700°C

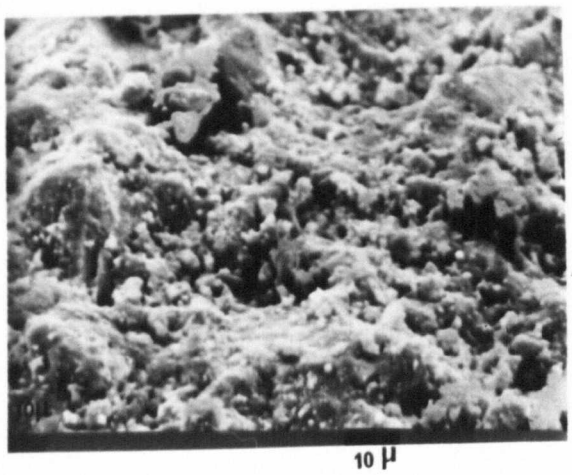

b

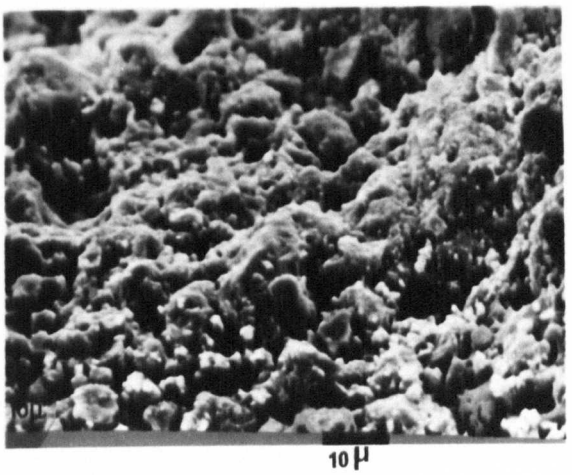

a

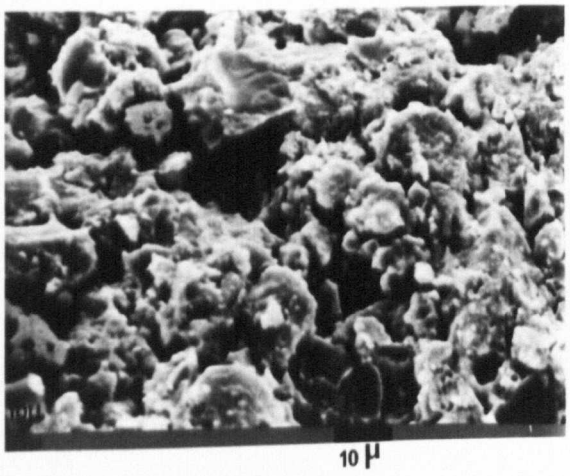

d

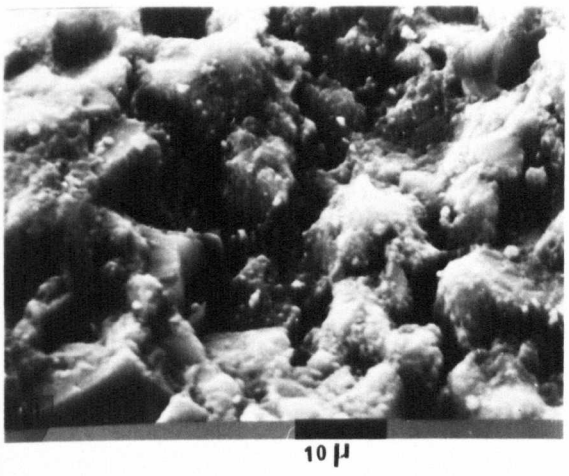

c

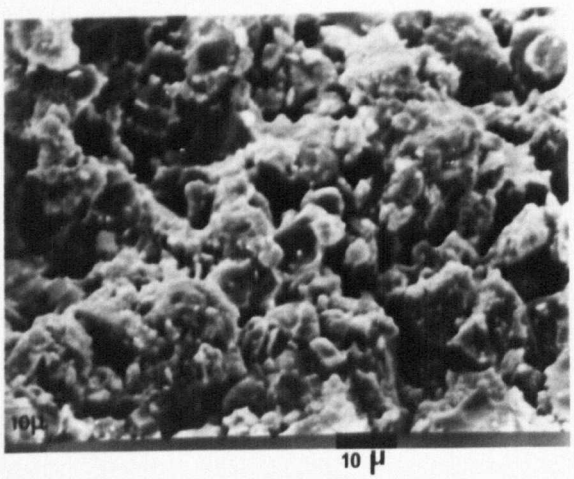

e

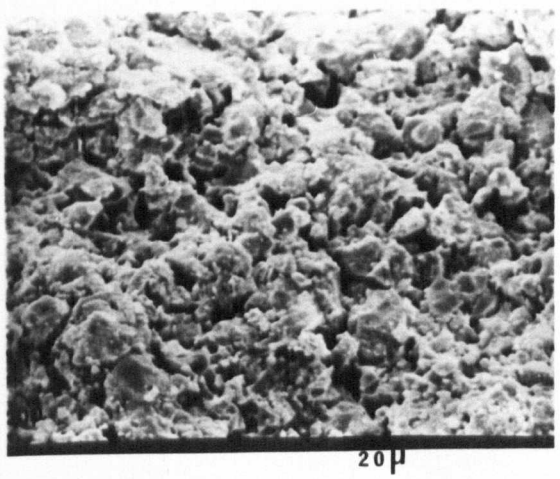

e

Fig. 7.10

SEM Micrographs of CA_2, hot-pressed under 207 MNm^{-2} pressure, for 30 minutes, at:

(a) 150°C

(b) 300°C

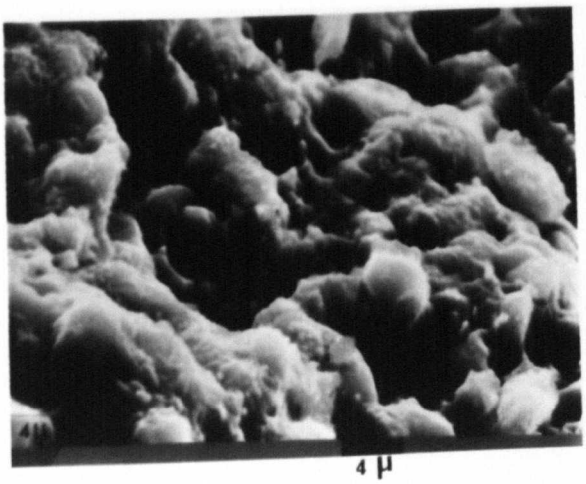

a

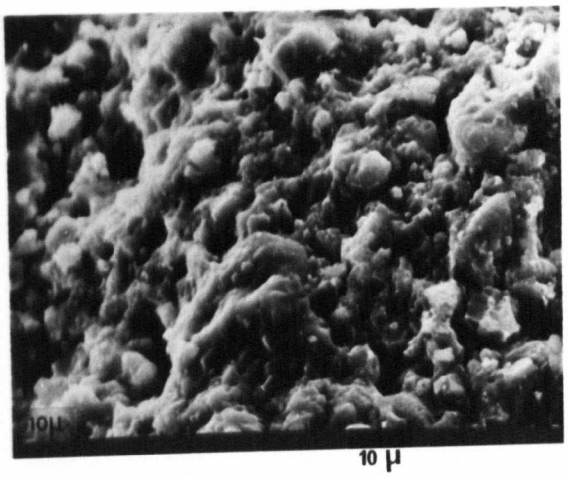

a

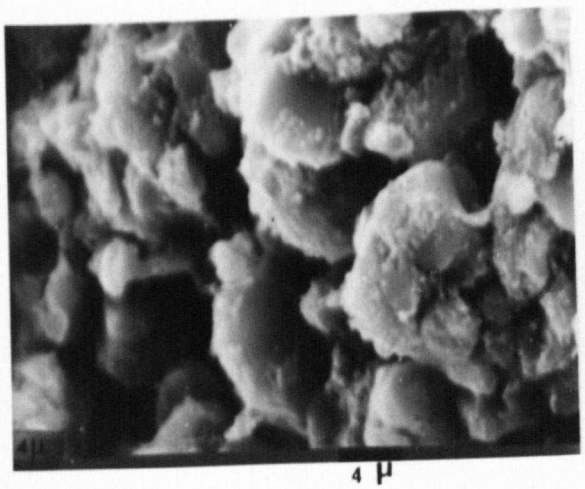

b

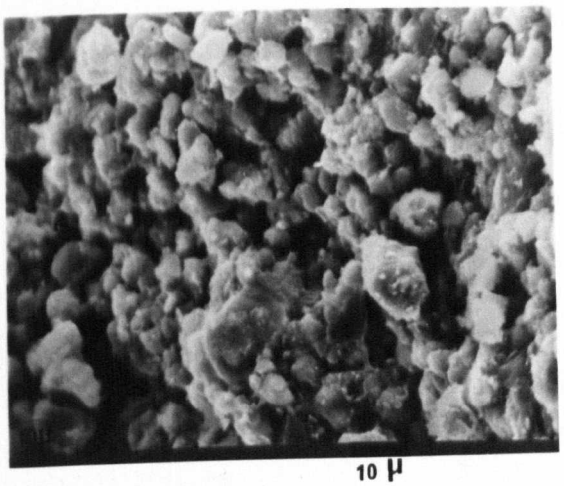

b

Fig. 7.11

SEM Micrographs of Secar "250" cement hot-pressed under 207 MNm^{-2} pressure, for 30 minutes, at:

(a) 150°C

(b) 300°C

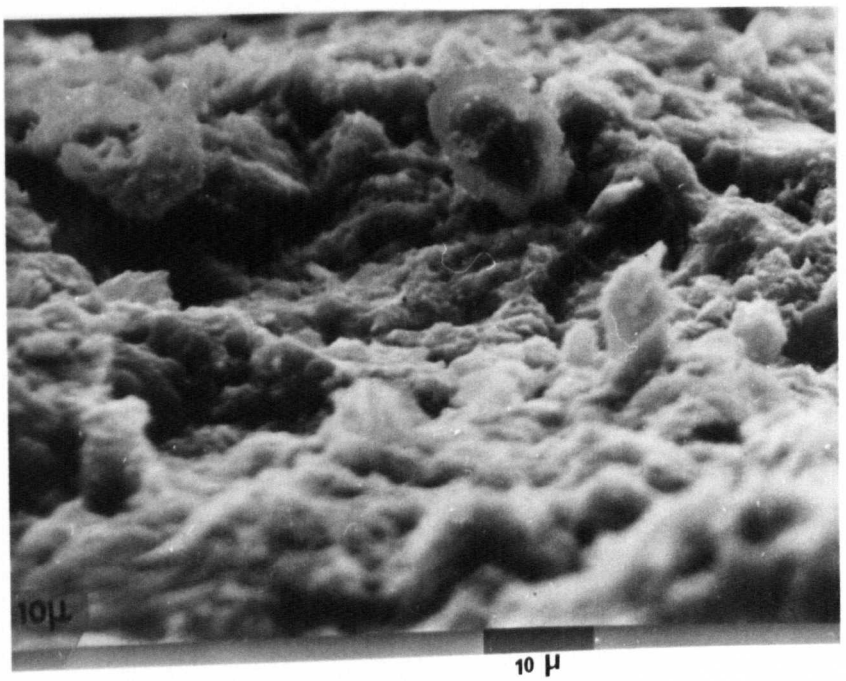

a

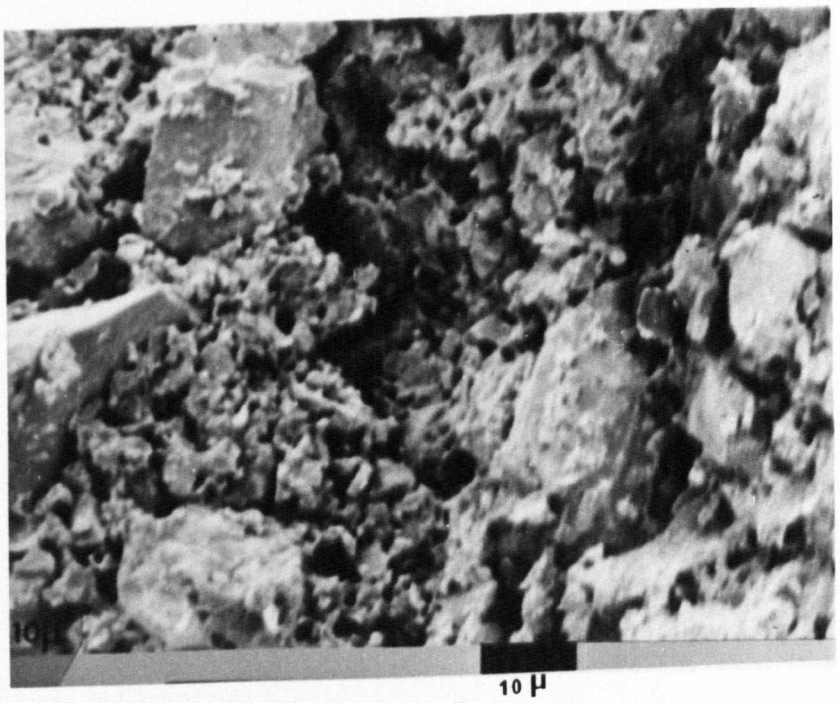

b

Material	Curing Time (days)	Phase Identification
CA	1	CA, C_3AH_6 (5.13, 2.81 and 2.30 Å), AH_3 (4.85 Å), C_2AH_8 (10.5 Å), C_4AH_{8-12}? (7.6 Å) and 11.3.
	5	CA, C_3AH_6 (5.13, 2.81 and 5.30 Å), AH_3 (4.85 Å), C_2AH_8 (10.7 Å)
	28	CA, C_3AH_6 (5.13, 2.81, 5.30 Å and others), AH_3 (4.85 and 4.37 Å), C_2AH_8 (10.7 Å) 11.3?
Secar "250" cement	1	CA, CA_2, C_3AH_6 (2.81, 2.30 and 2.04 Å) AH_3 (4.85 Å), C_2AH_8 (10.5 Å)
	5	CA, CA_2, C_3AH_6 (5.13, 2.81, 2.30 and 2.04 Å), AH_3 (4.85 and 4.37 Å), C_2AH_8 (10.56 Å), 11.3?
	28	CA, CA_2, C_3AH_6 (5.13, 2.81, 2.30 and 2.04 Å), AH_3 (4.85 and 4.37 Å).

Table 7.3: Summary of XRD results of CA and Secar "250" cement, hot-pressed under 207 MNm^{-2} at 150°C for 30 minutes, cured for 1, 5 and 28 days.

7.1.3 Hot-pressing, curing, followed by firing

Some calcium monoaluminate and secar "250" samples, hot-pressed (under 207 MNm^{-2} pressure, at 150°C, for 30 minutes) and cured for 28 days were subjected to heat treatment in the range 300 - 1300°C for 24 hours. As shown in Fig. 7.12 and Table 7.4, strength decreased to a minimum value at about 600°C, but increased again as the firing temperature approached 1300°C. XRD results, Table 7.5, showed that the hydrated products which had been formed during the hydration process were dehydrated. Microstructure of CA after firing at 1300°C is shown in Fig. 7.13B.

Material	Hot-pressing parameters			w/c ratio	Curing time (days)	Firing Conditions		% Change		Density g.cc	Strength MNm^{-2}		Porosity (%)
	Pressure MNm^{-2}	Temp. °C	Time min.			Time (hours)	Temp. (°C)	wt.	vol.		Compressive	Tensile	
CA	207	30	30	0.1	28	24	300			-	145.61	14.2	-
	207	30	30	0.1	28	24	600	-4.46	-	2.20	97.79	10.2	25.42
	207	30	30	0.1	28	24	900	-8.715	-2.64	2.22	125.73	12.5	24.72
	207	30	30	0.1	28	24	1200	-10.32	-6.38	2.31	144.38	16.0	21.69
	207	30	30	0.1	28	24	1300	-11.21	-9.30	2.40	177.56	20.8	18.64
Secar "250" cement	207	30	30	0.1	28	24	300	-	-	-	122.21	12.7	-
	207	30	30	0.1	28	24	600	-7.17	-	2.16	97.24	9.2	24.21
	207	30	30	0.1	28	24	900	-8.86	-2.30	2.17	118.3	10.7	23.81
	207	30	30	0.1	28	24	1200	-9.14	-7.036	2.33	157.9	20.0	18.24
	207	30	30	0.1	28	24	1300	-10.077	-9.494	2.41	183.8	23.4	15.43

Table 7.4: Mechanical properties and related physical properties of CA and Secar "250" cement, hot-pressed ($207\ MNm^{-2}$ pressure, at 150°C, for 30 minutes), cured for 28 days, before firing at different temperatures for 24 hours.

Material	Firing Temp. °C	Phase Identification
CA	300	CA, $C_4A_3H_3$ (3.59 and 3.24 Å)
	600	CA, $C_{12}A_7$ (4.89, 2.68 & 2.45 Å) and traces of $C_4A_3H_3$ (3.59, 3.24 Å)
	900	CA, traces of $C_{12}A_7$ (4.89, 2.45 Å)
	1200	CA, traces of $C_{12}A_7$ (4.89, 4.45 Å), traces of CA_2.
	1300	CA, and traces of CA_2.
Secar "250" cement	300	CA, CA_2, $C_4A_3H_3$ (3.59 & 3.24 Å)
	600	CA, CA_2 and traces of $C_{12}A_7$ (4.89, 2.45 Å)
	900	CA, CA_2, and traces of $C_{12}A_7$ (4.89, 2.68 & 2.45 Å)
	1200	CA, CA_2
	1300	CA, CA_2

Table 7.5: Summary of XRD results of CA and Secar "250" cement, hot-pressed (under 207 MNm^{-2} pressure, at 150°C, for 30 minutes), cured for 28 days before firing at different temperatures for 24 hours.

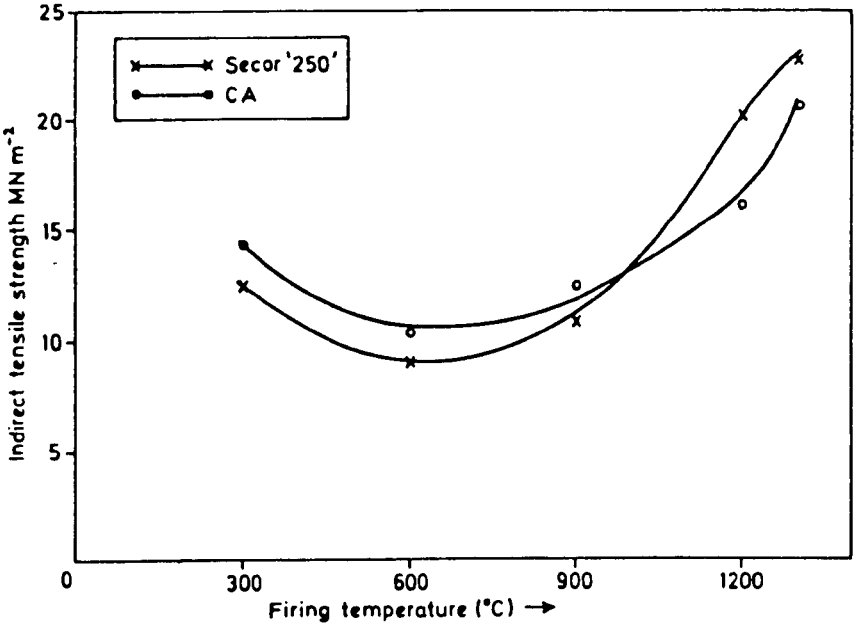

Fig. 7.12: Dependence of strength upon firing temperature. Samples cured for 28 days before firing for 24 hours.

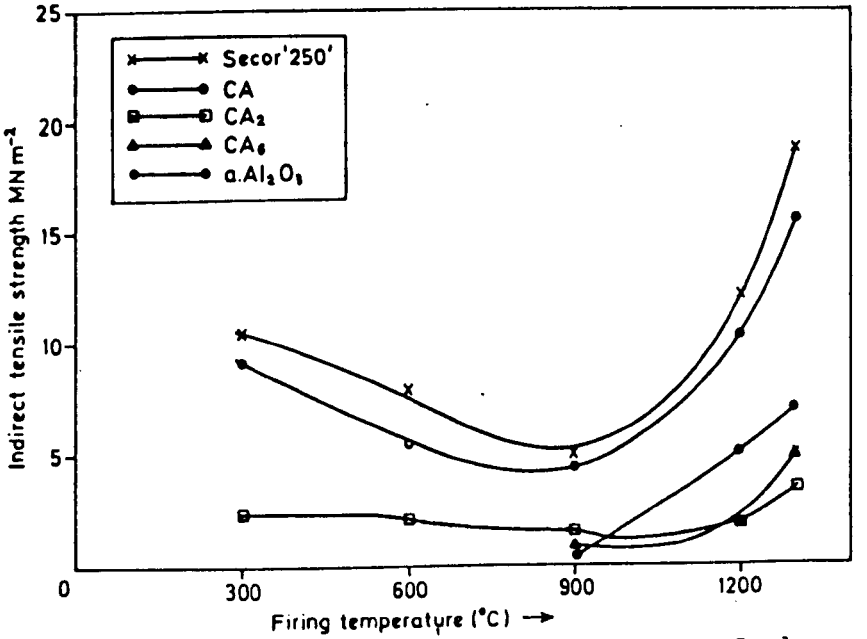

Fig. 7.14: Dependence of strength upon firing temperatures. Samples fired directly without curing.

Fig. 7.13A

SEM Micrographs of CA, hot-pressed under 207 MNm^{-2} pressure, for 30 minutes at 300°C, fired at 1300°C, 24 hours.

Fig. 7.13B

SEM Micrographs of CA, hot-pressed under 207 MNm^{-2} pressure, for 30 minutes at 150°C, cured 28 days, fired at 1300°C, 24 hours.

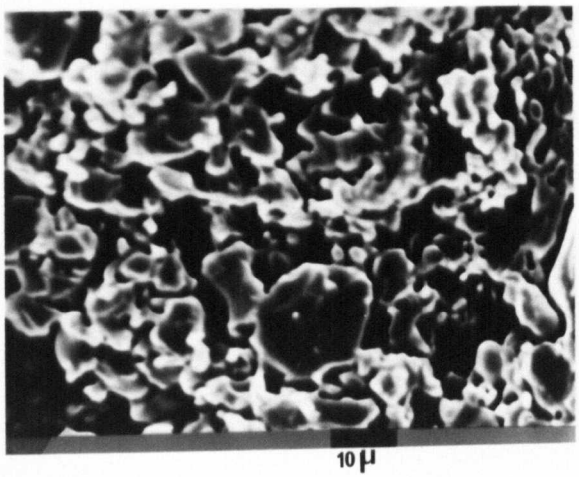
10 μ

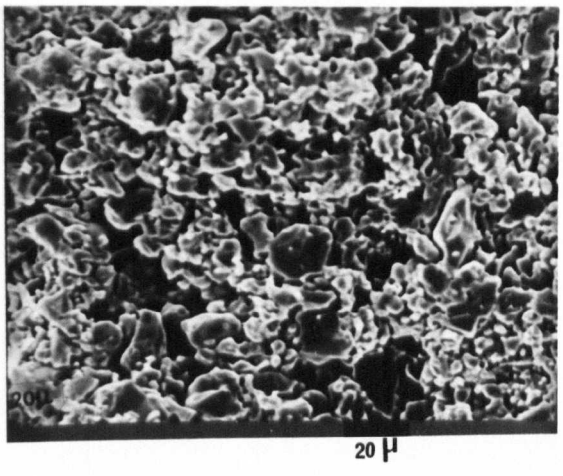
20 μ

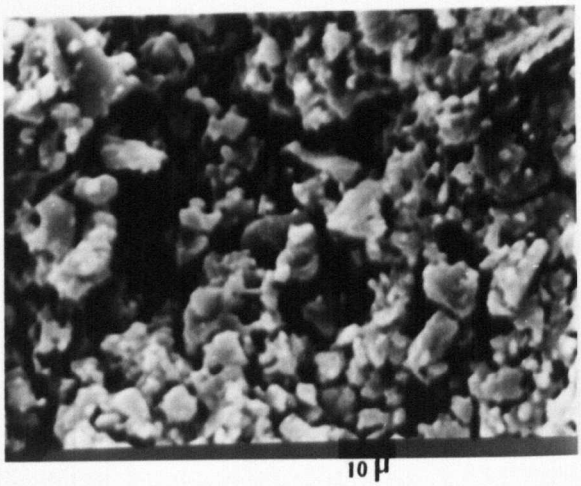
10 μ

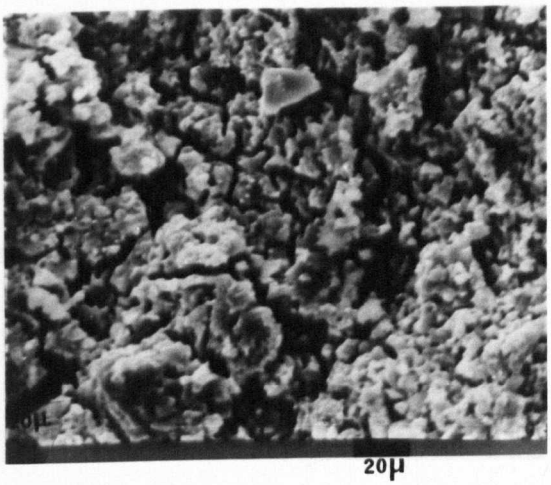
20μ

7.1.4 Hot-pressing followed by firing

Pure CA, CA_2, CA_6, α-Al_2O_3 and the commercial material secar "250" cement were hot-pressed at 300°C under 207 MNm^{-2} for 30 minutes. These samples were subjected to heating in the range 300-1300°C immediately after removing from the cell. The relationship between strength and firing temperature is given in Figure 7.14 and Table 7.6 with the other physical properties. Generally there was a decrease in strength to a minimum value at 900°C, but above 900°C it increased again. No strength values for CA_6 and α-Al_2O_3 fired below 900°C were obtained because the samples were very weak. XRD results are summarised in Table 7.7. Microstructure of CA, after firing at 1300°C, is shown in Figure 7.13A.

Material	Hot-pressing parameters			w/c ratio	Firing Conditions		% Change		Density g.cc	Strength MNm^{-2}		Porosity (%)
	Pressure MNm^{-2}	Temp. °C	Time min.		Temp. °C	Time hours	wt	vol.		Compressive	Tensile	
Pure CA	207	300	30	0.1	-	-	-	-	2.20	-	12.6	25.42
	207	300	30	0.1	300	24	-	-	-	-	9.1	-
	207	300	30	0.1	600	24	-1.9	-	2.13	64.34	5.5	27.79
	207	300	30	0.1	900	24	-2.2	-.82	2.09	51.44	4.4	29.15
	207	300	30	0.1	1200	24	-2.59	-2.00	2.15	80.5	10.2	27.12
	207	300	30	0.1	1300	24	-2.64	-2.08	2.25	116.25	15.6	23.73
Pure CA_2	207	300	30	0.1	-	-	-	-	2.05	-	4.08	28.32
	207	300	30	0.1	300	24	-	-	-	-	2.7	-
	207	300	30	0.1	600	24	-	-	-	-	2.2	-
	207	300	30	0.1	900	24	-1.509	-.206	2.007	-	1.4	29.82
	207	300	30	0.1	1200	24	-2.084	-2.6	2.013	-	2.1	29.61
	207	300	30	0.1	1300	24	-2.55	-2.7	2.02	-	3.6	29.37
Pure Secar "250"	207	300	30	0.1	-	-	-	-	2.21	-	13.4	22.45
	207	300	30	0.1	300	24	-	-	-	-	10.4	-
	207	300	30	0.1	600	24	-1.94	-	2.12	72.4	7.8	25.614
	207	300	30	0.1	900	24	-3.8	-.09	2.10	53.76	4.8	26.31
	207	300	30	0.1	1200	24	-3.92	-1.167	2.144	121.66	12.7	24.91
	207	300	30	0.1	1300	24	-5.67	-3.54	2.24	145.70	18.2	21.40

Table 7.6 (Cont.)

Table 7.6 (Cont.)

Material	Hot-pressing parameters			w/s ratio	Firing Conditions		% Change		Density g.cc	Strength MNm^{-2}		Porosity (%)
	Pressure MNm^{-2}	Temp. °C	Time min.		Temp. °C	Time hours	wt	vol.		Compressive	Tensile	
Pure CA_6	207	300	30	0.1	300	24	-	-	-	-	-	-
	207	300	30	0.1	900	24	-0.65	-2.00	2.23	-	0.8	39.56
	207	300	30	0.1	1200	24	-0.53	-2.23	2.30	-	2.1	37.66
	207	300	30	0.1	1300	24	1.38	-2.34	2.34	-	4.9	36.58
Pure α-Al_2O_3	207	300	30	0.1	300	24	-	-	-	-	-	-
	207	300	30	0.1	600	24	-	-	-	-	-	-
	207	300	30	0.1	900	24	-1.257	-.228	2.60	-	4.7	31.57
	207	300	30	0.1	1200	24	-1.207	-1.51	2.62	-	5.38	31.05
	207	300	30	0.1	1300	24	-1.798	-3.74	2.63	-	7.24	30.79

Table 7.6: Mechanical properties and related physical properties of CA, CA_2, Secar "250", CA_6 and α-Al_2O_3. Samples hot-pressed under 207 MNm^{-2} pressure, at 150°C, for 30 minutes, followed by firing at different temperatures for 24 hours.

Material	Firing Temp. °C	Phases Identified
CA	300	CA, traces of $C_4A_3H_3$
	600	CA, traces of $C_{12}A_7$ (4.89 Å)
	900	CA, traces of $C_{12}A_7$
	1200	CA, traces of CA_2 (3.52 Å)
	1300	CA, traces of CA_2 (3.52 Å)
Secar "250" cement	300	CA, CA_2, traces of $C_{12}A_7$ (4.89, & 4.45 Å)
	600	CA, CA_2, traces of $C_{12}A_7$ (4.89 & 2.45 Å)
	900	CA, CA_2, traces of $C_{12}A_7$ (4.89, 2.68 & 2.45 Å)
	1200	CA, CA_2
	1300	CA, CA_2
In the cases of CA_2, CA_6 and α-Al_2O_3, no significant change in the composition was noticed during the firing process.		

Table 7.7: Summary of XRD results for CA and Secar "250" cement, hot-pressed (under 207 MNm^{-2} pressure, for 30 minutes, at 300°C) followed by firing at different temperatures for 24 hours.

7.2 Discussion

The application of hot-pressing techniques in the cement field was recently reported.[36,96,97] In the present study the effect of hot-pressing temperature, over a wide range (i.e. 50 - 700°C), on strength properties of some calcium aluminate phases and the commercial secar "250" cement were investigated. In addition, the dependence of strength upon firing temperatures in the range 300 - 1300°C for 24 hours (after and without curing) was also studied.

The results of this work show that high strength values can be obtained by hot-pressing CA, CA_2 and secar "250" cement at low temperatures (i.e. 50 - 150°C).

From DTA results (Fig. 7.2 and Table 7.2), $C_2A.aq$ and C_3AH_6 were detected by two endothermic peaks at about 290 and 315°C, respectively. Peak areas for both of the hydrated compounds were calculated following the method described by Mackenzie and Ritchie[150]. It was found that the value of peak area estimated from the experimental DTA curves for C_3AH_6 increased as the hot-pressing temperature increased up to 150°C in all three materials. On the other hand, the peak area for $C_2A.aq$ decreased. The ratio between peak area of C_3AH_6/peak area of $C_2A.aq$ was plotted against hot-pressing temperature as shown in Fig. 7.15. Generally, this ratio was found to be increased when the hot-pressing temperature increased and more C_3AH_6 was formed. On the other hand, calcium dialuminate, CA_2, was found to have higher $C_3AH_6/C_2A.aq$ values, followed by secar "250" and finally calcium monoaluminate. This may explain why, when CA_2 is hydrated, it produced mainly C_3AH_6 and a small amount of $C_2A.aq$, whereas the amount of the latter is relatively higher in calcium monoaluminate after hydration.

The XRD results (Figures 7.3, 7.4, 7.5) indicated that C_3AH_6 and AH_3 were the main hydrated products between 50 - 150°C. After hot-pressing

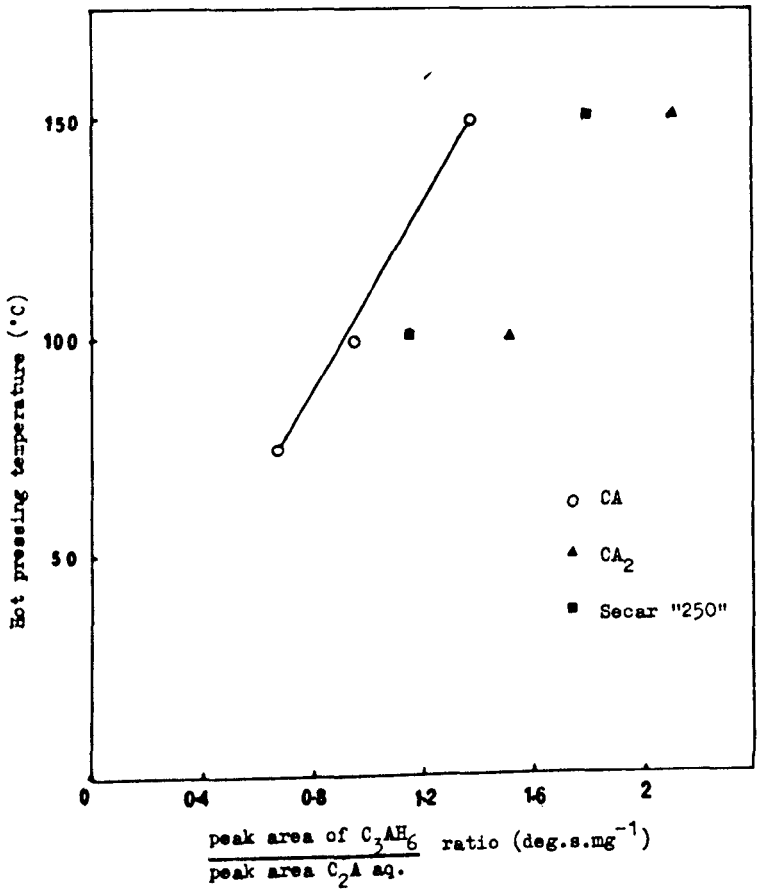

FIG. 7.15: Relationship between $\frac{\text{peak area of } C_3AH_6}{\text{peak area of } C_2A \text{ aq.}}$ ratio and hot pressing temperatures.

at relatively high temperatures (300°C), $C_4A_3H_3$ and traces of boehmite AlO.OH were detected. This might explain the marked fall in the strength values by hot-pressing at 300°C , Figure 7.1. The fall in strength is also established by the difference of microstructures shown in Figures 7.9, 7.10, 7.11. These results agree with the conclusions of other investigators[13,21] that C_3AH_6 is the stable hydrate compound of the C-A-H system up to about 215°C.

A scarcity of data on hydration of pure CA_2 is found in the literature[17]. On the other hand, no data is reported on the strength values of this material under hot-pressing conditions. Results of the present work have shown that pure CA_2 can give a high strength value by hot-pressing at low temperatures (i.e. ~ 150°C), as shown in Fig. 7.1. This can be explained by the formation of the hexa-hydrated compound C_3AH_6 (Figure 7.4) and the consequent relatively dense microstructure (Figure 7.10).

On the other hand, strength values showed a continuous decrease in the range 300 - 500°C without exception. The small increase in the strength values at 600 and 700°C could possibly be explained in terms of increased densification at relatively high hot-pressing temperatures.

The strength of calcium monoaluminate, CA, and Secar "250" cement samples hot-pressed at 150°C, under constant pressure (207 MNm^{-2}) for constant time (30 minutes) and cured for 1, 5 and 28 days were found to agree with data published elsewhere[36]. Generally, Table 7.3 shows that the amount of C_3AH_6 was increased by increasing the curing time.

Comparison between the data in Figures 7.12 and 7.14 and Tables 7.4 and 7.6, shows that firing after curing for 28 days is slightly better than firing without curing. The strength in the former is slightly better than in the latter. XRD analyses (Tables 7.5 and 7.7) show that the amount of $C_{12}A_7$ was higher in those samples fired after curing, than

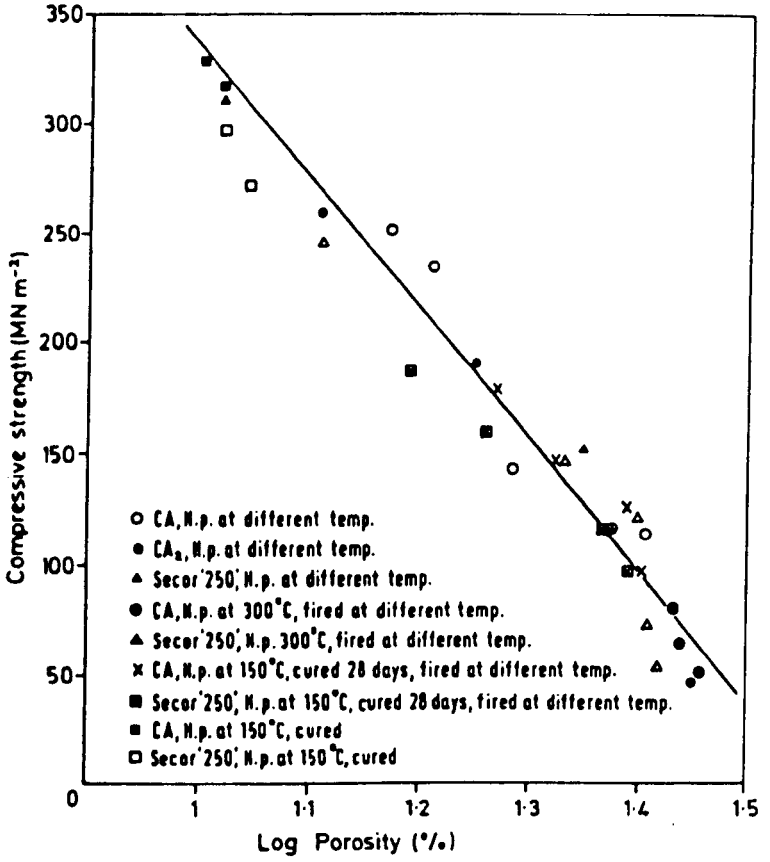

Fig. 7.16: Strength-log porosity relationship; data plotted on the basis of equation (2.10).

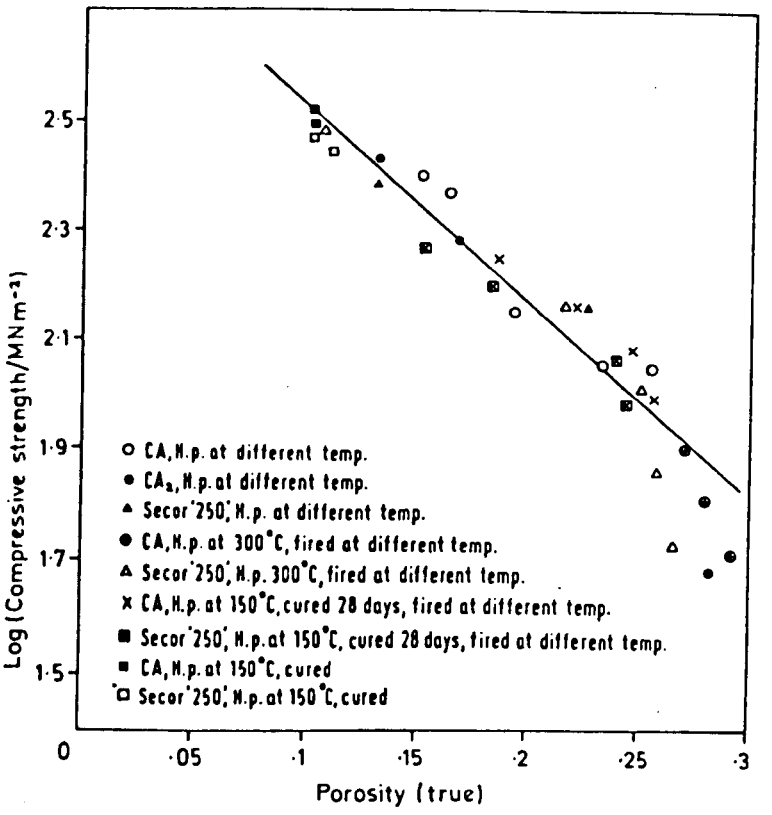

Fig. 7.11: Log strength-porosity relationship; data plotted on the basis of equation (2.7).

those which were fired directly[34]. Strength values of CA_2, CA_6 and α-Al_2O_3 after firing were, as expected, very low and increased slightly only at higher temperatures (i.e. 1200 and 1300°C) owing to sintering taking place.

The porosity-strength relationship developed by Roy[36,96,97] (equation 2.10) was found to fit the present results as shown in Fig. 7.16. The constant K is of the order of 2.73×10^{-5} when strength is expressed in psi, which is in reasonable agreement with the value (3.7×10^{-5}) reported by Roy. In addition, the empirical equation suggested by Ryskewitsch[108] (equation 2.7), was found also acceptable for fitting the same data, where n = 7.8, as shown in Fig. 7.17. The general trend is the lower the porosity, the higher is the strength.

CHAPTER 8

GENERAL CONCLUSIONS AND SUGGESTIONS FOR FUTURE WORK

8.1 General Conclusions

The results discussed in the preceding sections (4.3, 5.3, 6.3 and 7.3) can now be summarised and a number of features established.

8.1.1 Phosphoric acid and prefabricated aluminium phosphate additives

(a) Samples cast at room temperature, followed by firing

(1) The compressive strengths are directly related to the quantity of aluminium phosphate formed *in situ* (up to ~12% $AlPO_4$ when 10% H_3PO_4 is used).

(2) An increasing calcium oxide content is accompanied by a decrease in the strength by an amount which is dependent on the $\frac{C}{C+A}$ ratio.

(3) Increasing the calcium oxide content increases the degree of decomposition of aluminium phosphate formed *in situ* and decreases its thermal stability.

(b) Samples fabricated under hot-pressing conditions, followed by firing

(1) Under hot-pressing conditions, the reaction between the starting material and phosphoric acid to produce aluminium phosphate is almost complete in a short time (~30 minutes), and at relatively low temperature (200 - 700°C), depending on the $\frac{C}{C+A}$ ratio.

(2) Samples fired after hot-pressing at low temperature (300°C) show compressive strength values approximately five times (717 MNm^{-2} for α-Al_2O_3 mixture) those obtained from room temperature casting followed by firing (138 MNm^{-2} for α-Al_2O_3 mixture).

(3) When hot-pressing technique is used, the strength is not solely a function of aluminium phosphate content, but porosity also is a major contributing factor.

(4) When hot-pressing technique is used, slight changes of the unit cell dimensions of the $AlPO_4$ formed in situ are found.

(5) The aluminium phosphate (cristobalite form) does not behave like a cementitious material when added in prefabricated form. Negligible strength increases are obtained from samples cast at room temperature, and only a small improvement in strength if hot-pressing technique is used.

8.1.2 Phosphoric acid + boric acid mixture and prefabricated boron phosphate additives

(a) Samples cast at room temperature, followed by firing

(1) Small quantities ($\sim 5\%$) of phosphoric acid + boric acid mixture or prefabricated boron phosphate (cristobalite form) considerably increase the compressive strength of calcium mono-, and dialuminate after firing at higher temperatures. These compressive strengths are greater than when phosphoric acid alone is used (150 MNm^{-2} of CA + (H_3PO_4 + H_3BO_3), whereas the value is about 40 MNm^{-2} when phosphoric acid only is used, after firing at the same temperature).

(2) The large increase in compressive strength arises from increased densification and from the formation of $AlPO_4$ and uncharacterised compound.

(3) The binary compound $9Al_2O_3.2B_2O_3$ is found in many samples, but it does not appear to be a cementitious material.

(4) Boron phosphate is not detectable by XRD in any samples after firing above 900°C.

(b) Samples fabricated under hot-pressing conditions, followed by firing

(1) Samples fired after hot-pressing (at 300°C) generally show higher strength values (307 MNm^{-2} for CA mixture) than the corresponding samples cast at room temperature followed by firing (150 MNm^{-2} for CA mixture).

(2) When hot-pressing technique is used, the compound $9Al_2O_3.2B_2O_3$ is formed at about 300°C lower temperatures than in the case without hot-pressing.

(3) A sudden decrease in strength values at 900 - 1200°C in the mixture α-Al_2O_3 + 5% (H_3PO_4 + H_3BO_3) is observed in the absence of hot-pressing. This is avoided by hot-pressing at 300°C before firing.

8.1.3 Phosphoric acid + chromium trioxide mixture and prefabricated chromium phosphate additives

(a) Samples cast at room temperature, followed by firing

(1) High strength values in calcium monoaluminate mixtures (70 MNm^{-2}) can be obtained by using the mixture of (H_3PO_4 + CrO_3). If phosphoric acid only is used, the strength is much lower (40 MNm^{-2}).

(2) The ternary compound, $4CaO.3Al_2O_3.CrO_3$, is obtained when (H_3PO_4 + CrO_3) or CrO_3 only are mixed with calcium monoaluminate, and it is believed that this contributes to ultimate strength.

(3) Preformed chromium phosphate, $CrPO_4$ (amorphous, α and β forms) when used as a bonding agent is considerably less successful than if phosphoric acid + chromium trioxide mixture is used. Amorphous material was, however, more effective than the crystalline forms.

(b) Samples fabricated under hot-pressing conditions, followed by firing

A noticeable improvement in strength values can be obtained in samples fired after hot-pressing at relatively low temperature (300°C).

8.1.4 Hot-pressing of pure materials (no additives)

(1) Although pure calcium dialuminate does not under normal conditions hydrate to give hydrated compounds[8,9,10,17], the present study shows that if hot-pressed at low temperatures (100-150°C), it does hydrate and give C_3AH_6 and a product with very high compressive strength (190-260 MNm^{-2}).

(2) Hot-pressing of calcium monoaluminate, calcium dialuminate and Secar "250" cement shows a continuous increase in strength on increasing the hot-pressing temperatures up to 150°C. By hot-pressing at 300°C, a marked decrease in strength was observed.

(3) Strength values of hot-pressed calcium monoaluminate and Secar "250" cements, after firing at high temperatures, are slightly greater if the samples are cured for 28 days before firing than if curing is omitted.

The strength-porosity relationship was studied during the course of this work using three different empirical equations:

$$\sigma = \sigma_o \exp.(-nP) \quad [108],$$

$$P = P_o \exp.(-KS) \quad [36,96,97],$$

and

$$0.6P = \exp - \left[\frac{\sigma}{8000(1-P)} \right] \quad [109].$$

It was found that these empirical equations fit most of the data in a linear inverse relationship with different slope values. However, it must be pointed out that these observations support Evans and Tappin's[139] view that the use of a single empirical equation to represent this relationship could be misleading. On the other hand, it is believed that this relationship is affected to some extent by both the starting material and the additive which is used. This may be why the data in each group fits more than one straight line with different slope values. In addition, pore size, pore shape and pore size distribution are

in fact believed to play a great part in this relationship. Generally, the lower the porosity the higher is the strength.

Finally, it is apparent from the work in this thesis that, using any of the additives, hot-pressing at low temperature (300°C) for a short time (30 minutes) followed by firing at higher temperatures produces higher strength than room temperature casting followed by firing. In some mixtures in the $CaO-Al_2O_3$ system the strength can be increased by about four to five times, if certain additive combinations are used.

8.2 Suggestions for Future Work

(1) In view of the importance of the strength-porosity relationship which has been demonstrated, this topic should be further investigated. In particular, more information is needed on pore size, pore shape and pore size distribution.

(2) Since it is probable that an increase in hot-pressing time and/or pressure will lead to greater densification, and therefore higher strength, this is an obvious avenue for further investigation. Increasing the temperature during hot-pressing might also be looked into since the chemical reactions may not be the same at elevated temperatures.

(3) Certain fired mixes ($\alpha-Al_2O_3 + H_3PO_4$, CA + (H_3PO_4+H_3BO_3) or + BPO_4) showed a rapid build up of strength as the firing temperatures were increased in the range 1000-1300°C. Considerably greater strengths might be obtained if temperatures above 1300°C (but below the melting point of the mixes) are applied.

(4) More work could be carried out on the effect of other compounds, e.g. $FePO_4$ and $MnPO_4$ (isostructural with $AlPO_4$ and SiO_2), when formed *in situ*, on the strength properties of the products. The effect of these compounds added in prefabricated form might also be studied.

(5) Extended investigations in the system $CaO-Al_2O_3-P_2O_5-B_2O_3$ should be undertaken. This includes a more detailed study of the role of the compound $9Al_2O_3.2B_2O_3$ in the mixture $\alpha-Al_2O_3$ + $(H_3PO_4+H_3BO_3)$, especially after firing between 900-1200°C.

(6) Pure calcium dialuminate, CA_2, when hot-pressed at low temperatures for a short time, hydrates to give C_3AH_6, and a product with very high strength. Therefore, it is of interest that the study of hot-pressing conditions and also w/c ratio should be extended for this material.

APPENDIX 1: Calculation of Heat of Reaction (ΔH)

The fact that the area between the DTA curve and the extrapolated baseline of the peak is proportional to the heat evolved (absorbed) in the process investigated has been well established elsewhere.[151,152,153] The relationship between the peak area of a DTA curve and the value of the heat of reaction can be written in the general form:

$$\Delta H.M = K.A$$

where ΔH is the heat of reaction per unit of weight

M is the weight of the sample

K is the coefficient of conformity

A is the peak area of DTA curve.

Using DTA apparatus 673-4 (Stanton Redcroft), previously described (Section 3.8), the coefficient conformity K was calculated for different temperatures up to 930°C. The degree of packing and weight of sample (100 mg) were kept constant using 10°C/min heating rates. The experiments were carried out on the eight standard compounds previously studied by Mackenzie et al., which have known heats of transition. Table A1-1 gives the results of Mackenzie et al.[159] and Table A1-2 gives the results of the present study.

The relationship between heat of reaction and peak area is given in Fig. A1-1. All the points except those of KNO_3, Ag_2SO_4 and $SrCO_3$ lie relatively close to the straight line.

Compound	Peak Temp. °C	Peak Area (A) deg.sec.mg^{-1}	ΔH cal.mg^{-1}	Kx 10^{-3}cal/deg.sec.
KNO_3	127.7	.86	.013	15.1
$KClO_4$	299.5	3.21	.024	7.47
Ag_2SO_4	430	1.78	.006	3.37
SiO_2	573	.23	.002	8.69
K_2SO_4	583	1.12	.011	9.82
K_2CrO_4	665	1.27	.013	10.23
$BaCO_3$	810	2.86	.018	6.29
$SrCO_3$	925	3.75	.032	8.53

TABLE A1-1: Peak temperature, peak area, ΔH and K (constant) of standard compounds (Reference 150).

Compound	Peak Temp. °C	ΔT °C	Peak Area (A) deg.sec.mg^{-1}	ΔH cal.mg^{-1}	Kx 10^{-3}cal/deg.sec.
KNO_3	129	2.13	1.00	.013	13.00
$KClO_4$	300	3.23	2.907	.024	8.25
Ag_2SO_4	432	1.81	1.34	.006	4.48
SiO_2	573	0.38	.228	.00198	8.684
K_2SO_4	587	1.29	1.16	.011	9.48
K_2CrO_4	670	1.26	1.32	.013	9.84
$BaCO_3$	815	1.95	2.34	.018	7.7
$SrCO_3$	929	2.55	3.25	.032	9.85

TABLE A1-2: Peak temperature, ΔT, peak area, ΔH and K (constant) of standard compounds used in the present work.

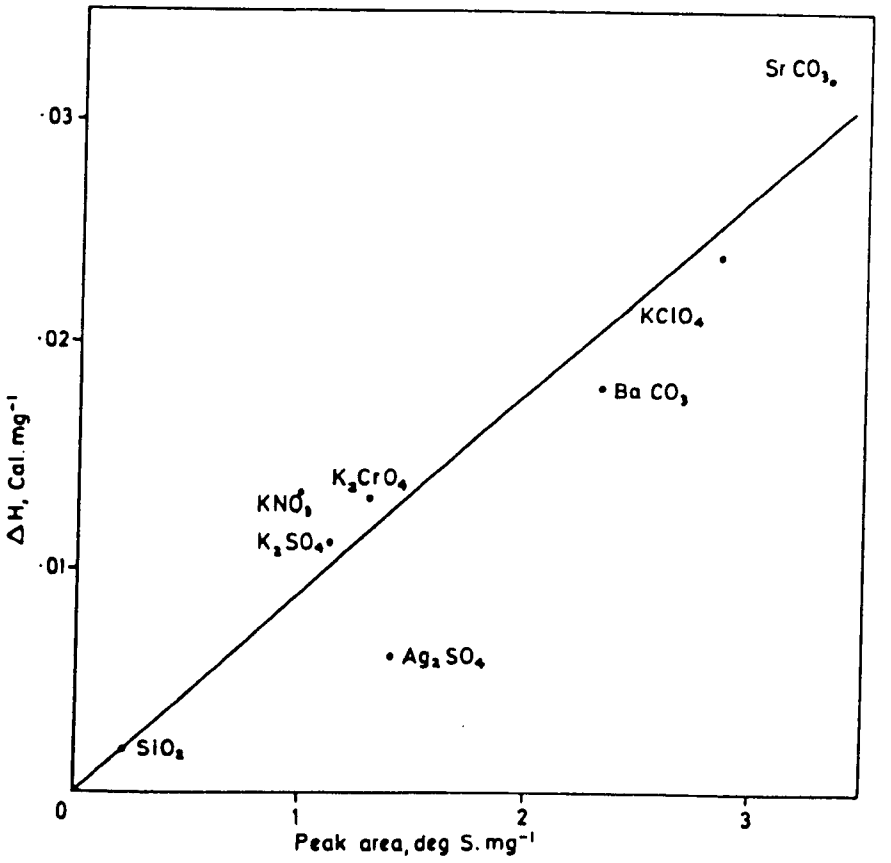

FIG. A1-1: Relationship between heat of transition (ΔH) and peak area for standard compounds.

APPENDIX 2

Hot-Pressed Cement Fondu Prepared with Additives

A2.1 Introduction

Hot-pressed cements were recently developed by Roy et al.[36,96,97,154] and very high strength values were reported. The present work is an attempt to investigate the role of some additives on the properties of the prepared cements. Some of the samples after hot-pressing were fired in air in the range of temperature 300- 1200°C for 24 hours, and some of them were cured for 1, 5 and 28 days. All the properties were compared with those for neat cement pastes (without additives), prepared under similar conditions. On the other hand, no report has appeared to date in the literature on the effect of H_3PO_4, CrO_3 and H_3BO_3 on the properties of cement fondu especially under hot-pressing conditions.

A2.2 Materials and Sample Preparation

The cement studied was cement fondu (supplied from Lafarge Aluminous Cement Co. Ltd., England). The chemical analysis and some physical properties are given in Table A2-1. The selected additives were phosphoric acid, chromium trioxide, (phosphoric acid + boric acid) and (phosphoric acid + chromium trioxide), and the percentage of the additives was fixed at 5 wt% throughout this work. All the samples were prepared under constant pressure (207 MNm^{-2}) for constant time (30 minutes) at constant temperature (150°C) before being subjected to heat treatment or curing.

Sample preparation either in disc or in cylindrical forms was carried out following the same procedure previously described (Section 3.3.2.2), using w/c ratio ~ 0.1.

	%
Al_2O_3	36.95
SiO_2	3.905
CaO	38.70
Fe_2O_3	12.00
FeO	4.33
MgO	1.06
TiO_2	1.77
Na_2O	0.30
K_2O	0.45
Colour	Dark
Density g/cc	3.12
Specific Surface Area (BET N_2 Absorption) m^2gm^{-1}	0.62
Phases present (XRD)	CA, $C_{12}A_7$ and C_4AF

Table A2-1: Chemical analysis and physical properties of cement fondu.

A2.3 Results and Discussion

Typical DTA curves for the cements mixed with the different additives as well as for neat cement paste are shown in Fig. A2-1. Neat cement paste shows three endothermic peaks at about 115, 148 and 300°C and an exothermic peak at about 886°C. The first endothermic peak is believed to represent alumina gel[34], whereas the second peak is probably due to decomposition of CA.aq.[148] The endothermic peak at about 300°C is presumably due to C_3AH_6[148], and the exothermic peak at about 886°C may be attributed to the crystallisation of CA. Ramachandran[148] reported that an exothermic peak at about 930°C is produced by this crystallisation. Samples mixed with phosphoric acid

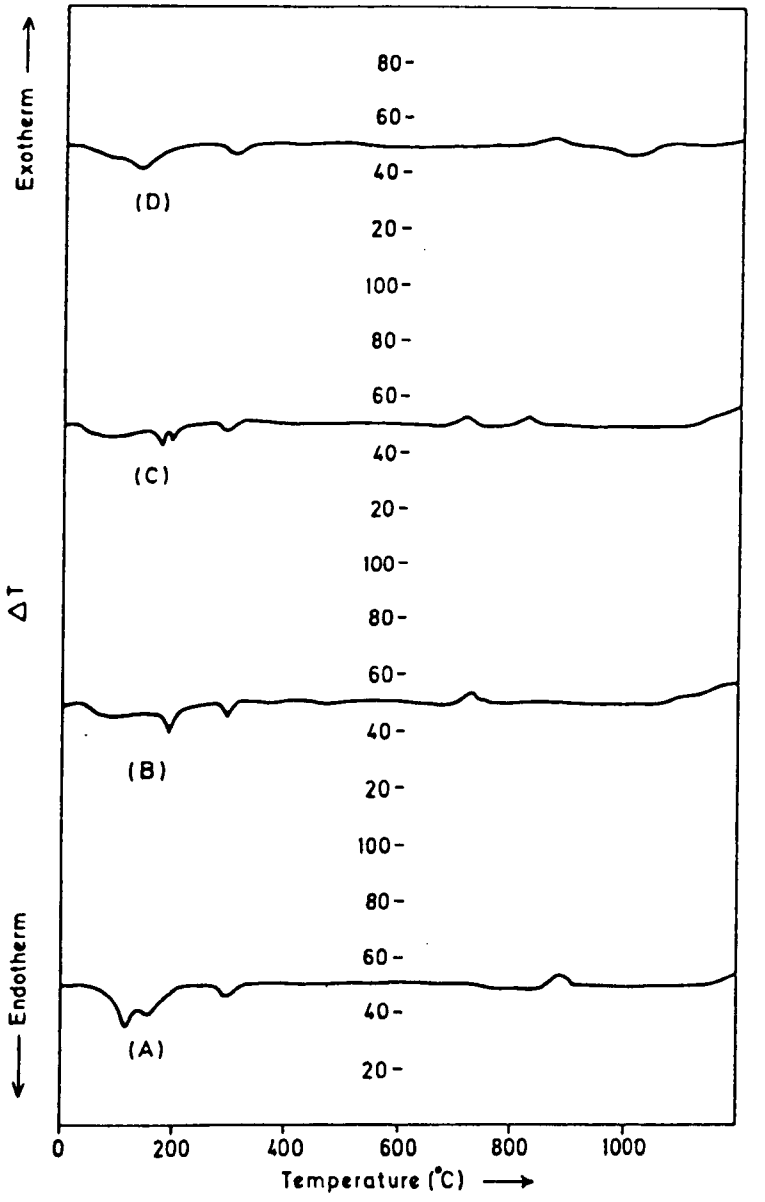

FIG. A2-1: DTA traces of: (A) neat cement fondu
(B) cement fondu + 5% H_3PO_4
(C) cement fondu + 5% (H_3PO_4+H_3BO_3)
(D) cement fondu + 5% (H_3PO_4+CrO_3)

show two endothermic peaks at about 192 and 297°C and an exothermic peak at about 720°C. No explanation can be given to the first endothermic peak, whereas the second one may represent C_3AH_6. The exothermic peak at about 720°C is believed to represent the reaction between the cement (especially CA) and the phosphoric acid (it may produce some form of anhydrous aluminium phosphate). Cements mixed with "H_3PO_4 + H_3BO_3" show three endothermic peaks at about 172, 192 and 295°C and two exothermic peaks at about 710 and 815°C. No explanation can be given of the first and second endothermic peaks, whereas the third one is most likely arising from C_3AH_6. In addition, the two exothermic peaks are believed to represent the reaction between phosphoric acid and cement at about 710°C and boric acid and cement at about 815°C. (The first reaction may produce anhydrous aluminium phosphate, whereas the second reaction may produce the aluminium-borate compound, "$9Al_2O_3.2B_2O_3$".) Finally, the reaction between cement and "H_3PO_4 + CrO_3" mixture shows three endothermic peaks at about 127, 298 and 1000°C and an exothermic broad peak at about 864°C. The first and the second endothermic peaks may represent CA.aq. and C_3AH_6 respectively, whereas the exothermic peak at about 864°C probably represents the crystallisation of the compound $4CaO.3Al_2O_3.CrO_3$, since its presence was confirmed by XRD. No explanation can be given to the endothermic peak at about 1000°C.

X-ray diffractometer analysis of the original, unhydrated cement powder shows that it is mainly composed of CA, $C_{12}A_7$, C_4AF and pleochroite as shown in Fig. A2-2. As expected, after hot-pressing at 150°C (under 207 MNm^{-2} pressure, for 30 minutes), a decrease in the original phases present was observed, and new peaks representing C_3AH_6 and AH_3 were detected. After firing the hot-pressed samples at 300°C in air for 24 hours, this resulted in the disappearance of the hydrated compounds (C_3AH_6 and AH_3). Small trace peaks were detected at 3.59 and 3.32 Å

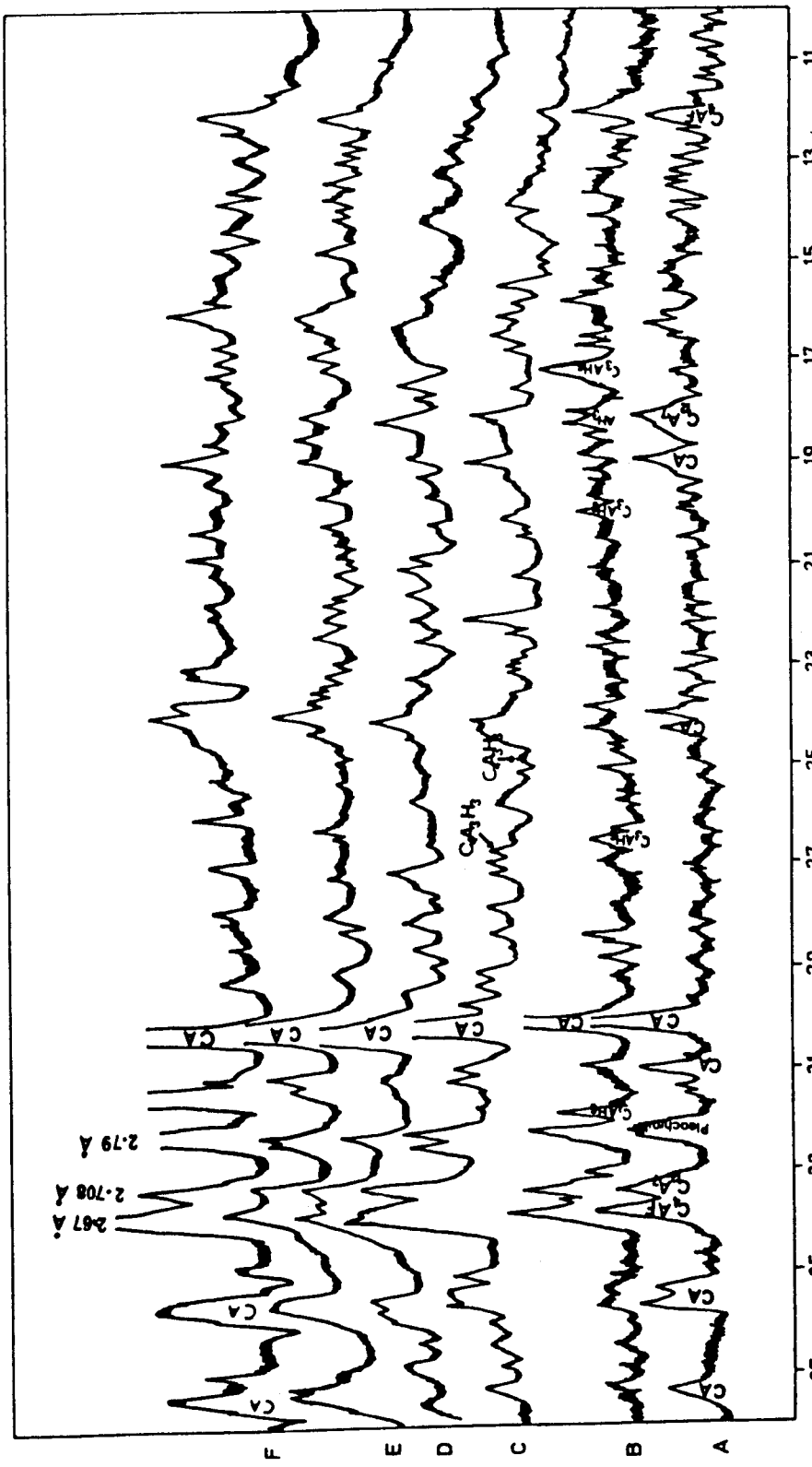

FIG. A2-2: X-ray diffractometer traces of neat cement fondu: (A) The original unhydrated cement; (B) hot-pressed at 150°C, under 207 MNm-2 pressure for 30 minutes. Samples followed by firing at (C) 300°C, (D) 600°C, (E) 900°C, (F) 1200°C, for 24 hours.

which possibly represent $C_4A_3H_3$. At the same time, CA, $C_{12}A_7$ and C_4AF could also be detected in the samples examined. After firing at 600°C, a small peak at 2.67 Å appeared which may represent C_2F, but CA, $C_{12}A_7$ and C_4AF were also detected. In addition, traces of CaO could also be detected.

After firing at 900°C, an increase in the intensities of the CA peaks was observed. This is supported by Midgeley's[34] observation that at this temperature some $C_{12}A_7$ reacts with Al_2O_3 to produce CA. Finally, after firing at 1200°C a noticeable increase in the CA peaks was observed. In addition, the group of peaks detected at 2.67, 2.708 and 2.79 Å may represent C_2F. All the above changes are shown in Fig. A2-2. X-ray analysis of fondu cement mixed with phosphoric acid after hot-pressing at 150°C (under 207 MNm^{-2} pressure for 30 minutes) shows that no reaction took place and no hydrated compounds were formed. Firing at 300°C produced no changes in the X-ray pattern. After increasing the firing temperature to 600, 900 and 1200°C, no difference in the X-ray patterns of these samples and those of neat cement fondu was evident (Fig. A2-3). X-ray analysis of cement fondu mixed with 5% "H_3PO_4 + H_3BO_3", hot-pressed at 150°C (under 207 MNm^{-2} pressure for 30 minutes), shows that no hydrated compounds were detected. After firing at 300, 600, 900 and 1200°C, the X-ray patterns were nearly similar to that of cement fondu + phosphoric acid mixture, as shown in Figure A2-4. The X-ray analytical results of fondu cement mixed with CrO_3 or "H_3PO_4 + CrO_3" show a great similarity over the range of firing, i.e. 300, 600, 900 and 1200°C, as shown in Figures A2-5 and A2-6. After hot-pressing at 150°C (under 207 MNm^{-2} pressure for 30 minutes), no hydrated compounds were detected. The only interesting phenomenon is the formation of the compound $4CaO.3Al_2O_3.CrO_3$ after firing both mixes at 900°C. This was confirmed by the appearance of the

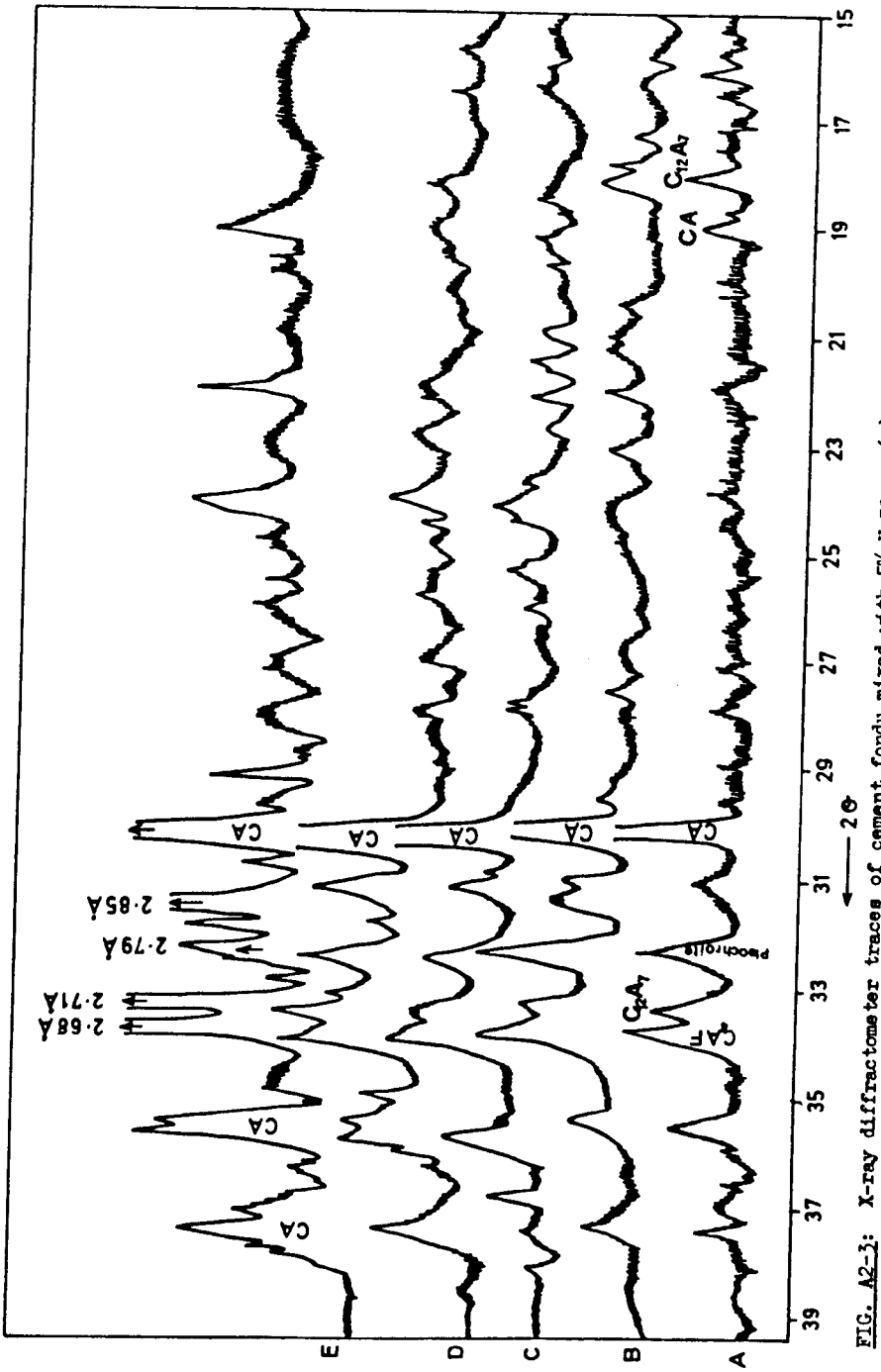

FIG. A2-3: X-ray diffractometer traces of cement fondu mixed with 5% H_3PO_4: (A) hot-pressed at 150°C, under 207 MNm^{-2} pressure, for 30 minutes. Samples followed by firing at: (B) 300°C, (C) 600°C, (D) 900°C, (E) 1200°C for 24 hours.

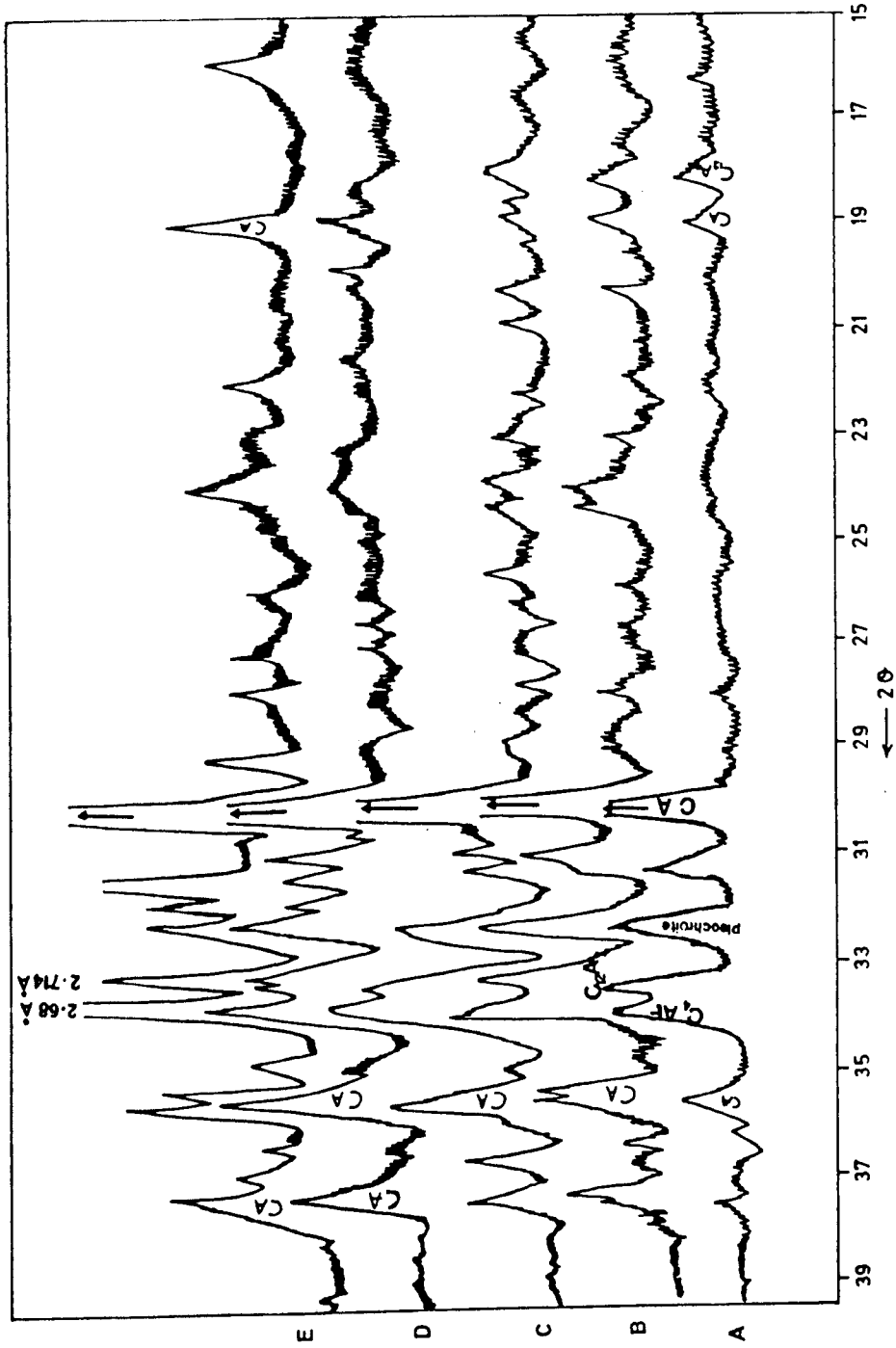

FIG. A2-4: X-ray diffractometer traces of cement fondu mixed with 5% "H_3PO_4+H_3BO_3", (A) hot-pressed at 150°C under 207 MNm^{-2} pressure for 30 minutes. Samples followed by firing at: (B) 300°C, (C) 600°C, (D) 900°C, (E) 1200°C for 24 hours.

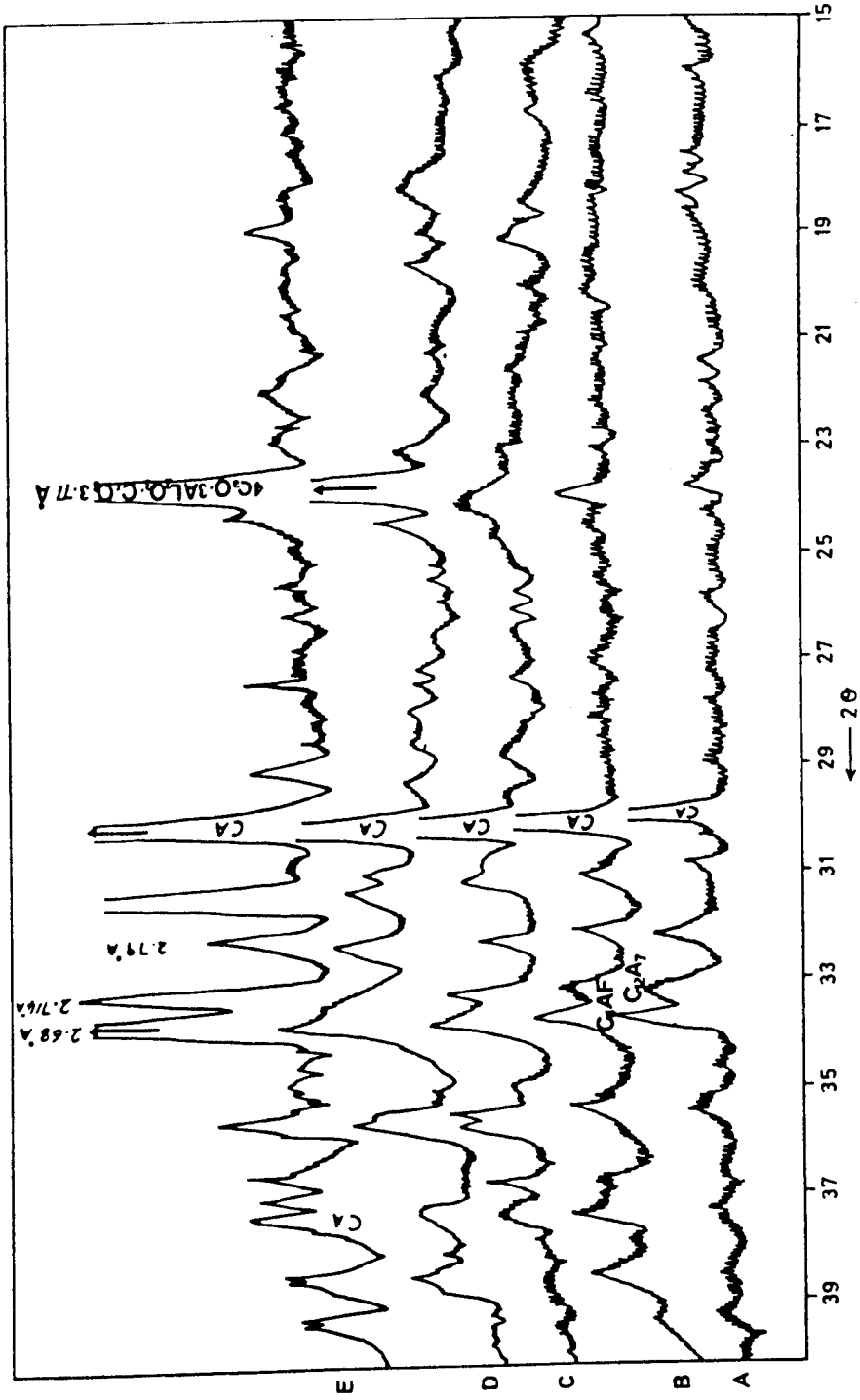

FIG. A2-5: X-ray diffractometer traces of cement fondu mixed with 5% CrO_3. (A) Sample hot-pressed at 150°C, under 207 MNm^{-2} pressure for 30 minutes. Samples followed by firing at: (B) 300°C, (C) 600°C, (D) 900°C, (E) 1200°C for 24 hours.

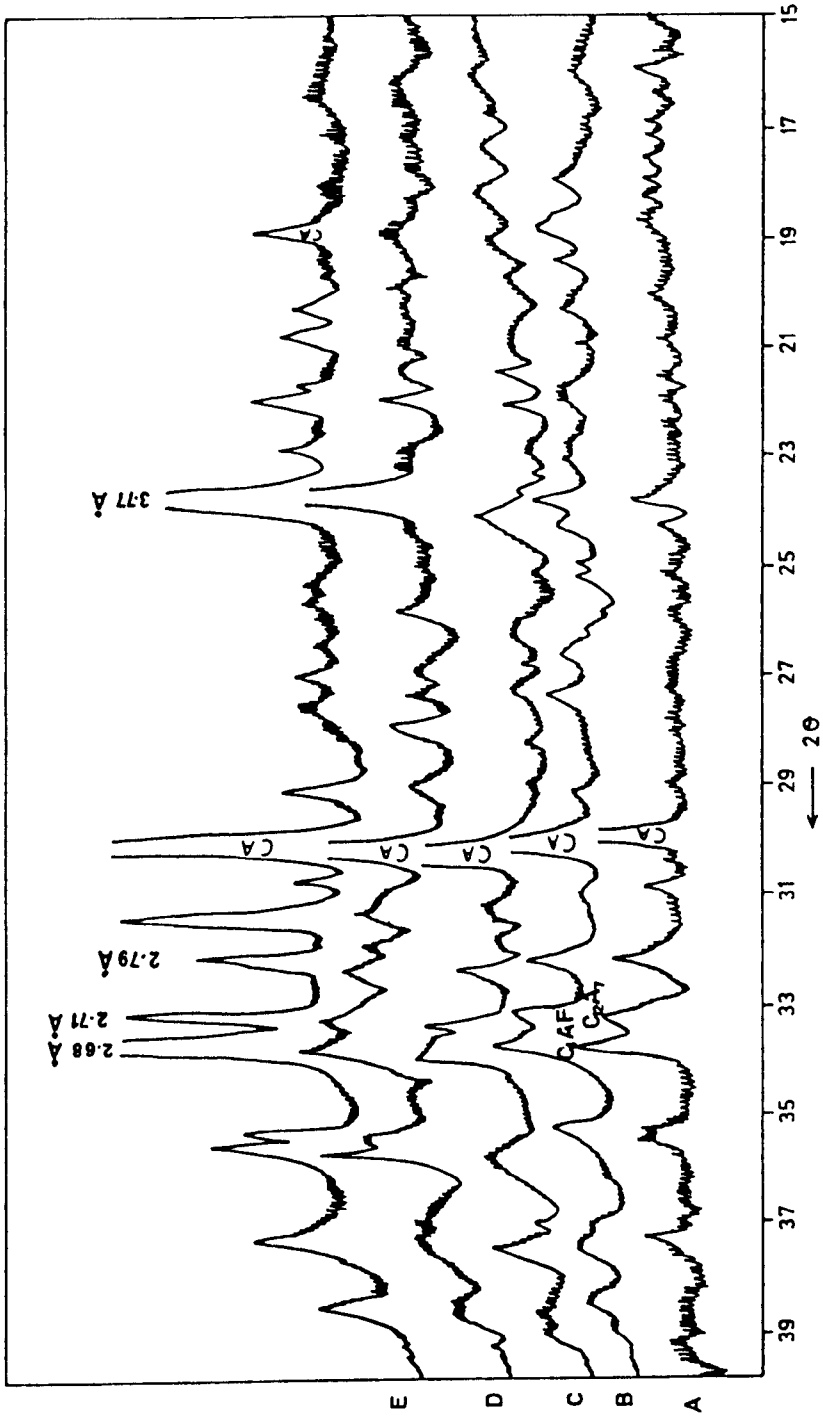

FIG. A2-6: X-ray diffractometer traces of cement fondu mixed with 5% "H_3PO_4+CrO_3". (A) Hot-pressed at 150°C under 207 MNm^{-2} pressure for 30 minutes. Samples followed by firing at: (B) 300°C, (C) 600°C, (D) 900°C, (E) 1200°C for 24 hours.

peaks at 3.769, 3.278, 2.67 and 2.474 Å. Increasing firing temperatures up to 1200°C produced an increase in the intensity of these peaks. The mechanical properties and related physical properties of all the above mixtures are given in Table A2-2. A continuous decrease in strength values of neat cement fondu was found up to 900°C. This is in agreement with Midgley's work[34] which can be explained on the basis of the decomposition of the cementing hydrates to various anhydrous phases. X-ray evidence (Fig. A2-2) shows that all the cementing hydrated compounds have disappeared after firing, forming anhydrous calcium aluminates. Cooper[155], in his investigation, suggested that the binding forces responsible for the strength above 400°C are due to degradation products of the hydrates such as $Ca(OH)_2$, $C_{12}A_7$, Al_2O_3 and possibly $C_4A_3H_3$. According to Taylor[156], at 600°C the loss of water from $Ca(OH)_2$ and $C_4A_3H_3$ should be complete. Therefore, the bonding above 600°C must be largely ceramic rather than hydraulic. After firing at 1200°C, the increase in the strength can be explained by the sintering process and the formation of a ceramic bond. Cement fondu mixed with phosphoric acid shows lower strength values after hot-pressing at 150°C than neat cement. This is most likely due to the absence of the hydrated compounds as shown in Fig. A2-3. After firing at 300 and 600°C, increases in strength were achieved. This may be due to the formation of some amorphous forms of aluminium phosphate. No explanation for the decrease in strength after firing at 900°C can be established from these results. This decrease was followed by an increase again after firing at 1200°C; this is most likely due to the sintering process.

Mixture	Hot-pressing parameters			w/c ratio	Firing Conditions		% Change		Density g.cc	Strength (MNm^{-2})		Porosity (%)
	Pressure (MNm^{-2})	Temp. (°C)	Time min.		Temp. (°C)	Time (hrs)	Wt.	Vol.		Tensile	Compressive	
Neat cement fondu	207	150	30	0.1	-	-	-	-	2.719	14.58	161.225	12.95
	207	150	30	0.1	300	24	-3.99	-	2.57	12.64	148.621	17.628
	207	150	30	0.1	600	24	-4.97	-0.47	2.53	11.2	113.4	18.90
	207	150	30	0.1	900	24	-5.22	-0.771	2.47	11.487	110.114	20.83
	207	150	30	0.1	1200	24	-6.55	-7.044	2.74	21.174	223.45	12.07
Cement fondu + 5% H_3PO_4	207	150	30	0.1	-	-	-	-	2.46	10.60	125.62	19.34
	207	150	30	0.1	300	24	-4.83	-0.94	2.55	13.69	166.5	16.123
	207	150	30	0.1	600	24	-5.44	-1.4	2.50	12.81	153.8	18.04
	207	150	30	0.1	900	24	-6.59	-	2.41	10.48	85.9	20.98
	207	150	30	0.1	1200	24	-8.50	-11.95	2.63	17.337	192.36	15.47
Cement fondu + 5% "H_3PO_4 + H_3BO_3"	207	150	30	0.1	-	-	-	-	2.385	3.6	46.6	22.71
	207	150	30	0.1	300	24	-2.00	-	2.315	1.9	25.9	25.35
	207	150	30	0.1	600	24	-2.15	+0.60	2.30	1.7	18.8	26.68
	207	150	30	0.1	900	24	-2.52	-1.60	2.365	2.9	35.8	23.2
	207	150	30	0.1	1200	24	-3.18	-28.4	2.865	32.9	370.0	8.7

TABLE A2-2 (Cont.)

Table A2-2 (Cont.)

Mixture	Hot-pressing parameters			w/c ratio	Firing Conditions		% Change		Density g.cc	Strength (MNm^{-2})		Porosity (%)
	Pressure (MNm^{-2})	Temp. (°C)	Time min.		Temp. (°C)	Time (hrs)	Wt.	Vol.		Tensile	Compressive	
Cement fondu + 5% "H_3PO_4 + CrO_3"	207	150	30	0.1	-	-	-	-	2.64	17.8	202.7	14.1
	207	150	30	0.1	300	24	-4.00	-0.53	2.48	13.7	168.2	18.4
	207	150	30	0.1	600	24	-5.034	-1.53	2.46	12.2	149.08	19.07
	207	150	30	0.1	900	24	-5.23	-	2.49	16.4	158.3	18.09
	207	150	30	0.1	1200	24	-6.46	-13.92	2.72	29.8	270.5	10.52
Cement fondu + 5% CrO_3	207	150	30	0.1	-	-	-	-	2.63	15.8	196.0	14.44
	207	150	30	0.1	300	24	-3.36	-0.745	2.42	6.49	73.0	21.91
	207	150	30	0.1	600	24	-4.27	-	2.42	6.8	64.6	21.67
	207	150	30	0.1	900	24	-4.77	-0.87	2.44	7.3	90.66	19.67
	207	150	30	0.1	1200	24	-5.26	-8.53	2.63	16.3	173.2	13.50

TABLE A2-2: Mechanical properties and related physical properties of neat cement fondu and cement fondu mixed with different additives. Samples were hot pressed at 150°C under 207 MNm^{-2} pressure for 30 minutes before firing in the range 300°-1200°C for 24 hours.

Cement fondu mixed with "H_3PO_4 + H_3BO_3" showed the lowest strength values over the range of firing up to 900°C, whereas after firing at 1200°C, a high degree of densification took place accompanied by a large decrease in volume. This shrinkage resulted in a high strength value. The two cement mixtures with CrO_3 or "H_3PO_4 + CrO_3" showed relatively high strength values after hot-pressing at 150°C (under 207 MNm^{-2} pressure for 30 minutes). This was followed by a continuous decrease in strength after firing up to 900°C, especially in the cement mixed with CrO_3. In the case of cement mixed with "H_3PO_4 + CrO_3", the strength loss was less. Both mixtures showed an increase in strength after firing to 1200°C.

The X-ray analyses of the hot-pressed neat cement fondu, after curing for 1, 5 and 28 days, are shown in Fig. A2-7. The results were found to agree with the work published by Roy and Gouda[36], whereas by increasing curing time, increases in the percentage of the hydrated compounds (C_3AH_6 and AH_3) were detected. X-ray analysis of hot-pressed cement mixed with phosphoric acid shows that no hydrated compounds can be detected after one day's curing. The presence of C_3AH_6 and AH_3 was detected after 5 days' curing. After 28 days' curing, no increase in the intensities of the peaks representing C_3AH_6 or AH_3 was observed, Fig. A2-8(1). The X-ray analysis of hot-pressed cements mixed with "H_3PO_4 + H_3BO_3" showed that a relatively small amount of C_3AH_6 and AH_3 could be detected after curing for 5 days, as shown in Fig. A2-9(1). On increasing curing time to 28 days, no increase in the hydrated compounds content was observed. X-ray analyses of hot-pressed cements mixed with CrO_3 or "H_3PO_4 + CrO_3" after curing are shown in Figs. A2-8(2) and A2-9(2). Cements mixed with "H_3PO_4 + CrO_3" showed the appearance of C_3AH_6 and AH_3 after 5 days' curing. A small increase in the amount of the above two hydrated compounds was observed after curing for 28 days. When CrO_3 was used as an additive, only traces of C_3AH_6 and AH_3 could be detected after

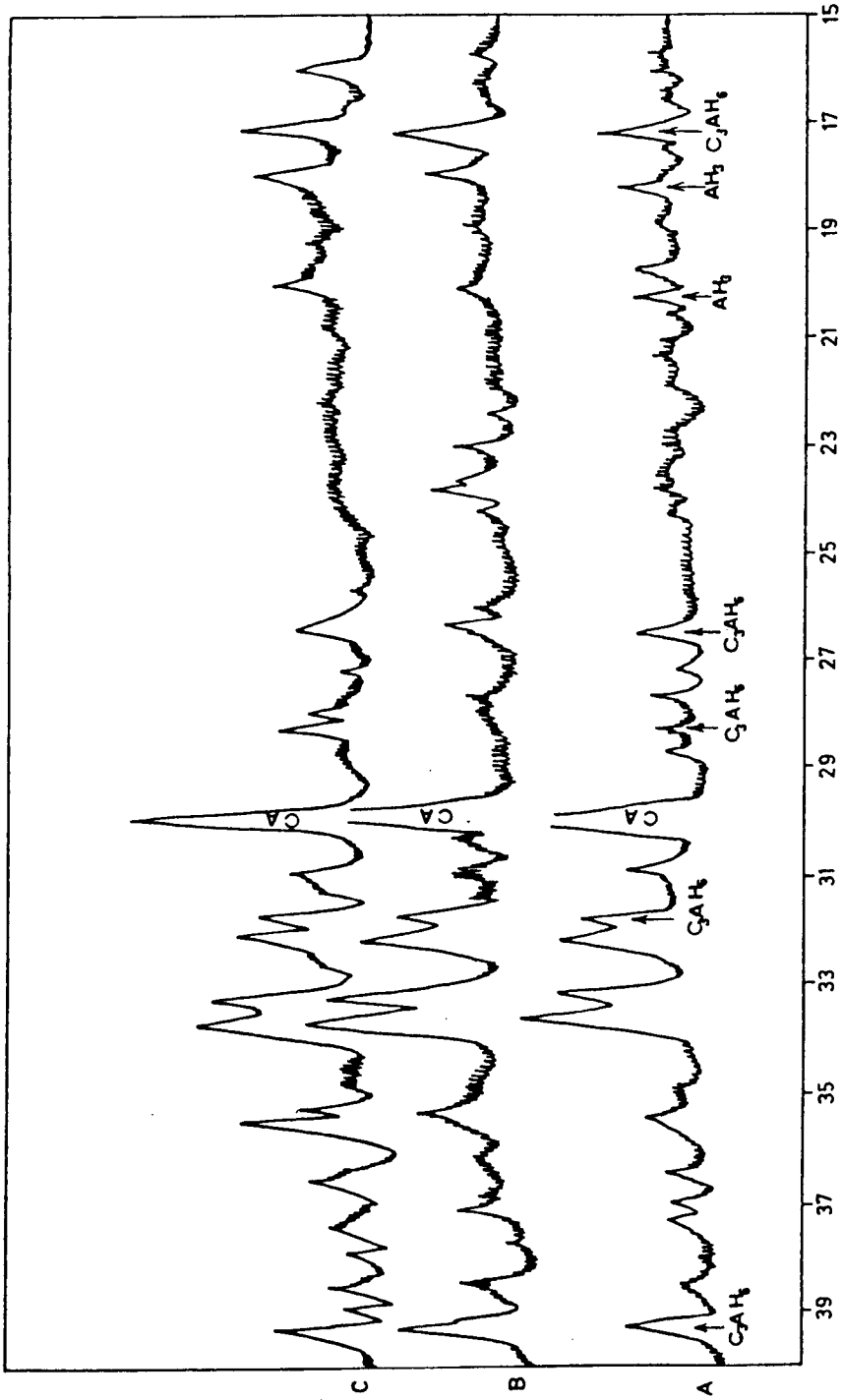

FIG. A2-7: X-ray diffractometer traces of neat cement fondu hot-pressed at 150°C, under 207 MNm^{-2} pressure for 30 minutes, and cured for (A) one day, (B) 5 days, (C) 28 days.

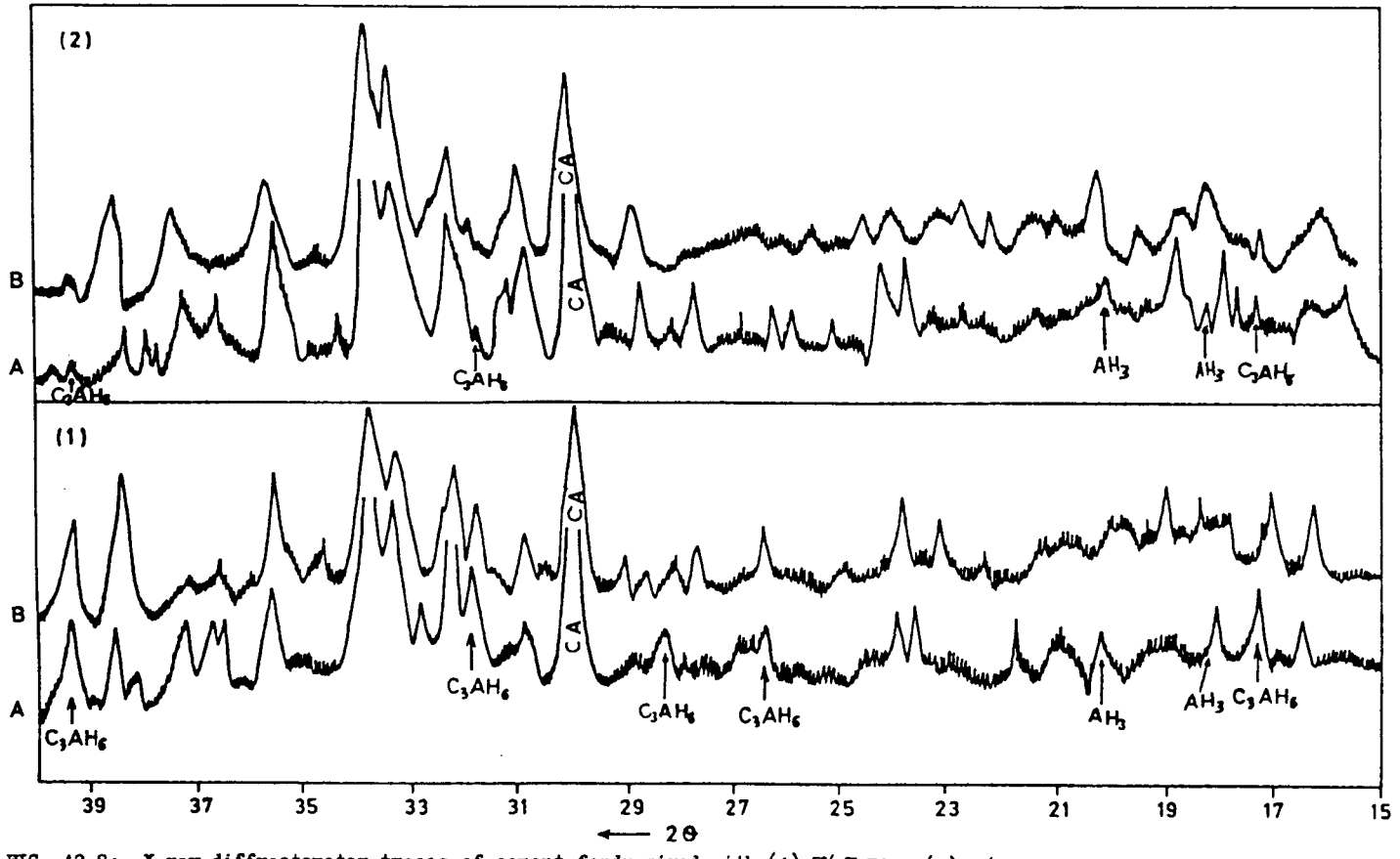

FIG. A2-8: X-ray diffractometer traces of cement fondu mixed with (1) 5% H_3PO_4, (2) 5% CrO_3. Samples cured for: (A) 5 days, (B) 28 days. (Samples were previously hot-pressed at 150°C under 207 MNm^{-2} for 30 minutes before curing.)

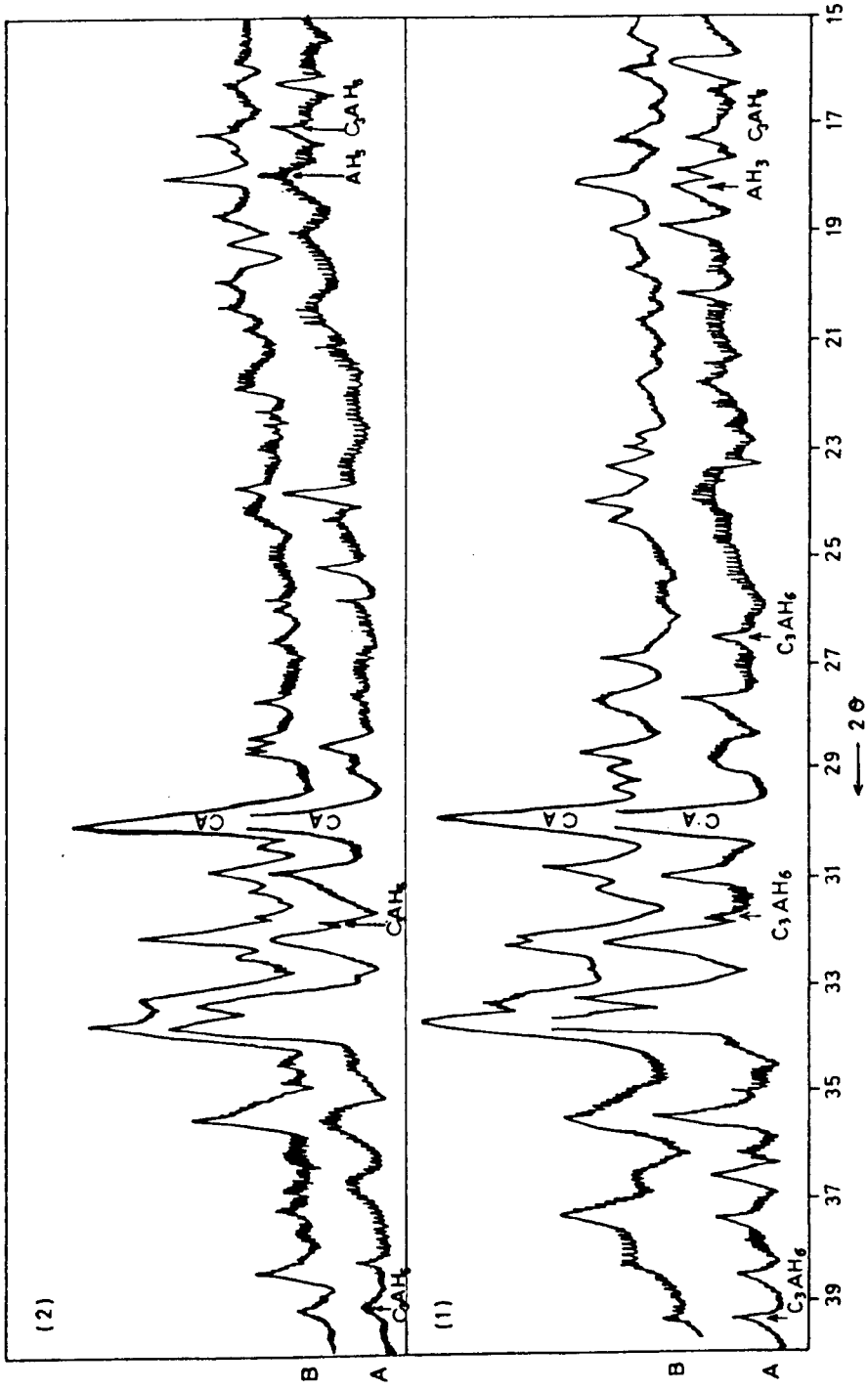

FIG. A2-9: X-ray diffraction traces of cement fondu mixed with: (1) 5% (H_3PO_4+H_3BO_3), (2) 5% (H_3PO_4+Cr_2O_3). Samples cured for (A) 5 days, (B) 28 days. (Samples were previously hot-pressed at 150°C under 207 MNm^{-2} for 30 minutes before curing.)

5 days' curing. After 28 days an increase especially in the AH_3 content was observed.

Mechanical properties and related physical properties of the above mixtures and neat cement fondu are given in Table A2-3. The results showed that strength increased in all the mixtures as the curing time was increased. However, all the additives used in this study retarded the early hydraulic activity of the cement by preventing the hydration of calcium monoaluminate in the early periods. Generally the results showed that the degree of retardation was higher when CrO_3 or "H_3PO_4 + H_3BO_3" were used, and relatively lower when phosphoric acid or "H_3PO_4 + CrO_3" were added. Mishima[157] reported that there was no obvious relationship between the quantities of crystalline hydrate products and the strength. This was because the structure of the whole body including the amorphous phases was considered to contribute to the strength. This may explain the relatively high strength value obtained when cement fondu is mixed with "H_3PO_4 + CrO_3" and hot-pressed at 150°C (under 207 MNm^{-2} pressure for 30 minutes).

The role that Cr_2O_3 and P_2O_5 play in the early strength of Portland cement clinker has been discussed by various investigators. Sakurai et al.[158] and Imlach[159] suggested that the early hydraulic activity of Portland cement clinker is remarkably promoted by the addition of small amounts of Cr_2O_3. The influence of P_2O_5 was reported by Nurse[65,160] and Welch and Gutt[161]. Akatsu et al.[162] reported that the proper amount of Cr_2O_3 or P_2O_5 (0.5%) promotes remarkable increase in strength of Portland cement, especially in the early age. Many reports have supposed that the effect of minor components on the early hydration and the early strength of clinker materials, is connected with the formation of crystal imperfection or defects[158].

Mixture	Hot-pressing parameters			w/c ratio	Curing time (days)	% change		Density g.cc	Strength (MNm^{-2})		Porosity (%)
	Pressure (MNm^{-2})	Temp. (°C)	Time min.			Wt.	Vol.		Tensile	Compressive	
Neat cement fondu	207	150	30	0.1	1	+0.84	+0.480	2.721	17.19	174.8	12.7
	207	150	30	0.1	5	+1.20	+0.672	2.731	20.30	211.08	12.46
	207	150	30	0.1	28	+2.04	+0.807	2.74	20.80	234.0	12.178
Cement fondu + 5% H_3PO_4	207	150	30	0.1	1	+2.4	-	2.59	15.60	138.0	16.45
	207	150	30	0.1	5	+3.15	+0.200	2.67	20.05	203.0	13.8
	207	150	30	0.1	28	+3.9	+0.57	2.67	17.88	185.0	13.8
Cement fondu + 5% "H_3PO_4 + H_3BO_3"	207	150	30	0.1	1	+5.9	-	2.33	2.6	31.0	23.6
	207	150	30	0.1	5	+8.88	+0.4823	2.56	14.3	120.0	16.66
	207	150	30	0.1	28	+10.30	+0.623	2.59	14.1	148.6	15.08

TABLE A2-3 (Cont.)

TABLE A2-3 (Cont.)

Mixture	Hot-pressing parameters			w/c ratio	Curing time (days)	% Change		density g.cc	Strength (MNm^{-2})		Porosity (%)
	Pressure (MNm^{-2})	Temp. (°C)	Time (min.)			wt.	Vol.		Tensile	Compressive	
Cement fondu + 5% "H_3PO_4 + CrO_3"	207	150	30	0.1	1	+3.5	-	2.68	19.07	192.0	13.54
	207	150	30	0.1	5	+4.6	+0.72	2.64	19.7	180.0	14.83
	207	150	30	0.1	28	+4.7	-	2.68	18.3	198.0	13.54
Cement fondu + 5% CrO_3	207	150	30	0.1	1	+4.4	-	2.51	4.1	52.0	19.06
	207	150	30	0.1	5	+4.4	-0.885	2.56	7.2	83.0	17.2
	207	150	30	0.1	28	+5.5	+0.93	2.64	14.8	157.0	14.87

TABLE A2-3: Mechanical properties and related physical properties of neat cement fondu and cement fondu mixed with different additives. Samples were hot-pressed at 150°C, under 207 MNm^{-2} pressure, for 30 minutes, cured for 1, 5 and 28 days.

The compressive strength of all the above mixtures as well as neat cement fondu were plotted against the porosity, in Figures A2-10 and A2-11, using two different empirical equations.

Figure A2-10 shows that except for three points representing cement mixed with "H_3PO_4 + H_3BO_3", the scatter of the results is considerable but an acceptable constant was obtained (n = 10.75). On the other hand, Fig. A2-11 showed a reasonable fitting to the data and the value of the constant (K) was 2.42×10^{-5} (if strength is expressed in psi). This is in acceptable agreement with the value (3.7×10^{-5}) reported by Roy et al.[36,97] for neat cement. Generally, in both curves there is an unmistakable trend of increasing strength with decreasing porosity.

It is believed that a more extensive study of the effects of P_2O_5 and CrO_3 on the properties of cement fondu could be profitably undertaken.

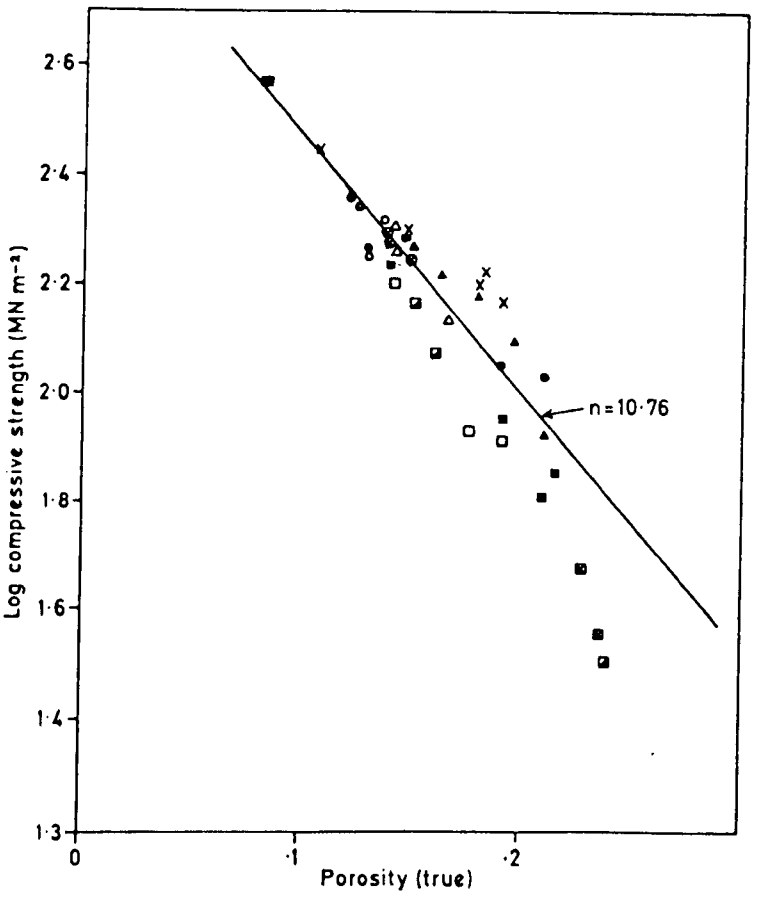

FIG.(A2-10): Log strength-porosity relationship. Data plotted on the basis of equation (2.7).

● ●	neat cement fondu	Samples hot-pressed at 150°C, fired at 300°, 600°, 900° and 1200°C for 24 hours.
▲ ▲	cement fondu + 5% H_3PO_4	
■ ■	" " + 5% CrO_3	
× ×	" " + 5% (H_3PO_4+CrO_3)	
■ ■	" " + 5% (H_3PO_4+H_3BO_3)	
o o	neat cement fondu	Samples hot-pressed at 150°C, cured for 1, 5 and 28 days.
▲ ▲	cement fondu + 5% H_3PO_4	
□ □	" " + 5% CrO_3	
● ●	" " + 5% (H_3PO_4+CrO_3)	
▨ ▨	" " + 5% (H_3PO_4+H_3BO_3)	

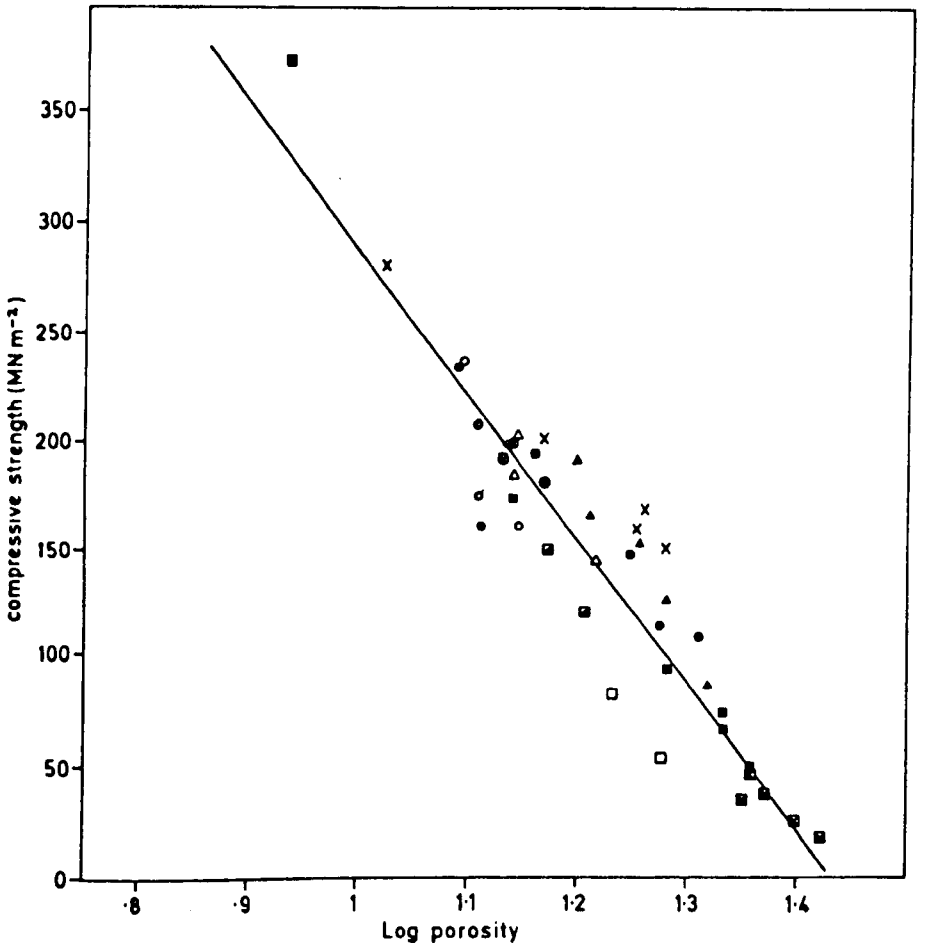

FIG.(A2-11): Strength-log porosity relationship. Data plotted on the basis of equation (2.10).

● ●	neat cement fondu	Samples hot-pressed at 150°C, fired at 300°, 600°, 900° and 1200°C for 24 hours.
▲ ▲	cement fondu + 5% H_3PO_4	
■ ■	" " + 5% CrO_3	
× ×	" " + 5% (H_3PO_4+CrO_3)	
■ ■	" " + 5% (H_3PO_4+H_3BO_3)	
○ ○	neat cement fondu	Samples hot-pressed at 150°C, cured for 1, 5 and 28 days.
△ △	cement fondu + 5% H_3PO_4	
□ □	" " + 5% CrO_3	
● ●	" " + 5% (H_3PO_4+CrO_3)	
▨ ▨	" " + 5% (H_3PO_4+H_3BO_3)	

REFERENCES

1. Davidge, R.W. "Fracture Mechanics of Ceramics" Vol. 2, Bradt, R.C., Hasselman, D.P.H. and Lange, F.F. (eds.), Plenum Press, pp. 447-468 (1973).
2. Shepherd, E.S., Rankin, G.A. and Wright, F.E. Amer. J. Sci. (4), 293 (1909).
3. Rankin, G.A. and Wright, F.E. Amer. J. Sci. (1) 39, No. 229 (1915).
4. Thorvaldson, T. and Grace, N.C. Canad. J. Res. 1, 45 (1929).
5. Lagerqvist, K., Wallmark, S. and Westgren, A. A. Anorg. Chem. 234, 1-16 (1937).
6. Toropov, N.A. and Stukalova, M.M. C.R. Acad. Sci., U.R.S.S., 24, 94 (1940).
7. Gentile, A.L. and Foster, W.R. J. Amer. Cer. Soc. 46, 74 (1963).
8. Nurse, R.W., Welch, J.H. and Majumder, A.J. Trans. Brit. Ceram. Soc. 64, 409-418 (1965).
9. Lea, F.M. The Chemistry of Cement and Concrete, Arnold Publishers, 3rd Ed., p.490 (1970).
10. Robson, T.D. Proc. 5th Int. Symp. of Chem. of Cement, Tokyo, 349-365 (1968).
11. Heller, L. Thesis, University of London (1951).
12. Dougill, M.W. Nature, 180 (4580), pp. 292-293 (1957).
13. Glasser, F.P. "Material Science and Technology" Vol. 2 (Alper, A.M., ed.), Academic Press, pp. 147-186 (1970).
14. Tavasci, B. Chim. el'Industr. 17, 461-471 (1935).
15. Bokyo, E.R. and Winsyi, L.G. Acta Cryst. 11, 444 (1958).
16. Goodwin, D.W. and Lindop, A.J. Acta Cryst. B26, 1320 (1970).
17. Bobrov, B.S., Zaldat, G.I. and Zalizovskii, E.V. Inorg. Mat. 10 (12), 1875-1877 (1975).
18. Filonenko, N.E. and Lourov, I.V. C.R. Acad. Sci. USSR, 66, No. 4, 673-676 (1949). Ceram. Abst. 1950, January, p.2f.
19. Jeffery, J.W. The Chemistry of Cements, Academic Press (London and New York), ed. Taylor, H.F.W., V.I, Chapter 4, p.151 (1964).

20. Nurse, R.W., Welch, J.H. and Majumdar, A.J. Trans. Brit. Ceram. Soc. 64, 323-332 (1965).

21. Jones, F.E. 4th Int. Symp. of Chem. of Cements, Washington, pp. 204-246 (1960).

22. Lhopitallier, P. 4th Int. Symp. of Chem. of Cements, Washington, pp. 1007-1034 (1960).

23. Seligmann, P. and Greening, N.R. J. Res. Dev. Labs. Portl'd Cem. Ass. 4 (2), 2 (1962).

24. Buttler, F.G. and Taylor, H.F.W. J. Chem. Soc. 2103 (1958).

25. Majumdar, A.J. and Roy, R. J. Amer. Ceram. Soc. 39, 434-442 (1956).

26. Aruja, E. Acta Cryst. 10, 337-339 (1957).

27. Parker, T.W. 3rd Symp. of Chem. of Cem., London, 485 (1952).

28. Midgley, H.G. Trans. Brit. Ceram. Soc. 67, 1 (1968).

29. Majumdar, A.J. Trans. Brit. Ceram. Soc. 63, 347 (1964).

30. Midgley, H.G. Cement & Concrete Res. 7, 669-672 (1977).

31. Lister, D.H. and Glasser, F.P. Trans. Brit. Ceram. Soc. 66, 293 (1967).

32. Robson, T.D. High Alumina Cement and Concrete, John Wiley & Sons (1962).

33. Percival, A., Buttler, F.G. and Taylor, H.F.W. 4th Int. Symp. of Chem. of Cements, Washington, 227 (1960).

34. Midgley, H.G. Trans. Brit. Ceram. Soc. 66, 161 (1967).

35. Turriziani, R. The Chemistry of Cements, ed. Taylor, H.F.W., Academic Press, Vol. 1, Chapter 6 (1964).

36. Gouda, C.R. and Roy, D.M. Cem. Concr. Res. 5, 551-564 (1975).

37. Midgley, H.G. and Midgely, A. Mag. Conc. Res. 27, 59-77 (1975).

38. Teychenne, D.C. Mag. Conc. Res. 27, 78-102 (1975).

39. Cattorji, S. and Jeffery, J.W. Trans. Brit. Ceram. Soc. 67, 171 (1968).

40. Neville, A.M. and Wainwright, P.J. High Alumina Cement Concrete, Halstead Press, John Wiley & Sons, New York, p.201 (1975).

41. Heindl, R.A. and Post, Z.A. J. Am. Ceram. Soc. 37, 206 (1954).

42. Schneider, S.J. J. Am. Ceram. Soc. 42, 184 (1959).

43. Tseung, A.C.C. and Carruthers, T.G. Trans. Brit. Ceram. Soc. 62, 305-320 (1963).

44. Wood, A.A.R. and Briebach, A.V. Trans. Brit. Ceram. Soc. 64, 333 (1965).

45. Dutta, B.M., Pramanik, S. and Ramakrishna, M.R. Trans. Ind. Ceram. Soc. Vol. 28 (5), sep-oc. 137-143 (1969).

46. Kingery, W.D. J. Am. Ceram. Soc. 33, 239 (1950).

47. Bechtel, H. and Floss, G. Ber. Dtsch. Keram. Ges. 37 (8), 362 (1960). Ceramic Abst. 40 (6), 141h (1961).

48. Bechtel, H. and Floss, G. Ber. Dtsch. Keram. Ges. 40 (7), 339 (1963). Ceramic Abst. 43 (6), 159i (1963).

49. Preuser, E. Silicattech. 12 (2), 81 (1961). Ceramic Abst. 41 (10), 239, (1962).

50. Reinhart, F. Glas. Emaill. Keram. Tech. 13 (1), 11 (1962). Ceramic Abst. 41 (8), 197 (1962).

51. Sheets, H.D., Bulloff, J.J. and Duckworth, W.H. Brick and Clay Record, 133, 55 (1958).

52. O'Hara, M.J., Duga, J.J. and Sheets, H.D. Am. Ceram. Soc. Bull. 51 (7), 590 (1972).

53. Ersin, E. and William, B.H. Amer. Ceram. Soc. Bull. 50, (7), 604-606 (1971).

54. Palfreyman, M. Amer. Ceram. Soc. Bull. 49 (7), 538 (1970).

55. Fisher, K. Proc. Brit. Ceram. Soc., Fabrication Sciences 2, 51 (1969).

56. Sicka, R.W. U.S. Pat. 3,625,723 (1971).

57. McCarthy, G.J. and Lovette, M. Am. Ceram. Soc. Bull. 5 (8), 655 (1972).

58. Chvetal, T. Ref. Jour. 42 (8), 333-336 (1966).

59. Birchall, J.D. and Cassidy, J.E. B.P. 1,322,724; B.P. 1,357,541.

60. Cassidy, J.E. B.P. 1,386,518.

61. Westman, A.E.R. Topics in Phosphorous Chemistry, Interscience, New York (ed. Griffith, E.J. and Grayson, M.), V.9, pp. 231-405 (1977).

62. Cassidy, J.E. Am. Ceram. Soc. Bull. 56, 7 pp. 640-643 (1977).

63. Mathers, J.P. and Manning, C.R. Am. Ceram. Soc. Bull., , 548 (1974).

64. Koyanagi, K. J. Soc. Chem. Ind. (Japan), 33 (7), 276 (1930). Ceram. Abst. 10A (3), 171 (1931).

65. Nurse, R.W. J. App. Chem. 2 (12), 708 (1952).

66. Stone, P.E., Egan, E.P.Jr. and Lehr, J.R. J. Am. Ceram. Soc. 39 (3), 89-98 (1956).

67. Horn, W.F. Ph.D. Thesis, Pennsylvania State University (1974).

68. Kolb, L. Silikattechnik, 16, 160 (1965).

69. Ershov, L.D. and Basman, R.M. Ukr. Khim Zh, 21 (6), 783 (1955). Ceram. Abst. 35 (10) 205 (1956).

70. Buerger, M.J. Amer. Mineral. 33 (5/6), 751 (1948).

71. Shafer, E.C., Shafer, M.W. and Roy, R. Z. Krist. 108, 263 (1956).

72. Corbridge, D.E.C. "The Structural Chemistry of Phosphorous". Elsevier Scientific Publishing Corp., pp. 103-105 (1974).

73. Trömel, G. and Winkhous, B. Fortscher. Mineral, 28 (1), 82-84 (1949).

74. Huttenlocher, H.F. Z. Krist. 90 (A), 508-516 (1935).

75. Strunz, H. Z. Krist. 103 (4), 228-229 (1941).

76. Brill, R. and De Bretteville, A.P. Amer. Mineral. 33 (7/8), 750-759 (1948).

77. Beck, W.R. J. Am. Ceram. Soc. 32 (4), 147-153 (1949).

78. Shafer, E.C. and Roy, R. Z. Physik. Chem. Neue. Folge. 11 (5), 30-40 (1957).

79. Folk, O.W. Z. Krist. 125, 134 (1967).

80. Englert, W.J. and Hummel, F.A. J. Soc. Glass Technol. 39, 126T (1955).

81. Dachille, F. and Glasser, L.S.D. Acta Cryst. 12, 820 (1959).

82. Mackenzie, J.D., Roth, W.L. and Wentorf, R.H. Acta. Cryst. 12, 79 (1959).

83. Mooney, R.C.L. Acta Cryst. 9, 728 (1956).

84. Schulze, G.E.R. Z. Physik. Chem. Abt. B.24, 215 (1934).

85. Wyckoff, R.W.G., in Crystal Structures, Vol. e, pp. 27-31, Interscience Publishers, New York (1965).

86. Hummel, F.A. and Kupinski, T.A. J. Am. Chem. Soc. 72 (10), 5318-5319 (1950).

87. Rickles, R.N. J. App. Chem. 15, 74-77 (1965).

88. Corbridge, D.E.C. Unpublished observations.

89. Vasilos, T. and Spriggs, R.M. Prog. in Ceramic Science (J.E. Burke, ed.), 4, 95-132 (1966).

90. Spriggs, R.M. and Dutta, S.K. Science of Sintering 6 (1), 1-24 (1974).

91. Morgan, P.E.D. and Scale, E. Am. Ceram. Soc. Bull. 45, 447 (1966).

92. Chaklader, A.C.D. and Baker, V.T. Am. Ceram. Soc. Bull. 44 (3), 258-259 (1965).

93. Steiner, C.J.P., Hasselman, D.P.H. and Spriggs, R.M. J. Amer. Ceram. Soc. 54 (8), 412-413 (1971).

94. Dutta, S.K. and Gazza, G.E. Am. Ceram. Soc. Bull. 52 (7), 552-554 (1974).

95. Rice, R.W. Am. Ceram. Soc. Bull. 41, 271 (1962).

96. Roy, D.M. and Gouda, G.R. Cem. Concr. Res. 3, 807 (1973).

97. Roy, D.M. and Gouda, G.R. Cem. Concr. Res. 5, 153 (1975).

98. Kelly, A. "Strong Solids", 2nd Edition, Oxford University Press, pp. 1-51 (1973).

99. Inglis, C.E. Inst. Naval Architects Trans. 55, 219 (1913).

100. Griffith, A.A. Phil. Trans. Roy. Soc. London 221A, 163 (1920).

101. Brown, W.F. and Srawley, J.E. ASTM S.T.P. 410 (1967).

102. Orowan, E. Report Progr. in Phys. 12, 185-232 (1949).

103. Petch, N.J. J. Iron Steel Inst. (London) 174 Part I, 25-28 (1953).

104. Knudsen, F.P. J. Am. Ceram. Soc. 42 (8), 376 (1959).

105. Rice, R.W. Proc. Brit. Ceram. Soc. 20, 205-257 (1972).

106. Davidge, R.W. and Evans, A.G. Mat. Sci. Eng. 6, 281 (1970).

107. Simpson, L.A. J. Am. Ceram. Soc. 56 (1), 7-11 (1973).

108. Ryskewitsch, E. J. Am. Ceram. Soc. 36 (2), 65 (1953).

109. Coble, R.L. and Kingery, W.D. J. Am. Ceram. Soc. 39, 11, 377-385 (1956).

110. Knudsen, F.P. J. Am. Ceram. Soc. 45 (2), 94 (1962).

111. Bailey, J.E. and Hill, N.A. Proc. Brit. Ceram. Soc. 15, 15-35 (1970).

112. Buist, D.S. Mineral. Mag. 281, 676-686 (1968).

113. Wright, A.F. and Leadbetter, A.J. Phil. Mag. 31, 1391 (1975).

114. Rudnick, A., Hunter, A.R. and Holden, F.C. Mat. Res. & Stds., 3 (4), 283-289 (1963).

115. Briggs, J. Ph.D. Thesis, University of Leeds (1972).

116. Spriggs, R.M., Brisette, L.A. and Vasilos, T. Mat. Res. and Stds. 4 (5), 218-220 (1964).

117. Grieb, W.E. and Werner, G. Proc. A.S.T.M. 62, 972-991 (1962).

118. Cullity, B.D. "Elements of X-ray Diffraction", Addison-Wesley Publ., p.391 (1967).

119. Mayer, D.J., Bacon, J. and Knott, P. Proc. Conf. Brit. Cer. Soc., April 1973.

120. Jung, H.J. Ph.D. Thesis, University of Leeds (1976).

121. Russell, J.D. Mineralogical Soc. Monog. 4 "The Infrared of Minerals", (ed. Farmer, V.C.), Mineral. Soc. Publ. Chapter 2, pp. 11-25 (1974).

122. Gitzen, W.H., Hart, L.D. and MacZura, G. Am. Ceram. Soc. Bull. 35 (6), 217-223 (1956).

123. Kingery, W.D. and Francois, B. J. Am. Ceram. Soc. 48 (1), 546-547 (1965).

124. Nichols, F.A. J. Nouc. Mat. 30, 143-165 (1969).

125. Roy, V.T. Z. Krist. 123, 263-314 (1968).

126. Kingery, W.D., Bowen, H.K. and Uhlmann, D.R. "Introduction to Ceramics", 2nd Ed., Wiley (Interscience), New York, p.459 (1975).

127. Evans, A.G. and Davidge, R.W. J. Mat. Sci. 5, 314-325 (1970).

128. Rice, R.W., in "Treatise on Material Science and Technology" (ed.MacCrone R.K.), Vol. 11, 199-381, Academic Press (1977).

129. Hasselman, D.P.H. J. Am. Ceram. Soc. 52 (11), 600-604 (1969).

130. Schiller, K.K., in "Mechanical Properties of Non-Metallic Brittle Materials" (ed. Walton, W.H.), 35-49, Wiley (Interscience), New York (1958).

131. Kumar, S. Bull. Cent. Glass Ceram. Res. Inst., Calcutta, 3 (4), 183-187 (1956).

132. Klein, R.M., Kolbeck, A.G. and Quackenbush, C.L. Am. Ceram. Soc. Bull. 57 (2), 199-202, 215-216 (1978).

133. Ramamoorthy, P. and Rackett, T.J. J. Am. Ceram. Soc. 57 (11), 501-502 (1974).

134. Giglioso, P.J.M. and Foster, W.R. Nature, 195 (4836), 69-70 (1962).

135. Kim, K.H. and Hummel, F.A. Phase Diagram of Ceramics (eds. Levin, E.M., Robbins, C.R. and McMurdie, H.F.), Fig. 308 (1964).

136. Baranova, T.F., Kolin, Yu.I. and Kurskaya, I.N. Glass Ceram. 32 (11), 26-27 (1957).

137. Brook, R.J. Science of Ceramics 9, 57-66 (1977).

138. Sawkow, J. and Sulikowski, J. Cem-wapno-Gips, 30 (10), 281-93 (1976). Ceram. Abst. 57, 59, g (1978).

139. Evans, A.G. and Tappin, G. Proc. Brit. Ceram. Soc. 20, 275-297 (1972).

140. Vogel, A.I. "Quantitative Inorganic Analysis", 2nd Edition, Longmans, Green & Co., London, p.453 (1951).

141. Chvatel, T. Tenth Int. Ceram. Congr., Stockholm, 377-391 (1966).

142. Grigor'ev, V.M., Gundarina, Z.I., Kopeikin, V.A., Kuz'minskaya, L.N. and Rashkovan, I.L. Izv. Akad. Nauk SSSR, Neorgan. Mat. 8 (7), 1187-1189 (1972).

143. Ford, W.F. and Rees, W.J. Trans. Brit. Ceram. Soc. 57, 233-241 (1958).

144. Nishino, T. and Moteki, K. Chem. Abstract. 60, 9000 (1964).

145. Klyucharov, Ya.V. and Gaenko, N.S. Izv. Akad. Nauk SSSR, Neorgan. Mat. 12 (4), 670-673 (1976) (translated).

146. Fedorova, R.A., Bondarev, K.T. and Shvorneva, L.I. Glass Ceram. 34 (7), 422-425 (1977).

147. Kobayashi, T. J. Ceram. Assoc. Japan, 74 (6), 190-195 (1966).

148. Ramachandran, V.S. Applications of Differential Thermal Analysis in Cement Chemistry, Chemical Publishing Co. Inc., New York (1969).

149. Henning, O. Mineralogical Soc. Monog. 4, "The Infrared of Minerals" (ed. Farmer, V.C.), Mineral. Soc. Publ. Chapter 19, pp. 445-463 (1974).

150. Mackinzie, R.C. and Ritchie, P.F.S. Thermal Analysis Vol. 1, Proc. Third ICTA, Davos, Switzerland (ed. Wiedemann, H.G.), pp. 441-452 (1972).

151. Bochardt, H.J. and Daniels, F. J. Am. Chem. Soc. 79, 41-46 (1957).

152. Read, R.L., Weber, L. and Gottfried, B.S. Ind. Eng. Chem. Fundamentals, 4, 38-46 (1965).

153. Berg, L.G., Kozhukhov, M.I. and Egunov, V.P., Thermal Analysis Vol. 1, Proc. Third ICTA, Davos, Switzerland (ed. Wiedemann, H.G.), pp. 425-439 (1971).

154. Sarkar, A.R. and Roy, D.M. Am. Ceram. Soc. Bull. 56 (11), 984-86, 900 (1977).

155. Cooper, C.F. Trans. Brit. Ceram. Soc. 64, 351-370 (1965).

156. Taylor, H.F.W. "Progress in Ceramic Science" Vol. 2, Pergamon Press, p.115 (1961).

157. Mishima, K. Proc. 5th Int. Symp. of Chem. of Cement, Tokyo, 167-174 (1968).

158. Sakuria, T., Sato, T. and Yoshinaga, A. Proc. 5th Int. Symp. of Chem. of Cement, Tokyo, 300-321 (1968).

159. Imlach, J.A. Am. Ceram. Soc. Bull. 54 (5), 519-522 (1975).

160. Nurse, R.W. Third Int. Symp. on the Chem. of Cement, London, pp. 56-90 (1952).

161. Welch, J.H. and Gutt, W. Proc. 4th Int. Symp. on Chem. of Cement, Washington, pp. 59-68 (1962).

162. Akatsu, K., Maeda, K. and Ikeda, I. Rev. 24th Gen. Meeting Cement Assn., Japan, pp. 20-23 (May 1970).